Department of Applied Chemistry

Sulfur Dioxide Leaching of Zinc Sulfide

Justin McGinnity

This thesis is presented as part of the requirements for
the award of the Degree of Doctor of Philosophy
of the Curtin University of Technology

August 2001

This work is dedicated to my beautiful wife, Sandra,
and our children, Mark, Maria, Francesca
and our babe in the womb,
in appreciation of their
loving support and encouragement.

It is also dedicated to my parents, Kevin and Dorothy McGinnity,
and father-in-law, Michael Siciliano,
in recognition of their
generous and loving assistance.

Acknowledgments

I would like to thank Pasminco Australia Ltd for the opportunity they provided in allowing me to undertake this study. In particular I am thankful for the support provided by Dr. Eric Roche and Dr. Mike Newman. Thanks also to my supervisors Assoc. Prof. Bill van Bronswijk and Graham S. Walker for their enduring guidance and patience.

I am also grateful for the financial support provided by Pasminco Australia Ltd, the Australian Research Council via the APRA(I) scheme, the AJ Parker CRC for Hydrometallurgy and Curtin University of Technology.

The work could not have been completed without the laboratories and facilities supplied by CSIRO Minerals, Curtin University of Technology and the AJ Parker CRC for Hydrometallurgy.

Special thanks also to the staff at CSIRO Minerals, particularly Peter Austin, Ric Hughes, Michael Verrall and Phan Khan for assistance with SEM and particle analyses, and to Peter Choo, Milan Chovancek, and Ian Davies for assistance with XRD and elemental analyses.

I gratefully acknowledge the support provided by Peter Chapman and the Vibrational Spectroscopy Facility at Curtin University for use of Raman and FTIR spectrometers.

I thank my pressure leaching "buddies" for giving up their time to assist me, in particular Assoc. Prof. Bill van Bronswijk, Graham S. Walker, Peter Miovski and Dr. Robbie MacDonald. I also wish to acknowledge the tremendous assistance rendered by Dave Walton and Glen Whiting of Curtin University for their assistance with the design and construction of various pieces of equipment and glassware used in the experimental work.

Abstract

Studies were conducted into the mechanism and kinetics of the dissolution of synthetic zinc sulfide and zinc concentrate in aqueous solutions containing sulfur dioxide.

Experiments at ambient temperature established that the dissolution of ZnS in aqueous solutions of sulfur dioxide proceeds via acidic non-oxidative dissolution and not by direct reaction of the sulfide with $SO_2(aq)$. The non-oxidative dissolution reaction generates $H_2S(aq)$ or $HS^-(aq)$ species which are thought to rapidly react with sulfurous acid species, $SO_2(aq)$ or $HSO_3^-(aq)$, to possibly produce initially sulfane monosulfonates as intermediates, followed by sulfane disulfonates and elemental sulfur. The formation of sulfane monosulfonates is postulated based upon inhibition observed in ZnS / SO_2 leaches which is not attributable to either $H_2S(aq)$ or occlusion by elemental sulfur.

At elevated temperatures (100°C – 200°C) the rate of ZnS dissolution in sulfurous acid is affected by the thermal decomposition of sulfurous acid, which produces sulfuric acid, which leaches the mineral non-oxidatively. Increasing the temperature increases the rate of thermal decomposition of sulfurous acid and consequently, the rate of sulfuric acid formation, increasing the rate of ZnS dissolution.

The kinetics of the dissolution of ZnS in solutions of sulfuric acid and sulfur dioxide were investigated at temperatures up to 200°C. At 100°C and 150°C, the dissolution of ZnS in H_2SO_4 was found to obey the relation

$$d[Zn^{2+}]/dt = k_f A_s [H^+] - k_r A_s [H_2S(aq)]^{1/2} [Zn^{2+}]^{1/2}$$

and equilibria and rate constants for the ZnS / H_2SO_4 reaction were obtained over the range, 100°C to 200°C. The activation energies of the forward and reverse reactions were found to be 56 ± 11 kJ mol^{-1} and 45 ± 15 kJ mol^{-1}, respectively. The equilibrium constants were 4.99×10^{-4}, 1.26×10^{-3} and 2.83×10^{-3} at 100°C, 150°C and 200°C, respectively.

In the presence of added SO_2, at low ZnS pulp density (0.5 g L^{-1}), the rate of ZnS dissolution in sulfuric acid increased due to the removal of $H_2S(aq)$ by reaction with $SO_2(aq)$ or $HSO_3^-(aq)$. However the increase in rate was much less than that expected for the complete removal of $H_2S(aq)$. As with leaches of ZnS in sulfurous acid at ambient temperature, the inhibition was not attributable to the presence of residual $H_2S(aq)$ or to occlusion of unreacted ZnS by elemental sulfur, but is thought to be due to aqueous species that are like "H_2S", in that they may react with Zn^{2+} to reprecipitate ZnS. To this end, sulfane monosulfonates have again been postulated. The rate of ZnS dissolution, under conditions of low pulp density, was independent of SO_2 concentration, suggesting that under these conditions the rate of the H_2S / SO_2 reaction is also independent of the SO_2 concentration.

At higher pulp densities (200 g L^{-1}), similar to those expected in an industrial application, synthetic zinc sulfide leached rapidly in H_2SO_4 / SO_2 solutions to approximately 60% zinc extraction, but was then inhibited by the large amounts of sulfur that formed. These caused agglomerates of zinc sulfide and elemental sulfur to form, even at temperatures below the melting point of sulfur, reducing the surface area of zinc sulfide available for reaction.

Leaches of zinc concentrate at low pulp densities in H_2SO_4 / SO_2 solutions and at temperatures above sulfur's meting point, were inhibited by the formation of molten sulfur. In contrast to synthetic zinc sulfide, zinc concentrate is readily wet by molten sulfur. Three surfactants orthophenylenediamine, quebracho and sodium ligninsulfonate were found to be reasonably effective in preventing molten sulfur from occluding the mineral surface. At high pulp densities, the H_2SO_4 / SO_2 leach solution was unable to effect the extraction of zinc from a zinc concentrate beyond approximately 10%.

Integral SO_2 / H_2SO_4 leaching of zinc concentrate was found not to be a commercial prospect. However, sidestream processing of zinc concentrate in an acid leach stage followed by reaction of generated H_2S with SO_2 from the roasting stage to produce elemental sulfur may be viable.

TABLE OF CONTENTS

LIST OF FIGURES

LIST OF TABLES

NOMENCLATURE OF SULFOXY SPECIES

Species composition	IUPAC name	Common name
SO_3^{2-}	sulfite	sulfite
HSO_3^-	hydrogen sulfite	bisulfite
SO_4^{2-}	sulfate	sulfate
HSO_4^-	hydrogen sulfate	bisulfate
$S_2O_3^{2-}$	thiosulfate	thiosulfate
$H_2S_2O_3^{2-}$	sulfane monosulfonic acid	thiosulfuric acid
$S_2O_4^{2-}$	dithionite	dithionite
$S_2O_5^{2-}$	disulfite	metabisulfite
$S_2O_6^{2-}$	dithionate	dithionate
$S_2O_7^{2-}$	disulfate	disulfate
$S_2O_8^{2-}$	peroxodisulfate	peroxodisulfate
$S_nO_3^{2-}$	sulfane monosulfonates	-
$S_3O_3^{2-}$, $n\geq3$	sulfane monosulfonates	-
$S_4O_3^{2-}$	disulfane monosulfonate	-
$S_5O_3^{2-}$	trisulfane monosulfonate	-
$S_6O_3^{2-}$	tetrasulfane monosulfonate	-
$H_2S_nO_3^{2-}$	sulfane monosulfonic acids	-
$S_nO_6^{2-}$, $n\geq3$	sulfane disulfonates	polythionates
$S_3O_6^{2-}$	sulfane disulfonate	trithionate
$S_4O_6^{2-}$	disulfane disulfonate	tetrathionate
$S_5O_6^{2-}$	trisulfane disulfonate	pentathionate
$S_6O_6^{2-}$	tetrasulfane disulfonate	hexathionate
$H_2S_nO_6^{2-}$, $n\geq3$	sulfane disulfonic acids	polythionic acids

1 INTRODUCTION

Most of the world's zinc sulfide hydrometallurgical processing plants use the roast-leach-electrowin (RLE) process to extract the metal from the ore. This process entails three main steps, roasting, leaching and electrowinning. The roasting step involves heating the zinc sulfide concentrate in air to remove the sulfur as sulfur dioxide gas and render the zinc as zinc oxide. The zinc oxide, or calcine, is then leached in sulfuric acid to produce a solution of zinc sulfate. In the final electrowinning stage, the zinc sulfate solution is transferred to electrolytic cells where zinc metal is electrochemically deposited onto cathodes.

The considerable quantity of sulfur dioxide gas produced in the roasting stage cannot be vented to the atmosphere, for environmental reasons, and is generally converted to sulfuric acid on site. Herein lies the cause of a significant commercial problem faced by the industry, namely that storage of sulfuric acid on site is limited and the worldwide market for this acid is oversupplied. In order to counter this problem, this study sought to investigate the possibility of utilising the sulfur dioxide gas produced in the roasting stage as a leachant for zinc sulfide. Incorporation of a successful zinc sulfide – sulfur dioxide leach stage in a conventional RLE process might enable all sulfide to be converted to elemental sulfur. This would be an attractive outcome as it would reduce the sulfuric acid storage problems and produce a more saleable product, sulfur.

1.1 THE PRESENT SITUATION FOR ZINC PRODUCTION

Zinc occurs predominantly as zinc blende, ZnS, also known as sphalerite, and Australia has 9.5% of the world's zinc reserves (Habashi 1997a).

Both pyrometallurgical and hydrometallurgical techniques are currently employed to extract zinc metal from zinc ores. There is one commonly used pyrometallurgical process and a number of hydrometallurgical processes. Hydrometallurgical routes in commercial operation include the "Roast-Leach–Electrowin" process, oxidative pressure leaching and ferric leaching.

1.1.1 Pyrometallurgy

The oldest method of refining zinc is to roast the ore in air, producing zinc oxide (calcine), and then to reduce the zinc oxide to zinc metal using carbon.

$$ZnS + O_2 \rightarrow ZnO + SO_2 \quad (1.1)$$

$$ZnO + C \rightarrow Zn + CO \quad \Delta H = 353\ kJ \quad (1.2)$$

The reaction temperature of the carbon reduction step is in the range 1100°C to 1300°C and zinc produced is in the gaseous state (bp 920°C). It is then condensed to the liquid state and cast into ingots.

Production using this method began in the early 1800s. Various methods have been used over the years, each improving over the other, to obtain the highest yields using the above reactions. The most common and efficient pyrometallurgical process now in use since 1960 is the Imperial Smelting Shaft Furnace process.

The main advantage of pyrometallurgy is its ability to treat ores of complex composition. A disadvantage is that the zinc produced needs to be further refined by distillation, since it typically contains Pb (0.7-3%), Fe (< 0.2%) and Cd (<0.3%) (Habashi 1997b).

An additional problem is that the process produces sulfur dioxide (Eqn. 1.1), which needs to be converted to sulfuric acid and sold. As with other sulfur dioxide

producing processes, zinc production is tied to the market for sulfuric acid, since, due to storage difficulties, the acid must be sold as produced. If there is little demand for sulfuric acid, then the zinc production must be reduced.

1.1.2 Roast-Leach-Electrowin

Prior to the early part of this century the only commercial methods used to produce zinc from zinc ores were pyrometallurgical (Veltman and Bolton 1980). Research then led to the development of the electrolytic process, so called because zinc metal is electrowon from zinc sulphate solutions. This is a mainly hydrometallurgical process and as such a radical departure from the traditional pyrometallurgical techniques. The first commercial plants using the electrolytic process began operating in 1916 (Veltman and Bolton 1980).

The advantages of the electrolytic process over older pyrometallurgical retort processes are many. Some of which are that it is less labor intensive (Veltman and Bolton 1980) and that hydrometallurgically produced zinc does not need to be refined, whereas pyrometallurgically produced zinc has impurities and thus requires purification by distillation. By 1997 approximately 80% of the world's metallic zinc was produced by the electrolytic process (Habashi 1997c). This process is also known as the roast-leach-electrowin process and involves the following three stages:

1. Roasting (heating) the ore in air to produce zinc oxide.

$$ZnS + O_2 \rightarrow ZnO + SO_2 \qquad (1.3)$$

2. Leaching the zinc oxide in sulfuric acid to produce a zinc sulfate solution.

$$ZnO + H_2SO_4 \rightarrow ZnSO_4 + H_2O \qquad (1.4)$$

3. Electrowinning the zinc metal from the zinc sulphate solution.

$$ZnSO_4 + H_2O \rightarrow Zn(s) + H_2SO_4 + \tfrac{1}{2}\,O_2(g) \qquad (1.5)$$

One of the disadvantages of this process is again the production of sulfur dioxide gas

in the roasting stage. For environmental and, to a lesser degree, economic reasons the sulfur dioxide cannot be vented to atmosphere but must be recovered. The most common method of sulfur dioxide recovery is conversion to sulfuric acid (Adams and Matthew 1981). Hence, this again does not solve the sulfur dioxide problem completely as RLE companies still have to reduce zinc production so that sulfuric acid production does not exceed storage capacity.

Another disadvantage is that roasting produces zinc ferrite ($ZnFe_2O_4$) which is not amenable to leaching during the "neutral" leach stage of a conventional electrolytic zinc process (Adams and Matthew 1981), but requires separate treatment using higher acid concentrations ($[H_2SO_4] = 50 - 150$ g L^{-1}) (Habashi 1997c).

1.1.3 Pressure leaching

Research into leaching of zinc sulfide in sulfuric acid under oxygen pressure at elevated temperatures began in the 1950's (Bjorling 1954; Forward and Veltman 1959) and commercial production began in 1981 (Masters, Doyle and Weir 1989).

Acidic oxidative pressure leaching is one of the few commercial zinc concentrate processes that produces elemental sulfur. In this process the zinc concentrate is leached directly (i.e. no prior roasting step) in sulfuric acid solution at around 140 - 150°C with 700 kPa oxygen partial pressure (Berezowsky et al. 1991; Chalkley, Collins and Ozberk 1993). An important aspect of this process is the conversion of the sulfide sulfur in zinc sulfide to elemental sulfur. The overall equation is (Veltman and Bolton 1980):

$$ZnS + H_2SO_4 + \tfrac{1}{2}O_2 \rightarrow ZnSO_4 + H_2O + S^o \qquad (1.6)$$

being the sum of the reactions:

$$ZnS + Fe_2(SO_4)_3 \rightarrow ZnSO_4 + 2FeSO_4 + S^o \qquad (1.7)$$

$$2FeSO_4 + H_2SO_4 + \tfrac{1}{2}O_2 \rightarrow Fe_2(SO_4)_3 + H_2O \qquad (1.8)$$

The reaction requires the presence of dissolved iron, but the addition of iron is not generally required as it is already present in most zinc concentrates. The dissolution

of ZnS is accomplished by ferric ions (Peters 1993), themselves being reduced to ferrous ions (Eqn. 1.7). The ferrous ions are subsequently re-oxidised to ferric by oxygen (Eqn. 1.8).

In the absence of iron the addition of oxygen to an acidic leach of ZnS has only a marginal effect on the extent of dissolution. Tronev and Bondin (1939) studied the dissolution of ZnS in neutral, acidic and basic solutions under high pressures of air (up to 85 atm, 8600 kPa). In 0.1 N (0.05 M) H_2SO_4 at 100°C increasing the air pressure from 1 to 85 atm (101 - 8600 kPa) increased the zinc extracted from a low 0.069g L^{-1} to only 0.104 g L^{-1}. Bjorling (1954) studied the leaching of ZnS in H_2SO_4 under O_2 pressure and reported the formation of $ZnSO_4$ and elemental sulfur. However, the rate of the reaction was very slow in comparison to the same reaction with FeS. In contrast Forward and Veltman (1959) when leaching zinc concentrates, found that 99 % zinc extraction was possible in 2 – 4 hours when using 100 g L^{-1} H_2SO_4, 20 psi (~140 kPa) O_2 and a temperature of 110°C. Attempts to increase the reaction rate by increasing the temperature above the melting point of sulfur (119°C) were unsuccessful, giving only 65 – 72 % zinc extraction, since although the reaction initially proceeded rapidly, occlusion of unreacted mineral by molten sulfur soon occurred, preventing further leaching.

The favourable leaching results obtained by Forward and Veltman in their initial study fostered considerable further research into the system. A major advance was made when suitable surfactants were identified for keeping molten elemental sulfur from adhering to the mineral (Kawulka, Haffenden and Mackiw 1975). This allowed temperatures in excess of the melting point of sulphur (119°C) to be used. In practice leaches are undertaken at 140 – 150°C (Chalkley, Collins and Ozberk 1993). Increasing the temperature above 150°C has little advantage as, although the viscosity of molten sulphur has its minimum at 153°C, it increases rapidly beyond that temperature (Veltman and Bolton 1980). In addition, above about 150°C, elemental sulfur begins to oxidise forming sulfuric acid (Kawulka, Haffenden and Mackiw 1975).

1.1.4 Ferric leaching

Ferric ions in either chloride or sulfate media can be used to leach zinc sulfide to yield zinc ions and elemental sulfur (Scott and Nicol 1978). There is little difference in the chloride and sulfate systems (Dutrizac 1992; Palencia Perez and Dutrizac 1991) as the active reagent in each is the ferric ion. The overall stoichiometry is:

$$ZnS + 2Fe^{3+} \rightarrow Zn^{2+} + 2Fe^{2+} + S^{o} \qquad (1.9)$$

The mechanism has been considered to have both non-oxidative and oxidative reactions occurring depending on the nature of the sphalerite (Scott and Nicol 1978). The non-oxidative mechanism involves acidic dissolution of ZnS followed by ferric oxidation of hydrogen sulfide to elemental sulfur.

$$ZnS + 2H^{+} \leftrightarrow Zn^{2+} + H_2S \qquad (1.10)$$

$$H_2S + 2Fe^{3+} \rightarrow S^{o} + 2Fe^{2+} + 2H^{+} \qquad (1.11)$$

The oxidative process being

$$ZnS + 2Fe^{3+} \rightarrow Zn^{2+} + 2Fe^{2+} + S^{o} \qquad (1.12)$$

Sphalerites containing low levels of impurities (< 0.4% total) leach non-oxidatively in ferric sulfate – sulfuric acid solutions. However, when impurities having electrical conductivity are present, such as iron, lead and copper ions, oxidative dissolution occurs in competition with the non-oxidative mechanism (Scott and Nicol 1978).

Many studies indicate that the mechanism of the dissolution of zinc concentrates is oxidative (electrochemical), the rate being controlled by charge transfer between ZnS and ferric ions (Crundwell 1987; Palencia Perez and Dutrizac 1991; Warren, Henein and Jin 1985). Sphalerites with higher iron contents leach at faster rates than those with lower iron contents, the rate of reaction being a linear function of the concentration of iron in the zinc sulfide lattice, and the activation energy decreases as

the iron content of the sphalerite increases (Palencia Perez and Dutrizac 1991). The reaction order with respect to Fe^{3+} is 0.5 at low concentrations of Fe^{3+} (Crundwell 1987; Jin, Warren and Henein 1984; Warren, Henein and Jin 1985) but is zero at high concentrations ($[Fe^{3+}] > \sim 0.8$ M) (Jin, Warren and Henein 1984; Warren, Henein and Jin 1985). This is because iron-containing sphalerite is an n-type semiconductor and being an n-type semiconductor its dissolution rate is limited by the rate of diffusion of holes to the solid – solution interface. Hence, when the saturation current is reached with a given concentration of ferric ions any further increase in the concentration of ferric ions does not increase the dissolution rate (Crundwell 1988).

Using ferric chloride – hydrochloric acid solutions, Dutrizac and MacDonald (1978) observed that the accumulation of ferrous ions severely impeded the dissolution rate, whereas the presence of dissolved zinc chloride only slightly impeded it. In addition the dissolution appeared to be dominated by ferric leaching at low HCl concentrations (<1 mol L^{-1}), but by non-oxidative acidic leaching at higher concentrations (>2-3 mol L^{-1}). They also found that, of the sulfide present in ZnS, approximately 95% is converted to elemental sulfur, the remaining 5% being converted to sulfate.

The leaching kinetics of the two systems, $Fe_2(SO_4)_3$–H_2SO_4 and $FeCl_3$–HCl, are similar (Palencia Perez and Dutrizac 1991). The reaction is generally considered to be chemically controlled (Crundwell 1987; Jin, Warren and Henein 1993; Jin, Warren and Henein 1984), but becomes diffusion controlled as elemental sulfur passivates the mineral surface (Bobeck and Su 1985; Lochmann and Pedlik 1995). Ligninsulfonate has been successfully used to prevent passivation of the surface by elemental sulphur at 80°C (Lochmann and Pedlik 1995).

The commercial application of the ferric leach to zinc concentrates is only recent, with Korea Zinc commencing production in 1994 and Outokumpu Zinc Oy commencing in 1998. Both companies have integrated the atmospheric ferric leach process with their existing roast–leach–electrowin operations (Buban et al. 2000; Takala 1999). In the Outokumpu process, zinc concentrate is leached in the presence of ferric ions, oxygen and jarosite nuclei in 10-40 g L^{-1} sulfuric acid at a temperature

in the range 80°C to the solution boiling point. The presence of jarosite nuclei ensure that, while the concentrate is being leached, iron is simultaneously precipitated as jarosite (Fugleberg and Järvinen 1998).

1.1.5 Non-commercialised approaches

A number of other approaches to the oxidative dissolution of ZnS have been studied. These include bacterial leaching, peroxide leaching, chlorine leaching, caustic leaching and ammoniacal leaching.

Bacterial leaching

Bacterial leaching of ZnS was first studied in 1922 (Dutrizac and MacDonald 1974). Leaching of ZnS using Thiobacillus ferrooxidans produces zinc ions in solution and the sulfide sulfur is oxidised to elemental sulfur. The mechanism of this reaction is being debated in the literature, especially as to whether the bacteria directly or indirectly oxidise the mineral. For the direct mechanism the reaction is given as

$$ZnS + 2H^+ + \tfrac{1}{2}O_2 \xrightarrow{bacteria} Zn^{2+} + S^o + H_2O \qquad (1.13)$$

In the indirect mechanism the mineral is oxidised by ferric ions. Bacteria are indirectly involved, in that they oxidise ferrous ions already present in the system to ferric ions (Driessens, Fowler and Crundwell 1999).

$$ZnS + 2Fe^{3+} \rightarrow Zn^{2+} + S^o + 2Fe^{3+} \qquad (1.14)$$

$$4Fe^{2+} + 4H^+ + O_2 \xrightarrow{bacteria} 4Fe^{3+} + 2H_2O \qquad (1.15)$$

Recently, however, there appears to be agreement that the indirect mechanism is the mechanism that actually occurs (Driessens, Fowler and Crundwell 1999; Hansford and Vargas 1999; Sand et al. 1999; Tributsch 1999). Under similar conditions, the bacterial and chemical leach rates are initially equivalent, however at longer reaction times the bacterial leach rate increases with respect to the chemical rate. This is

considered to be due to bacteria oxidising elemental sulfur to sulfate, thus preventing elemental sulfur from passivating the mineral surface (Driessens, Fowler and Crundwell 1999).

Despite the recent strong interest in the bacterial leaching of sulfide minerals and the mechanisms involved, its commercial application is presently limited to the extraction of only gold, copper and cobalt from sulfidic ores (Brierley and Brierley 2001).

Chlorine / hydrochloric acid leaching

Chlorine has also been used to leach sphalerite at temperatures between 30 and 60°C at pH 2, producing zinc ions, sulfate and elemental sulfur. Increasing the HCl concentration from 0 to 2.5 mol L^{-1} increased the percentage of sulfide sulfur converted to elemental sulfur from 50 to 75% (Lotens and Wesker 1987).

The commercialisation of this process would be inhibited by difficulties associated with electrowinning zinc from chloride solutions and handling corrosive chlorine / hydrochloric acid solutions (Roche 1993).

Peroxide / hydrochloric acid leaching

Aqueous solutions of hydrogen peroxide (3 mol L^{-1}) and hydrochloric acid (6 mol L^{-1}) have been successfully employed to extract up to 97% Zn from a zinc–lead concentrate (slurry = 40% solids) at a temperature of 95°C (Vazarlis 1987). The reaction is given as

$$ZnS + H_2O_2 + 2HCl \rightarrow ZnCl_2 + S^o + 2H_2O \qquad (1.16)$$

Approximately 92.5% of the sulfide sulfur reported as elemental sulfur with the remainder being sulfate. Increasing the concentration of H_2O_2 decreased the yield of sulfur and increased the yield of sulfate. In another study 4% peroxide solutions at 20°C were able to extract 65-100% of the zinc from mechanically activated sphalerite within 2 hours, and convert 40% of the sulfur to elemental sulfur (Balaz and Ebert 1991).

This process has not been commercialised probably because of the high cost of peroxide in addition to difficulties previously mentioned for the chlorine / hydrochloric acid process (Roche 1993).

Sodium hydroxide leaching

Synthetic ZnS readily dissolves in 4 mol L^{-1} NaOH at 150°C, the sulfide sulfur being oxidised to sulfate and zinc being present in solution as the zincate ion. Elemental sulfur is not produced in this system (Tronev and Bondin 1939). Problems associated with the commercialisation of this method include the high cost of sodium hydroxide and the production of sulfate and its subsequent removal and disposal (Roche 1993).

Ammoniacal leaching

Zinc concentrate has been successfully leached using ammoniacal solutions in the presence of excess oxygen (Bjorling 1954; Stanczyk and Rampacek 1960). The zinc sulfide is oxidised to zinc oxide, which is dissolved by ammonia yielding a zinc-ammonia complex. The reactions are considered to be:

$$2ZnS + 3O_2 \rightarrow 2ZnO + 2SO_2 \quad (1.17)$$

$$SO_2 + 2NH_4OH \rightarrow (NH_4)_2SO_3 + H_2O \quad (1.18)$$

$$2(NH_4)_2SO_3 + O_2 \rightarrow 2(NH_4)_2SO_4 \quad (1.19)$$

$$ZnO + (NH_4)_2SO_4 + 2NH_3 \rightarrow Zn(NH_3)_4SO_4 + H_2O \quad (1.20)$$

Extractions of up to 98% Zn were obtained when leaching a 5% pulp for one hour at 200°C (Stanczyk and Rampacek 1960). An advantage of this process is that the iron is precipitated as ferric hydroxide, which is another reason for working under an overpressure of oxygen to ensure any ferrous is converted to ferric. Again, however, high reagent costs and the production of sulfate and its subsequent removal and disposal are obstacles to its commercialisation (Roche 1993).

1.2 POSSIBLE SOLUTIONS FOR RLE PLANTS

The generation and utilisation of sulfur dioxide is a major problem for Roast-Leach-Electrowin (RLE) plants. A preferred option is to have elemental sulfur as a by-product instead of sulfuric acid. Elemental sulfur is preferred because:

- Elemental sulfur is easier and cheaper to stockpile and transport.
- Elemental sulfur is a more saleable product.
- Production of elemental sulfur avoids the need for a sulfuric acid plant
- Production of elemental sulfur eliminates the dependency of zinc production on sulfuric acid sale / disposal.

Production of elemental sulfur instead of sulfuric acid from sulfur dioxide gas can be achieved in a number of ways. Four potential strategies are given below.

1. Conversion of sulfur dioxide generated in the roasting stage to elemental sulfur using a sulfur recovery unit. Sulfur recovery units are being developed to convert SO_2 gas (dry) or SO_2 absorbed in a liquid solution (wet) into elemental sulfur. Dry units produce elemental sulfur by the reaction of SO_2 gas with a reducing gas, such as methane, in the presence of a catalyst (Kwong and Meissner 1995). Wet units involve absorption of the SO_2 gas into a buffered aqueous solution followed typically by reaction with aqueous H_2S (Pay et al. 1994) to produce elemental sulfur. Another option is to use bacteria instead of H_2S to convert sulfur dioxide to elemental sulfur (Kwong and Meissner 1995).

2. Shutting down the RLE plant altogether and building an acidic oxidative pressure leaching plant. However, this is an enormous change and costly, and hence unlikely. The preferable option is to retrofit a new process onto the existing plant.

3. Incorporation of a ferric leaching stage to the existing RLE process. The ferric leaching stage directly leaches zinc concentrate, yielding zinc sulfate solution and elemental sulfur. This reduces the amount of zinc concentrate requiring roasting and so reduces the amount of SO_2 generated and the amount of sulfuric acid produced. This is a feasible option as demonstrated by its successful

implementation at the Korea Zinc (Onsan) and Outokumpu (Kokkola) plants (Buban et al. 2000; Takala 1999).

4. Leaching of ZnS with aqueous solutions of SO_2, using SO_2 generated from the roasting stage of an RLE plant. The idea of incorporating an SO_2 leach circuit into the roast-leach-electrowin zinc flowsheet has been suggested by Linkson (1985). ZnS and aqueous solutions of SO_2, with or without added sulfuric acid, react to give zinc ions in solution and, under certain conditions, elemental sulfur (Adams and Matthew 1981; Foerster and Janitzki 1931; Henderson and Weiser 1913; Larsen 1984; Larsen and Linkson 1993; Linkson and Larsen 1984; Makovetskii 1934; Sobol and Frash 1974; Thom 1977; Thom, Waters and Hadermann 1978b; Wohler, Martin and Schmidt 1923). Although, at ambient temperatures, the degree of zinc extraction is not sufficient for commercial viability, the use of higher temperatures, similar to those used in pressure leach plants, may increase the degree of zinc extraction.

The last option is attractive as it has the potential to solve the two problems:

- The need to remove roaster generated SO_2 without making H_2SO_4, as the SO_2 would be converted to elemental sulfur rather than H_2SO_4.
- The need to convert sulfide sulfur to elemental sulfur. This is a process whereby, potentially, zinc concentrate can be treated without generating SO_2.

In addition, there may be no need to build a new plant, as it may be possible to retrofit an existing RLE plant, running the roast-leach–electrowin process and an SO_2 leach process in parallel.

Hence, this work, in the first instance, investigated the direct leaching of sphalerite by aqueous sulfur dioxide.

2 SULFUR DIOXIDE LEACHING OF SULFIDES

2.1 SULFUR DIOXIDE LEACHING APPROACHES

Three approaches have been reported for leaching sulfides with sulfur dioxide. These are:

- Leaching in aqueous solutions containing only sulfur dioxide
- Leaching with aqueous sulfur dioxide solutions containing additional reagents, such as sulfuric acid, hydrochloric acid, ferric ions, cupric ions and oxygen
- Non-aqueous SO_2 leaching

2.1.1 *Leaching in aqueous solutions containing only sulfur dioxide*

The first reported investigation into the use of sulfur dioxide as a lixiviant for a metal occurred in 1833, and by 1913 it was well known that FeS, ZnS and MnS were readily soluble in a concentrated aqueous solution of sulfur dioxide (Henderson and Weiser 1913). The relative reactivities of some common sulfide ores toward aqueous SO_2 solutions have been reported by Thom, Waters and Hadermann (1978a). They report that pyrrhotite (FeS) and galena (PbS) are more readily leached than sphalerite (ZnS) and chalcopyrite ($CuFeS_2$), which are relatively unreactive, and that pyrite (FeS_2) and chalcocite (Cu_2S) exhibit very little reaction.

The aqueous sulfur dioxide / metal sulfide reaction yields metal ions in solution with a complex mixture of oxysulfur compounds and elemental sulfur. Thiosulfate, polythionates, sulfate, and elemental sulfur have all been observed. The ability of bisulfite to react with the reaction products and the interconversion between polythionates ensures a varied product mixture whose composition is dependent on

the reaction time and the relative amounts of metal sulfide and sulfurous acid.

The relative proportions of sulfur species also vary with different metal sulfides. For example, the reaction with ZnS yields tetrathionate as the major product with lesser amounts of sulfate, thiosulfate, trithionate, pentathionate and elemental sulfur, whereas FeS and MnS yield thiosulfate as the major product. Elemental sulfur, thiosulfate (Brual, Byerley and Rempel 1983; Kunda and Rudyk 1970), trithionate (Brual, Byerley and Rempel 1983; Foerster and Janitzki 1931; Kunda and Rudyk 1970), tetrathionate (Brual, Byerley and Rempel 1983; Foerster and Janitzki 1931) and in some cases pentathionate are also observed in the reaction with FeS, whereas in the reaction with MnS thiosulfate is by far the dominant product with some elemental sulfur and trithionate also being present (Foerster and Janitzki 1931).

Most research has focussed on the mechanism of the dissolution reactions and two reaction mechanisms have been advocated. The first proposes that dissolution is non-oxidative and occurs via acid attack on the metal sulfide generating H_2S which subsequently reacts with SO_2, setting up a chain of reactions yielding the aforementioned complex mixture of oxysulfur species and elemental sulfur. This mechanism has been proposed for the dissolution of the ZnS (Henderson and Weiser 1913) and FeS (Brual, Byerley and Rempel 1983; Kunda and Rudyk 1970). The second mechanism proposes that dissolution is oxidative and occurs via reaction with aquated sulfur dioxide (Brual, Byerley and Rempel 1983; Larsen 1984; Thom, Waters and Hadermann 1978b).

Both oxidative and non-oxidative mechanisms are considered to occur concurrently in the FeS – SO_2 system. Brual, Byerley and Rempel (1983) studied the kinetics and mechanism of dissolution of FeS in aqueous sulfur dioxide solutions with and without added perchloric acid. The acidic dissolution (non-oxidative) mechanism dominates when there is a high concentration of hydrogen ions relative to sulfur dioxide (Eqns. 2.1-2.2) and elemental sulfur is eventually produced by reaction of SO_2 with generated H_2S (Eqn. 2.3b).

$$FeS + H^+ \rightarrow FeSH^+ \quad (2.1)$$

$$FeSH^+ \rightarrow Fe^{2+} + HS^- \quad (2.2)$$

$$HS^- + H^+ \rightarrow H_2S \quad (2.3a)$$

$$H_2S + SO_2 \rightarrow S^o + SO_4^{2-} + H_2S_xO_6 \quad (x \geq 3) \quad (2.3b)$$

The aquated SO_2 dissolution (oxidative) mechanism dominates when the concentration of $SO_2(aq)$ is high relative to the hydrogen ion concentration. Dissolution is postulated to proceed via adsorption of aquated SO_2 onto the FeS surface followed by release of a proton, leaving HSO_3^- adsorbed on FeS. Reaction between these species occurs at the surface releasing Fe^{2+}, HS^- and SO_3^{2-} (Eqns. 2.4-2.6).

$$FeS + SO_2.H_2O \rightarrow FeS\ SO_2\ H_2O \quad (2.4)$$

$$FeS\ SO_2\ H_2O \rightarrow FeS.HSO_3^- + H^+ \quad (2.5)$$

$$FeS.HSO_3^- \rightarrow Fe^{2+} + HS^- + SO_3^{2-} \quad (2.6)$$

H_2S subsequently reacts with SO_2 via the Wackenroder reaction to produce elemental sulfur (Eqn. 2.3b).

Another aquated SO_2 dissolution mechanism has been proposed by Thom, Waters and Hadermann (1978a; 1978b) for the dissolution of FeS, PbS, ZnS, $CuFeS_2$, FeS_2 and Cu_2S in sulfurous acid. They consider the reaction between aqueous SO_2 and the metal sulfide to be similar to the aqueous phase reaction of SO_2 and H_2S, which is a complex reaction that proceeds via many steps and involves the generation and interconversion of numerous oxysulfur intermediates. The reaction is addressed in more detail in Section 2.2.2.3. With regard to FeS they propose the following mechanism.

$$FeS + SO_2(aq) \leftrightarrow FeS{\cdot}SO_2(ads) \rightarrow Fe^{2+} + S_2O_2^{2-} \quad (2.7)$$

$$S_2O_2^{2-} + 2H^+ \leftrightarrow H_2S_2O_2 \quad (2.8)$$

$$H_2S_2O_2 + HSO_3^- \leftrightarrow H_2S_2O_3 + HSO_2^- \quad (2.9)$$

$$H_2S_2O_3 + HSO_2^- \leftrightarrow HO_3SS\text{-}SOH + OH^- \quad (2.10)$$

$$HO_3SS\text{-}SOH + HSO_3^- \leftrightarrow HO_3SSS\text{-}SO_3H + OH^- \quad (2.11)$$

Thiosulfate is considered one of the main oxysulfur intermediates, and the production of elemental sulfur is proposed to occur via acidic decomposition of thiosulfate.

$$8S_2O_3^{2-} + 8H^+ \rightarrow S_8 + 8HSO_3^- \quad (2.12)$$

In contrast, Larsen (1984) observed tetrathionate as the major intermediate, with the eventual formation of sulfur after 14 hours, and proposed the reaction,

$$ZnS + 3SO_2 \rightarrow Zn^{2+} + S_4O_6^{2-} \quad (2.13)$$

The observation of tetrathionate is in accord with thermodynamic studies. E_h - pH diagrams of the Zn – S – SO_2 – H_2O system indicate that tetrathionate ($S_4O_6^{2-}$) is a metastable intermediate species (Larsen 1984). The dissolution reaction was considered to be composed of the following electrochemical reactions:

$$\text{Anodic:} \quad 2ZnS + 3H_2O \rightarrow 2Zn^{2+} + \tfrac{1}{2} S_4O_6^{2-} + 6H^+ + 9e^- \quad (2.14)$$

$$\text{Cathodic:} \quad 6SO_2 + 6H^+ + 9e^- \rightarrow \tfrac{1}{2} S_4O_6^{2-} + 3H_2O \quad (2.15)$$

This reaction has $\Delta G^o_{rxn,298K}$ = -84.1 kJ mol^{-1} (Larsen 1984) and thus is thermodynamically favourable, but no mechanism for this process was put forward. Elemental sulfur, observed after prolonged leaching, is postulated to occur via decomposition of tetrathionate (Eqn. 2.16),

$$2S_4O_6^{2-} + 4H^+ \rightarrow 3S^o + 2H_2O + 5SO_2 \quad (2.16)$$

the overall reaction being

$$ZnS + \tfrac{1}{2} SO_2 + 2H^+ \rightarrow Zn^{2+} + \tfrac{3}{2} S^o + H_2O \quad (2.17)$$

Since a number of mechanisms of the ZnS – SO_2 reaction have been proposed, but not resolved, this question needs to be addressed.

Only a handful of studies has been conducted on the reaction between metal sulfides and sulfur dioxide solutions at elevated temperatures (Kunda and Rudyk 1970; Sobol and Frash 1974; Sobol and Timoshenko 1992; Timoshenko et al. 1991). Sobol and Frash (1974) examined the ability of aqueous solutions of sulfur dioxide at 100 - 110°C to leach a number of sulfides and sulfidic concentrates, namely, FeS, Fe_7S_8, FeS_2, NiS, Ni_3S_2, MoS_2, $CuFeS_2$, $NiFeS_2$, zinc concentrate and pentlandite concentrate. They found that only FeS (pyrrhotite) and Fe_7S_8 (troilite) could be leached successfully. The extractions for metals from the other minerals varied from 33% for nickel in Ni_3S_2 to only 0.5% for zinc from zinc concentrate. All of the other reported research into SO_2 leaching at elevated temperatures is focussed on pyrrhotite, probably because of its ease of dissolution.

The reaction between pyrrhotite (FeS) and aqueous solutions of sulfur dioxide has been studied at temperatures up to 130°C (Kunda and Rudyk 1970; Sobol and Frash 1974; Sobol and Timoshenko 1992; Timoshenko et al. 1991). The products are ferrous sulfate and elemental sulfur.

$$FeS + 2SO_2 \rightarrow FeSO_4 + 2S^o \qquad (2.18)$$

At temperatures above the melting point of sulfur (119°C), iron extraction is diminished due to molten sulfur coating the mineral (Kunda and Rudyk 1970). Sulfur is also produced by the disproportionation of sulfur dioxide to sulfate and elemental sulfur.

$$3SO_2 + 2H_2O \rightarrow 2H_2SO_4 + S^o \qquad (2.19)$$

Dissolution occurs via reaction of FeS with hydrogen ions, generating H_2S.

$$FeS + 2H^+ \rightarrow Fe^{2+} + H_2S \qquad (2.20)$$

SO_2 reacts with H_2S removing it from solution to form elemental sulfur. No reason has been given as to why aqueous sulfur dioxide solutions are able to leach FeS and Fe_7S_8, but are unable to leach zinc sulfide. If dissolution of the iron sulfides occurs

via acidic dissolution (Eqn. 2.20), then it is reasonable to expect that zinc sulfide, which is also amenable to dissolution by acidic solutions, should also be leachable. The fact that it is not raises the question of 'why not?', which also needs to be addressed.

2.1.2 Leaching with aqueous sulfur dioxide solutions containing additional reagents

Sulfur dioxide has also been used in combination with other leaching agents, usually acids and oxidants. In these systems leaching is generally accomplished by the acid or oxidant, and sulfur dioxide is present to remove undesirable products or to assist in re-oxidising reduced oxidants.

Sulfur dioxide solutions containing added hydrochloric acid and sodium chloride have been successfully used to leach lead sulfide at 90°C. Both naturally occurring pure lead sulfide (galena) and a lead sulfide concentrate (27% Pb, 7% Zn) were amenable to the leach solution. The mechanism for lead sulfide extraction involves non-oxidative dissolution of the sulfide followed by SO_2 oxidation of the aqueous hydrogen sulfide to elemental sulfur. The rate is first order with respect to hydrogen ions and chloride ions when the total chloride ion concentration is less than 2 mol L^{-1}. Above 2 mol L^{-1} total chloride, the rate increases considerably, probably because of chloride ions complexing lead at the lead sulfide surface (Han 1985).

Whereas galena is readily leached, sphalerite and chalcopyrite were less amenable to the leach solution. Using a hydrochloric acid (1 mol L^{-1}) solution at 90°C, with added NaCl (3.4 mol L^{-1}) and saturated with SO_2, galena (-52+25 μm) was 100% leached after 30 minutes. In contrast, sphalerite (-90+75 μm) was ~40% leached after 30 minutes and ~71% leached after 2 hours. Chalcopyrite (-106+75 μm) was the most refractory to the leach solution, being only 3% leached after 2 hours. It is also of interest to note that whereas zinc is satisfactorily leached from pure sphalerite (71% after 2 hours) it is not so readily leached from a concentrate (3% after 2 hours) (Han 1985).

Although sulfur dioxide solutions acidified with HCl are not very reactive toward chalcopyrite at temperatures below 150°C (Han 1985; Meyers, Hamersma and Kraft 1975), increasing the temperature to 180°C increases the extraction dramatically (Meyers, Hamersma and Kraft 1975). Using a SO_2 (0.86 mol L^{-1}) / HCl (3.6 mol L^{-1}) solution at 180°C, extractions of 99.7% and 96.6% for copper and iron, respectively, were attained when a chalcopyrite concentrate (8 g L^{-1}) was leached for only 30 minutes. In addition, complete conversion of the sulfide sulfur to elemental sulfur was achieved. The stoichiometry for the reaction is

$$4CuFeS_2 + 3SO_2 + 12HCl \rightarrow 4CuCl_2 + 4FeCl_2 + 11S^o + 6H_2O \quad (2.21)$$

Sulfur dioxide solutions acidified with sulfuric acid have also been examined for their reactivity toward metal sulfides (Adams and Matthew 1981; Larsen 1984; Sobol and Frash 1974; Tiwari 1977). Thermodynamically, the dissolution of the iron, nickel and zinc sulfides in sulfurous acid, with and without added sulfuric acid, is favourable at 110°C. The ZnS dissolution reaction (Eqn. 2.22) has ΔG (25°C) = -73.2 kJ mol^{-1} and ΔG (110°C) = -68.1 kJ mol^{-1} (Sobol and Frash 1974).

$$ZnS + H_2SO_4 + \tfrac{1}{2} SO_2(aq) \rightarrow ZnSO_4 + \tfrac{3}{2} S^o + H_2O \quad (2.22)$$

Furthermore, E_h-pH diagrams for the Zn-S-SO_2-H_2O system (Larsen 1984) indicate that dissolution of ZnS is thermodynamically possible up to at least 200°C, producing zinc ions and elemental sulfur (Figure 2.1). The diagrams indicate that ZnS may dissolve, generating zinc ions, either via non-oxidative dissolution of the sulfide or via direct oxidation of the sulfide by SO_2. Non-oxidative dissolution would yield aqueous H_2S(aq) which would then be oxidised to sulfur by the SO_2(aq) present in solution. Direct oxidation of ZnS by SO_2 would yield elemental sulfur, with the sulfide sulfur being oxidised to elemental sulfur or tetrathionate and the sulfur in SO_2 being reduced to elemental sulfur or tetrathionate.

However, of the common iron, nickel, copper and zinc sulfides, only pyrrhotite (Kunda and Rudyk 1970; Sobol and Frash 1974) and troilite (Sobol and Frash 1974)

have been successfully leached by solutions of sulfur dioxide and sulfuric acid. When a zinc sulfide concentrate was leached at 105-110°C in sulfuric acid in the presence of SO_2, only 0.5 % zinc extraction was achieved, suggesting significant kinetic retardation (Sobol and Frash 1974).

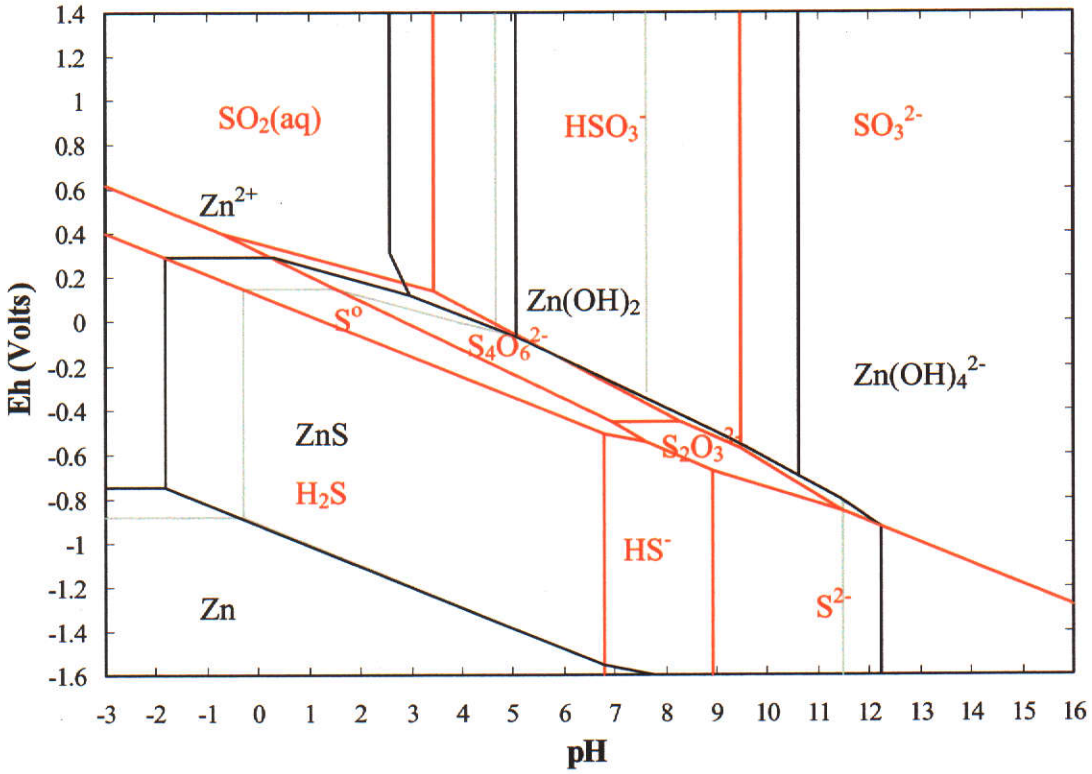

Figure 2.1 E_h-pH diagram for the Zn-S-SO_2-H_2O system at 200°C (after Larsen (1984)). The black lines identify predominance areas for the situation when aqueous species have activities of 1, and the grey lines indicate the situation when the activities of aqueous species are 0.001.

At ambient temperatures, when zinc sulfide is leached in SO_2 solutions containing added sulfuric acid, non-oxidative dissolution of the sulfide occurs followed by reaction of SO_2 with generated H_2S to form elemental sulfur (Larsen 1984; Tiwari 1977).

$$ZnS + 2H^+ \leftrightarrow Zn^{2+} + H_2S \quad (2.23)$$

$$H_2S + {}^1/_2\, SO_2 \rightarrow {}^3/_2\, S^o + H_2O \quad (2.24)$$

Increasing the acidity increased the initial dissolution rate, but had little effect on the extent of the reaction. The highest zinc extractions obtained were only ~60%, and

Tiwari (1977) attributed the limited zinc extraction to the formation of a film of sulfur covering the unreacted core of the zinc sulfide particles and inhibiting the diffusion of reagents (H^+) and products (H_2S) to and from the reaction interface.

This reaction has been carried out at temperatures no greater than 70°C, which is below the melting point of elemental sulfur. The problem of sulfur occluding the zinc sulfide surface may be overcome by increasing the temperature above the melting point of sulfur (119°C), and using a surfactant to keep the molten sulfur from adhering to the zinc sulfide surface. Increasing the temperature may also increase the zinc extraction (akin to the way elevated temperatures increase the dissolution of $CuFeS_2$ in hydrochloric acid (Meyers, Hamersma and Kraft 1975)). As there have been no studies on this reaction at elevated temperatures, higher temperature work needs to be investigated.

Sulfur dioxide solutions containing added oxygen and ferrous or ferric ions have been used to leach synthetic ZnS. Ferric ions are necessary as they catalyse the oxidation of SO_2 in the presence of O_2 to H_2SO_4 (Eqn. 2.25) (Adams and Matthew 1981; Larsen 1984). Ferric ions are regenerated from ferrous ions by the SO_2 / O_2 mixture (Eqn. 2.26).

$$2SO_2 + O_2 + 2H_2O \xrightarrow{Fe^{3+}} 2H_2SO_4 \qquad (2.25)$$

$$2\,Fe^{2+} + SO_2 + O_2 \longrightarrow 2Fe^{3+} + SO_4^{2-} \qquad (2.26)$$

The formation of sulfuric acid enhances the leach rate and non-oxidative dissolution occurs via the sulfuric acid generated *in situ*. In the absence of iron, sulfuric acid is not formed and the oxygen acts merely as a diluent of the sulfur dioxide gas (Larsen 1984). For zinc concentrates, the addition of dissolved iron is not required, as iron present in the concentrate passes into solution and is sufficient to facilitate the formation of sulfuric acid (Adams and Matthew 1981). The overall reaction is

$$2ZnS + 3SO_2 + {}^5/_2O_2 + H_2O \rightarrow 2ZnSO_4 + 2S^o + H_2SO_4 \qquad (2.27)$$

2.1.3 Summary of aqueous sulfur dioxide leaching of zinc sulfide

Leaching ZnS with aqueous sulfur dioxide solutions at ambient temperatures is not commercially viable because the dissolution rate is too slow. In addition, the conversion of sulfide sulfur to elemental sulfur is slow and incomplete. However, at higher temperatures it may prove to be viable as increasing temperature increases the SO_2 leach rate (Larsen 1984) and polythionates decompose to elemental sulfur more rapidly (Meyer and Ospina 1982).

In contrast, when ZnS is leached in aqueous sulfur dioxide solutions containing sulfuric acid at ambient temperatures, promising reaction rates have been observed (Larsen 1984). However, elemental sulfur may inhibit dissolution by occluding the mineral surface (Tiwari 1977). A possible way to avoid this is to conduct leaches above the melting point of sulfur (119°C) and to use a surfactant to prevent the molten sulfur from adhering to the sulfide surface. Surfactants have successfully been used for this purpose in acidic oxidative pressure leaching studies (Owusu, Dreisinger and Peters 1995a) and in commercial processes (Collins et al. 1994; Kawulka, Haffenden and Mackiw 1975).

2.2 Dissolution of Zinc Sulfide in Sulfuric Acid and Conversion of Hydrogen Sulfide to Elemental Sulfur by Sulfur Dioxide

The mechanism of dissolution in the SO_2 / H_2SO_4 system is considered to involve non-oxidative dissolution of ZnS by H_2SO_4 (Eqn. 2.23, p. 20) followed by SO_2 oxidation of H_2S (Eqn. 2.24, p. 20) (Tiwari 1977).

2.2.1 Dissolution of Zinc Sulfide in Sulfuric Acid

In sulfuric acid ZnS dissolves non-oxidatively, yielding the products Zn^{2+} ions and $H_2S(g)$ (Romankiw and de Bruyn 1965)

$$ZnS + H_2SO_4(aq) \leftrightarrow ZnSO_4(aq) + H_2S(aq) \quad (2.28)$$

$$H_2S(aq) \leftrightarrow H_2S(g) \quad (2.29)$$

To date, equilibrium constants for this reaction have been measured using synthetic sulfides whose composition has included sphalerite and wurtzite. Equilibrium constants have not been measured using pure sphalerite. Using a synthetic zinc sulfide composed of 75% sphalerite and 25% wurtzite, Romankiw and De Bruyn (1965) obtained an equilibrium constant of 1.13×10^{-3} at 25°C, whilst using another synthetic ZnS (58% wurtzite, 42% sphalerite), Corriou, Gely and Viers (1988) determined the equilibrium constant at 25°C to be 1.05×10^{-4}. The cause of the discrepancy between these two values is unknown. The low equilibrium constant indicates that in a closed system at 25°C, the extent of reaction is very low.

For temperatures above 100°C, there is only one reported study on the equilibrium constant for this reaction. Corriou, Gely and Viers' (1988) study of the dissolution of ZnS (58% wurtzite, 42% sphalerite) in sulfuric acid was undertaken over the temperature range 25°C to 200°C. They found that the equilibrium constant increased with temperature, from 1.05×10^{-4} at 25°C to 7.2×10^{-2} at 200°C. Hence, increasing the temperature increases the extent of dissolution, but not to a commercially significant level. For example, in 0.125 mol L^{-1} H_2SO_4 the concentration of dissolved zinc at equilibrium increases from 3.12 mmol L^{-1} at 25°C to only 12.85 mmol L^{-1} at 200°C.

The kinetics of this reaction at ambient temperatures have been studied in detail by a number of authors, however, there is no reported data for the kinetics at elevated temperatures (> 100°C)

Romankiw and de Bruyn (1965) examined the dissolution of a synthetic zinc sulfide (75% sphalerite, 25% wurtzite) in H_2SO_4 (0.125 mol L^{-1} to 8.75 mol L^{-1}) at temperatures from 0.6°C to 65°C, and concluded that in the concentration range 0.5 mol L^{-1} to 5 mol L^{-1} H_2SO_4 the dissolution rate is expressed by

$$d[Zn^{2+}]/dt = k_f A_s [H^+] - k_r A_s \, p(H_2S)^{1/2} [Zn^{2+}]^{1/2} \quad (2.30)$$

where A_s is the surface area of ZnS

This expression (Eqn. 2.30) has been confirmed by Locker and de Bruyn (1969) and Crundwell and Verbaan (1987). Locker and de Bruyn (1969), who studied the dissolution kinetics of two types of zinc sulfide, one being 100% sphalerite, the other 75% sphalerite – 25% wurtzite, in H_2SO_4 (0.5 to 4 mol L-1) over the range 0.2°C to 59°C, also found that the activation energy for each type of ZnS was the same (Table 2.1). Crundwell and Verbaan (1987), who studied the dissolution of synthetic and natural sphalerites (0.45 – 10.74% Fe content) in 0.25 – 2 mol L^{-1} H_2SO_4 over the range 25 – 54°C, additionally found that the activation energies of the forward reaction and reverse reactions are independent of iron content (Table 2.1).

Table 2.1 Activation energies for zinc sulfides of varying iron content.
a-(Locker and deBruyn 1969), b-(Crundwell and Verbaan 1987), c-(Romankiw and de Bruyn 1965)

Material	Crystal structure	Fe (%)	Activation energy (kJ mol^{-1})	
			Forward	Reverse
Synthetic [a]	Sphalerite	0.0001	39.7 ± 4.2	24.3 ± 4.2
Synthetic [c]	Sphalerite(~75%),Wurtzite(~25%)	0.006	46.4 ± 4.2	32.6 ± 4.2
Synthetic [a]	Sphalerite(~75%),Wurtzite(~25%)	0.1	41.4 ± 4.2	28.0 ± 4.2
Synthetic [b]	Sphalerite	0.12	37.9	25.4
Natural [b]	Sphalerite	0.45	43.9	31.6
Natural [b]	Sphalerite	7.25	44.3	30.4
Natural [b]	Sphalerite	10.74	37.4	21.1

The equilibrium constants for the dissolution of sphalerite in sulfuric acid and the kinetics of the reaction at temperatures above 100°C have not been reported and still need to be examined.

Studies have also been conducted into the mechanism by which the non-oxidative dissolution of ZnS in acidic solutions takes place. Two dissolution theories have been proposed – the adsorption theory (Locker and deBruyn 1969; Majima and Awakura 1985; Majima, Awakura and Misaki 1981) and the ionic charge transfer or electrochemical theory (Crundwell and Verbaan 1987; Nicol 1983; Scott and Nicol 1977).

According to the adsorption theory hydrogen ions adsorb onto the sulfide surface, react with sulfide forming HS^- and are then released from the surface together with zinc ions. The rate determining step being either the adsorption of hydrogen ions onto the sulfide surface (Locker and deBruyn 1969) or the release of hydrogen sulfide ions from the sulfide surface (Majima and Awakura 1985; Majima, Awakura and Misaki 1981).

$$ZnS + H^+ \xleftrightarrow{K} ZnS:H^+_{ad} \tag{2.31}$$

$$ZnS:H^+_{ad} \longrightarrow Zn^{2+} + HS^- \tag{2.32}$$

$$HS^- + H^+ \xrightarrow{\text{fast}} H_2S \tag{2.33}$$

The charge transfer theory for the dissolution of sulfides, first advocated by Scott and Nicol (1977), is based upon an electrochemical theory for the dissolution of ionic compounds (Nicol 1983; Scott and Nicol 1977). According to this theory, dissolution proceeds by transfer of ions across the double layer from the solid surface to the solution. The rate determining step is the transfer of ions across this double layer, with the rate being dependent upon the potential difference between the solid surface and the solution. For example, Crundwell and Verbaan (1987) expressed the rates of dissolution of the zinc and sulfur lattice ions using a Butler-Volmer expression with the equation for zinc dissolution being given by

$$r_+ = \vec{k}_+[Zn_{lat}]e^{(\alpha_+ z_+ F\phi/RT)} - \overleftarrow{k}_+[Zn]e^{\{-(1-\alpha_+)z_+ F\phi/RT\}} \tag{2.34}$$

where ϕ is the potential across the Helmholtz plane (double layer), α_+ is the cation transfer coefficient, $\vec{k}_+$ and $\overleftarrow{k}_+$ are rate constants for the removal and deposition processes, F is the Faraday constant, z_+ the charge on the cation, R the universal gas constant and T the temperature in Kelvin.

These two theories have been evaluated by Nicol (1983) and Crundwell and Verbaan (1987). They have shown that the non-oxidative dissolution of ZnS in sulfuric acid is more adequately described by the electrochemical model; one advantage being that it is able to account for the effect of variations in the potential across the double layer.

2.2.2 The Reaction of Sulfur Dioxide with Hydrogen Sulfide in Aqueous Solutions

The species present in aqueous solutions of SO_2 and H_2S and the products from their reaction, particularly the postulated initial products, are pertinent to gaining an understanding of the processes occurring in the SO_2 leaching system. In addition, attention is given to evidence for the existence of the polysulfane monosulfonic acids (HSS_nSO_3H, $n \geq 1$) in aqueous solutions, as these could be involved.

2.2.2.1 Aqueous solutions of SO_2

SO_2 readily dissolves in aqueous solutions, with Henry's constant for the solubility of SO_2 in water being 73.4 kPa mol^{-1} kg at 20°C (Rumpf and Maurer 1992). This equates to a SO_2 solubility of 1.38 mol kg^{-1} when the pressure of SO_2 is 101.3 kPa. Although aqueous solutions of SO_2 are often referred to as "sulfurous acid', the sulfurous acid molecule (H_2SO_3) is not present. (The H_2SO_3 molecule has only been produced in the gas phase by dissociative ionization (70 eV) of diethyl sulfite or ethanesulfonic acid followed by collision induced neutralization of the $H_2SO_3^{+\bullet}$ radical cation (Sulzle et al. 1988).) Aqueous solutions of SO_2 contain predominantly dissolved SO_2 in the molecular state (Schroeter 1966a). Aqueous SO_2 exists in equilibrium with bisulfite (HSO_3^-) and hydrogen ions, the equilibrium constant being 0.0139 at 25°C (Huss and Eckert 1977).

$$SO_2(aq) + H_2O \leftrightarrow HSO_3^- + H^+ \qquad (2.35)$$

Dissociation of HSO_3^- to SO_3^{2-} is negligible, $K_2^{25^\circ C} = 6.24 \times 10^{-8}$ (Schroeter 1966b).

$$HSO_3^-(aq) + H_2O \leftrightarrow SO_3^{2-} + H_3O^+ \qquad (2.36)$$

There are two isomers of the bisulfite ion; one with the proton bonded to the sulfur atom (HSO_3^-) and the other with the proton bonded to an oxygen atom ($HOSO_2^-$).

The equilibrium quotient (Q_1) (Eqn. 2.37) for this isomerisation is 4.98 at 25°C in solutions of ionic strength 1 mol kg^{-1} (Horner and Connick 1986).

$$Q_1 = [HOSO_2^-]/ [HSO_3^-] \quad (2.37)$$

Another reaction that occurs in aqueous solutions of SO_2 is the dimerization of bisulfite ion to form disulfite (Connick, Tam and von Deuster 1982).

$$2HSO_3^-(aq) \leftrightarrow S_2O_5^{2-} + H_2O \quad (2.38)$$

$$Q_d = [S_2O_5^{2-}]/ [HSO3-]^2 \quad (2.39)$$

The equilibrium quotient for this reaction, Q_d, is 0.062 mol L^{-1} at an ionic strength of 1 mol L^{-1} (Littlejohn, Walton and Chang 1992). However this only occurs at high concentrations of bisulfite (Connick, Tam and von Deuster 1982) and thus, in aqueous solutions of SO_2, the concentration of disulfite is negligible.

2.2.2.2 Aqueous solutions of H_2S

Hydrogen sulfide is also soluble in aqueous solutions, though much less so than SO_2. For H_2S, Henrys constant is 46 740 kPa mol^{-1} kg (at $\mu = 0$) (Suleimenov and Krupp 1994). This equates to a H_2S solubility of 2.2×10^{-3} mol kg^{-1} when $p(H_2S) = 101.3$ kPa. For the first acid dissociation of H_2S (Eqn. 2.40), $pK_{a1} = 6.99$ at 25°C (Suleimenov and Seward 1997). Thus, at pH < 7, $H_2S(aq)$ is the dominant species, whereas $HS^-(aq)$ is the main species at higher pH values.

$$H_2S(aq) \leftrightarrow HS^-(aq) + H^+(aq) \quad (2.40)$$

2.2.2.3 H_2S / SO_2 reaction in aqueous solutions

The reaction between aqueous solutions of SO_2 and H_2S, often referred to as the Wackenroder reaction, has been studied since 1846 (Volynskii 1971). It is also referred to as the wet Claus reaction (Siu and Jia 1999), the Claus reaction being the

gas phase reaction between SO_2 and H_2S. In the gas phase, these react at around 350°C, in the presence of an appropriate catalyst (e.g. Al_2O_3), to form elemental sulfur and water (Habashi 1997d).

$$SO_2 + 2H_2S \rightarrow 3S^\circ + H_2O \qquad (2.41)$$

However, in aqueous solutions the reaction products include not only elemental sulfur, but also polythionic acids, $H_2S_nO_6$ (Steudel, Gobel and Holdt 1989). Polysulfane oxides are also formed at room temperature and below (Schenk and Steudel 1965). The resulting solution is a complex mixture of sulfur-oxy species due to the ability of polythionic acids to react with sulfurous acid forming lower polythionates (Schroeter 1966c).

The products of this reaction depend strongly on the SO_2:H_2S ratio (Schroeter 1966d). When SO_2 is in excess polythionates predominate, and when H_2S is present in stoichiometric or greater amounts, elemental sulfur predominates (Table 2.2).

Table 2.2 SO_2 / H_2S reaction products and their dependence on the SO_2 : H_2S ratio. From Schroeter (1966d)

SO_2: H_2S	Main products	Notes
0.5:1	S°	-
0.5-1:1	S°, $H_2S_nO_6$ $n = 4 - 8$. Main product is $H_2S_4O_6$	2/3 of the S in $H_2S_nO_6$ provided by H_2S, 1/3 by SO_2. Ratio is essentially independent of $[SO_2]$ and $[H_2S]$
<1:1 + heat	polythionates, $S_nO_6^{2-}$	A milky liquid cont. mainly $H_2S_3O_6$ and $H_2S_5O_6$, called Wackenroder's solution.
>1:1	polythionates, $S_nO_6^{2-}$	A milky liquid cont. mainly $H_2S_3O_6$ and $H_2S_5O_6$, called Wackenroder's solution.
50:1	polythionates, $S_nO_6^{2-}$	Main product out of $H_2S_xO_6$ is $H_2S_4O_6$ 1/2 of the S in $H_2S_nO_6$ provided by H_2S, 1/2 by SO_2.

The reaction products are also dependent upon the pH. Low pHs favour the formation of elemental sulfur (Nikolaev, Ivanov and Akulova 1939). With pH <1 and a large excess of SO_2(aq), the major products are tetra- and pentathionate,

whereas with increasing pH the formation of tetra- and pentathionates decreases and the yield of trithionate and thiosulfate increases (Magers 1940). At pH values in excess of certain, ionic strength dependent values (pH 7, $\mu = 0.5$ mol L^{-1}; pH 8, $\mu = 3$ mol L^{-1}), no reaction occurs (Teder and Wilhelmsson 1975). This is supported by Heunisch (1977) who reports that free SO_3^{2-} ions do not react with HS^- ions at room temperature.

When H_2S is reacted with aqueous solutions of sulfite salts, containing an excess of sulfite and at pH 6–7, the major product is thiosulfate (Urban 1975). The equation for thiosulfate formation is (Heunisch 1977)

$$2HS^- + 4HSO_3^- \rightarrow 3S_2O_3^{2-} + 3H_2O \qquad (2.42)$$

2.2.2.4 Mechanism of the H_2S / SO_2 reaction

The mechanism of the H_2S / SO_2 reaction is not yet completely understood. It is generally accepted that H_2S and SO_2 react in aqueous solution to produce an initial intermediate sulfoxylic acid, $H_2S_2O_2$ (Eqn. 2.43) (Kozak 1987; Schenk and Steudel 1965; Thorne and Roberts 1948).

$$H_2S + SO_2 \rightarrow H_2S_2O_2 \qquad (2.43)$$

The existence of this species in aqueous solutions has not been reported, but it has been generated in the gas phase by electron impact decomposition of diisopropoxy disulfide ($C_3H_7OSSOC_3H_7$) followed by collision induced neutralisation of the cation. The structure of the molecule formed in this manner was HO-S-S-OH (Schmidt et al. 1992). It is expected that isomers of the hypothetical anion, $HS_2O_2^-$, are also formed by reaction with water (Eqn. 2.44), the most stable of which has been calculated to be $HSSO_2^-$ (Miaskiewicz and Steudel 1994).

$$H_2S_2O_2 + H_2O \rightarrow H_3O^+ + HS_2O_2^- \qquad (2.44)$$

Subsequent reactions produce short chain sulfanemono- and disulfonates, which increase in sulfur chain length until an S_8 ring, is able to form.

Numerous side reactions occur in this system. Many of the reactions are nucleophilic displacement reactions between one of the many nucleophiles, *viz.*, bisulfite (HSO_3^-), thiosulfite ($S_2O_3^{2-}$), sulfane monsulfonates ($^-S_xSO_3H$) and relatively positively charged sulfur atoms in species containing sulfur chains, *viz.*, elemental sulfur, S_n ($n = 6$ - 10) and polythionic acids ($HO_3SS_xSO_3H$). For example, thiosulfate displaces the sulfite group of polythionates ($^-O_3SS_nSO_3^-$, $n > 1$) generating a polythionate with one extra sulfur atom ($^-O_3SS_{n+1}SO_3^-$) in the process.

$$S_nO_6^{2-} + S_2O_3^{2-} \leftrightarrow S_{n+1}O_6^{2-} + SO_3^{2-} \qquad (2.45)$$

Although, the equilibrium for this reaction lies to the left, the building-up process occurs under acidic conditions, where sulfite is removed as hydrogen sulfite (Foss and Kringlebotn 1961). Polythionates ($S_nO_6^{2-}$, $n = 4$ - 6) also rearrange into higher ($S_{n+1}O_6^{2-}$) and lower ($S_{n-1}O_6^{2-}$) polythionates via a mechanism catalysed by thiosulfate (Eqn. 2.46). This mechanism may also involve the polysulfane monosulfonates ($S_nO_3^{2-}$) (Foss 1961).

$$2S_nO_6^{2-} \leftrightarrow S_{n+1}O_6^{2-} + S_{n-1}O_6^{2--} \qquad (2.46)$$

Under acidic conditions ($0 \leq pH \leq 2$), the bisulfite ion present in sulfurous acid solutions attacks polythionates ($H_2S_nO_6$), displacing thiosulfate and generating the next lower polythionate (Schroeter 1966c).

$$S_4O_6^{2-} + HSO_3^- \rightarrow S_3O_6^{2-} + S_2O_3^{2-} + H^+ \qquad (2.47)$$

$$S_5O_6^{2-} + HSO_3^- \rightarrow S_4O_6^{2-} + S_2O_3^{2-} + H^+ \qquad (2.48)$$

$$S_6O_6^{2-} + HSO_3^- \rightarrow S_5O_6^{2-} + S_2O_3^{2-} + H^+ \qquad (2.49)$$

It is postulated that the mechanism involves the breaking of the bond between the second and third sulfur atoms of the polythionate ion, with the addition of HSO_3^- and H^+ yielding $H_2S_3O_6$ and $H_2S_{n-2}O_3$. Sulfurous acid then reacts with the

sulfanemonosulfonic acid ($H_2S_{n-2}O_3$) to give $H_2S_2O_3$ and $H_2S_{n-3}O_6$. For pentathionate the reactions are

$$HO_3SSSSSO_3H + HSO_3^- \rightarrow HO_3SSSO_3H + HSSSO_3H \quad (2.50)$$

$$HSSSO_3H + H_2SO_3 \rightarrow 2HSSO_3H \quad (2.51)$$

Elemental sulfur (S_8) is considered to form via ring closure of the sulfur chain of $HS_8SO_3^-$.

$$HS_8SO_3^- \rightarrow S_8 + HSO_3^- \quad (2.52)$$

In addition, elemental sulfur is also formed when sulfide or hydrogen sulfide reacts with polythionates (Silberman and Fridman 1946).

Also finely dispersed sulfur is capable of reacting with sulfurous acid to produce thiosulfuric acid (Schroeter 1966e).

$$S_8 + 8H_2SO_3 \rightarrow 8H_2S_2O_3 \quad (2.53)$$

In reactions involving H_2S it seems that $H_2S(aq)$ is the active species rather than HS^- (aq), as in the reaction with sulfite for polythionate formation, decreasing the pH of sulfite / sulfide reaction mixtures, in the range $4 \leq pH \leq 7$, resulted in higher concentrations of polythionates being produced (Kask and Teder 1998).

Barbieri (1961) observed that in $H_2S_nO_6$ the outer sulfur atoms are from SO_2, whereas the inner sulfur atoms are from H_2S and SO_2. In the presence of excess SO_2 the inner sulfur atoms in $H_2S_nO_6$ are formed from H_2S and SO_2 at the ratio 1:1 (i.e. 50% of the sulfur atoms are from H_2S and the other 50% are from SO_2). In the presence of excess H_2S the inner sulfur atoms in $H_2S_nO_6$ are formed from H_2S and SO_2 at a ratio 2:1. However, in the elemental sulfur that is also produced in the reaction, the sulfur atoms originate from H_2S and SO_2 in the ratio 2:1, regardless of which reagent is in excess (Barbieri and Sosi 1961; van der Heijde and Aten 1953).

2.2.2.5 Polysulfane monosulfonic acid formation

Thiosulfate (monosulfane sulfonic acid) is the first in the series of the polysulfane monosulfonic acids, and can be prepared by the following reaction in ether at low temperatures (Schmidt and Siebert 1973).

$$HSH + SO_3 \rightarrow HSSO_3H \quad (2.54)$$

Using this same method higher sulfanemonosulfonic acids (HS_nSO_3H, n = 1 - 6) can be prepared using higher sulfanes (Schmidt and Siebert 1973), i.e.

$$HS_nH + SO_3 \rightarrow HS_nSO_3H \quad (2.55)$$

Although these acids have been prepared and are stable in ethereal solutions at low temperatures, they decompose rapidly in water and aqueous alkali yielding mainly thiosulfate, sulfur dioxide and elemental sulfur. The acids and their anions, $HS_nSO_3^-$ and $S_nSO_3^{2-}$, have not been detected in aqueous solutions to date. However, they have been observed indirectly, and are postulated as key intermediates in many reactions involving polythionates and the formation of elemental sulfur. Thermodynamic data for such species has also been calculated (Williamson and Rimstidt 1992).

Schroeter (1966f), citing Schmidt and Heinrich (1958), mentions that the existence in aqueous solutions of sulfane monsulfonates as products of the reaction between finely dispersed elemental sulfur and sulfurous acid (Eqns. 2.56 – 2.58), has been "established by titration techniques and by isolation of their insoluble silver salts".

$$S_8 + H_2SO_3 \rightarrow H_2S_9O_3 \quad (2.56)$$

$$H_2S_9O_3 + H_2SO_3 \rightarrow H_2S_8O_3 + H_2S_2O_3 \quad (2.57)$$

$$\vdots$$

$$H_2S_3O_3 + H_2SO_3 \rightarrow H_2S_2O_3 + H_2S_2O_3 \quad (2.58)$$

Sulfane monosulfonates are also produced via the reaction of HSO_3^- with sulfane disulfonates (Schmidt 1965b).

$$\begin{array}{l} \quad\quad H\vdots SO_3H \\ \quad\quad + \\ HO_3S–S_n–S–\vdots S–SO3H \end{array} \quad \rightarrow \quad H_2S_3O_6 \quad + \quad HO_3S–S_n–S–H \qquad (2.59)$$

$$\begin{array}{l} \quad\quad H\vdots SO_3H \\ \quad\quad + \\ HO_3S–S_{n-1}–S–\vdots S–H \end{array} \quad \rightarrow \quad H_2S_2O_3 \quad + \quad HO_3S–S_{n-1}–S–H \qquad (2.60)$$

$$\begin{array}{l} \quad\quad H\vdots SO_3H \\ \quad\quad + \\ HO_3S–S_{n-2}–S–\vdots S–H \end{array} \quad \rightarrow \quad H_2S_2O_3 \quad + HO_3S–S_{n-2}–S–H \qquad (2.61)$$

Sulfanemonosulfonates are also considered to be key intermediates in the acidic decomposition of thiosulfate (Davis 1958; Steudel, Gobel and Holdt 1988). The reaction produces predominantly long chain polythionates ($S_nO_6^{2-}$) (average chain length of $n = 29$), and elemental sulfur with smaller amounts of SO_2, H_2S and sulfate (Steudel, Gobel and Holdt 1988). Sulfanemonosulfonates are thought to be involved in the formation of polythionates (Steudel, Gobel and Holdt 1988) and elemental sulfur (Davis 1958), via the following reactions:

polythionate formation

$$n S_2O_3^{2-} + (n+1)H^+ \rightarrow HS_nSO_3^- + nHSO_3^- \qquad (2.62)$$

$$2\,HS_nSO_3^- \rightarrow H_2S + S_{2n+1}O_6^{2-} \qquad (2.63)$$

$$S_mO_6^{2-} + nS_2O_3^{2-} \rightarrow S_{m+n}O_6^{2-} + nSO_3^{2-} \qquad (2.64)$$

sulfur formation

$$S_2O_3^{2-} + H^+ \rightarrow HS_2O_3^- \qquad (2.65)$$

$$HS_2O_3^- + S_2O_3^{2-} \rightarrow HS_3O_3^- + SO_3^{2-} \qquad (2.66)$$

$$HS_3O_3^- + S_2O_3^{2-} \rightarrow HS_4O_3^- + SO_3^{2-} \qquad (2.67)$$

$$\vdots$$

$$HS_9O_3^- \rightarrow S_8 + HSO_3^- \qquad (2.68)$$

Sulfanemonosulfonates are also considered to be initial products of the hydrolysis of polythionates (Meyer and Ospina 1982; Steudel et al. 1987; Wagner and Schreier 1978)

$$^{-}O_3S—S_n—SO_3^{-} + H_2O \rightarrow {}^{-}O_3S—S_n^{-} + HSO_4^{-} + H^{+} \quad (2.69)$$

In addition, sulfanemonosulfonic acid intermediates are considered essential for the synthesis, degradation and transportation of polysulfur compounds in aqueous acidic solutions (Steudel et al. 1987).

$$2HS_2SO_3^{-} \leftrightarrow HS_4SO_3^{-} + HSO_3^{-} \quad (2.70)$$

$$2HS_4SO_3^{-} \leftrightarrow HS_8SO_3^{-} + HSO_3^{-} \quad (2.71)$$

$$HS_8SO_3^{-} \leftrightarrow S_8 + HSO_3^{-} \quad (2.72)$$

$$2HS_2SO_3^{-} \leftrightarrow HS_5O_6^{2-} + H_2S \quad (2.73)$$

2.2.2.6 Kinetics of the H_2S / SO_2 reaction

Compared to the many studies on the mechanism and products of the H_2S / SO_2 reaction, there have been only a few studies on the kinetics.

In excess sulfite and at pH ≥ 7, sulfide and sulfite react to form predominantly thiosulfate (Eqn. 2.74) (Heunisch 1977).

$$2HS^{-} + 4HSO_3^{-} \rightarrow 3S_2O_3^{2-} + 3H_2O \quad (2.74)$$

Siu and Jia (1999) report that in basic solutions (pH = 8-9) at 20°C, with sulfide being in excess the rate of thiosulfate formation is

$$d[S_2O_3^{2-}]/dt = k_A[HS^{-}][HSO_3^{-}]^2 \quad (2.75)$$

and the rate of bisulfite removal is

$$-d[HSO_3^{-}]/dt = k_B[H^{+}]^{-0.6}[HS^{-}]^{0.7}[HSO_3^{-}]^{1.5} \quad (2.76)$$

Teder and Wilhelmsson (1975) studied the rate of reaction between aqueous solutions of NaSH and Na_2SO_3 over the temperature range 30-70°C and at pHs from 3 to 8.5. They observed complex kinetics and were unable to provide a general rate equation to describe the reaction. When sulfite was added to the hydrogen sulfide solution, the reaction obeyed first order kinetics. However, when sulfide was added to sulfite there was initially a rapid reaction, followed by a slower reaction that had the same rate as that observed for the addition of sulfite to hydrogen sulfide. The rate increased with decreasing pH. Increasing the temperature only marginally increased the rate, the apparent activation energy being only 2 kJ mol^{-1}. The actual rate may have been much higher as they mention that with increasing temperature, increasing losses of H_2S from the aqueous phase to the gas phase occurred.

Keller (1956) found that, whereas the overall reaction stoichiometry is given by equation 2.24 (p. 20),

$$2H_2S + SO_2 \rightarrow 3S^\circ + 2H_2O$$

when H_2S reacts with SO_2 in aqueous solutions buffered to pHs of 4 to 6, SO_2 is consumed rapidly and almost completely by reaction with only 0.3 to 0.5 mole of H_2S per mole of sulfur dioxide, yielding thiosulfuric acid and trace amounts of polythionic acids (Eqn. 2.77). Little or no elemental sulfur is formed initially. Instead, sulfur results from the subsequent reaction of H_2S with thiosulfuric and polythionic acids.

$$2H_2S + 4SO_2 + H_2O \rightarrow 3H_2S_2O_3 \qquad (2.77)$$

Keller (1956) also observed that the initial reaction between H_2S and SO_2 is faster than the subsequent reactions between H_2S and thiosulfuric and polythionic acids where sulfur is formed. In addition, he notes that decreasing the pH increases the rate of H_2S consumption but that increasing the pressure of H_2S has no effect on the rate. Increasing the temperature from 25 to 40°C increased the rate of H_2S consumption by a factor of almost four.

Tiwari (1977) studied the rate of reaction between SO_2 and H_2S at an aqueous interface, where one of the gases was in a sulfuric acid solution (0.044 to 1 mol L^{-1}) and the other in the gas phase above the solution. To determine the reaction rate, the rate of decrease in pressure of the gas in the gaseous phase was measured. Assuming that sulfur is produced quantitatively according to equation 2.24 (p. 20), the following rate equation was obtained

$$dn(S)/dt = k_c A [SO_2] [H_2S] \quad (2.78)$$

where k_c is the rate constant and A is the reaction surface area of the aqueous solution in contact with the gas phase. At 24.5°C in 1 mol L^{-1} H_2SO_4, k_c was determined to be 15.14 litre^2 m^{-2} mol^{-1} min^{-1}. Increasing the temperature (14.7°C to 36.3°C), significantly increased the rate of the reaction, the activation energy for the reaction being 118 ± 4 kJ mol^{-1}.

In the H_2SO_4 dissolution of ZnS, H_2S will be generated at pH values less than 2. Most of the reported studies have been conducted at pH values of 3 and higher, with only one being conducted at pHs below this (Tiwari 1977). The applicability of Tiwari's study is limited since the reaction was carried out at the gas – liquid interface and not in solution. Furthermore, since there have also been no reported studies on the rate of the reaction at temperatures above 70°C, low pH and higher temperature studies are required.

2.3 AIMS OF THIS STUDY

The review of the literature highlighted areas that require further research in order to gain a fuller understanding of the chemistry associated with SO_2 leaching of zinc sulfide. These areas are:

- The mechanism for the dissolution of ZnS in sulfurous acid solutions has not yet been decisively determined.

- The use of aqueous solutions of SO_2 results in slow leach rates at ambient temperatures. Whether or not satisfactory results can be obtained at elevated temperatures needs to be established.

Faster leaching rates are obtained when SO_2 is used in conjunction with an acid. The leaching of zinc sulfide in acidified SO_2 solutions has been shown to progress via non-oxidative acidic dissolution of the sulfide (Eqn. 2.23, p. 20) followed by reaction of generated H_2S with SO_2 to produce sulfur (Eqn. 2.24, p. 20).

Dissolution of ZnS in acid alone is limited as the equilibrium favours the reagents even at elevated temperatures. However, dissolution should be enhanced by the addition of SO_2, provided the rate of the H_2S / SO_2 reaction (Eqn. 2.24, p. 20), which removes H_2S from solution, is faster than the rate of dissolution of ZnS (Eqn. 2.23, p. 20). Otherwise, there will be a build up of H_2S, which will inhibit the dissolution of ZnS. There is no reported data on the rates of these reactions at elevated temperatures, particularly at the expected operating temperature of 150°C. Hence there is a need to know the rates (or at least the relative rates) of these reactions at elevated temperatures.

To these ends, the following aims were set:

- to elucidate the role of SO_2 in leaching ZnS in sulfurous acid solutions
- to determine the comparative rates of the non-oxidative dissolution of ZnS and the SO_2 / H_2S reaction at elevated temperatures
- to evaluate the SO_2 pressure leaching of zinc sulfide
- to trial the process on zinc concentrates

3 MATERIALS AND METHODS

3.1 MATERIALS

3.1.1 Common Reagents

- Sulfur dioxide (Industrial grade), BOC Gases
- Nitrogen gas (High Purity), BOC Gases

- Sulfuric acid (AR grade), BDH
- Hydrochloric acid (AR grade), BDH and Ajax Chemicals
- Sodium hydroxide (AR), Rowe Scientific Pty. Ltd.
- Sodium hydroxide convol, BDH
- Zinc sulfate ($ZnSO_4.7H_2O$) (AR), APS Ajax Finechem
- Lead acetate $Pb(CH_3COO)_2.3H_2O$ (AR), BDH
- Barium chloride ($BaCl_2.2H_2O$) (AR), Merck

- Surfactants
  - Quebracho, Imtrade Mining
  - Sodium ligninsulfonate (Ligninsulfonic acid, sodium salt), Aldrich
  - Orthophenylenediamine (1,2-Phenylenediamine), Aldrich

- Milli-Q water was used in all ambient temperature experiments
- Deionised water was used in all pressure leaching experiments

3.1.2 Zinc Sulfide

Each sample was characterised using the following techniques: Laser diffraction for particle size distribution, BET nitrogen adsorption for surface area determination, XRD for crystal structure analysis. Approximate crystal phase compositions were obtained by comparison of XRD spectra with spectra in the International Crystallographic Diffraction Database (Set 49, 1999). Table 3.1 lists the various zinc sulfides used and their relevant physical properties. Chemical analyses of the various synthetic zinc sulfides used are given in Table 3.2.

Table 3.1 Structure, size and surface area of synthetic zinc sulfides.
[a] - D[4,3] denotes volume weighted mean particle size

Material	Structure	Surface Area ($m^2 g^{-1}$)	Mean Particle Size D[4,3][a] (μm)	Size Range (μm) (90% of particles)	Source
ZnS-A	sphalerite	13.2	5.39	-11.8 +1.75	Ventron
ZnS-B	sphalerite (~80%) wurtzite (~20%)	7.8	1.11	-2.68 +0.14	BDH
ZnS-C	wurtzite (~53%) sphalerite (~47%)	7.7	12.35	-30.8 +2.68	Alfa, Johnson Matthey
ZnS-F1	sphalerite	1.143	8.45	-22.4 +1.95	Aldrich
ZnS-F2	sphalerite	0.568	27.3	-52.3 + 4.10	Aldrich
ZnS-F3	sphalerite	0.3	107.9	-184 +56.2	Aldrich
ZnS-F4	sphalerite	0.425	425.4	-710 +240	Aldrich

Table 3.2 Chemical analysis of synthetic zinc sulfides.

Material	Zn (%)	S/S (%)	S/SO_4^{2-} (%)	ZnO (%)	Fe (%)	Pb (%)	Cu (%)
ZnS-A	64.1	29.7	0.48	0.25	<0.01	0.02	<0.005
ZnS-B	65.7	31.7	0.67	0.59	<0.01	0.01	<0.005
ZnS-C	66.4	33.1	0.18	0.31	0.01	0.04	<0.005
ZnS-F	67.9	33.6	<0.05	0.03	0.04	0.05	<0.005

3.1.2.1 Preparation of narrow size fractions

The size fractions: ZnS-F1, ZnS-F2, ZnS-F3 and ZnS-F4 were prepared from ZnS chips (3 – 12 mm) obtained from Aldrich. These ZnS chips were manually ground in an agate mortar and pestle. The larger size fractions (ZnS-F3 and ZnS-F4) were obtained by dry screening through sieves. All fractions were rinsed successively with deionised water, ethanol and acetone to remove fines. The rinsed fractions were then dried at 60°C for 45 minutes and stored in an evacuated desiccator.

The preparation of the smaller size fractions, ZnS-F1 and ZnS-F2, required sieving and settling / decantation in deionised water to obtain the desired narrow size ranges. One hundred grams, in five gram portions, of the –212+106 μm fraction were slurried with deionised water and each ground in a mechanical agate mortar and pestle (Morris Mill) for 4 minutes. The resulting slurry was sieved through 38 μm and 10 μm sieves. The +38 μm fraction was reground until all passed through the 38 μm sieve. This yielded two fractions: "-38+10 μm" and "–10 μm", however the actual size distributions were much broader. To obtain narrower size distributions, each fraction was slurried in deionised water, allowed to settle for certain times, and decanted. The settling times used were determined by applying Stoke's law (Eqn. 3.1) (Micromeritics 1991),

$$D = k v^{1/2} \tag{3.1}$$

where
$$k = \left[18 \frac{\eta}{(\rho - \rho_o) g} \right]^{1/2} \tag{3.2}$$

and

D = diameter of ZnS particle

v = equilibrium sedimentation velocity

η = viscosity of water

ρ = density of ZnS

ρ_o = density of water

g = acceleration due to gravity

The settling time, t, for a given settling distance, h, being

$$t = \frac{k^2 h}{D^2} \tag{3.3}$$

The ZnS-F1 fraction was obtained by removing particles less than 1 μm and greater than 15 μm from the "-10 μm" fraction. Particles larger than 15 μm were removed by repeatedly settling and decanting the fraction. A settling distance of 10 cm was used with a settling time of 4.5 minutes. To remove the fines (< 1 μm) the slurry was repeatedly settled and decanted. A settling distance of 10 cm was used with settling times varying from 120 - 240 minutes. The slurry was also sonicated three times at intervals throughout the process to break up loose agglomerates. The resulting fraction was pressure filtered through a 0.45 μm 142 mm Supor membrane (Pall Gelman). The collected particles were rinsed first with five 50 mL aliquots of deionised water and then five 50 mL aliquots of ethanol. The solids were air dried on the filter membrane for 5 minutes, then transferred to a watchglass and dried at 50°C for one hour, at room temperature for 18 hours and then at 50°C for 2 hours. The solids were stored in an evacuated desiccator.

The ZnS-F2 fraction was obtained by adding the decanted +15 μm fraction to the sieved "–38+10 μm" fraction. The slurry was pressure filtered through a 0.45 μm 142 mm Supor membrane, washed with five 50 mL aliquots of deionised water, rinsed with five 50 mL aliquots of ethanol and then air dried on the filter for five minutes. The partially dried solid was transferred to a petri dish and dried for 2 hours at 50°C, 16.5 hours at room temperature and then another 2 hours at 50°C. The size distributions of these two smaller size fractions are shown in Figure 3.1.

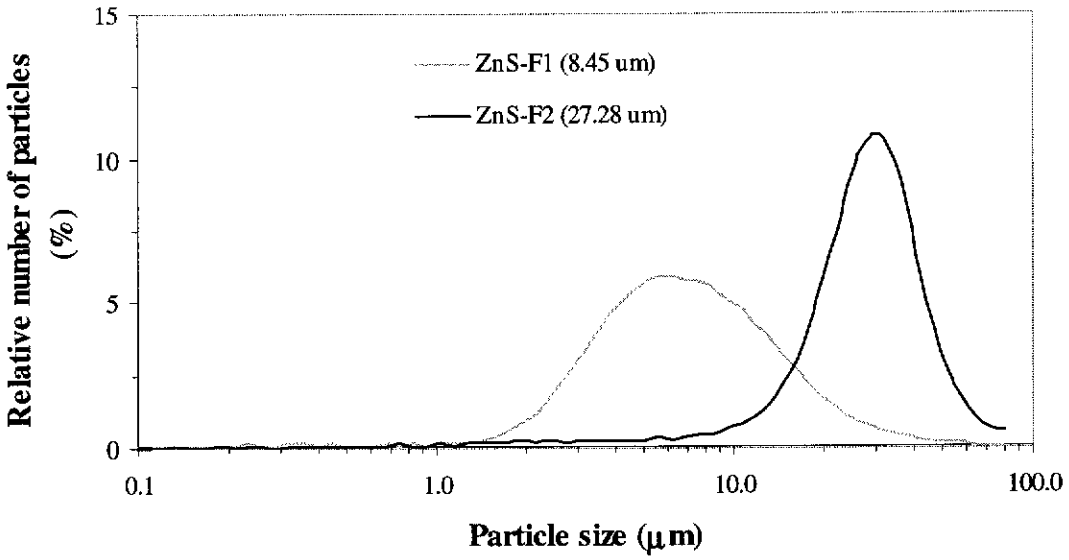

Figure 3.1 Particle size distribution for ZnS-F1 (8.45 μm) and ZnS-F2 (27.3 μm)

3.1.3 Zinc Concentrate

Three batches of Elura concentrate from Pasminco Australia Ltd were used. One batch was used as a source of narrow size fractions, while the other two were used for leaching experiments on the bulk.

3.1.3.1 Preparation of narrow size fractions

Elura concentrate, which since receipt had been stored under vacuum, was ground gently by hand in an agate mortar and pestle to remove the larger agglomerates until the concentrate was <710 μm. Subsamples (150 g) were then slurried with 500 mL deionised water and sonicated for 7 minutes to break down the smaller agglomerates. The sonicated slurry was sieved through a 53 μm sieve and the -53 μm fraction was allowed to settle and subsequently decanted to remove fines. The resulting slurry was cyclosized in a Warman Cyclosizer (Model no. M-4) to produce five size fractions, Elura C1 to Elura C5, with average sizes and specific surface area ranging from 51.26 to 12.57 μm, and 0.27 to 0.89 m^2 g^{-1}, respectively. X-ray diffraction spectra of the size fractions were similar, revealing sphalerite as the major mineral phase with pyrite present in minor amounts. Diffuse reflectance infrared Fourier

transform spectroscopy (DRIFT), a surface sensitive analytical technique, did not detect the presence of xanthates in the cyclosized fractions.

3.1.3.2 Preparation of Elura bulk concentrate for leaching

The Elura concentrates used for bulk leaching studies contained some very hard agglomerates. To crush these agglomerates it was slurried with ethanol and ground gently in a rod mill. It was then stored under ethanol. Before leaching the slurry was filtered and the solid dried in an oven at 50°C overnight. The filter cake was gently crushed by hand in a porcelain mortar and pestle and forced through a 1 mm screen. The material was then split using a riffle splitter to obtain the mass required for leaching.

Each sample was characterised using the following techniques: XRD for crystal structure analysis, laser diffraction for particle size distribution, BET nitrogen adsorption for surface area determination. Table 3.3 lists the bulk samples and smaller size fractions used and their relevant physical properties. Chemical analyses of the samples are given in Table 3.4.

Table 3.3 Composition, size and surface area of zinc concentrate fractions.
[a]-D[4,3] denotes volume weighted mean particle size

Material	Structure	Surface Area ($m^2 g^{-1}$)	Mean Particle Size D[4,3][a] (μm)	Size Range (μm) (90% of particles)
Elura Bulk #1	sphalerite	-	16.20	-39.9 +1.3
Elura Bulk #2	sphalerite	-	15.91	-35.6 +1.3
Elura C1	sphalerite	0.27	51.26	-83.4 +31.1
Elura C2	sphalerite	0.30	35.20	-56.2 +21.0
Elura C3	sphalerite	0.66	25.21	-42.7 +15.3
Elura C4	sphalerite	0.72	17.18	-30.8 +9.58
Elura C5	sphalerite	0.89	12.57	-22.4 +6.27

Table 3.4 Chemical composition of Elura zinc concentrate samples.

Sample	Zn (%)	Fe (%)	Cu (%)	Cd (%)	Pb (%)	As (%)	Si (%)	Ni (ppm)	Hg (ppm)	Ag (ppm)
Elura Bulk 1	47.7	10.5	0.39	0.11	4.0	0.20	-	-	-	-
Elura Bulk 2	44.9	10.4	0.27	0.11	2.2	0.16	0.19	<10	82	-
Elura C1	47.3	14.4	0.21	0.11	1.00	0.22	0.16	<10	70	70
Elura C2	49.3	12.8	0.21	0.11	0.61	0.20	0.16	<10	75	72
Elura C3	52.3	11.9	0.21	0.12	0.42	0.18	0.11	<10	76	66
Elura C4	52.6	10.5	0.21	0.12	0.36	0.16	0.10	<10	86	64
Elura C5	54.6	9.4	0.21	0.12	0.36	0.14	0.05	<10	88	66

3.2 AMBIENT LEACHING APPARATUS AND METHODS

3.2.1 Ambient leaching apparatus

Leaching reactions were performed in a 1 L flat-bottomed cylindrical glass reactor (Figure 3.2 and 3.3). Three perspex baffles were added (attached to the glass walls with silicone) to ensure the slurry was well mixed. Agitation was provided via a polypropylene Rushton impeller attached to a Teflon covered stainless steel stirrer shaft.

The vessel had a glass lid with five inlets, to accommodate the stirrer shaft, gas inlet tube, thermometer, and sampling tube. Gases exited at the fifth port and at the required times pH measurements were undertaken via this port also. The vessel needed to be gas tight to prevent air from entering the vessel. To this end, a stirrer shaft seal was made to ensure that no gas exited or entered via the stirrer shaft port. All other connections were gas tight.

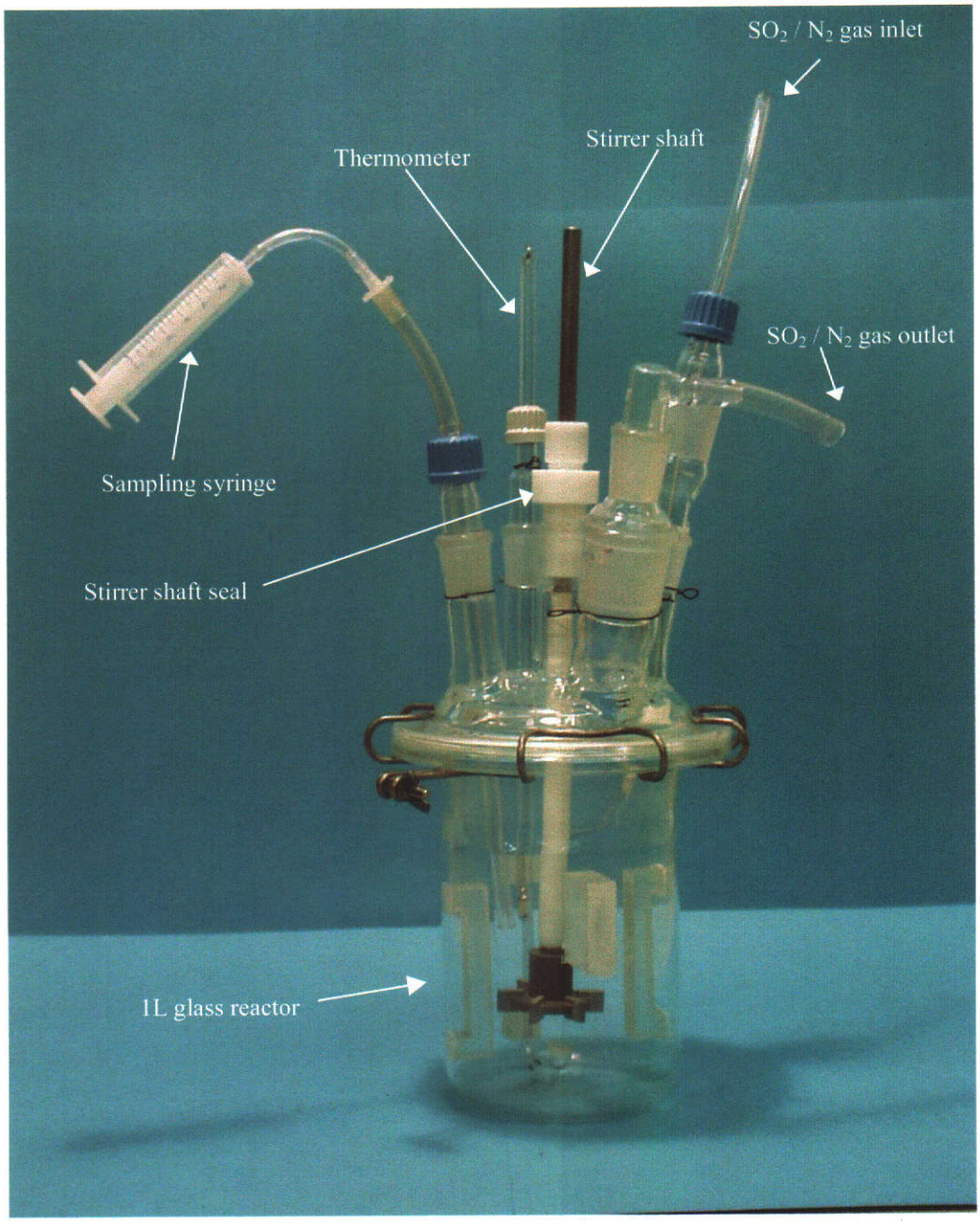

Figure 3.2 Photograph of ambient leaching vessel.

Gases were sparged into the solution through a sintered glass frit (9 mm diameter, porosity no. 1) situated at the bottom of the vessel. PVC tubing was used to connect all glassware. The exit bubbler, mixer bubbler, water bubbler and traps were all glass Buchner flasks. Samples were withdrawn from the vessel via a glass dip tube attached to a 10 mL polypropylene syringe.

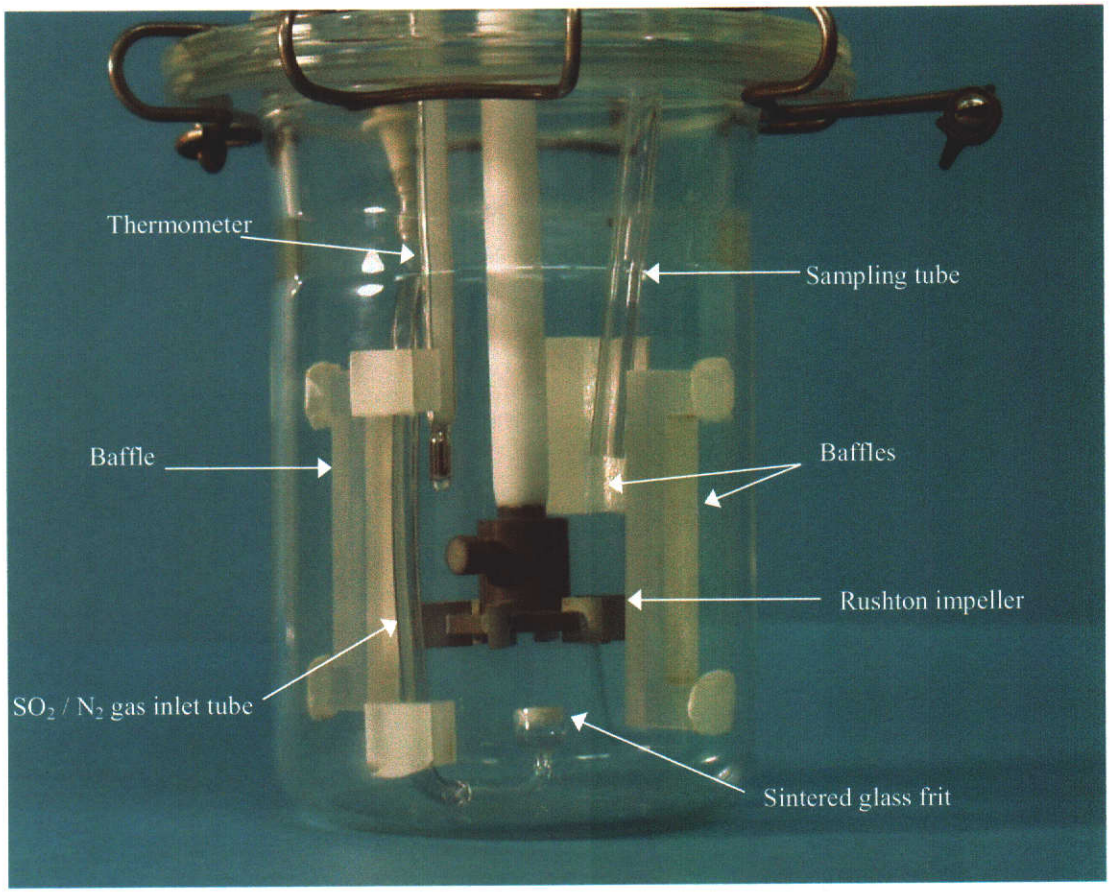

Figure 3.3 Photograph of ambient leaching vessel – close up view.

The reaction vessel was immersed in a heated water bath. All experiments were conducted at 25 ± 0.2°C.

Gas flow rates were measured using Gapmeter flow meters fitted with Gapmeter C6 and A1 flow tubes and duralium floats. Each Gapmeter was calibrated for use with sulfur dioxide and nitrogen gases.

A schematic diagram of the experimental set-up is shown in Figure 3.4

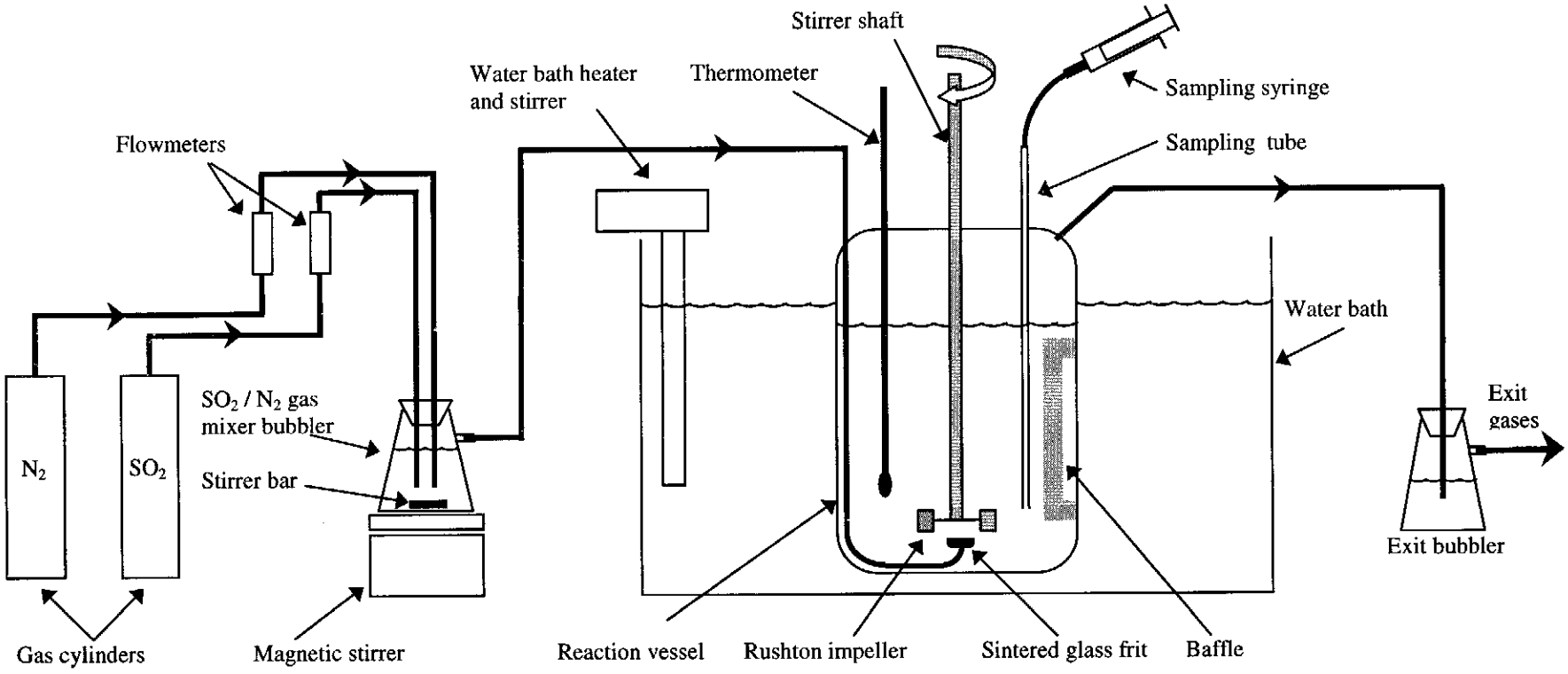

Figure 3.4 Schematic diagram of ambient leaching apparatus.

3.2.2 Calibration of Gas Flow Meters

The concentration of sulfur dioxide in the leach solution was adjusted by varying the SO_2 / N_2 gas mixture that was introduced to the reactor vessel. Three Gapmeters were used to vary the SO_2 and nitrogen flow rates whilst maintaining a constant total flow rate. Prior to use the flow meters were calibrated by timing the period taken by a film of soap in a graduated vertical tube to traverse a given distance. Timing was done manually with a Casio HS-30W stopwatch.

The flow meters used were:

- C6 Gapmeter tube with hollow duralium (HD) float
- A1 Gapmeter tube with hollow duralium (HD) float.
- C1D Platon meter with hollow duralium (HD) float

The C6 and A1 Gapmeters were calibrated for use with nitrogen and sulfur dioxide gases. The C1D Platon flow meter was calibrated for use with sulfur dioxide only. The calibration measurements were performed at room temperature (21.8 - 22.5°C) and gave the following useable ranges.

Table 3.5 Ranges of sulfur dioxide and nitrogen gas flow rates using available flow meters.

Gapmeter	Flow Rate Range (mL min^{-1})	
	Nitrogen	Sulfur dioxide
C6 + HD float	150 – 1730	210 – 1770
A1 + HD float	65 – 655	70 – 595
C1D + HD float	–	18 – 126

The higher gas flow rates were adjusted using stainless steel needle valves. A Nupro metering needle valve was used to control the lower sulfur dioxide flow rates (< 130 mL min^{-1}).

3.2.3 Method

A typical experiment involved

- preparation of sulfurous acid solution of desired concentration
- addition of zinc sulfide
- sampling of reactor slurry
- filtration of slurry at the end of the leach

Sulfurous acid preparation

Milli-Q water (794.7 ± 0.2 mL) was added to the reaction vessel and purged of air by sparging for approximately 20 minutes with high purity nitrogen gas (650 mL/min) while stirring at 500 rpm. The nitrogen was humidified prior to sparging to minimise the loss of H_2O from the reactor via evaporation. Nitrogen and sulfur dioxide gases, with a total combined flow rate of 1050 mL min^{-1}, were mixed in the 'mixer bubbler' by sparging the two gases into a stirred solution of water. The gas mixture exiting the 'mixer bubbler' was then sparged into the deoxygenated water in the reaction vessel. After 25 minutes of SO_2/N_2 sparging the water heater was turned on and the water bath heated such that the reaction solution attained 25.0°C. The sparging was continued for at least 90 minutes while stirring at 600 rpm, before the zinc sulfide was added. Gas sparging was continued throughout the duration of the leach, except in leaches where no gas flow was desired. Prior to the addition of zinc sulfide measurements of the concentration of $SO_2(aq)$ and pH of the solution were made. The increase in volume due to dissolved sulfur dioxide (Rumpf and Maurer 1992) was taken into account when determining the total solution volume.

Zinc sulfide addition

After preparation of sulfurous acid of desired concentration a known mass of ZnS was added to the reactor solution via a funnel fitted with a 15 cm piece of 10 mm i.d. PVC tube. ZnS powder adhering to the funnel was rinsed off using a previously sampled 40 mL aliquot of sulfurous acid solution. The end of the tube had slots cut into it and was long enough to be submerged beneath the solution surface. This

facilitated the delivery of the rather hydrophobic ZnS *into* the solution instead of on top of the solution.

Sampling of reactor slurry

Sampling was performed by withdrawing approximately 8 mL of slurry via a glass dip tube with a 10 mL polypropylene syringe. The dip tube was cleared of slurry before and after each sample by flushing with the SO_2/N_2 gas mixture.

Samples were syringe filtered through 25 mm 0.1 μm Supor filter membranes (Gelman Sciences). Filtrates were collected in 20 mL glass vials and sealed with a screw cap polypropylene lid. These were analysed for zinc and some for total soluble sulfur. Residues were allowed to dry and were stored for later analysis. Residues were examined via scanning electron microscopy and FT-Raman spectroscopy.

Filtration of slurry at the end of the leach

On completion of the leach, the slurry was filtered under applied air pressure through a 0.1 μm Supor membrane (47 mm diam.) using a stainless steel Sartorius pressure filter. The filtrate and residue were collected and stored for subsequent analysis.

3.3 PRESSURE LEACHING APPARATUS AND METHODS

3.3.1 Pressure leaching apparatus

Pressure leaching experiments were undertaken using a Parr 2 L zirconium (Zr 702) autoclave (Figures 3.5 and 3.6). The autoclave internals included a stirrer shaft, stirrer shaft bracket, two axial flow impellers, dip tube for slurry sampling, thermocouple well and cooling coils arranged in a serpentine fashion. These were all made from zirconium. The bushing used in the bracket was made of Teflon.

The solid sample injection tube was 10 mm titanium tube. The plug was made from teflon with an EPDM (ethylene-propylene-difunctional monomer copolymer) O–ring seal.

All valves and fittings external to the reactor vessel were stainless steel 316. Swagelok valves and fittings were used.

The temperature was controlled to ± 1°C by a Parr 4842 heater and temperature controller.

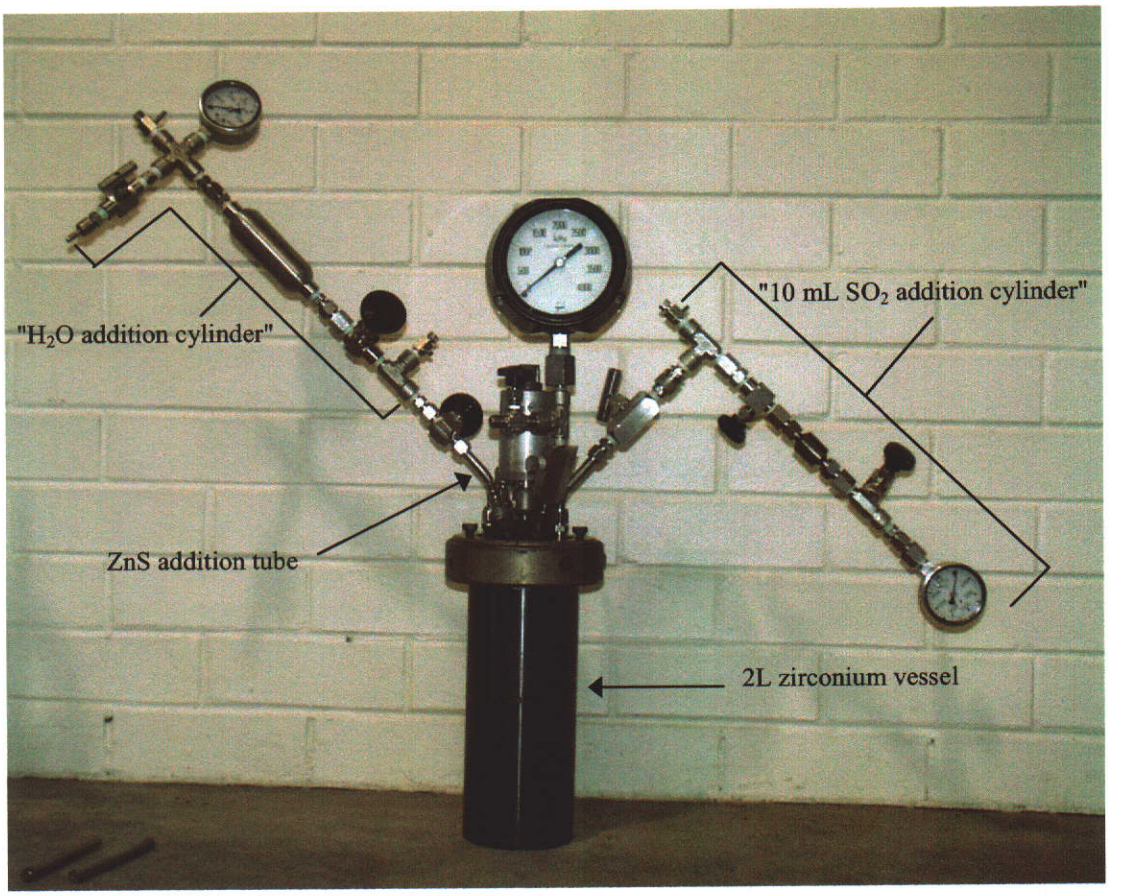

Figure 3.5 Photograph of 2 L Zirconium pressure vessel with the H_2O addition cylinder and the 10 mL SO_2 addition cylinder attached.

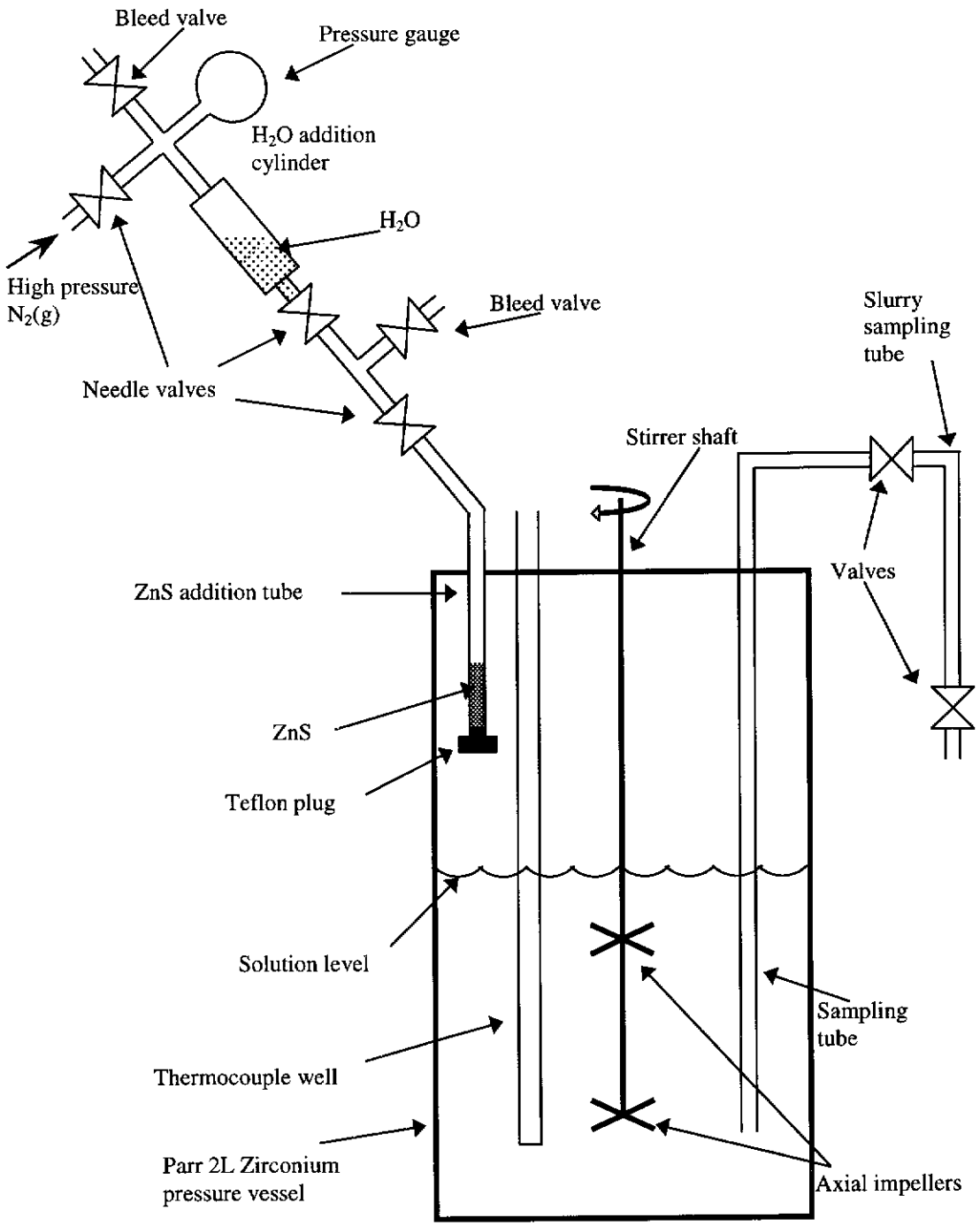

Figure 3.6 Schematic diagram of 2 L zirconium pressure vessel, showing H_2O addition cylinder, ZnS addition tube and slurry sampling tube.

3.3.2 Techniques common to leaching experiments

3.3.2.1 Pressure testing

Prior to each experiment the reaction vessel was pressure tested to a pressure in excess of that which was expected for the experiment; typically 2500 – 3000 kPa.

3.3.2.2 SO_2 liquefaction

Depending on the mass of SO_2 required for a given experiment SO_2 gas was liquefied into a 10 mL or 150 mL "SO_2 addition cylinder", which consisted of a 10 or 150 mL stainless steel 316 sample cylinder fitted with needle valves, bleed valve, check valve, pressure gauge and a fitting for connection to the outlet of the dip tube (Figure 3.7).

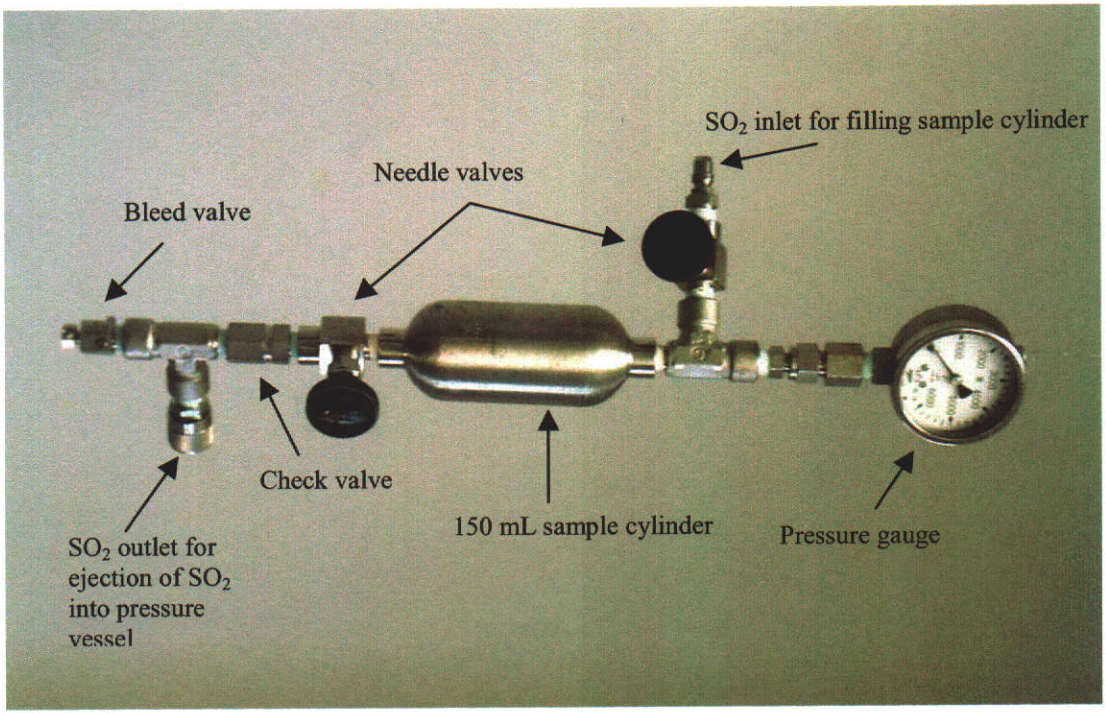

Figure 3.7 150 mL SO_2 addition cylinder

Prior to liquefaction the cylinder was evacuated and weighed. It was then flushed with nitrogen gas, and filled with $SO_2(g)$ and evacuated, three times, to ensure the absence of air.

The SO_2 inlet of the cylinder was then connected to a SO_2 gas cylinder via Teflon

tubing and SO_2 was added to it by immersing it in a crushed ice and salt slush bath (approx. $-15^{\circ}C$ to $-20^{\circ}C$). Approximately 30 minutes was sufficient to liquefy approximately 100 g of SO_2. The cylinder was then removed from the ice/salt slush, disconnected from the SO_2 gas cylinder, rinsed of salt solution and dried. Excess SO_2 was bled from the cylinder until the desired mass was achieved. It was re-weighed after injecting the SO_2 into the pressure vessel, the difference in weight being the mass of SO_2 injected.

3.3.2.3 SO_2 injection

SO_2 was injected into the pressure vessel, when it had reached the desired temperature. The SO_2 outlet of the cylinder was attached to the dip tube outlet. Air was excluded from the connection by flushing it with nitrogen gas. The cylinder was then heated using a hot air gun until the pressure in the cylinder was ~3000 kPa. The dip tube valve was then opened allowing SO_2 to enter the pressure vessel. Not all of the SO_2 was added in one injection. To add more SO_2 the dip tube valve was closed, the cylinder heated again until the pressure in the cylinder exceeded the pressure in the vessel by at least 200 kPa and then the valve re-opened to allow more SO_2 to enter the pressure vessel. This was repeated until there was insufficient SO_2 in the cylinder to generate the required pressure. The cylinder was fitted out with a check valve to prevent any possible flow of gas or liquid back into the cylinder.

3.3.2.4 ZnS injection

ZnS (synthetic or Elura concentrate) was injected into the pressure vessel, at leach temperature, via the solid addition tube (Figure 3.6). The maximum mass of solid able to be injected in this manner was ~10 g.

Prior to fitting the head of the vessel to the body, the solid addition tube was plugged at the end with a teflon plug fitted with an EPDM O–ring (SO_2 resistant). A known mass of ZnS was transferred into the solid addition tube via a glass funnel, followed by 5 mL of deionised water. Air was flushed from the tube by a slow stream of

nitrogen gas. The ZnS/H_2O mixture in the solid addition tube was injected/washed into the reaction vessel by a flow of water under high pressure, sufficient to pop open the teflon plug, using an "H_2O addition cylinder" consisting of a 75 mL stainless steel sample cylinder fitted with inlet and outlet valves, bleed valve, pressure gauge and Swagelok fitting for connection to the solid addition tube (Figure 3.8).

The cylinder was charged with 45 mL of deionised water and purged of air by a flow of nitrogen gas through the water for 15 minutes. It was then attached to the valve of the solid addition tube and nitrogen gas was flushed through the connecting pieces. To inject the ZnS/H_2O mixture, the cylinder was pressurised to approximately 2000 kPa and then the appropriate valves were opened, causing the water and ZnS to force out the teflon plug, thus allowing the contents to enter the pressure vessel.

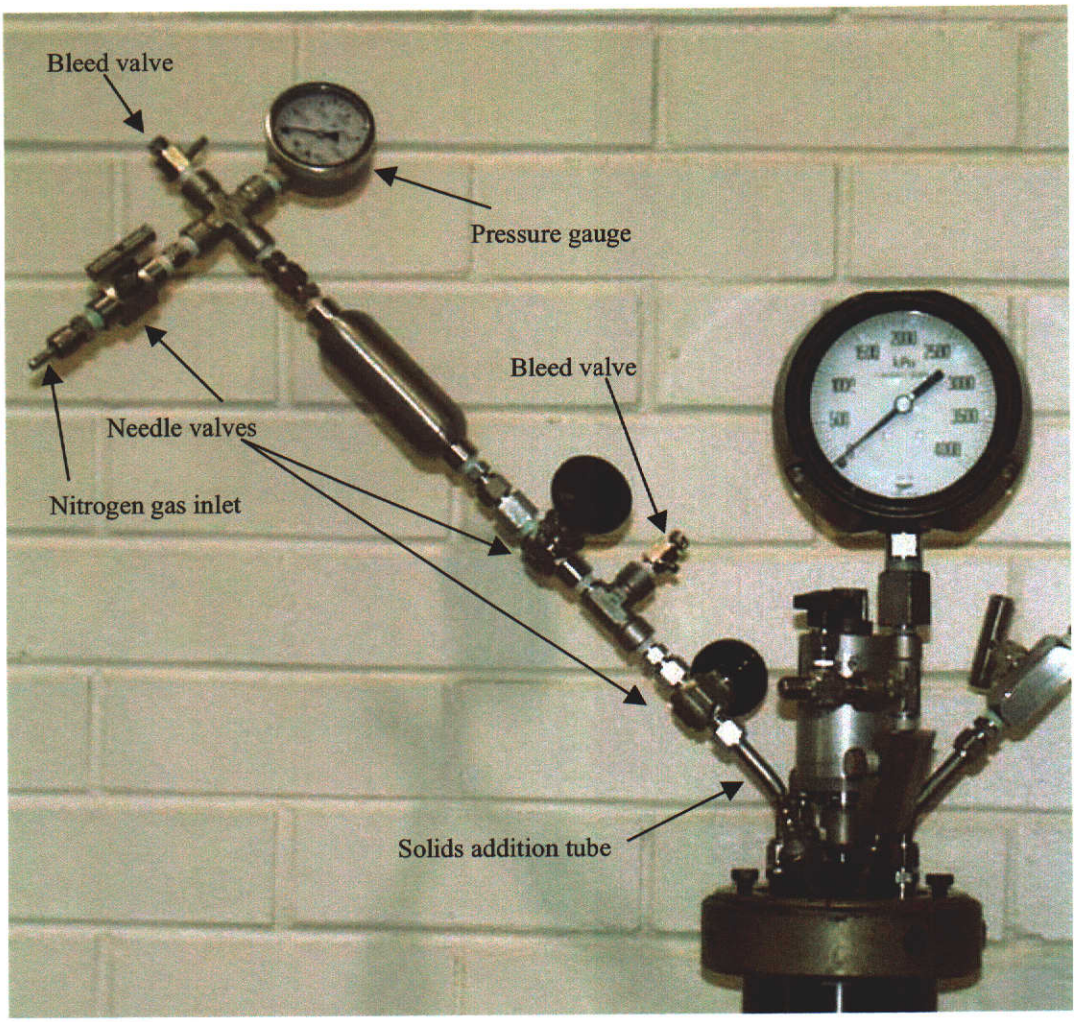

Figure 3.8 Photograph of H_2O addition cylinder connected to solids addition tube.

3.3.2.5 Surfactant addition

When desired, surfactants were injected at the same time as the concentrate or ZnS using the same method as for ZnS / water injection, except that instead of using 45 mL of deionised H_2O to inject the Elura concentrate / H_2O slurry held in the solid addition tube, 45 mL of surfactant solution was used.

3.3.2.6 Sampling of slurry and gases

Slurry

Sampling slurry from the reactor vessel involved the following steps. The slurry sampling assembly was attached to the to dip tube, and to clear the dip tube of solution, it was backflushed with nitrogen. With the valves of the slurry sampling assembly closed, the dip tube valve was opened, allowing the slurry to enter the slurry sampling assembly (Figure 3.9). The sampled solution (8 – 12 mL) was drained from the slurry sampling assembly, via PVC tubing, to a syringe with syringe filter attached and filtered through 0.1 μm Supor membranes (25 mm) immediately after sampling. The filtrates were collected in 20 mL glass containers fitted with a polypropylene screw caps and analysed for zinc. The filter residues were washed with two 5 mL portions of deionised water and left to dry in air for subsequent analysis by Raman spectroscopy or scanning electron microscopy.

After sampling the slurry, the dip tube was cleared of solution by again backflushing with high pressure nitrogen gas. Between samples, the slurry sampling assembly was disconnected from the dip tube of the vessel, rinsed with deionised water, followed by ethanol and dried using compressed air. To assist with rapid sampling (2 minute intervals) in the initial stages of a leach, two slurry sampling assemblies were used; one being rinsed while the other was being used.

Gases

Gases were sampled from the headspace using a gas sampling assembly (Figure 3.10). After sampling the headspace gas into the high pressure region (vol ~ 8 mL), it was bled into an evacuated 500 mL glass sample cylinder.

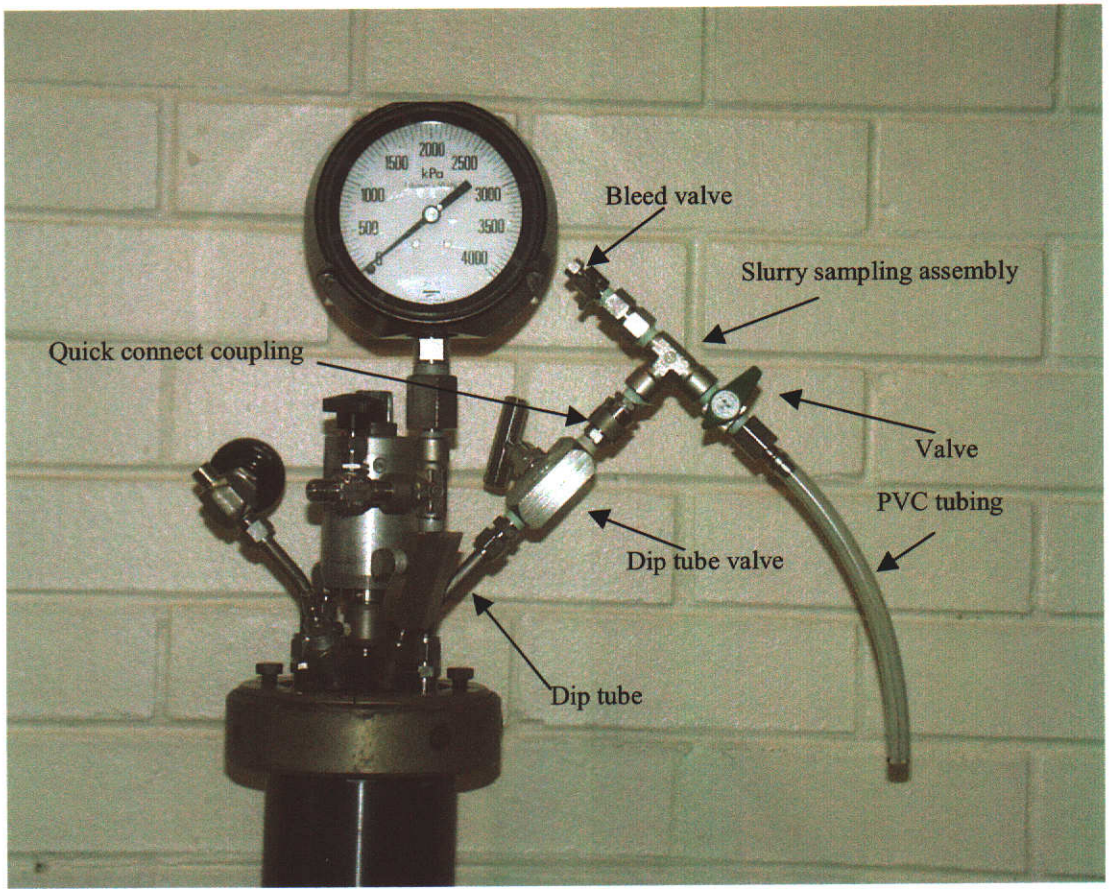

Figure 3.9 Photograph showing slurry sampling assembly connected to valve at the end of the dip tube.

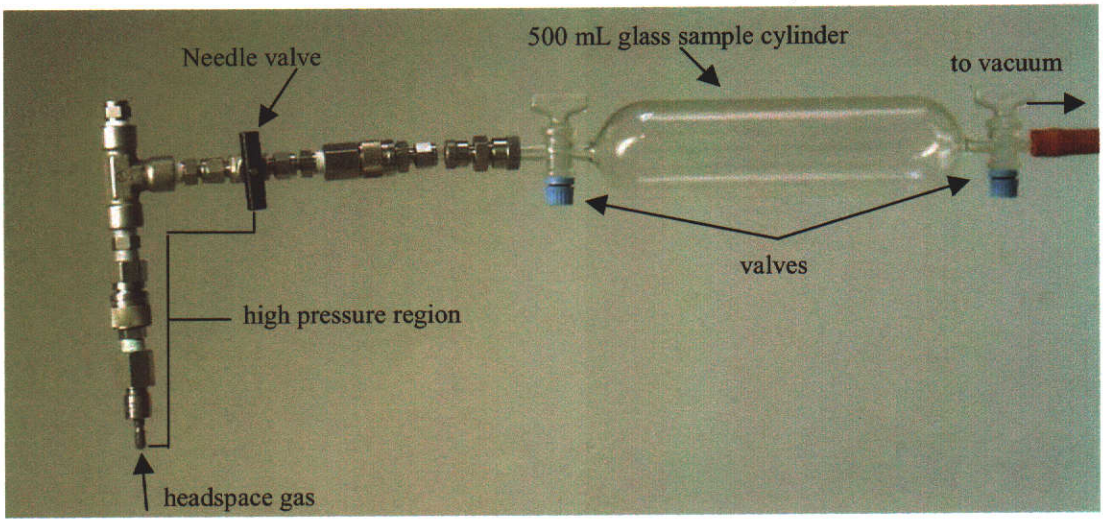

Figure 3.10 Photograph of headspace gas sampling assembly and glass sample cylinder.

3.3.2.7 Shut down procedure

After taking the final sample the pressure vessel was cooled to 35°C or lower and the overpressure of nitrogen and SO_2 gas was released and bubbled through a 250 g L^{-1} NaOH solution contained in a 1L Parr pressure vessel and a 250 ml Dreschel bottle connected in series. To assist with the removal of unreacted SO_2 from the leach solution, nitrogen was flushed through the leach solution until no odour of SO_2 could be detected. The vessel was opened after the SO_2 had been removed.

In some experiments where low masses of SO_2 were used, it was possible to simply cool the autoclave to around 35°C, vent off excess $SO_2(g)$ to atmosphere under a fume extractor. The SO_2 laden leach solutions were filtered under a fume extractor.

3.3.3 General operational sequences

Table 3.6 details the four general operating sequences used for the different leaches.

For the ZnS / H_2O / SO_2 leaches the reaction was initiated by the addition of sulfur dioxide at the set temperature.

For the ZnS / H_2SO_4 and ZnS / H_2SO_4 / SO_2 low pulp density leaches, where the amount of zinc sulfide was less than 10 g, the zinc sulfide could be injected into the leach solution containing H_2SO_4 and SO_2 at temperature, initiating the reaction.

In ZnS / H_2SO_4 / SO_2 high pulp density leaches, where larger amounts of zinc sulfide were required, the material could not be injected into the vessel at temperature and so was first added to the reaction vessel and slurried with water. The reaction was initiated by the injection of the other reagents, sulfuric acid and/or sulfur dioxide.

Table 3.6 Operational sequences for pressure leaching experiments.

Step	Type of leach			
	ZnS / H_2O / SO_2	**ZnS / H_2SO_4**	**ZnS / H_2SO_4 / SO_2**	
			Low pulp density	High pulp density
1	Add ZnS and H_2O.	Add H_2SO_4	Add H_2SO_4	Add ZnS (or concentrate) and H_2O.
2	Purge with N_2(g) for 15 minutes.	Purge with N_2(g) for 15 minutes.	Purge with N_2(g) for 15 minutes.	Purge with N_2(g) for 15 minutes.
3	Heat to set temperature.	Heat to set temperature.	Heat to set temperature.	Heat to set temperature.
4	At set temperature, set stirring speed to required rate.	At set temperature, set stirring speed to required rate.	At set temperature, set stirring speed to required rate.	At set temperature, set stirring speed to required rate.
5	Inject SO_2.	Inject ZnS.	a) Inject SO_2. b) Inject ZnS	a) Inject H_2SO_4. b) Inject SO_2.
6	Take samples	Take samples	Take samples	Take samples
7	Shut down	Shut down	Shut down	Shut down
8	Filter slurry	Filter slurry	Filter slurry	Filter slurry

3.3.4 Operating sequences for high pulp density zinc concentrate leaches in H_2SO_4 and SO_2

Elura concentrate leaches were conducted at 100°C, 150°C and 180°C. Since the method of reagent addition varied slightly between each leach, typical details of each method are given below.

- ***100°C Elura concentrate leach***

1. Elura concentrate (204.36 g) was added to the open vessel.
2. 1200 mL of water was added to the open vessel.
3. High purity nitrogen gas was bubbled through the solution via the dip tube for 15 minutes while stirring at 300 rpm.
4. After the nitrogen purge, heating of the pressure vessel to the set temperature commenced.
5. On attaining the set temperature, the stirring speed was increased to 800 rpm and two samples were taken (blanks).
6. Concentrated H_2SO_4 (224.06 g) was injected from the "H_2SO_4 addition cylinder", initiating the reaction.
7. SO_2 (109.95 g) was injected from the "SO_2 addition cylinder".

   Note: In some cases the order of steps 6 and 7 was reversed. Also in some cases SO_2 was injected only after the Elura concentrate / H_2SO_4 system had attained equilibrium.
8. Samples were taken throughout the duration of the leach.
9. At the completion of the leach, the vessel was cooled and the excess gas vented through a sodium hydroxide solution.
10. The leach solution was vacuum filtered, initially through Whatman 541 filter paper and then 0.45 μm Supor membrane (47 mm) and the filtrate collected. The residue was rinsed with deionised water and allowed to dry in an oven at 50°C.
11. The filtrate was analysed for zinc, iron (Elura concentrate samples), total sulfur, sulfate and occasionally hydrogen ion content.

- ***150°C Elura concentrate leach***

1. Elura concentrate (264.19 g), quebracho (0.2 g L^{-1}) and sodium ligninsulfonate (0.1 g L^{-1}) were added to the open vessel.

2. 1200 mL of 1.8 mol L^{-1} H_2SO_4 was added to the open vessel.
3. High purity nitrogen gas was bubbled through the solution via the dip tube for 25 minutes while stirring at 100 rpm.
4. After the nitrogen purge, heating of the pressure vessel to the set temperature commenced. SO_2 (117.62 g) was added on commencement of heating (T=15°C). The temperature reached 65°C by the time all the SO_2 had been added.
5. On attaining the set temperature (25 min after SO_2 addition), the stirring speed was increased to 800 rpm and two samples were taken (blanks).
   Following this, steps 8 – 11 from the 100°C leach were followed.

- ***180°C Elura concentrate leach***

1. Elura concentrate (260.28 g), deionised water (1200 mL), quebracho (0.2 g L^{-1}) and sodium ligninsulfonate (0.1 g L^{-1}) were added at room temperature prior to fitting the head to the reactor.
2. The headspace purged with nitrogen (high purity) for 25 minutes while stirring the pulp at 500 rpm.
3. After the nitrogen purge, heating of the pressure vessel to the set temperature commenced.
4. On attaining the set temperature, the stirring speed was increased to 800 rpm and two samples were taken (blanks).
5. SO_2 (105.3 g) was injected from the "SO_2 addition cylinder" over a period of 4 minutes.
6. 7.3 minutes after SO_2 addition had commenced, concentrated H_2SO_4 (224.8 g) was added. The commencement of the reaction (time zero) was taken as the time addition of H_2SO_4.
   Following this, steps 8 – 11 from the 100°C leach were followed.

3.3.5 Pressure leaching safety

Before each experiment the vessel and attached valves were pressure tested to a pressure in excess of the operating pressure. The SO_2 and H_2O addition cylinders were regularly pressure tested.

For any procedures requiring the addition of reagents to, or the taking of samples from the vessel while under pressure an assistant was always present. The assistant was required to be familiar with the equipment and experimental procedure so that the operator's actions could be cross-checked.

3.4 ANALYTICAL METHODS

3.4.1 Determination of zinc

For the determination of zinc, solutions were diluted to give a zinc concentration in the range 0-10 ppm, which was suitable for analysis by flame atomic absorption spectroscopy. This was done by transferring 5 mL of the filtrate to an appropriate volumetric flask. Concentrated HCl was also added to give 2% v/v HCl. AAS analyses were performed using a Varian SpectrAA-800, operating under the following conditions:

Wavelength	:	213.9 nm
Fuel/Support	:	Acetylene/air –oxidising flame
Lamp current	:	5 mA
Slit	:	1 nm

3.4.2 Determination of the concentration of aqueous sulfur dioxide in leach solutions at ambient temperature

To determine the concentration of $SO_2(aq)$ in the ambient temperature leach solutions, the solutions were first analysed for total sulfur ($SO_2(aq)$ and HSO_3^-). 10 mL aliquots of the aqueous sulfur dioxide solution were pipetted into a stirred solution of ~50 mL 0.5 $molL^{-1}$ NaOH and 50 mL water, converting all sulfur species to sulfite (Eqn. 3.1) and thus preventing loss of $SO_2(g)$ to the atmosphere.

$$SO_2(aq) + 2OH^- \rightarrow H_2O + SO_3^{2-} \qquad (3.1)$$

These were then oxidised to sulfate with 2 mL of 30% v/v H_2O_2, transferred to 500 mL volumetric flasks, made to 2% v/v HCl using concentrated HCl and then made up to the mark with either deionised or Milli-Q water. These solutions were further diluted to give [S] < 100 ppm and analysed for total sulfur via ICP-AES. A blank was included with each set of determinations.

The concentration of $SO_2(aq)$, $HSO_3^-(aq)$ and $H^+(aq)$ at equilibrium was determined using the total sulfur (SO_2, HSO_3^-) concentration and the equilibrium constant, K_{a1}, for the reaction of $SO_2(aq)$ with water (Eqn. 3.2). At 25°C, $K_{a1}^{25^\circ C} = 0.0139$ mol L^{-1} (Huss and Eckert 1977)

$$SO_2(aq) + H_2O \leftrightarrow H^+(aq) + HSO_3^-(aq) \qquad K_{a1} \qquad (3.2)$$

$$K_{a1}^{25^\circ C} = \frac{[H^+][HSO_3^-]}{[SO_2(aq)]} \qquad (3.3)$$

$$[S]_{Total} = [SO_2(aq)] + [HSO_3^-] \qquad (3.4)$$

At equilibrium,

$$[HSO_3^-] = [HSO_3^-]_{eqm}$$

$$[H^+] = [H^+]_{eqm}$$

$$\text{and } [SO_2(aq)] = [S]_{Total} - [HSO_3^-]_{eqm}$$

After substituting these expressions into equation 3.3, a quadratic expression in $[HSO_3^-]_{eqm}$ is obtained (Eqn. 3.5); the solution of which is given by equation 3.6.

$$[HSO_3^-]_{eqm}^2 + K_{a1}^{25^\circ C}[HSO_3^-]_{eqm} - K_{a1}^{25^\circ C} \times [S]_{Total} = 0 \qquad (3.5)$$

$$[HSO_3^-]_{eqm} = \frac{-K_{a1}^{25^\circ C} \pm \sqrt{(K_{a1}^{25^\circ C})^2 - 4 \times K_{a1}^{25^\circ C} \times [S]_{Total}}}{2} \qquad (3.6)$$

3.4.3 Estimation of the concentration of aqueous sulfur dioxide in leach solutions at elevated temperatures

The concentration of aqueous sulfur dioxide in the zirconium pressure vessel at elevated temperatures was determined using the total mass, partial pressure and molar volume of sulfur dioxide and equations 3.7 – 3.9.

$$V_{hdspc} = V_{reactor} - V_{soln} \tag{3.7}$$

$$V_{soln} = V_{H_2O} + n(SO_2(aq))\upsilon_{SO_2} \tag{3.8}$$

where V_{hdspc} = the volume of the head space in the vessel in litres

$V_{reactor}$ = the volume of the reactor vessel

V_{soln} = the volume of the solution in the vessel

υ_{SO_2} = the molar volume of SO_2 in water

$$n(SO_2)_{total} = \frac{m(SO_2)}{W_{SO_2}} = n(SO_2(aq)) + n(SO_2(g)) \tag{3.9}$$

where $m(SO_2)$ = mass of sulfur dioxide added to the vessel

W_{SO_2} = molecular weight of sulfur dioxide

$$n(SO_2(g)) = \frac{pV_{hdspc}}{RT} \tag{3.10}$$

$$= \frac{p}{RT}\left[V_{reactor} - V_{H_2O} - n(SO_2(aq))\upsilon_{SO_2}\right]$$

$$= \frac{p}{RT}\left[V_{reactor} - V_{H_2O} - (n(SO_2)_{total} - n(SO_2(g)))\upsilon_{SO_2}\right]$$

$$= \frac{\left[V_{reactor} - V_{H_2O} - n(SO_2)_{total}\,\upsilon_{SO_2}\right]}{\frac{RT}{p} - \upsilon_{SO_2}} \tag{3.11}$$

where p = partial pressure of SO_2

T = temperature in Kelvin

R = the universal gas constant = 8.314 J K^{-1} mol^{-1}

Substituting equation 3.11 into equation 3.9 and solving for $n(SO_2(aq))$ gives

$$n(SO_2(aq)) = \frac{\frac{m(SO_2)RT}{W_{SO_2}} - p(V_{reactor} - V_{H_2O})}{RT - p\upsilon_{SO_2}} \tag{3.12}$$

The concentration of aqueous sulfur dioxide is then

$$[SO_2(aq)] = \frac{n(SO_2(aq))}{V_{H_2O} + n(SO_2(aq))\upsilon_{SO_2}} \tag{3.13}$$

Estimation of molar volume of SO_2 in water at elevated temperatures

Values for the partial molar volume of sulfur dioxide in water (υ_{SO_2}) at temperatures above 393 K were obtained by extrapolation of a quadratic curve fitted to Rumpf and Maurer's (1992) data (Figure 3.11, Table 3.7). The expression for the fitted curve, where T is in Kelvin, is

$$\upsilon_{SO_2} = 6.3490\times10^{-4}T^2 - 3.3484\times10^{-1}T + 84.199 \tag{3.14}$$

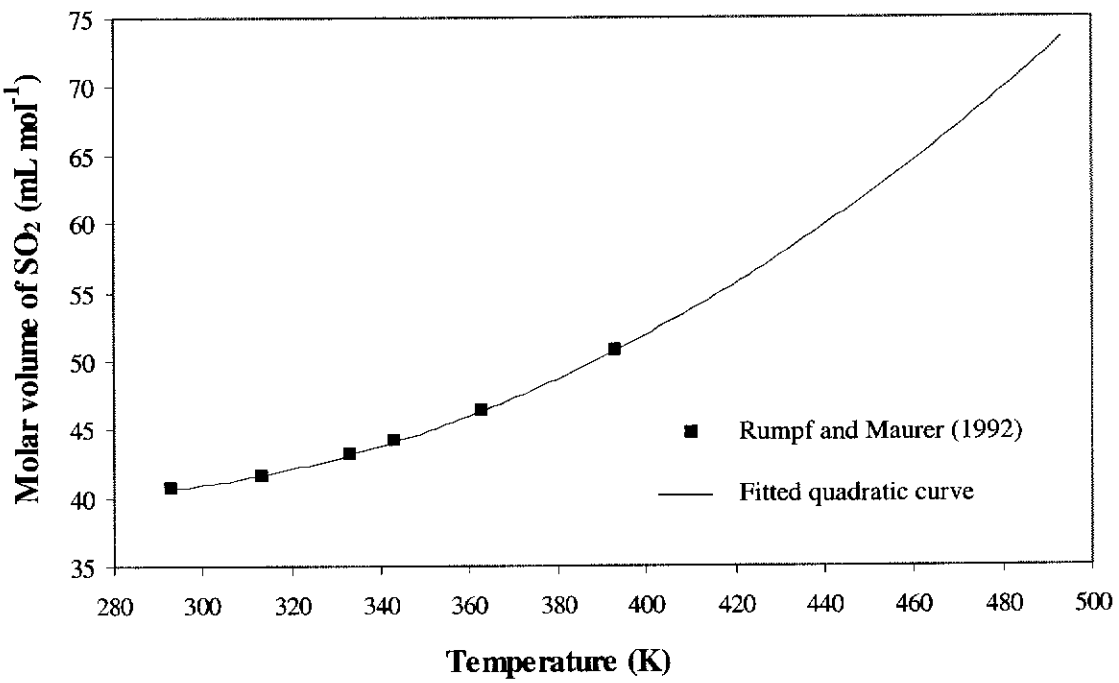

Figure 3.11 Curve fit to literature values for the molar volume of SO_2 in water and extrapolation to 200°C.

Table 3.7 Literature[a] and extrapolated[b] values for molar volume of SO_2 in water at 100°C to 200°C.

Temperature (K)	Molar volume of SO_2 in water /(mL mol^{-1})
293.16	40.6[a]
313.16	41.6[a]
333.15	43.1[a]
343.17	44.1[a]
363.17	46.3[a]
393.17	50.7[a]
403.15	52.4[b]
423.15	56.2[b]
453.15	62.8[b]
473.15	67.9[b]

[a] – Rumpf and Maurer (1992), [b] – Equation 3.14

3.4.4 Determination of sulfate

Solutions were analysed for sulfate by determination of the total sulfur content via ICP-AES at 180.734 nm using a Varian Liberty 220 ICP Emission Spectrometer. Prior to analysis solutions were diluted to give [S] < 100 ppm and acidified with HCl to give 2% v/v HCl.

3.4.5 Detection of H_2S

Lead acetate was used to test for H_2S.

In ambient leaching experiments, the gases exiting the reaction vessel were bubbled through a basic solution of saturated lead acetate or passed over filter paper which had been soaked in the lead acetate solution.

In pressure leaching experiments, the headspace gases were sampled using the gas

sampling tube according to the method given in Section 3.3.2.6. Prior to gas sampling approximately 1 mL of saturated basic lead acetate was added to the ~500 mL glass sample cylinder of the gas sampling tube. The presence of $H_2S(g)$ was evident by the formation of a brown / black precipitate (PbS), the darker the colour, the higher the concentration of H_2S.

Semi-quantitative determinations of H_2S were achieved by visual comparison of precipitates with those formed by the reaction of known amounts of $H_2S(g)$ with the lead acetate solution.

3.4.6 Determination of $[H^+]$

3.4.6.1 Determination of $[H^+]$ in sulfuric acid solutions

The hydrogen ion concentration in sulfuric acid solutions used for leaching experiments was determined by titrating the acid against a standard sodium tetraborate solution. Sodium tetraborate (AR) was recrystallised prior to use, according to the method given by Vogel (1979). Standard solutions were stored in tightly sealed Nalgene bottles. Titrations were performed using a "B" grade 50mL burette and methyl red indicator was used to determine the endpoint.

3.4.6.2 Determination of sulfuric acid in solutions containing sulfur dioxide

To determine the sulfuric acid concentration, the solutions were initially purged of sulfur dioxide. This was achieved by pipetting 10mL of the analyte into 2-4 mL of deionised water at 60-65°C, which had previously been sparged with nitrogen gas for 5 minutes. Nitrogen sparging (200-300 mL min^{-1}) was continued at this temperature for at least 5 minutes.

The resulting sulfur dioxide free solution was then titrated against a sodium hydroxide solution which had been standardised by titrating against a standard 0.5 mol L^{-1} HCl solution (Convol). Titrations were performed using a Metrohm 716 DMS Titrino automatic titrator.

3.4.6.3 pH measurements

Measurements of pH were made using an Orion Ross combination pH probe (Model 815600) and an Orion 290A pH meter. The pH meter was calibrated prior to use using the following pH buffers.

- pH 4 and 7, BDH and Radiometer Copenhagen
- pH 1.01 (25°C), Merck (Titrisol)
- pH 1.681 (25°C), the buffer solution was prepared by dissolving 3.1525 g of potassium tetroxalate dihydrate ($KH_3(C_2O_4)_2.2H_2O$) in approximately 150 ml of Milli-Q water and making up to 250 mL at 22.1°C. The potassium tetroxalate dihydrate was a certified secondary reference material supplied by Merck (Batch no. B682361 542).

3.4.7 Gravimetric determination of elemental sulfur

The amount of elemental sulphur in the leach residues was determined gravimetrically. The leach residue was weighed into a pre-weighed extraction thimble, which was then placed in a 60 mL Soxhlet apparatus fitted with a condenser and 250 mL round bottom flask. Whatman cellulose, single thickness extraction thimbles (28mm x 80 mm) were used. Approximately 100 mL of tetrachloroethylene was used as the extractant. Each reflux cycle took about 6 minutes and extractions were carried out for a total of 90 minutes. The thimble was removed, allowed to dry in a fume cupboard and further dried in an oven at 50°C. The dried thimble, containing residue, was then weighed, the difference in weight being the mass of elemental sulfur.

3.4.8 Raman spectroscopy

Two Raman spectrometers were utilised to obtain Raman spectra.

FT-Raman spectra were obtained using a Nd:YAG laser (1064 nm) with up to 800 mW of power and a Bruker RFS 100 spectrometer. A resolution of 4 cm^{-1} was used and at least 256 scans were accumulated. Spectra were manipulated using OPUS 2.0 software.

Dispersive Raman spectra were obtained with a Dilor Labram 1A spectrometer using the 514.532 nm line from a 75 mW Argon ion laser or the 632.817 nm line from a 17 mW Helium-Neon laser.

For Raman analysis approximately 1.5 mL of each filtrate was transferred to 8 mm × 39 mm borosilicate glass vials fitted with polypropylene caps. To exclude air, the headspaces were purged with high purity nitrogen gas prior to sealing.

Intensities (areas) of peaks obtained using the Bruker RFS 100 and Dilor Labram 1A spectrometers were determined by integrating peaks using OPUS 2.0 and Dilor Labspec V 2.0 software, respectively. Errors in measured peak areas from the Dilor Labram 1A spectrometer were determined by performing at least 10 area measurements of a given peak and calculating the standard deviation. Peak intensities for aqueous species were normalised relative to the 1650 cm^{-1} peak of H_2O.

3.4.9 X-ray powder diffraction

Mineral phases were identified from X-ray powder diffraction data. Diffraction data were obtained with a Philips X'Pert automatic powder diffractometer using cobalt Kα X-rays, and were analysed by comparison with spectra in the International Crystallographic Diffraction Database (Set 49, 1999). Analyses were undertaken using XPLOT for Windows (Version 1.34). As an example, a spectrum of a synthetic zinc sulfide containing sphalerite and wurtzite is compared with ICDD peaks for the pure sphalerite and wurtzite phases in Figures 3.12 and 3.13, respectively. The specific phase is shown in red in each figure.

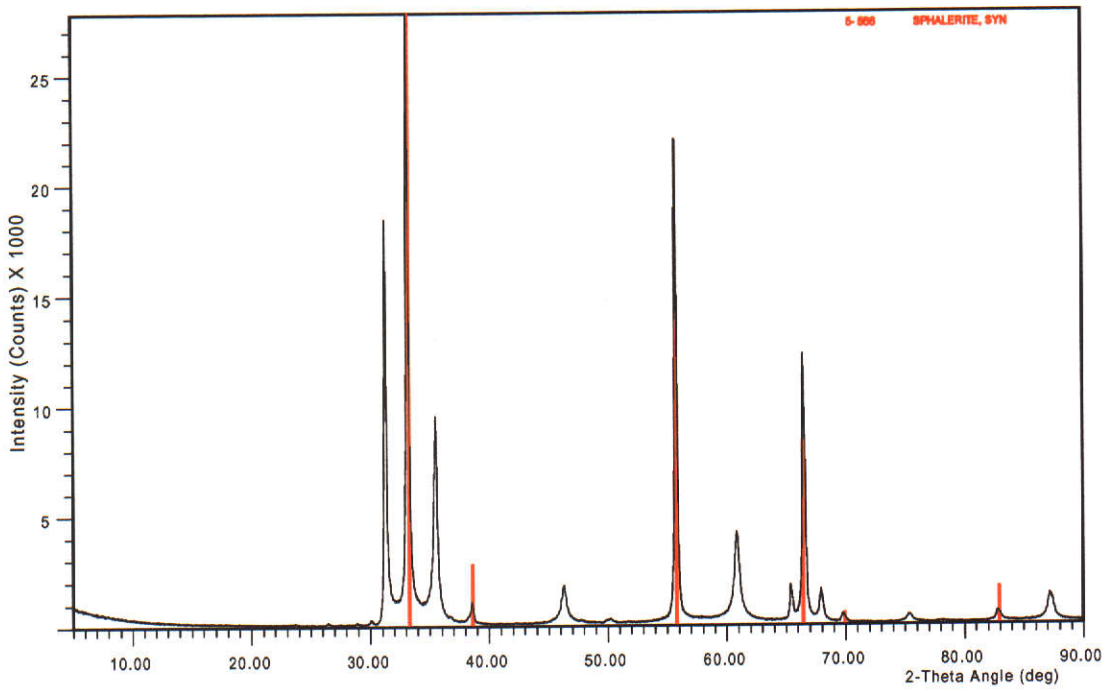

Figure 3.12 XRD of synthetic ZnS (Alfa, Johnson Matthey) with ICDD peaks for sphalerite overlaid.

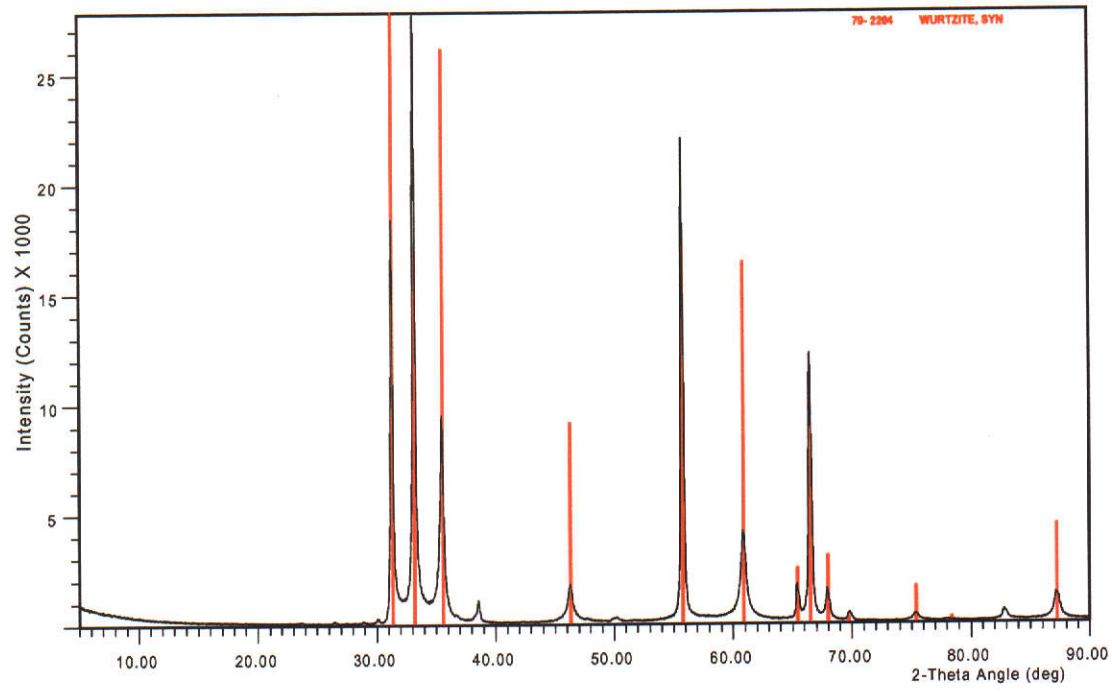

Figure 3.13 XRD of synthetic ZnS (Alfa, Johnson Matthey) with ICDD peaks for wurtzite overlaid.

Semi-quantitative phase composition analysis of synthetic sulfides was obtained as follows. The 38.58° peak of sphalerite and the 46.30° peak of wurtzite were found to be unique to each spectra and these were used in the analysis. The area of each peak was determined using Traces (Version 4.0) software. Using the International Crystallographic Diffraction Database (Set 49, 1999) these peaks had relative intensities of 10 and 32.7, respectively. In order to estimate the relative abundance of each phase the peaks were scaled to an intensity of 100. The sphalerite composition was calculated using equation 3.15, with *A*(sphalerite) and *A*(wurtzite) being, respectively, the areas of the sphalerite and wurtzite peaks.

$$\%\ \text{sphalerite} = \frac{A(\text{sphalerite}) \times \frac{100}{10}}{A(\text{sphalerite}) \times \frac{100}{10} + A(\text{wurtzite}) \times \frac{100}{32.7}} \times 100\% \qquad (3.15)$$

The phase compositions of the synthetic zinc sulfides used in this work are listed in Table 3.1 (p. 39).

3.4.10 Scanning electron microscopy

Images were obtained using Jeol JSM–LV and Philips XL40/CP scanning electron microscopes. The accelerating voltage was typically 20 k eV and both secondary electron and backscatter electron images were collected. Samples were mounted on adhesive carbon tape or set in resin and then either carbon or gold coated using a Dynavac Mini Coater.

3.5 MEASUREMENT OF INITIAL REACTION RATES FROM LEACH DATA

Initial zinc dissolution rates were obtained from plots of measured zinc concentration (mol L^{-1}) versus time. The initial rate (at t=0) was taken from the slope of the

polynomial curve of best fit to the first three or four points. In some cases, the slope was taken as the average slope of all polynomials that fitted the first three or more points. Polynomials that had the origin as point of inflexion, or which showed strong deviations in curvature at t=0 were discounted. The error in the slope was taken as the standard deviation of the measured slopes, or if only one polynomial curve was fitted to the data points the error was taken as the error in the polynomial's first order term.

4 AMBIENT LEACHING OF ZINC SULFIDE BY AQUEOUS SULFUR DIOXIDE

4.1 KINETICS AND MECHANISM OF ZnS DISSOLUTION IN SO_2(aq)

Since two differing views of the mechanism for the reaction between ZnS and aqueous solutions of sulfur dioxide have been proposed *viz.*, non-oxidative dissolution and oxidative dissolution, this investigation was aimed at clarifying the mechanism under ambient conditions.

The orders of reaction with respect to $[H^+]$ and $[SO_2(aq)]$ are likely to differ between an oxidative process and a non-oxidative process. Thus, by determining the order of reaction with respect to hydrogen ions and sulfur dioxide it should be possible to identify which process is occurring.

4.1.1 Optimisation of leaching parameters

Being a heterogeneous system, it was necessary to first optimise parameters such as the stirring speed and gas flow rate so that possible diffusion effects could be eliminated. The effect of varying pulp density was also investigated in these optimisation experiments as it was considered that it might affect the leaching kinetics, if dissolution occurred via the non-oxidative pathway.

Experiments on the effect of H^+ and $SO_2(aq)$ on the reaction rate were conducted using the optimum conditions.

4.1.1.1 Agitation

In SO_2 saturated solutions, increasing the agitation from 600 to 950 rpm had no effect on the leaching rate, indicating that the reaction rate was not diffusion controlled, but controlled by reaction at the solution mineral interface (Figure 4.1). If it had been diffusion controlled the leaching rate would have been expected to increase with increasing stirring speed.

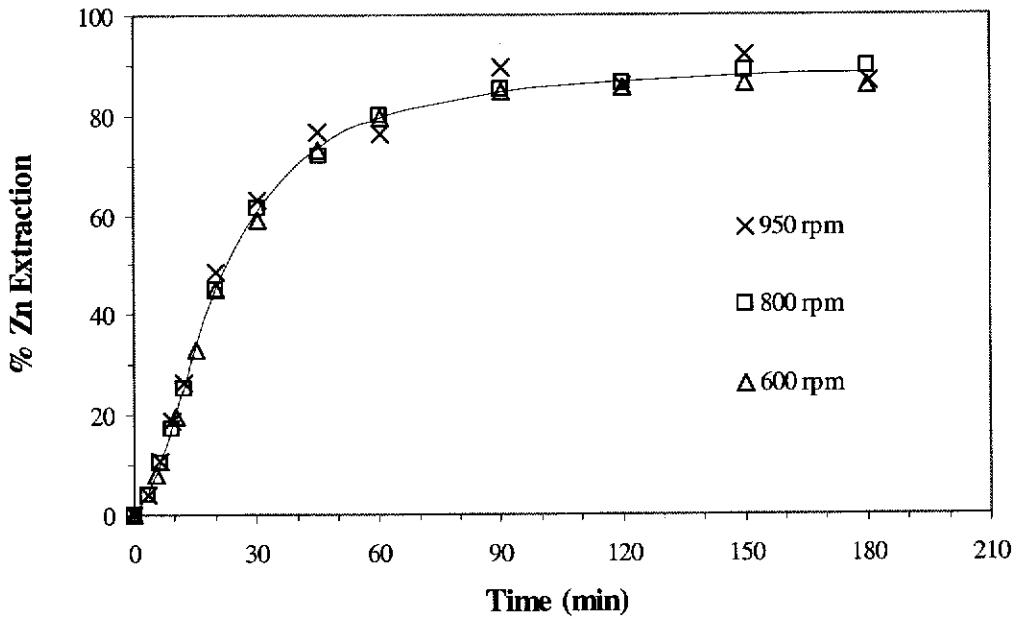

Figure 4.1 Effect of stirring speed on the rate of dissolution of ZnS-A (5.39 μm) in $SO_2(aq)$. $[SO_2(aq)]$ = 1.3 mol L^{-1}, T = 25°C, Pulp density = 4 g L^{-1}, $SO_2(g)$ flow rate = 1050 mL min^{-1}

4.1.1.2 SO_2 flow rate

Varying the SO_2 flow rate from zero to 1050 mL min^{-1} also had no effect on the dissolution rate (Fig. 4.2). This also suggests that under these conditions the reaction rate is not controlled by diffusion of species to or from the solid / solution interface.

Subsequent measurements were conducted using a total gas flow rate (i.e. SO_2 and/or

N_2) of 1050 mL min^{-1} because, with the flow meters available, it was more accurate to prepare SO_2 / N_2 mixtures at higher flow rates.

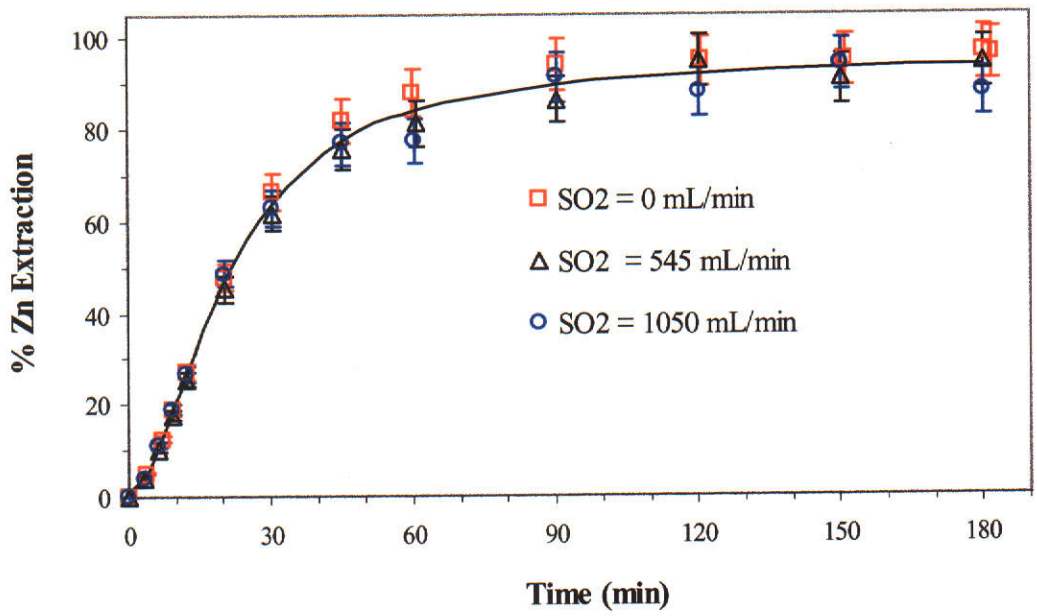

Figure 4.2 Effect of $SO_2(g)$ flow rate on zinc extraction.
$[SO_2(aq)]$ = 1.3 mol L^{-1}, T = 25°C, Stirring speed = 950 rpm, Pulp density = 4 g L^{-1}.

4.1.1.3 Pulp density

It has been postulated that the dissolution of ZnS could proceed non-oxidatively, i.e. by acid dissolution (Eqn. 1.10, p. 6). Since, the non-oxidative dissolution reaction is reversible with the overall dissolution rate described by equation 2.27 (p. 21), it is necessary that the dissolution reaction (the forward reaction) be isolated as much as possible from any possible reverse reaction. This can be achieved by reducing the pulp density.

Reducing the pulp density below 0.98 g L^{-1} caused little increase in the initial dissolution rate (% Zn vs time) under the chosen conditions (Figure 4.3), indicating that at pulp densities below 0.98 g L^{-1} the rate of the reverse reaction was negligible. In subsequent experiments where the effects of H^+ and SO_2 on the rate of the dissolution reaction were of interest, a pulp density of 0.5 g L^{-1} was employed.

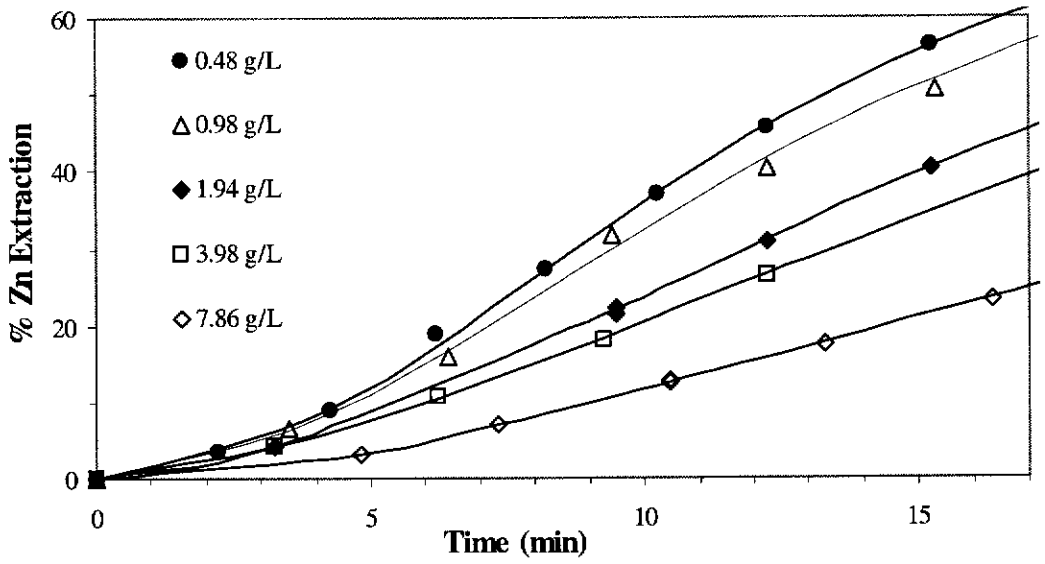

Figure 4.3 Effect of pulp density on zinc extraction in initial stages.
T = 25°C , $[SO_2(aq)]$ = 1.3 mol L^{-1}, SO_2 flow = 1050 mL min^{-1}, Stirring speed = 800 rpm.

Increasing the pulp density above 0.98 g L^{-1} caused the dissolution rate to decrease, but not the amount of zinc extracted (Figure 4.4). This effect indicates the presence of a reverse reaction whereby the products react to re-precipitate ZnS.

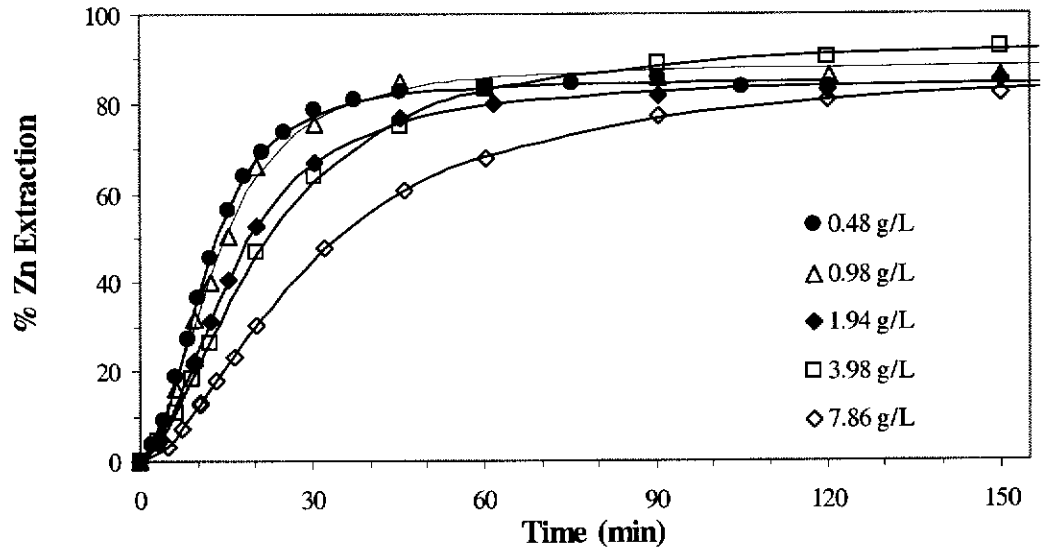

Figure 4.4 Effect of pulp density on zinc extraction.
T = 25°C , $[SO_2(aq)]$ = 1.3 mol L^{-1}, SO_2 flow = 1050 mL min^{-1}, Stirring speed = 800 rpm.

SEM and Raman microscopy of sample residues taken after 30 minutes of leaching from the leach that experienced the greatest inhibition (pulp density = 7.86 g L^{-1})

showed that the residue consisted mainly of zinc sulfide particles with only a few particles of sulfur, the presence of sulfur and zinc sulfide being confirmed by Raman spectroscopy (Figures 4.5 and 4.6). The surfaces of some of the ZnS particles were examined via Raman spectroscopy to see if a thin layer of sulfur was coating the particles, however none was detected. In this leach, which experienced the greatest inhibition, elemental sulfur ought to have been readily observed if it had caused inhibition by coating the ZnS particles. That sulfur was not observed to coat the ZnS particles and that it was not abundant in the leach residue suggests that elemental sulfur is not a cause of the decrease in the dissolution rate. The exclusion of elemental sulfur as a cause of inhibition in aqueous SO_2 leaching of ZnS has also been proposed by Larsen (1984).

The reduction in leach rate also cannot be attributed to a lack of reagents as the constant flow of SO_2 through the solution and the rapid rate of hydrolysis of SO_2 (De Maeyer and Kustin 1963) would have ensured that $SO_2(aq)$ and $H^+(aq)$ concentrations remained constant.

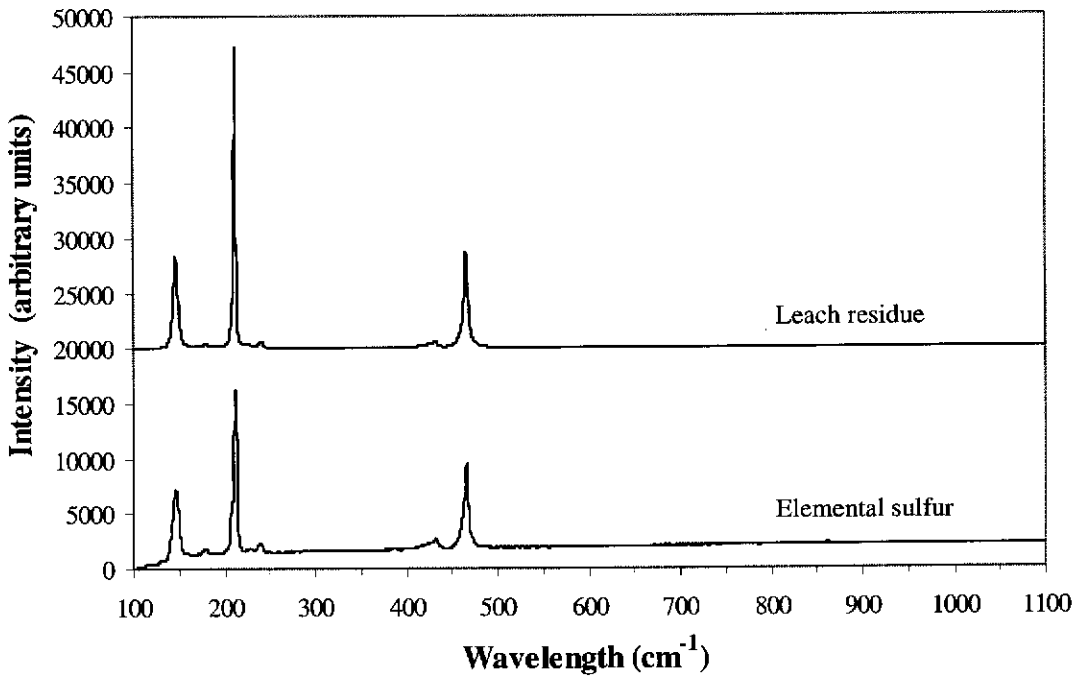

Figure 4.5 Dispersive Raman spectrum (He-Ne, 632.817 nm) showing the presence of elemental sulfur in the solids of a sample taken after 30 minutes of leaching.
Leach conditions are the same as in Figure 4.4 with pulp density = 7.86 g L^{-1}.

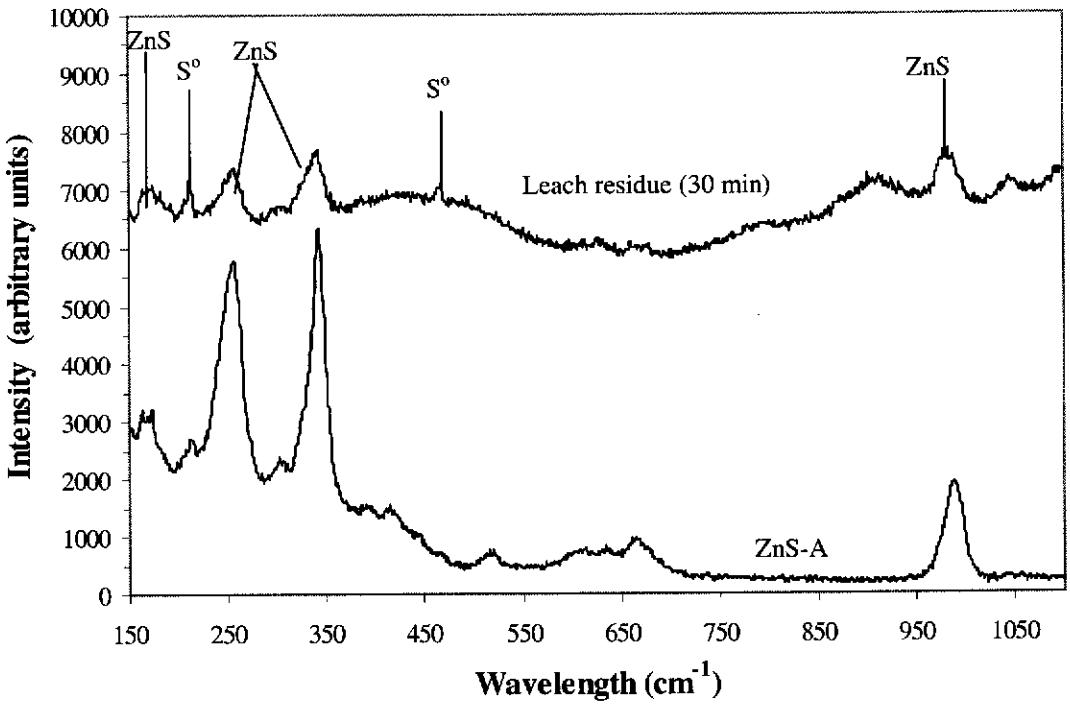

Figure 4.6 Dispersive Raman spectra (He-Ne, 632.817 nm) of ZnS-A (5.39 μm) and the leach residue (after 30 min leaching) showing the presence of zinc sulfide and elemental sulfur in the residue of a sample taken after 30 minutes of leaching.
Leach conditions are the same as in Figure 4.4 with pulp density = 7.86 g L^{-1}.

4.1.1.4 Leach curve shape and reproducibility of initial rates

The leach curves obtained were all S-shaped (Figures 4.1, 4.2 and 4.3). This was most probably caused by the ZnS powder, on addition to the solution, not completely dispersing immediately, but some remaining together in loose aggregates. Over time, these aggregates would be gradually broken down by the action of the impeller, increasing the overall surface area. The formation of agglomerates was probably due to the hydrophobicity and small particle size of the ZnS powder.

The breakdown of aggregates was confirmed by separate stirring tests. Figure 4.7 shows that, when ZnS-A (5.39 μm) is added to a stirred solution of water that has nitrogen gas flowing through it, after 2 minutes of agitation, about 14% of the particles are larger than 100 μm, but as stirring continues the percentage of particles greater than 100 μm decreases.

Increasing stirring time also increases the number of particles smaller than 10 μm. However, even after 60 minutes of stirring the average particle size (12.55 μm) is still greater than the average sonicated / dispersed particle size (5.39 μm), indicating that the agitation is not vigorous enough to break up the aggregates.

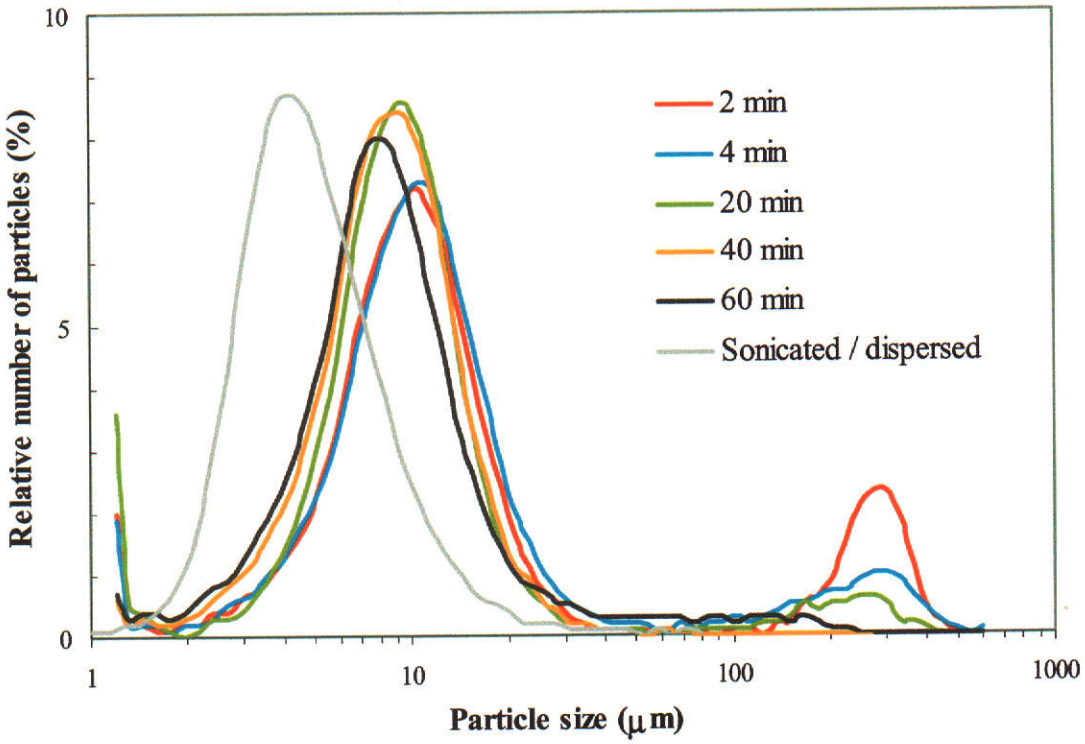

Figure 4.7 Effect of stirring time on particle size distribution of 0.4 g ZnS-A (5.39 μm) powder in 760 mL H_2O stirred at 800 rpm.
Nitrogen flow = 1050 mL min^{-1} T = 25.0°C

Although the ZnS surface area increased with stirring time, it did so consistently since reproducible kinetics were obtained (Figure 4.8, Table 4.1).

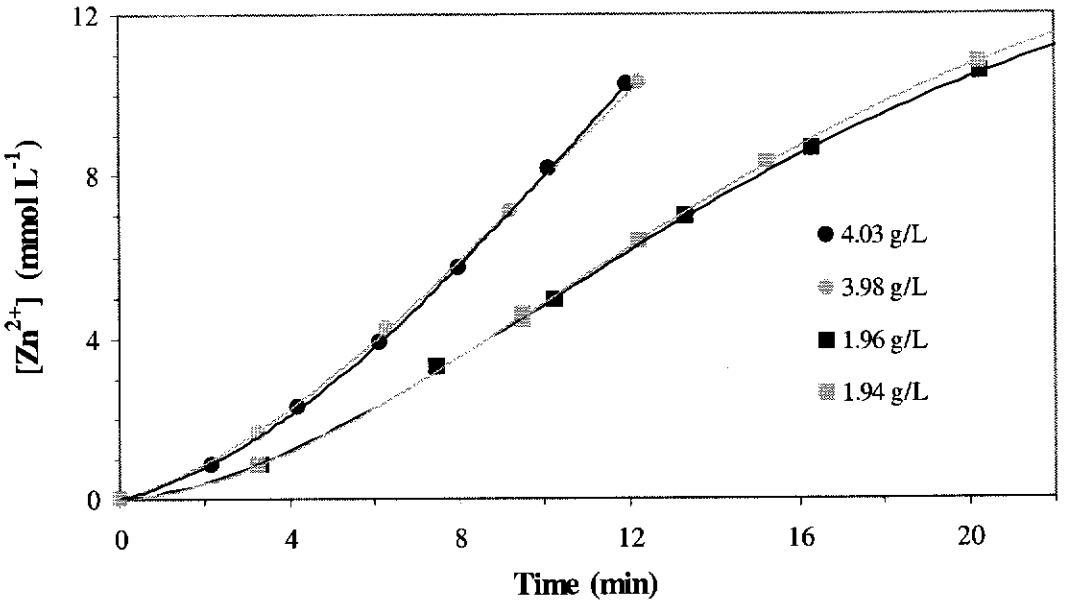

Figure 4.8 Reproducibility of dissolution kinetics.
T = 25°C , $[SO_2(aq)]$ = 1.3 mol L^{-1}, SO_2 flow = 1050 mL min^{-1}, Stirring speed = 800 rpm

Table 4.1 Reproducibility of initial rates of dissolution of ZnS-A (5.39 μm) in sulfurous acid.
Experimental conditions are as given in Figure 4.8

Pulp density ($g\ L^{-1}$)	Rate ($d[Zn^{2+}]/dt$) at t=0 ($mmol\ L^{-1}\ min^{-1}$)
1.94	0.14 ± 0.06
1.96	0.12 ± 0.06
4.03	0.33 ± 0.04
3.98	0.31 ± 0.08

4.1.2 Effect of SO_2 on initial dissolution rate

The effect of $SO_2(aq)$ on the initial dissolution rate was investigated under the determined optimal experimental conditions, i.e.

Stirring speed : 800 rpm
Total (SO_2/N_2) gas flow rate : 1050 mL min^{-1}
ZnS pulp density : 0.5 g L^{-1}

It was found that the dissolution of ZnS increased with increasing concentration of SO_2 (Figure 4.9).

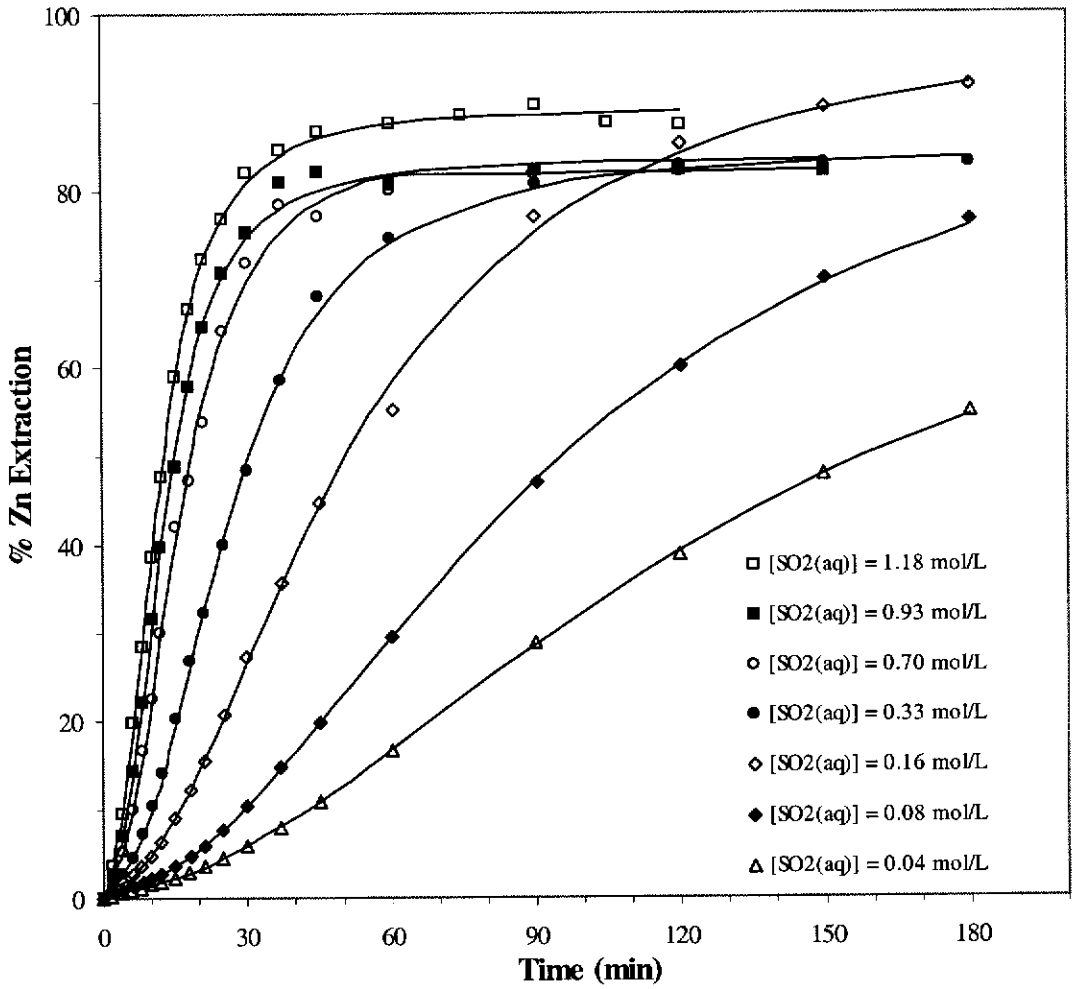

Figure 4.9 Effect of $[SO_2(aq)]$ on dissolution of ZnS in aqueous solutions of $SO_2(aq)$ at 25°C. Pulp density = 0.5 g L^{-1}. 800 rpm. Total gas flow rate = 1050 mL min^{-1}.

The initial dissolution rate ($d[Zn^{2+}]/dt$) was found to be half order with respect to $SO_2(aq)$ (Figure 4.10). The intercept is zero, within experimental error ($1\times10^{-6} \pm 3\times10^{-6}$).

$$\frac{d[Zn^{2+}]}{dt} = (4.1\times10^{-5} \pm 0.5\times10^{-5})\times[SO_2(aq)]^{0.5} \qquad (4.1)$$

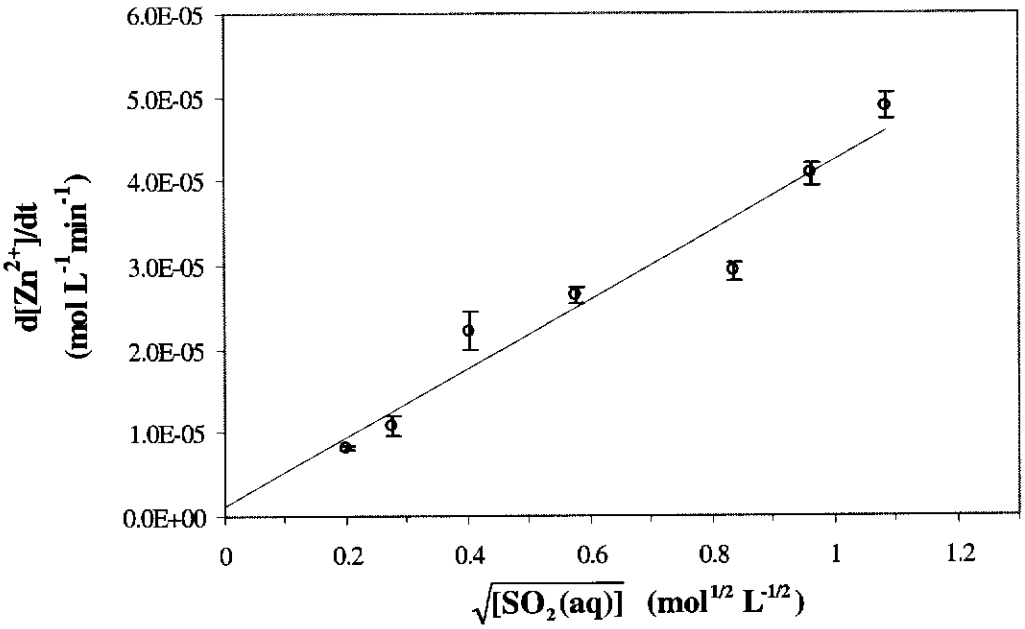

Figure 4.10 Effect of $[SO_2(aq)]$ on initial dissolution rate of ZnS-A (5.39 μm) in $SO_2(aq)$ at 25°C. Pulp density = 0.5 g L^{-1}, 800 rpm, $SO_2(g)$ flow rate = 1050 ml min^{-1}

However, this does not necessarily indicate that SO_2 is involved in the reaction, as hydrogen ions are also present in the solution, via the equilibrium shown in equation 2.35 (p. 26), i.e.

$$SO_2(aq) + H_2O \leftrightarrow H^+(aq) + HSO_3^-(aq)$$

The concentration of hydrogen ions was determined using the equilibrium constant for the dissociation of aquated sulfur dioxide, $K_{a1}^{25^\circ C} = 0.0139$ mol L^{-1} (Huss and Eckert 1977), which gives

$$[H^+(aq)] = 0.1179[SO_2(aq)]^{0.5} \quad (4.2)$$

and when the effect of hydrogen ion concentration on the reaction rate was evaluated, a linear relationship was observed (Eqn. 4.3, Figure 4.11).

$$\frac{d[Zn^{2+}]}{dt} = \left(3.5\times10^{-4} \pm 0.4\times10^{-4}\right)[H^+(aq)] \quad (4.3)$$

The intercept was zero, within experimental error ($1\times10^{-6} \pm 3\times10^{-6}$), as before, indicating that the line of best fit passes through the origin and hence, that this is a true first order relationship.

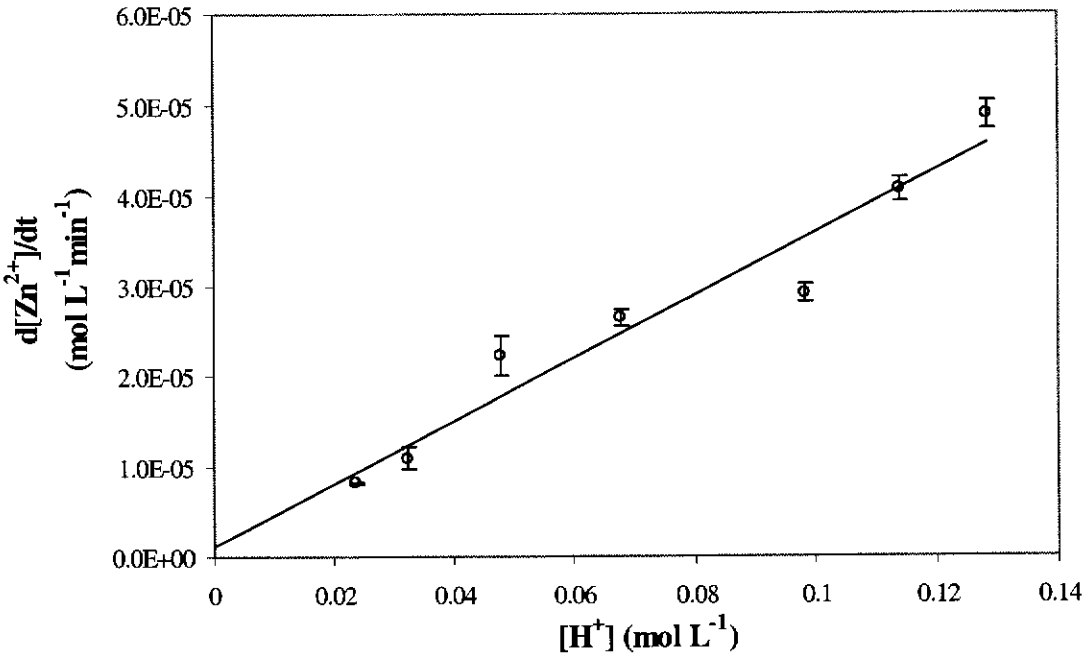

Figure 4.11 Effect of $[H^+(aq)]$ on dissolution rate of ZnS-A (5.39 μm) in $SO_2(aq)$ at 25°C. Pulp density = 0.5 g L^{-1}, 800 rpm, $SO_2(g)$ flow rate = 1050 ml min^{-1}

This result suggests that dissolution of ZnS is occurring non-oxidatively since a first order relationship between the dissolution rate and $[H^+]$ is also observed in acids, where ZnS undergoes non-oxidative dissolution, *viz.* sulfuric (Crundwell and Verbaan 1987; Locker and deBruyn 1969; Romankiw and de Bruyn 1965; Tiwari 1977) and hydrochloric acids (Locker and deBruyn 1969; Majima and Awakura 1985; Majima, Awakura and Misaki 1981).

The observed half order of reaction with respect to $[SO_2(aq)]$ is thus most likely a consequence of the relationship between $[H^+]$ and $[SO_2(aq)]$ in aqueous solutions (Eqn. 4.2).

Hence, in sulfurous acid at ambient temperatures, ZnS dissolution occurs via non-oxidative reaction between hydrogen ions and the solid (Eqn. 1.10, p. 6). SO_2 does not play a direct role in the leaching of ZnS, but by reaction with water acts as a source of hydrogen ions (Eqn. 2.35, p. 26).

4.1.3 Sulfurous vs sulfuric acid leaching

Because of the similarity between sulfurous and sulfuric acids, it was appropriate to compare the leaching kinetics of ZnS in each of these acids, as a means of dispelling any doubts that SO_2 is not an active species in the reaction.

In sulfuric acid, ZnS dissolution is affected by the presence of $H_2S(aq)$ due to the equilibrium equation 2.23 (p. 20), i.e.

$$ZnS + 2H^+ \leftrightarrow Zn^{2+} + H_2S$$

In the absence of any gas flow, equilibrium is attained as expected, since H_2S is not removed, but when nitrogen gas is flushed through the solution, removing H_2S, the reaction goes to completion (Figure 4.12). The initial dissolution rates ($0 < t < 8$ min) were equivalent with or without a flow of nitrogen gas indicating that, under the chosen conditions, the rate of the reverse reaction was negligible (Figure 4.13). When these leach curves are compared with that for the dissolution of ZnS in sulfurous acid, similar initial leach rates are observed (Figure 4.13). Since ZnS dissolves in sulfuric acid non-oxidatively (Crundwell and Verbaan 1987; Locker and deBruyn 1969; Romankiw and de Bruyn 1965; Tiwari 1977), this is added evidence in support of the previous conclusion that dissolution in sulfurous acid occurs via reaction with hydrogen ions. It is highly unlikely that acid dissolution and an SO_2 based reaction would have coincidentally identical rates.

The leach curves (Figures 4.12 and 4.13) also indicate that removal of hydrogen sulfide by reaction with aqueous sulfur dioxide is more effective than physically removing it with a flow of nitrogen gas. In the case of the sulfurous acid leach, the gas flow rate was zero and consequently the hydrogen sulfide was not removed physically but rather by reaction with aqueous sulfur dioxide.

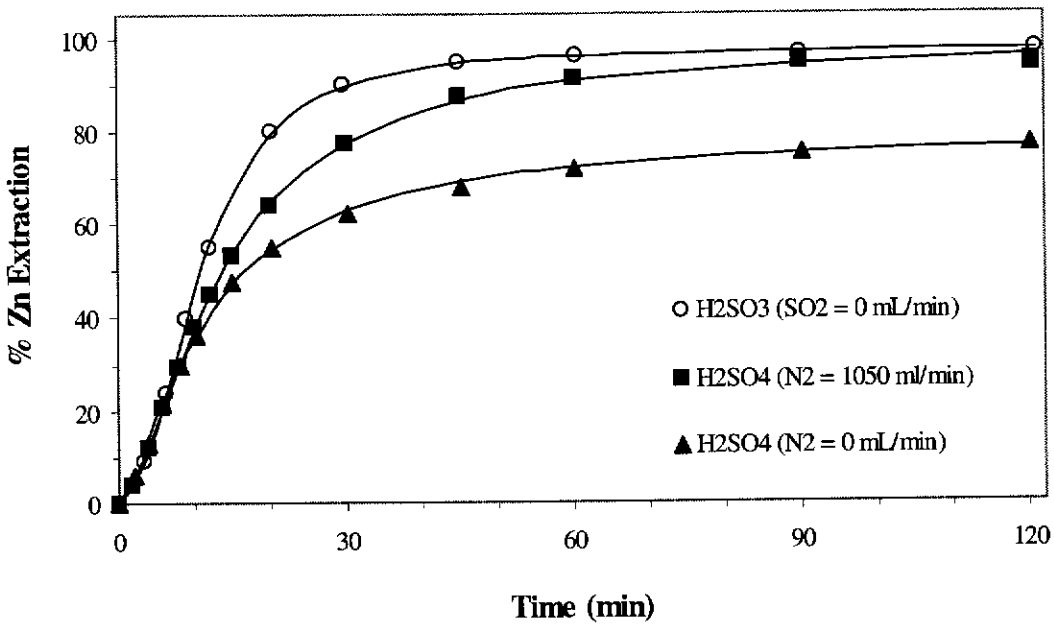

Figure 4.12 Dissolution of ZnS in sulfurous and sulfuric acids at pH 0.90.
T = 25°C, Stirring speed = 800 rpm (except for H_2SO_3 - 950 rpm), $[SO_2(aq)]$ = 1.32 mol L^{-1} ZnS = 0.5 g L^{-1}

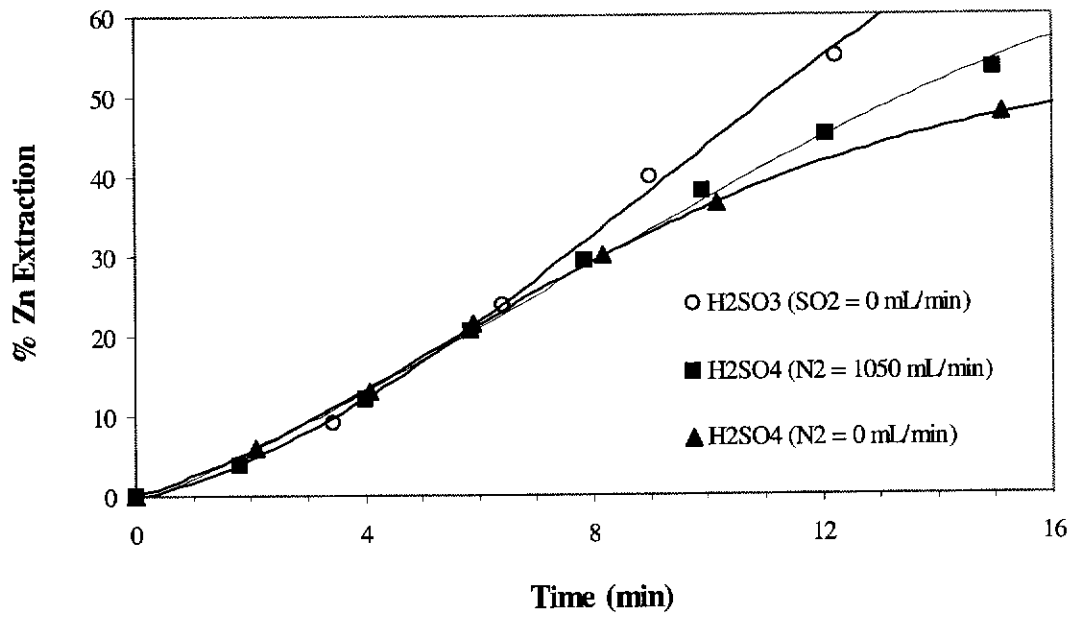

Figure 4.13 Initial stage of dissolution of ZnS in sulfurous and sulfuric acids at pH 0.90.
T = 25°C, Stirring speed = 800 rpm (except for H_2SO_3 - 950 rpm), ZnS = 0.5 g L^{-1} In the sulfurous acid solution $[SO_2(aq)]$ = 1.32 mol L^{-1}

At pH 1.52, the presence of sulfur dioxide initially inhibits, but then enhances ZnS dissolution (Figure 4.14). The observed enhancement is further evidence that the removal of H_2S by reaction with sulfur dioxide is more effective than its physical removal by displacement with nitrogen gas. Although apparently contradictory, the observed inhibition is likely due to the presence of other species that interact with zinc ions in the same way as H_2S. This is addressed in Section 4.2.

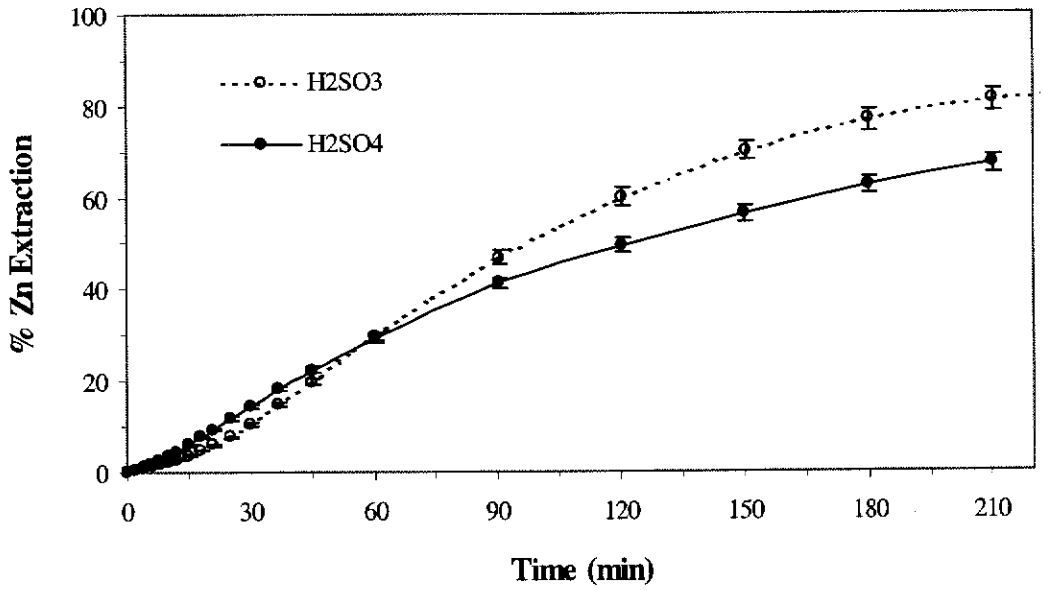

Figure 4.14 Dissolution of ZnS in sulfurous and sulfuric acids at pH 1.52
T = 25°C, Stirring speed = 800 rpm. For H_2SO_4, N_2 = 1050 mL min^{-1}. For H_2SO_3, SO_2/N_2(5.5%) = 1050 mL min^{-1} ZnS = 0.5 g L^{-1}

4.2 INHIBITION IN SO_2 LEACHES

The earlier observation that the ZnS dissolution rate decreases with increasing pulp density would seem to indicate, in the absence of evidence for occlusion by elemental sulfur (4.1.1.3), that the dissolution is inhibited by the build up of H_2S, and that the H_2S / SO_2 reaction is not fast enough to remove H_2S from solution.

Since in sulfurous acid, the evidence indicates that ZnS dissolves non-oxidatively, it may be expected that $H_2S(g)$, $H_2S(aq)$ or $HS^-(aq)$ would be formed. However, results from experiments with varying gas flow rates (Figure 4.2) suggest that $H_2S(g)$ is not present in significant quantities in the solution. A pulp density of 4 g L^{-1} was

sufficient to cause inhibition (Figure 4.3), and if $H_2S(g)$ was the cause of inhibition it would be expected that increasing the sulfur dioxide gas flow rate would increase the dissolution rate, in the same way that increasing the nitrogen gas flow rate increases the dissolution of ZnS in sulfuric acid by displacing $H_2S(g)$ from solution (Figure 4.14). However increasing the $SO_2(g)$ flow rate had no effect on the reaction rate (Figure 4.2). In addition, when the exit gases were bubbled through a lead acetate solution, no H_2S was detected. The absence of $H_2S(g)$ indicates also that neither $H_2S(aq)$ nor $HS^-(aq)$ were present, since if these were present, the low pH's would also ensure the presence of $H_2S(g)$.

Thus, if non-oxidative dissolution was occurring, no $H_2S(g)$ was formed or, if it was formed, it rapidly reacted to form a soluble species. Similarly, Larsen (1984) also reported that he did not detect H_2S when leaching ZnS in sulfurous acid.

Evidence that the source of inhibition is unlikely to be a surface solid, e.g. elemental sulfur, was given in 4.1.1.3. This is supported by ZnS leaches in sulfurous acid at pH 1.52. The dissolution is inhibited initially (with respect to the sulfuric acid dissolution rate), but then increases and eventually exceeds the sulfuric acid dissolution rate (Figure 4.14). If a surface layer were inhibiting dissolution then the inhibition would be expected to continue and even increase throughout the leach, since it would be expected that the surface layer would increase in thickness and that the extent of surface coverage would also increase. The leach residue obtained from a sample taken after 30 minutes of leaching did not contain any sulfur, confirming that sulfur is not the cause of the observed inhibition (Figure 4.15).

Further evidence, in support of the inhibitor being a solution species, is that the dissolution rate of ZnS in sulfurous acid, conducted under conditions promoting inhibition (i.e. pulp density = 4 g L^{-1}), is suppressed even further by the addition of zinc ions (Figure 4.16).

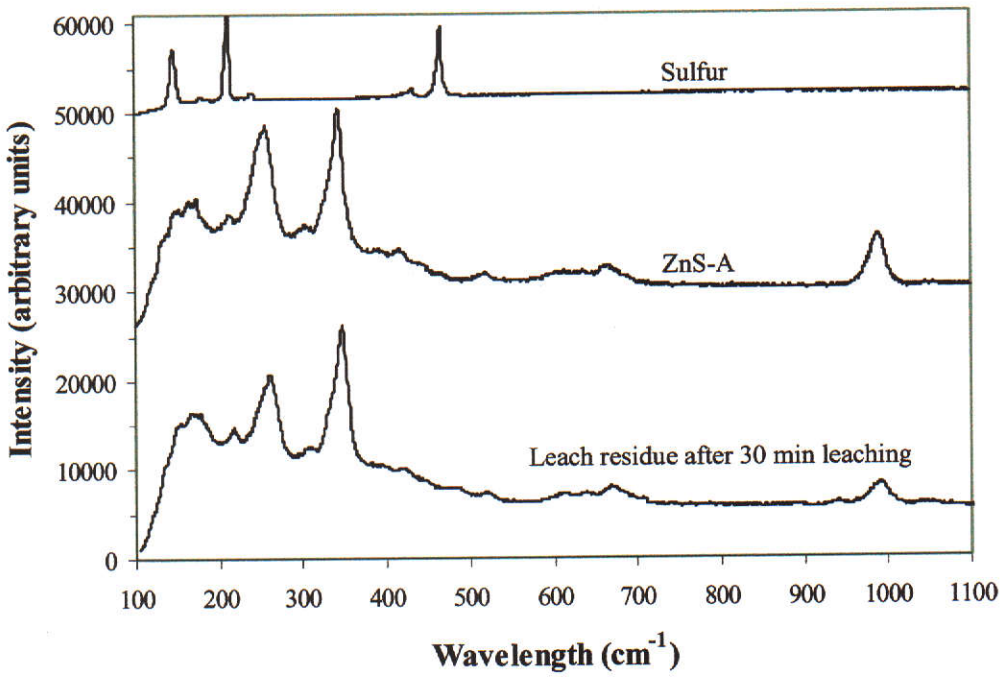

Figure 4.15 Dispersive Raman spectrum (He-Ne, 632.817 nm) of solid residue after 30 minutes leaching from leach of ZnS-A (5.39 µm) in sulfurous acid at pH 1.52.
T= 25°C, 800 rpm, SO_2/N_2(5.5%) = 1050 mL min^{-1}, ZnS = 0.5 g L^{-1}

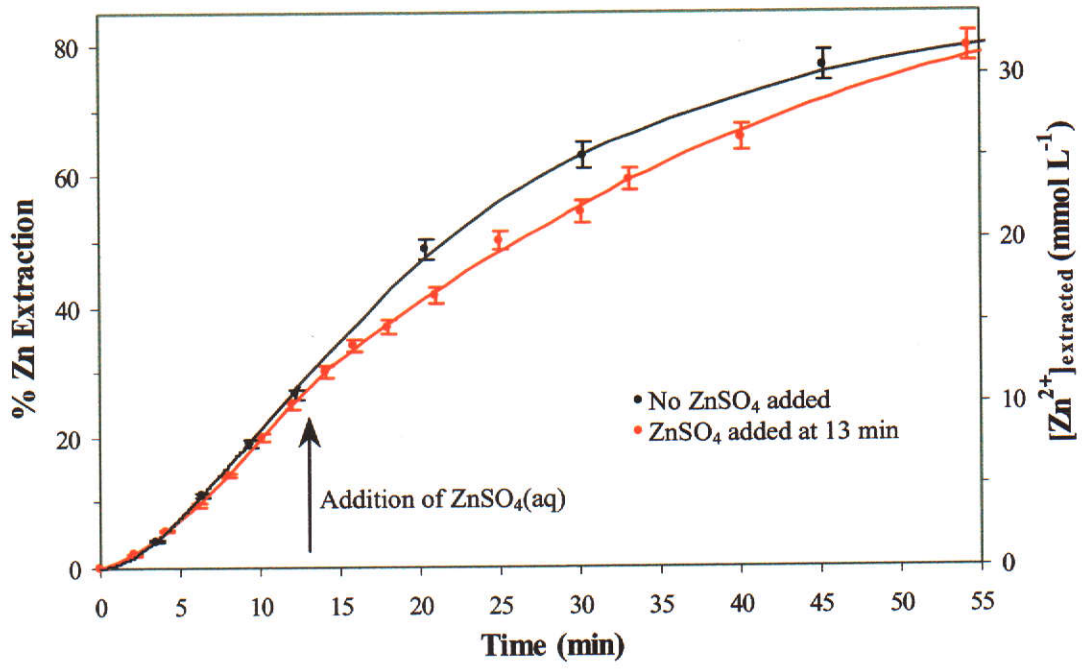

Figure 4.16 Effect of $ZnSO_4$ addition on Zn extraction.
$[SO_2(aq)]$ = 1.3 mol L^{-1}, T = 25°C, Stirring speed = 950 rpm, ZnS = 4 gL^{-1}, Solution volume = 800 mL, 10 mL of 1.5 mol L^{-1} $ZnSO_4$ added at t = 13 min

The addition of the concomitant sulfate ions (Figure 4.16) would not have affected the pH, since the excess $SO_2(aq)$ continuously flushing through the solution would have ensured that the equilibrium concentration of $SO_2(aq)$ and consequently the equilibrium hydrogen ion concentration was maintained. Thus, the cause of inhibition is likely to be a solution species which is able to react with zinc ions and re-precipitate ZnS (Figure 4.17).

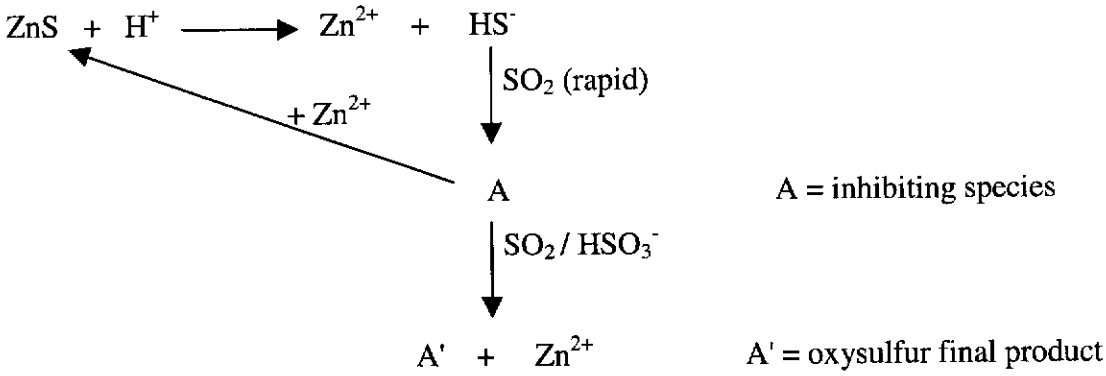

Figure 4.17 Possible reaction pathways involving an inhibiting species, A.

The inhibiting effect of zinc ions was also observed by Larsen (1984). In his study, the addition of 0.1 mol L^{-1} Zn^{2+} to a sulfurous acid leach of ZnS (43 g L^{-1}) at 25°C, severely retarded the dissolution rate, reducing the zinc extraction after two hours from 31.1% to 8.3%.

It seems reasonable to assume that the inhibiting species (or multiple species) is reactive toward zinc ions in a similar manner to H_2S, i.e. it is "H_2S-like". Only tetrathionate, sulfate, bisulfite and aqueous sulfur dioxide were observed in the solution, using Raman spectroscopy (Figure 4.18), however none of these reacts with zinc ions to precipitate ZnS. This does not necessarily exclude the possibility of other species being present, since the Raman technique is relatively insensitive and the concentrations of these species could easily be below their detection limit.

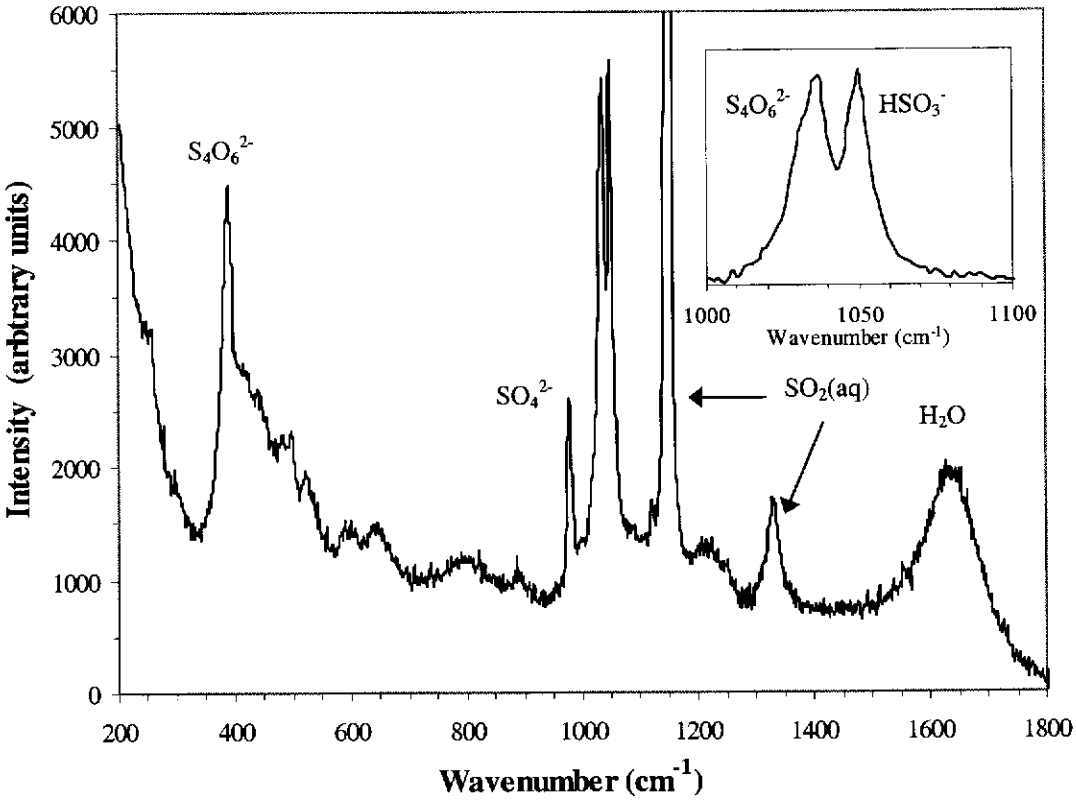

Figure 4.18 Dispersive Raman spectrum (He-Ne, 632.817 nm) of solution from SO_2(aq) leach of ZnS.
Conditions: [SO_2(aq)] = 1.3 mol L^{-1}, T = 25°C, Stirring speed = 950 rpm, ZnS = 4 gL^{-1}, Solution volume = 800 mL, 10 mL of 1.5 mol L^{-1} $ZnSO_4$ added at t = 13 min.

It is unlikely that any sulfane disulfonic acids ($HO_3SS_xSO_3H$) or sulfane disulfonates ($^-O_3SS_xSO_3^-$) would react with zinc ions to precipitate ZnS as the sulfur atoms all bear a positive charge (Meyer, Peter and Spitzer 1977). Intermediates causing inhibition are more likely to be sulfane monosulfonic acids, HS_nSO_3H, or their ions, $^-S_nSO_3H$, $HS_nSO_3^-$ and $^-S_nSO_3^-$ (n = 2 – 7), because these contain negatively charged sulfur atoms (Table 4.2) and as such may behave like H_2S or HS^- towards zinc ions. Even though these species have not been detected in aqueous solutions, they are generally accepted as being intermediates in the reaction between H_2S and SO_2 in aqueous solutions (Meyer, Peter and Spitzer 1977; Schmidt 1965a).

Table 4.2 Calculated charges on the atoms in sulfane monosulfonic acids and their ions.

From Meyer, Peter and Spitzer (1977)

Specie	Atom	HS_xSO_3H	$HS_xSO_3^-$	$^-S_xSO_3H$	$^-S_xSO_3^-$
$H_2S_2O_3$	H	0.133	0.072		
	S	0.189	0.132	-0.167	-0.244
	S	0.405	0.290	0.258	0.127
	O*(a)*	-0.401	-0.496	-0.514	-0.628
	O	-0.244	-0.502	-0.312	-0.628
	H	0.318		0.252	
$H_2S_3O_3$	H	0.045	0.006		
	S	0.122	0.079	-0.295	-0.365
	S	0.193	0.110	-0.012	-0.114
	S	0.387	0.279	0.297	0.175
	O*(a)*	-0.406	-0.491	-0.480	-0.567
	O	-0.243	-0.491	-0.295	-0.562
	H	0.308		0.265	
$H_2S_4O_3$	H	0.000	-0.018		
	S	0.090	0.060	-0.367	-0.422
	S	0.127	0.088	-0.106	-0.174
	S	0.182	0.124	0.067	0.011
	S	0.382	0.267	0.325	0.216
	O*(a)*	-0.418	-0.510	-0.458	-0.544
	O	-0.246	-0.502	-0.276	-0.542
	H	0.302		0.273	
$H_2S_5O_3$	H	-0.013	-0.023		
	S	0.067	0.042	-0.403	-0.415
	S	0.080	0.050	-0.167	-0.213
	S	0.108	0.064	0.017	-0.056
	S	0.170	0.102	0.112	0.054
	S	0.376	0.267	0.337	0.230
	O*(a)*	-0.420	-0.504	-0.453	-0.535
	O	-0.249	-0.496	-0.272	-0.529
	H	0.301		0.282	
$H_2S_6O_3$	H	-0.025	-0.031		
	S	0.030	0.018	-0.423	-0.446
	S	0.052	0.034	-0.209	-0.234
	S	0.076	0.050	-0.042	-0.088
	S	0.116	0.080	0.047	0.016
	S	0.175	0.121	0.124	0.078
	S	0.375	0.261	0.352	0.243
	O*(a)*	-0.423	-0.514	-0.437	-0.525
	O	-0.250	-0.503	-0.260	-0.518
	H	0.297		0.285	

(a) Each molecule contains two oxygen atoms of this type

A possible reaction scheme for the reaction of sulfane monosulfonates with zinc ions is given below

$$Zn^{2+} + {}^{-}SS_{n-1}O_3H \rightarrow Zn\text{-}S\text{-}S\text{-}S_{n-2}O_3H^{+} \quad (4.7)$$

$$Zn\text{-}S\text{-}S\text{-}S_{n-2}O_3H^{+} + {}^{-}SS_{n-1}O_3H \rightarrow ZnS + HO_3S_{2n-1}O_3H \quad (4.8)$$

Overall: $$Zn^{2+} + 2\,{}^{-}S_nO_3H \rightarrow ZnS + H_2S_{2n-1}O_6 \quad (4.9)$$

Sulfane monosulfonates may also be used to explain why the sulfurous acid leach at pH 1.52 is inhibited with respect to a sulfuric acid leach at the same pH (Figure 4.14), whereas the sulfurous and sulfuric acid leaches at pH 0.90 have equivalent dissolution rates (Figures 4.12 and 4.13).

Sulfane monosulfonic acids are known to react spontaneously with sulfurous acid, e.g. the reaction of trisulfane monosulfonic acid (HO_3SS_3H) with H_2SO_3 is considered to be (Schmidt 1965b),

$$\begin{array}{l} H\,|\,SO_3H \\ + \\ HO_3S\text{–}S\text{–}S\text{–}\,|\,S\text{–}H \end{array} \rightarrow H_2S_2O_3 + HO_3S\text{–}S\text{–}S\text{–}H \quad (4.14)$$

$$\begin{array}{l} H\,|\,SO_3H \\ + \\ HO_3S\text{–}S\text{–}\,|\,S\text{–}H \end{array} \rightarrow H_2S_2O_3 + H_2S_2O_3 \quad (4.15)$$

i.e. sulfurous acid removes sulfane monosulfonic acids from solution, producing thiosulfuric acid.

Consequently, inhibition is not observed in the pH 0.90 leach, in contrast to the pH 1.52 leach, because in the pH 0.90 leach the concentration of sulfurous acid (1.19 mol L^{-1}) is sufficiently high to react with the inhibiting species (the sulfane

monosulfonic acids) removing them from solution and producing thiosulfuric acid, which is a non-inhibiting species. In the pH 1.52 leach the concentration of sulfurous acid, being about 15 times lower (0.075 mol L^{-1}), is insufficient to completely remove the inhibiting sulfane monosulfonic acids, and inhibition occurs as a result.

4.3 ANALYSIS OF DATA ACCORDING TO HETEROGENEOUS REACTION MODELS

To assist in elucidating the reaction mechanism the experimental data was evaluated according to two common heterogeneous reaction models; the surface reaction controlled and diffusion controlled shrinking particle models (Sohn and Wadsworth 1979b).

In the surface reaction controlled shrinking particle model the solid particles are assumed to be isometric, with the radius decreasing uniformly (i.e. shrinking particles) during dissolution and the dissolution reaction is assumed to be first order and irreversible. The model also requires the size distribution to be narrow. The model relates an expression of the fraction of the solid reacted (α) to the leach time (t).

$$1 - (1 - \alpha)^{1/3} = k_r t \qquad (4.16)$$

where $k_r = CVk_o k'/r_o$ and C is the concentration of the leaching agent, V the molar volume of the solid, k_o the concentration of potentially reactive surface sites, k' the rate constant, and r_o the initial radius of the particles (Sohn and Wadsworth 1979b). A linear relationship between $1 - (1 - \alpha)^{1/3}$ and t is suggestive of surface reaction controlled dissolution kinetics.

The expression for the situation where the reaction rate is controlled by diffusion of species through a product layer on the surface of the particle is given by

$$1-\frac{2}{3}\alpha-(1-\alpha)^{2/3}=k_d t \qquad (4.17)$$

where $k_d=\frac{2VDC}{\rho r_o^2}t$ with ρ being the density of the particles, and D the diffusion coefficient (Sohn and Wadsworth 1979c).

Figures 4.19 and 4.20 show that neither model correlated well with the experimental leach data. In the initial stages poor correlations with either model were observed, as expected, since the particles were somewhat agglomerated and took time to be dispersed throughout the solution (see Section 4.1.1.4). The straight lines in Figures 4.19 and 4.20 show the periods of time during the leaches where the dissolution kinetics followed the respective models.

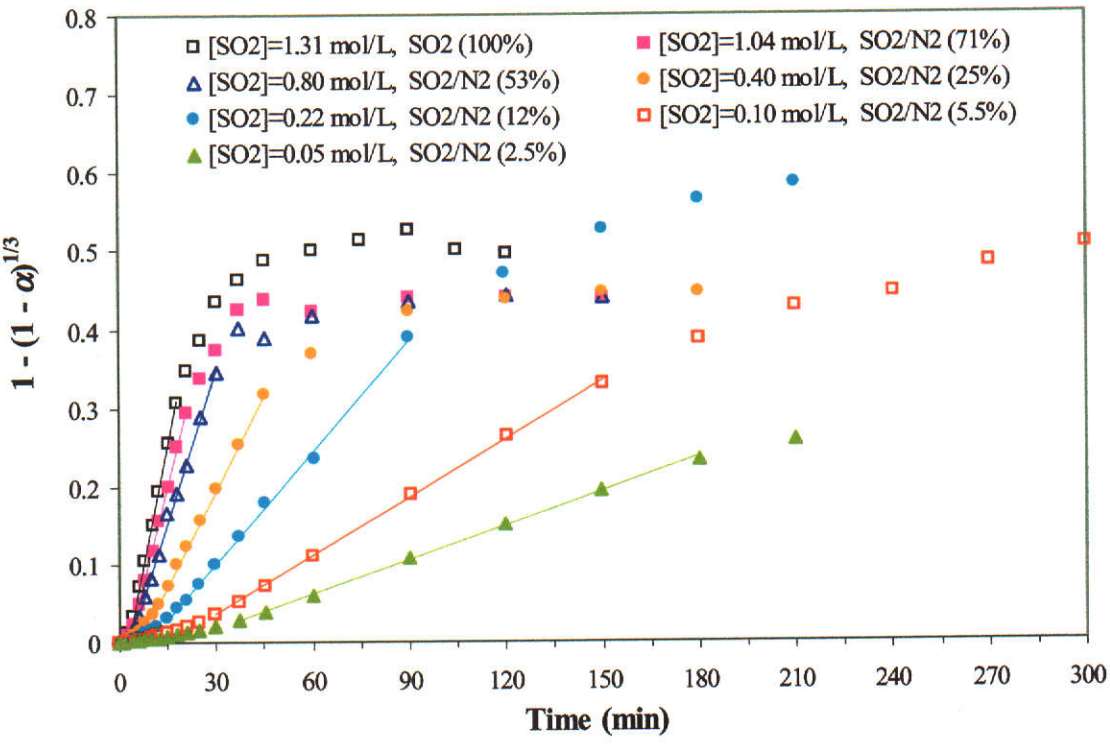

Figure 4.19 Surface reaction model for dissolution data presented in Figure 4.9.

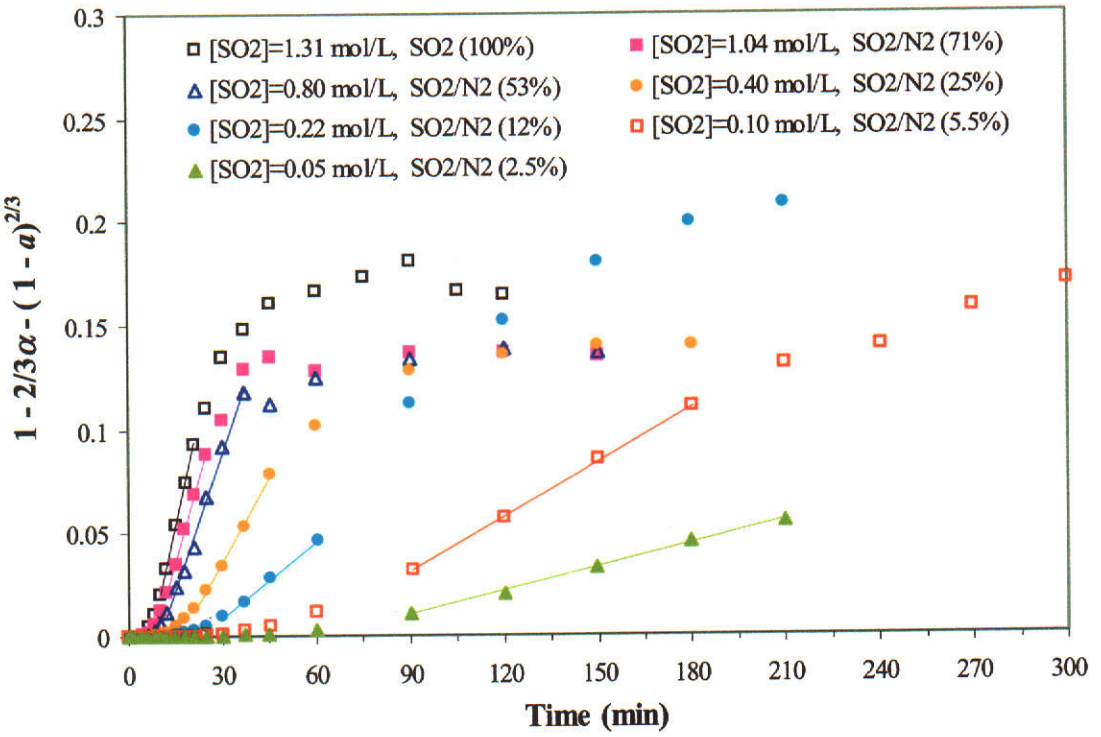

Figure 4.20 Diffusion controlled model for dissolution data presented in Figure 4.9.

The results suggest that in each leach there are periods of time where the dissolution rate is simultaneously controlled by the rate of the surface reaction and by the rate of diffusion. This indicates that neither a surface reaction model nor a diffusion controlled model alone is able to account for the kinetics of zinc sulfide dissolution in aqueous sulfur dioxide solutions. These observations are not in conflict with the previously advanced positions that the dissolution rate is inhibited by species which cause the re-precipitation of ZnS and that inhibition is not due to the formation of a sulfur layer.

4.4 SUMMARY

On the basis of the observed SO_2(aq) and H_2SO_4 leaching rates, the inhibition of the dissolution at higher pulp densities, and the eventually higher reaction rates observed in the presence of SO_2, it is concluded that the reaction between ZnS and aqueous

solutions of sulfur dioxide at ambient temperatures involves non-oxidative acidic dissolution of ZnS. Oxidative dissolution does not occur and the polythionates observed in this work and the work of other researchers are the result of the reaction between "sulfurous acid" and H_2S or HS^-, produced by non-oxidative dissolution of ZnS.

Inhibition is observed at higher pulp densities and in the presence of added soluble zinc, and it is postulated that the H_2S or HS^- species produced react rapidly with either $SO_2(aq)$ or $HSO_3^-(aq)$, forming species that are "H_2S – like", in that they are capable of reacting with Zn^{2+} to precipitate ZnS. It is postulated that these "H_2S – like" species may be sulfane monosulfonates.

5 PRESSURE LEACHING OF ZINC SULFIDE IN SO_2(aq)

The rate of dissolution of ZnS in sulfurous acid at ambient temperatures is too slow to be commercially viable. It was considered a possibility that higher, commercially viable, rates could be obtained at elevated temperatures. This necessitated the use of higher pressures to maintain high concentrations of SO_2(aq) in solution, and all leaching experiments were conducted in an autoclave.

Preliminary experiments were conducted to determine whether a surfactant was necessary in leaches above the melting point of sulfur and to determine the optimum stirring speed for leach tests. The effect of temperature (100 – 200°C) was investigated.

The concentrations of SO_2 in solution at these elevated temperatures were calculated using the mass, partial pressure and molar volume of sulfur dioxide. The method is given in Section 3.4.3.

5.1 EFFECT OF SURFACTANT

Raman spectra of preliminary leaches showed that elemental sulfur is produced in the reaction between synthetic ZnS and sulfur dioxide solutions at elevated temperatures. As molten sulfur could occlude the unreacted mineral, a surfactant was evaluated for keeping the surface clear of molten sulfur.

Sodium ligninsulfonate was chosen for this study as it has been used with success in the acidic oxidative leaching of zinc concentrate at 150°C (Kawulka, Haffenden and Mackiw 1975). Addition of sodium ligninsulfonate (0.1 g L^{-1} – 0.3 g L^{-1}) had

negligible effect on the reaction rate, causing only minor variations in zinc extraction at 150°C (Figure 5.1) and 180°C (Figure 5.2). This suggests that molten sulfur does not wet the surface and does not occlude synthetic ZnS.

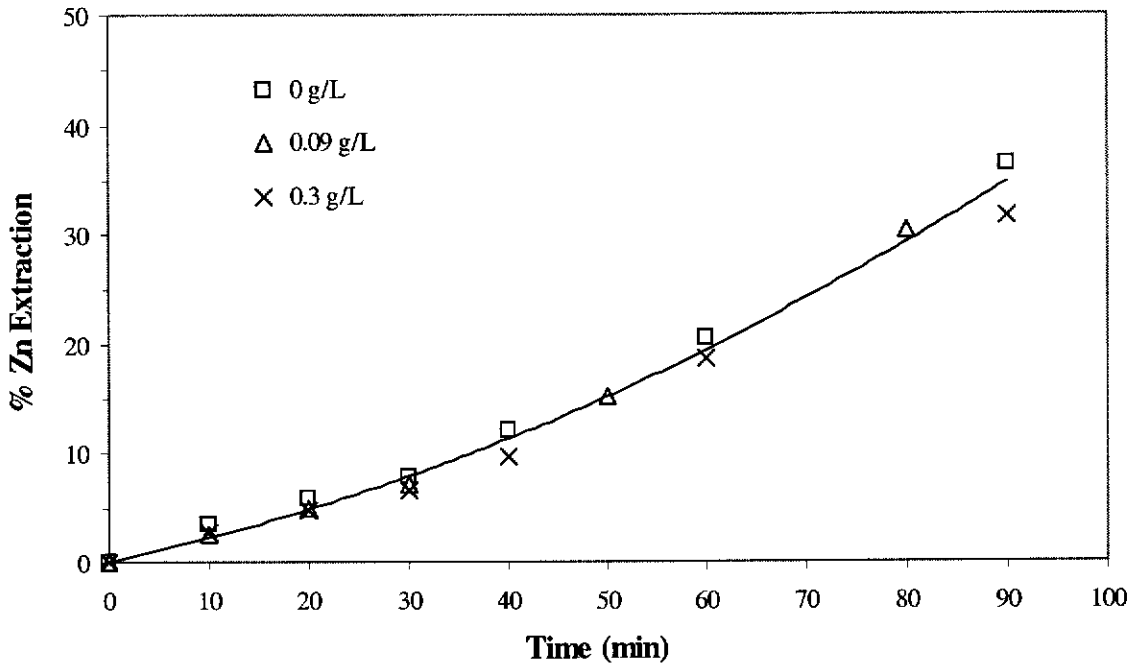

Figure 5.1 Effect of sodium ligninsulfonate concentration on %Zn extraction at 150°C. $[SO_2(aq)]$ = 1 mol L^{-1}, ZnS-F3 (107.93 μm) = 2 g L^{-1}, stirring speed = 600 rpm

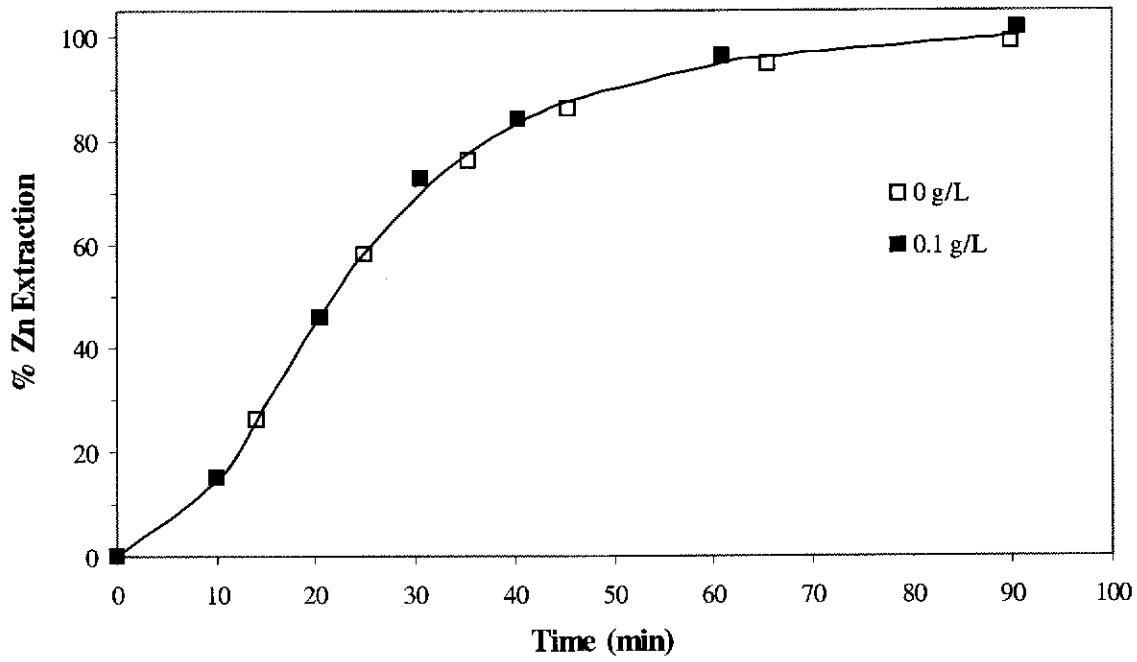

Figure 5.2 Effect of sodium ligninsulfonate on % Zn extraction at 180°C. $[SO_2(aq)]$ = 1 mol L^{-1}, ZnS-F3 (107.93 μm) = 2 g L^{-1}, stirring speed = 800 rpm

Although no effect on the rate was observed upon addition of a surfactant, there was a marked difference in the appearance of the residue. Without surfactant the residue consisted mainly of clumps containing sulfur and ZnS and the sulfur tended to adhere to the wall, cooling coil and stirring shaft of the autoclave. With surfactant present the residue consisted predominantly of finely divided yellow sulfur particles, some larger lumps of sulfur and particles of unreacted ZnS. The inside surfaces of the autoclave were also left free of residue.

This is in contrast to natural sphalerite, which is occluded by molten sulfur (Forward and Veltman 1959). Since, in these leaches using synthetic ZnS, elemental sulfur did not inhibit dissolution of the mineral, no surfactant was used in subsequent leaches.

5.2 EFFECT OF AGITATION

To eliminate the effect of diffusion (of reagents to the solid surface) on the reaction rate, stirring speeds in excess of 700 rpm were required (Figure 5.3). This differs from the result obtained under ambient conditions, where 600 rpm was sufficient to eliminate diffusion effects. However, the ambient temperature experiments used ZnS-A (5.39 μm) whereas these experiments used ZnS-F3 (107.93 μm). The larger size fraction was used to obtain manageable rates and required higher stirring speeds to lift the material off the bottom of the vessel. Subsequent reactions were carried out at a stirring speed of 800 rpm.

5.3 EFFECT OF TEMPERATURE

Figure 5.4 shows the effect of temperature on the rate of ZnS dissolution in SO_2(aq). Increasing the temperature from 100°C to 130°C produced only a slight increase in the reaction rate. At 150°C the reaction rate was initially constant, however after approximately 30 minutes the rate began to increase. Increasing the temperature to 180°C and 200°C dramatically increased the reaction rate.

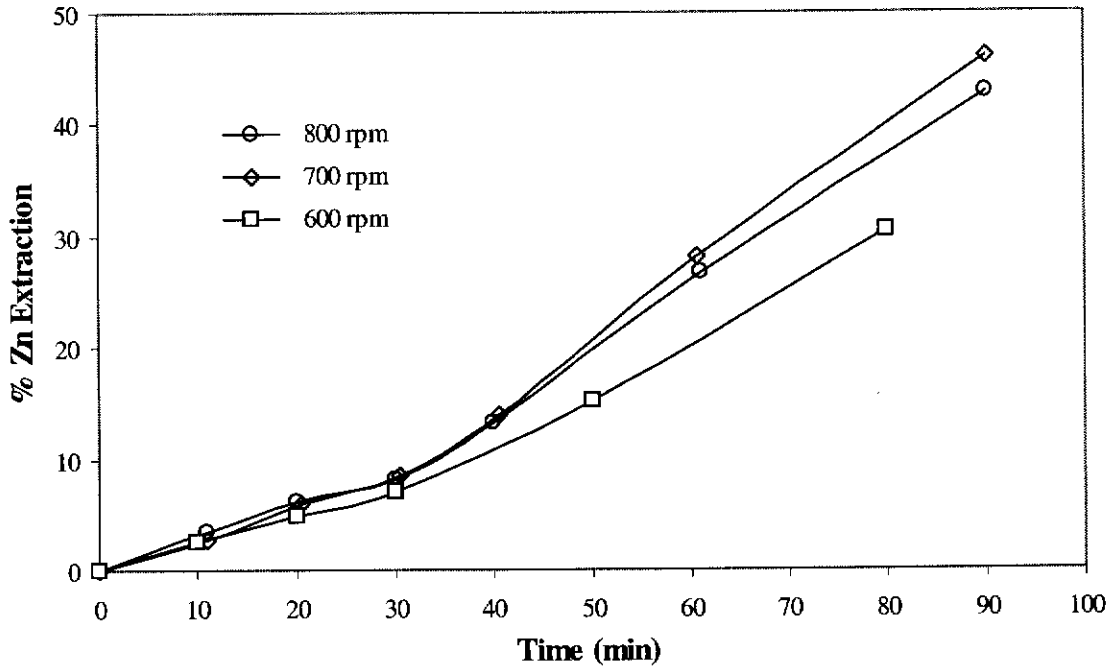

Figure 5.3 Effect of stirring speed on zinc extraction.
Temp = 150°C, $[SO_2(aq)]$ = 1 mol L^{-1}, [Na Ligninsulfonate] = 0.1 g L^{-1}, ZnS-F3 (107.93 μm) = 2 g L^{-1}

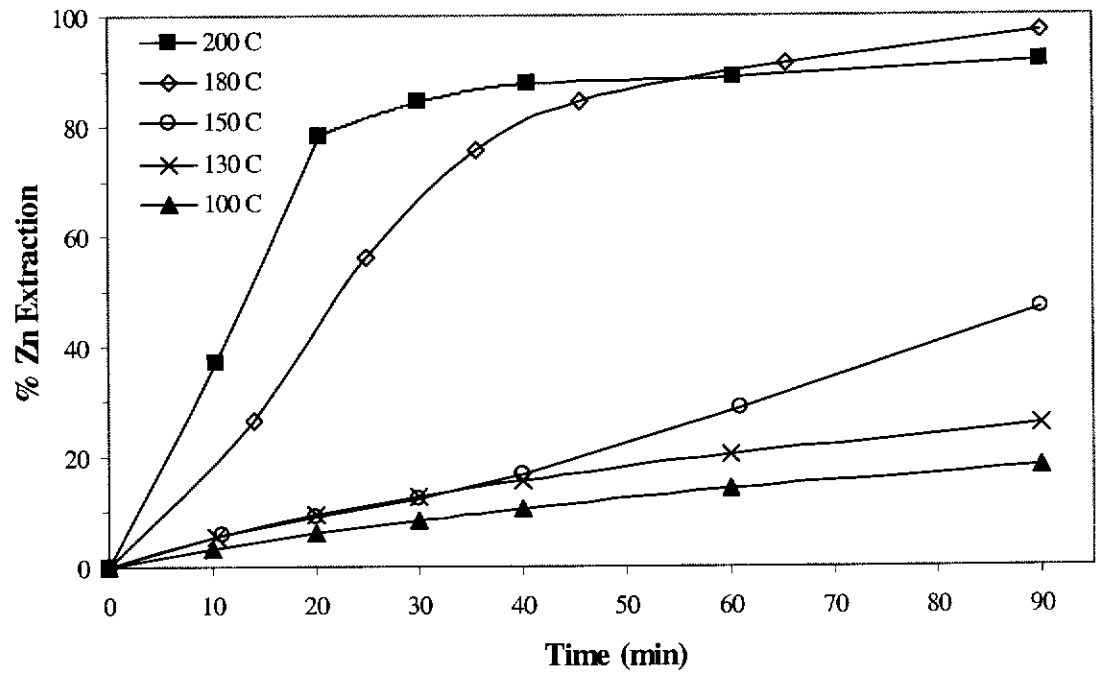

Figure 5.4 Effect of temperature on dissolution of ZnS in $SO_2(aq)$.
$[SO_2(aq)]$ = 1 mol L^{-1}, stirring speed = 800 rpm, ZnS-F3 (107.93 μm) = 2 g L^{-1}

Leaches at temperatures above 130°C exhibited an induction period, after which the rate increased. The induction period decreased with increasing temperature. At 150°C it was 40 minutes, whereas at 180°C and 200°C it was less than 10 minutes.

The products of the reaction included zinc ions, elemental sulfur, sulfate ions and hydrogen ions. Increasing the temperature reduced the concentration of sulfur dioxide but increased the sulfate and hydrogen sulfate concentrations, as shown by Raman spectra of the solutions after 90 minutes of leaching (Figure 5.5). Also, elemental sulfur was observed in amounts exceeding that expected based upon the reaction of ZnS with sulfurous acid solutions (Eqn. 2.17, p. 16), i.e.

$$ZnS + 2H^+ + \tfrac{1}{2}SO_2 \leftrightarrow Zn^{2+} + \tfrac{3}{2}S^o + H_2O$$

According to this equation the ratio $n(S^o):n(Zn^{2+})$ should be 1.5, however, at temperatures less than or equal to 130°C, the ratio was less than 1.5, whereas at 150°C this ratio was greater than 6, increasing to 8 at 180°C and 11 at 200°C (Figure 5.6).

To explain the observed low $n(S^o):n(Zn^{2+})$ ratios at temperatures less than or equal to 130°C, it is necessary to recall that while the above equation (Eqn. 2.17, p. 16) describes the overall reaction stoichiometry for the final end products, the reaction also produces the metastable intermediate, tetrathionate. Tetrathionate, observed using Raman spectroscopy in leaches conducted at 25°C (Figure 4.18, p. 90), was also observed in leaches at 100, 130 and 150°C. Consequently, since the leach residues were analysed before tetrathionate had decomposed to elemental sulfur, the observed $n(S^o):n(Zn^{2+})$ ratios were lower than that expected according to equation 2.17 (p. 16).

At temperatures greater than or equal to 150°C, the $n(S^o):n(Zn^{2+})$ ratio was much higher than 1.5, suggesting that in this system thermal decomposition of aqueous SO_2 occurred.

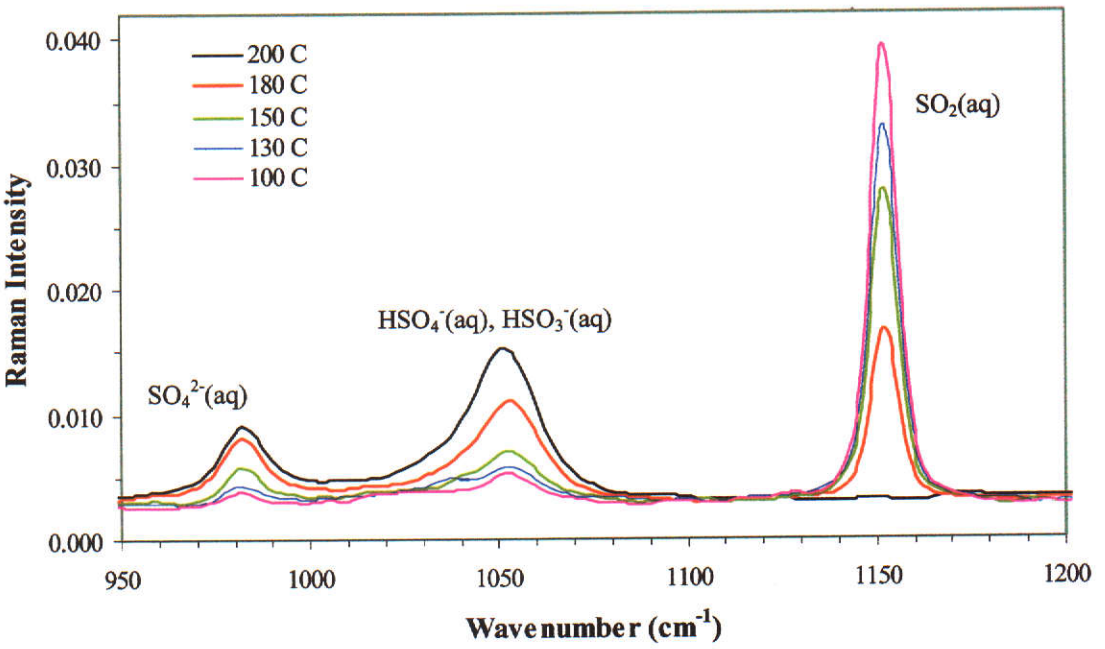

Figure 5.5 FT-Raman spectra of SO_2 leach solutions after 90 minutes leaching showing increasing sulfuric acid and decreasing sulfur dioxide concentration with increasing temperature.

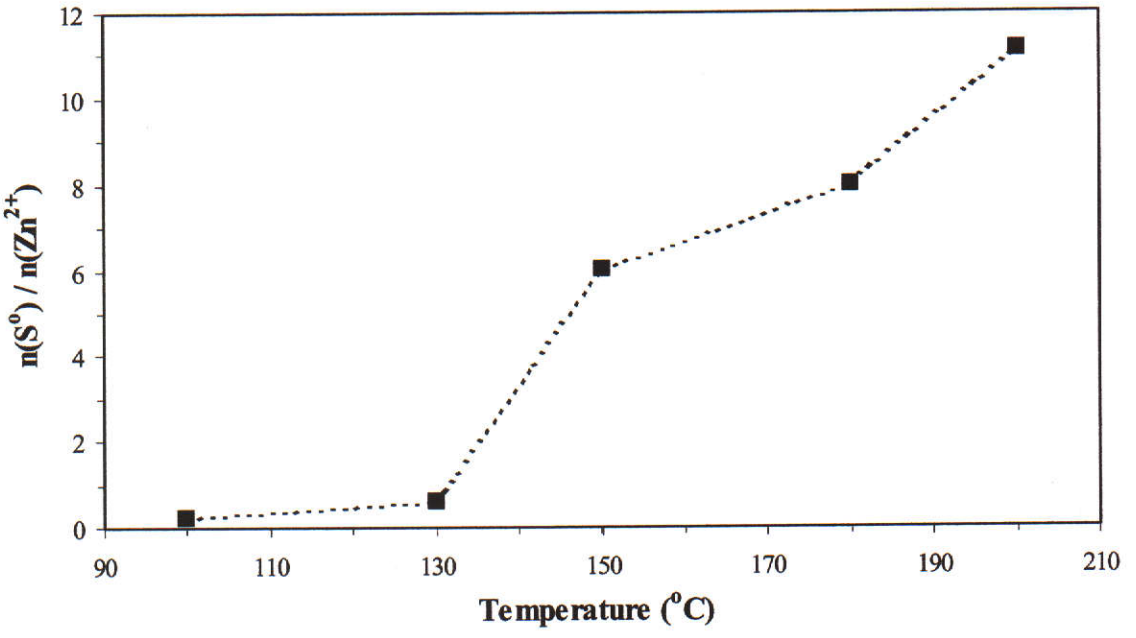

Figure 5.6 Elemental sulfur to zinc ion ratio versus temperature in ZnS / SO_2 leaches. $[SO_2(aq)]_{initial}$ ~ 1.1–1.2 mol L^{-1}, ZnS-F3 (107.93 µm) = 2 g L^{-1}

The decomposition of aqueous solutions of SO_2 at elevated temperatures is known to yield elemental sulfur and sulfuric acid, the reaction given by equation 2.19 (p. 17) (Ryabinina and Oshman 1972), citing (Foerster et al. 1923; and Slavik 1961), i.e.

$$3SO_2(aq) + 2H_2O \rightarrow S^\circ + 2H_2SO_4$$

Thus the observed increase in dissolution rate at 150°C, 180°C and 200°C was due to the formation of sulfuric acid, occasioned by the thermal decomposition of $SO_2(aq)$.

Confirmation that thermal decomposition of SO_2 occurred was arrived at by comparing the concentrations of sulfate and hydrogen ions present in solution with expected values based upon the observed mass of elemental sulfur and that calculated using equation 5.2. In determining the calculated values, corrections were made for the effect of other reactions occurring simultaneously, *viz.*, the consumption of hydrogen ions by the acidic dissolution of ZnS (Eqn. 2.23, p. 20), and the formation of elemental sulfur by the reaction of H_2S with SO_2 (Eqn. 2.24, p. 20), i.e.

$$ZnS + 2H^+ \leftrightarrow Zn^{2+} + H_2S$$
$$2H_2S + SO_2 \rightarrow 2H_2O + 3S^\circ$$

Thus the number of moles of elemental sulfur produced by thermal decomposition of sulfur dioxide (Eqn. 2.19, p. 17) is equal to the total measured number of moles less the amount generated via reaction 2.24 (p. 20). Knowing the number of moles of zinc ions produced it was possible to determine the number of moles of H_2S produced and hence the number of moles of elemental sulfur generated via reaction 2.24 (p. 20). The number of moles of elemental sulfur produced via the SO_2 thermal decomposition reaction thus becomes

$$n(S^\circ)_{\text{prod by SO2 decompn.}} = n(S^\circ)_{\text{total, measured}} - 3/2\ n(Zn^{2+})_{\text{measured}} \qquad (5.2)$$

Similarly, hydrogen ions while being produced via SO_2 thermal decomposition (Eqn. 2.19) are also being consumed via reaction with ZnS (Eqn. 2.23). So the actual number of moles of hydrogen ions produced via equation 2.19 is equivalent to the

number of moles of hydrogen ions measured at the end of the leach plus the number of moles consumed via reaction with ZnS (Eqn. 2.23, p. 20).

$$n(H^+)_{\text{prod by SO2 decomp}} = n(H^+)_{\text{measured}} + 2\,n(Zn^{2+})_{\text{measured}} \qquad (5.3)$$

At the completion of each leach the solutions were analysed for the concentration of zinc ions, hydrogen ions and total soluble sulfur. The total soluble sulfur concentration was taken as the equivalent to the concentration of sulfate, since the concentration of tetrathionate was negligible.

Table 5.1 shows that the expected number of moles of soluble sulfur (sulfate) and hydrogen ions, calculated from the observed mass of elemental sulfur produced using equation 2.19, compare favourably with the observed values. This confirms that in these leaches thermal decomposition of SO_2 occurred, generating elemental sulfur, sulfate and hydrogen ions according to reaction 2.19 (p. 17).

Table 5.1 Comparison of calculated and measured amounts of hydrogen ions and soluble sulfur in solutions after 90 minutes of SO_2 leaching.
ZnS pulp density ~ 2g L^{-1}, $[SO_2(aq)]_{initial}$ =1.1 – 1.2 mol L^{-1}

Temperature(°C)	**$n(S^o)_{obs}$ (mole)**	**$n(SO_4^{2-})_{obs}$ (mole)**	**$n(SO_4^{2-})_{calc}$ (mole)**	**$n(H^+(aq))_{obs}$ (mole)**	**$n(H^+(aq))_{calc}$ (mole)**
100	0	0.03	0	0.04	0
130	0	0.05	0	0.05	0
150	0.064	0.16	0.13	0.28	0.23
180	0.174	0.32	0.35	0.58	0.66
200	0.241	0.43	0.48	0.81	0.93

The thermal decomposition of SO_2 is known to exhibit an induction period (Ryabinina and Oshman 1972), which accounts for the induction period observed in these leaches (Figure 5.4). The rate of dissolution of ZnS is dependent upon the concentration of hydrogen ions, which in turn is dependent upon the rate of decomposition of SO_2. Hence the rate of ZnS dissolution reflects the rate of thermal decomposition of $SO_2(aq)$.

When an exponential curve of the form,

$$t_{induction} = ae^{-bT}$$

where

$t_{induction}$ is the induction period

T the temperature in Kelvin

a and b are constants,

is fitted to a plot of Ryabinina and Oshman's (1972) induction periods versus temperature and extrapolated to higher temperatures, the calculated induction periods correspond closely to the induction periods observed in this work (Figure 5.7).

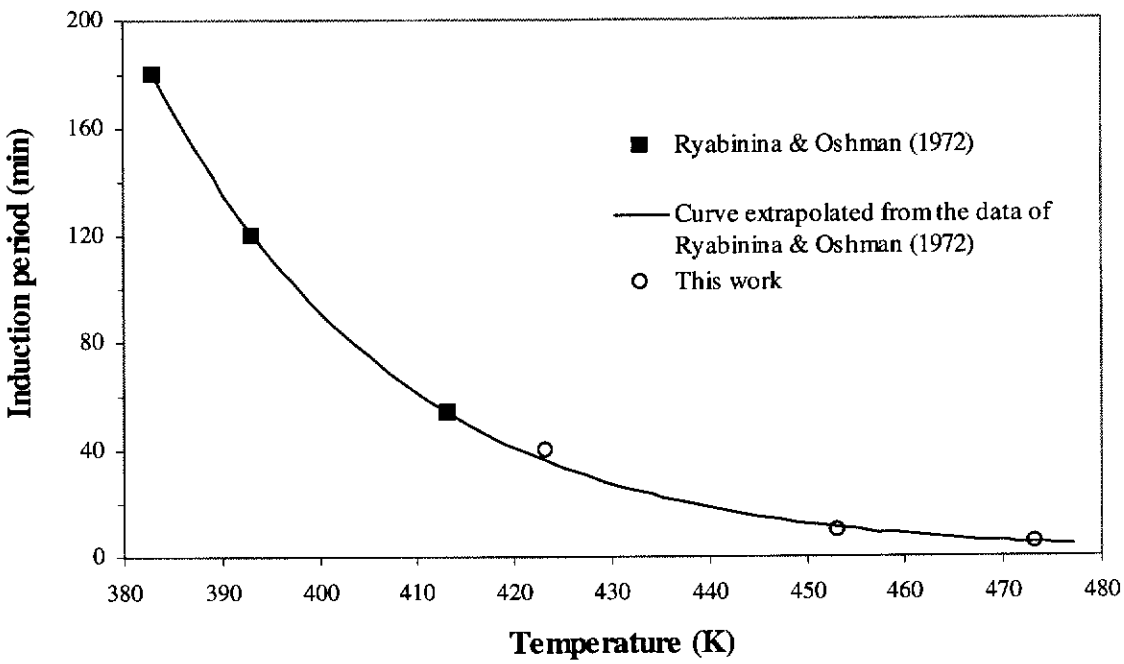

Figure 5.7 Induction period versus temperature for thermal decomposition of SO_2 in water.

5.3.1 Other oxy-sulfur species present in leach solutions

Raman spectra confirmed the presence of the expected major species, $SO_2(aq)$, HSO_3^-, SO_4^{2-} and HSO_4^-, in all leach solutions, a typical spectrum is shown in Figure 5.8.

In addition, the presence of tetrathionate ($S_4O_6^{2-}$), as predicted by Larsen (1984) from thermodynamic data, was shown by peaks attributable to it (1038cm^{-1}, 388cm^{-1}) in leaches conducted at 100°C, 130°C, and 150°C (Figure 5.9). It is, however only a minor component of the solutions. Tetrathionate was not observed in the 180°C and 200°C leaches. This is not unexpected, as aqueous solutions of tetrathionate are increasingly unstable with increasing temperature, decomposing to yield elemental sulfur and sulfate (Meyer and Ospina 1982) (Eqn. 5.7).

$$3S_4O_6^{2-} + 2H_2O \rightarrow \tfrac{7}{8}\ S_8 + 5SO_4^{2-} \qquad (5.7)$$

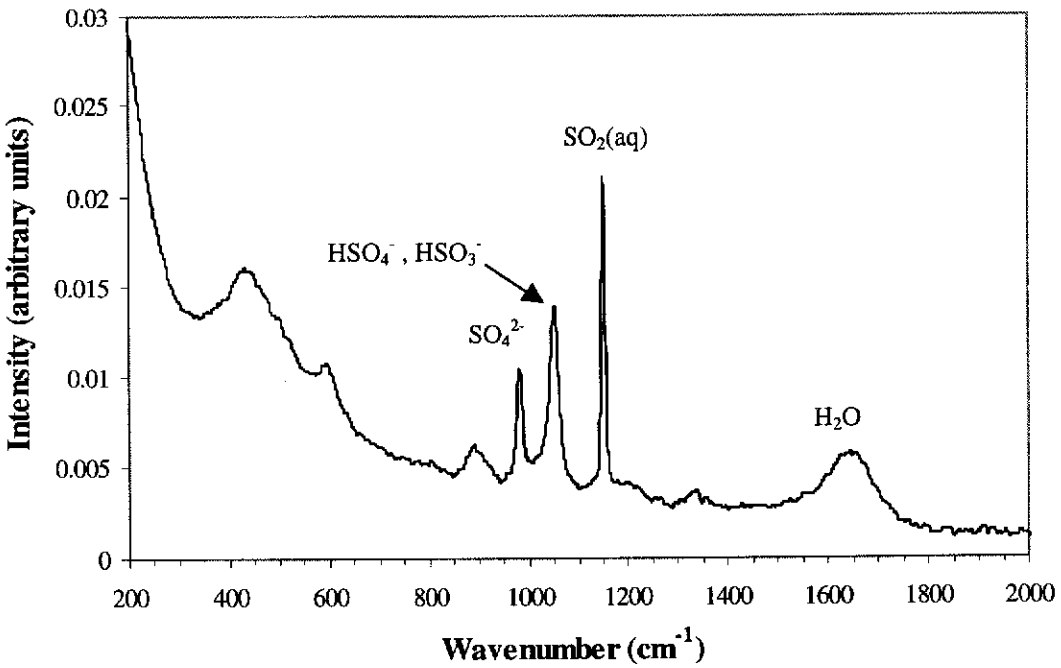

Figure 5.8 FT-Raman spectrum of solution after leaching ZnS in $SO_2(aq)$ at 180°C for 90 minutes. ZnS-F3 (107.93 μm) = 2 g L^{-1}, $[SO_2(aq)]_{initial}$ = 1.1 mol L^{-1}

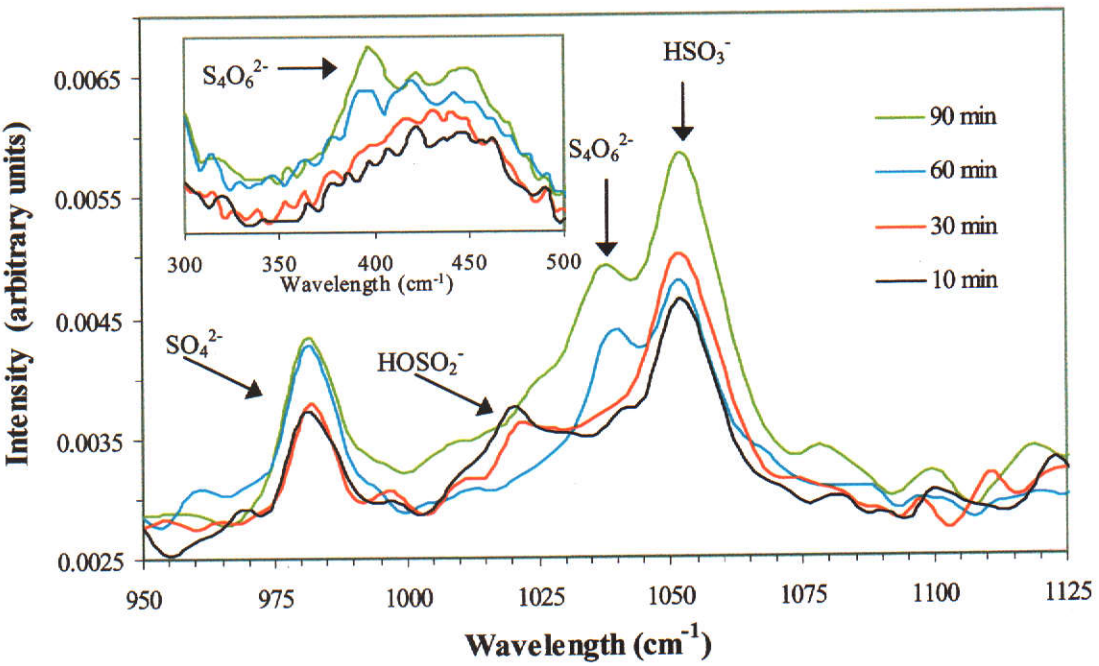

Figure 5.9 FT-Raman spectra of the leach solution from a leach of ZnS in SO_2(aq) at 130°C. ZnS-F3 (107.93 μm) = 2 g L^{-1}, $[SO_2(aq)]_{initial}$ ~ 1.1 mol L^{-1}.

The rate of decomposition is second order with respect to tetrathionate ion (Meyer and Ospina 1982; Ospina 1982).

$$d[S_4O_6^{2-}]/dt = k_d[S_4O_6^{2-}]^2 \qquad (5.8)$$

Ospina (1982) measured the rate of reaction 5.7 at temperatures from 20°C to 70°C, but there is no reported data for temperatures above this.

To estimate the rate at elevated temperatures (up to 200°C), Ospina's data was extrapolated by determining its Arrhenius parameters (z, E_a) at 20°C – 70°C, and assuming that they remain constant. The activation energy was determined from an Arrhenius plot of Ospina's rate constants. The pre-exponential factor was calculated by substituting the activation energy and rate constants for the given temperatures into the Arrhenius equation and averaging the results. Using these, rate constants were calculated for temperatures up to 200°C. From the rate constants, half-lives for the tetrathionate ion were estimated (Table 5.2, Figure 5.10) using the equation for a

second order reaction (Eqn. 5.9) (Atkins 1982). The concentration of tetrathionate used in the equation (0.05 mol L^{-1}) was the maximum concentration observed in the experiments.

$$t_{1/2} = \frac{1}{k_d [S_4O_6^{2-}]_o} \tag{5.9}$$

Half-lives calculated using extrapolated rate constants compare favourably with half-lives calculated using experimentally determined rate constants (Figure 5.10). The short half-lives at 180 °C and 200°C, of 24 and 12 minutes, respectively, explain why tetrathionate is not observed at these temperatures.

Table 5.2 Effect of temperature on half-life of tetrathionate ion in water.
Data above 70°C was extrapolated from Ospina's data obtained at 20°C – 70°C..

Temp (°C)	Half – life (hrs min) (0.05 mol L^{-1} $S_4O_6^{2-}$)	Rate constant, k_d	Source of k_d *a* – Ospina (1982)
20	4900 hrs	4.1×10^{-3}	*a*
35	720 hrs	2.79×10^{-2}	*a*
50	630 hrs	3.18×10^{-2}	*a*
70	81 hrs	2.48×10^{-1}	*a*
100	15 hrs	1.35×10^{0}	calculated
130	3 hrs 14 min	6.20×10^{0}	calculated
150	1 hr 19 min	1.52×10^{1}	calculated
180	24 min	5.01×10^{1}	calculated
200	12 min	1.02×10^{2}	calculated

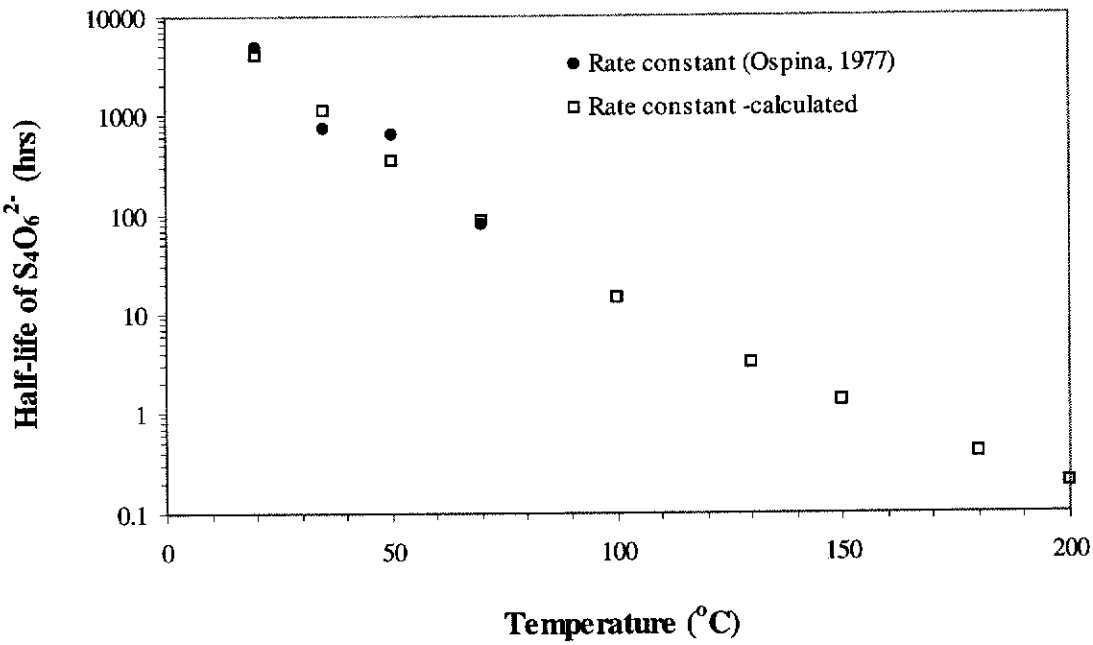

Figure 5.10 Effect of temperature on half-life of tetrathionate ion in water.
Data above 70°C was extrapolated from data obtained by Ospina .

5.4 SUMMARY

At elevated temperatures, it appears that the same dissolution mechanism is operating as in leaches under ambient conditions – the dissolution being driven by hydrogen ions. Increasing the temperature above 130°C dramatically increases the dissolution rate, because thermal decomposition of aqueous SO_2 occurs, generating sulfuric acid.

Tetrathionate, observed in leaches at ambient temperatures and predicted to be present at elevated temperatures (Larsen 1984), was also observed in leaches up to 150°C. However, at elevated temperatures above 150°C tetrathionate decomposes rapidly and as such was not observed at 180 °C or 200°C

The practicability of leaching ZnS in sulfurous acid solutions above 120°C is limited due to the tendency of sulfur dioxide to decompose to elemental sulfur and sulfuric acid. It would be simpler to add sulfuric acid to the leach to enhance the rate.

6 PRESSURE LEACHING OF ZINC SULFIDE IN H_2SO_4

Prior to studying the ZnS – H_2SO_4 – SO_2 leaching system the kinetics and equilibria of the ZnS – H_2SO_4 system was investigated, so that the effect of SO_2 on this system could be evaluated unambiguously.

Most of the previous work on this system has been done at temperatures below 70°C. Some equilibrium data has been obtained up to 200°C (Corriou, Gely and Viers 1988), but no rate data were presented.

At temperatures less than 70°C, it has been shown that the rate of dissolution of ZnS in sulfuric acid solutions is dependent on the difference between the rate of production of Zn^{2+} by acidic dissolution of ZnS (forward reaction) and the rate of Zn^{2+} consumption by precipitation with H_2S (reverse reaction) (Eqn. 2.28, p. 23) and obeys equation 2.30 (p. 23) (Crundwell and Verbaan 1987; Romankiw and de Bruyn 1965).

$$ZnS(s) + 2H^+(aq) \leftrightarrow Zn^{2+}(aq) + H_2S(aq)$$

$$d[Zn^{2+}]/dt = k_f A_s [H^+] - k_r' A_s p(H_2S)^{1/2} [Zn^{2+}]^{1/2}$$

or

$$d[Zn^{2+}]/dt = k_f A_s [H^+] - k_r A_s [H_2S(aq)]^{1/2} [Zn^{2+}]^{1/2} \qquad (6.1)$$

as

$$H_2S(aq) \leftrightarrow H_2S(g)$$

A_s is the surface area of ZnS in the reaction.

$p(H_2S)$ is the partial pressure of $H_2S(g)$.

k_f, k_r and k_r' are forward and reverse reaction rate constants, respectively.

It was necessary to determine, firstly, whether this rate equation (Eqn. 6.1) was obeyed at elevated temperatures and, secondly, the values of the equilibrium constant, rate constants and activation energy.

6.1 VALIDATION OF THE RATE EQUATION

Equation 6.1 suggests that in the initial stage the rate of the reverse reaction ought to be negligible, with the dissolution equation being reduced to

$$(d[Zn^{2+}]/dt)_o = k_f \, A_{so} \, [H^+]_o \qquad (6.2)$$

where $(d[Zn^{2+}]/dt)_o$ = initial rate

$[H^+]_o$ = initial hydrogen ion concentration

A_{so} = initial surface area

Under conditions where equation 6.2 holds, it then becomes a simple matter to determine the effect of surface area and hydrogen ion concentration on the forward reaction rate term. To this end, the effects of the following factors on the rate were examined:

- stirring speed
- pulp density
- effect of hydrogen ion concentration
- effect of surface area

6.1.1 Effect of stirring speed

The effect of stirring speed was investigated to determine a speed at which the reaction rate was unaffected by diffusion of species to and from the reaction interface.

425.4 μm fraction

In an attempt to reduce the reaction rate, a larger size fraction, ZnS-F4 (425.4 μm, -710 +240 μm) was also used. However, the dissolution rate of this fraction was significantly affected by stirring speed (Figure 6.1), with the dissolution rate increasing with increasing stirrer speed. This suggested that attrition of the particles was occurring, with higher stirring speeds causing greater attrition, increasing the reactive surface area and thus the dissolution rate. This variation in surface area made it unsuitable for determining absolute dissolution rates. Nonetheless, it could be utilised in experiments where knowledge of the surface area was not critical, e.g. equilibrium measurements and comparative studies. Subsequent experiments using this material were conducted at 800 rpm to minimise the effect of variation in stirring speed as much as possible and for consistency with other work.

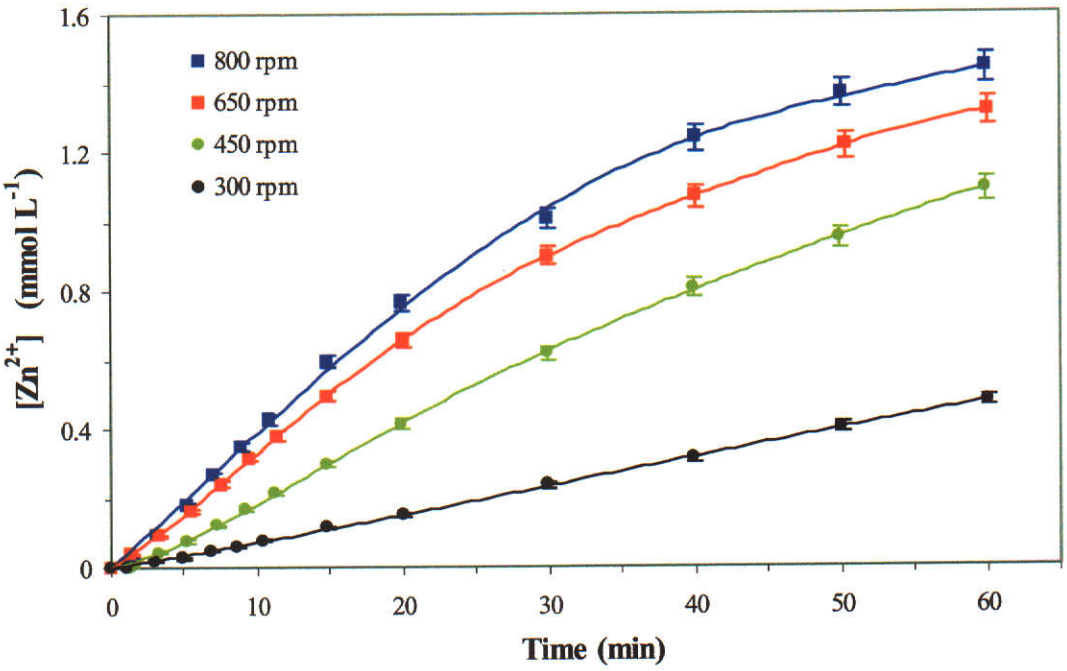

Figure 6.1 Effect of stirring speed on the dissolution of ZnS-F4 (425.4 μm) in 0.1 mol L^{-1} H_2SO_4 at 150°C.

27.3 μm fraction

To overcome the problem of attrition a smaller size fraction, ZnS-F2 (27.3 μm, -52.3 +4.10 μm), was employed. Using this size fraction the dissolution rate was unaffected by increasing the stirring speed (Figure 6.2), indicating that the

dissolution of ZnS in H_2SO_4 was not diffusion controlled at the stirring speeds employed. In addition, the results indicate that there was no attrition of particles in the initial stages. A stirring speed of 800 rpm was used in subsequent experiments.

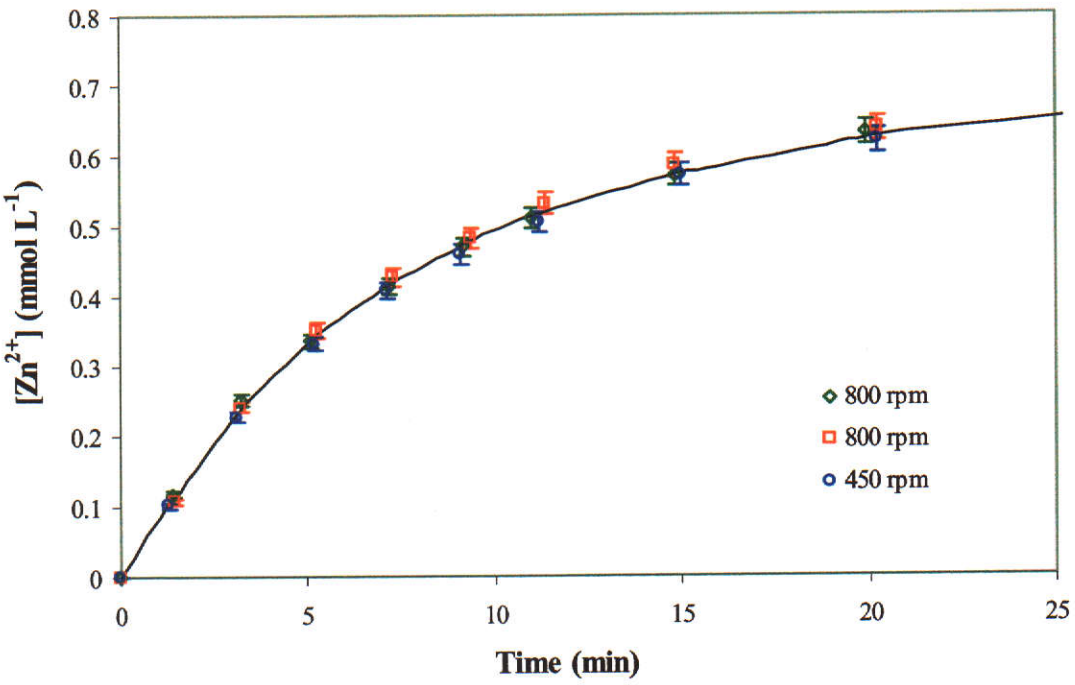

Figure 6.2 Effect of stirring speed on the dissolution of ZnS-F2 (27.3 μm) in 0.025 mol L^{-1} H_2SO_4 at 150°C.

6.1.2 Effect of pulp density

To study the forward reaction it is necessary to isolate it from the reverse reaction, i.e. render the rate of the reverse reaction negligible. This can be achieved by reducing the pulp density, and was studied using both size fractions.

425.4 μm fraction

Decreasing the pulp density below 0.2 g L^{-1} did not significantly increase the initial dissolution rate when leaching the 425.4 μm fraction in 0.09 mol L^{-1} H_2SO_4 at 150°C (Figure 6.3). This indicates that the contribution from the reverse reaction to the initial rate is negligible provided the pulp density is at most 0.2 g L^{-1}. Subsequent experiments where this size fraction was used to ascertain the applicability of equation 6.2 were undertaken using a pulp density of 0.2 g L^{-1}. The upward

curvature evident in the initial stage of each leach curve is due to increasing ZnS surface area caused by attritioning of the ZnS particles.

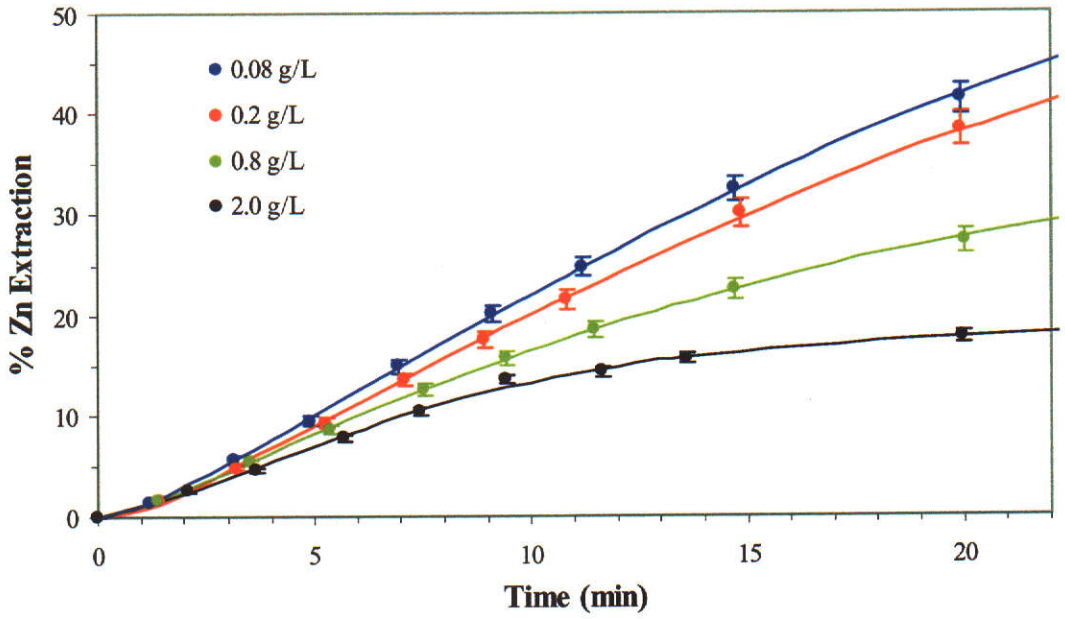

Figure 6.3 Effect of pulp density on dissolution of ZnS-F4 (425.4 μm) in 0.09 mol L^{-1} H_2SO_4 at 150°C.

27.3 μm fraction

Due to the higher surface area of this fraction, a lower acidity was used (0.024 mol L^{-1}) in order to reduce the dissolution rate to measurable values at 150°C. When the pulp density of this fraction was reduced to 0.2 and 0.08 g L^{-1}, similar initial dissolution rates were observed (Figure 6.4 and Figure 6.5), indicating that the rate of the reverse reaction was insignificant in the initial stages at these pulp densities. At higher pulp densities the reverse reaction becomes increasingly significant, decreasing the initial dissolution rate.

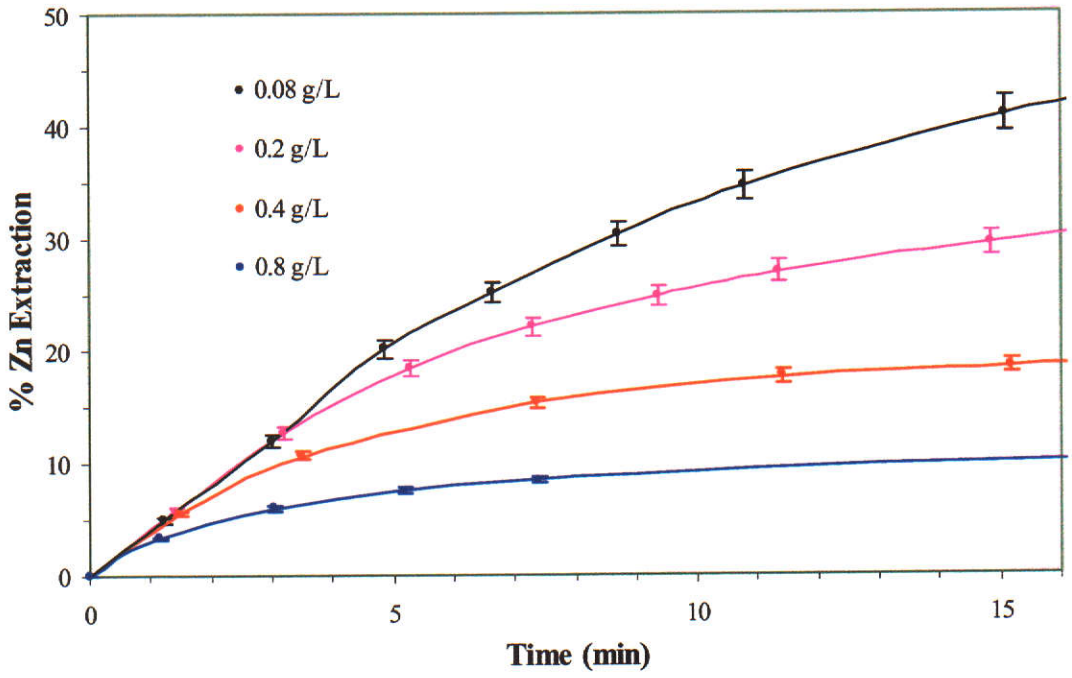

Figure 6.4 Effect of ZnS pulp density on dissolution of ZnS-F2 (27.3 μm) in 0.024 mol L^{-1} H_2SO_4 at 150°C in the initial stages.

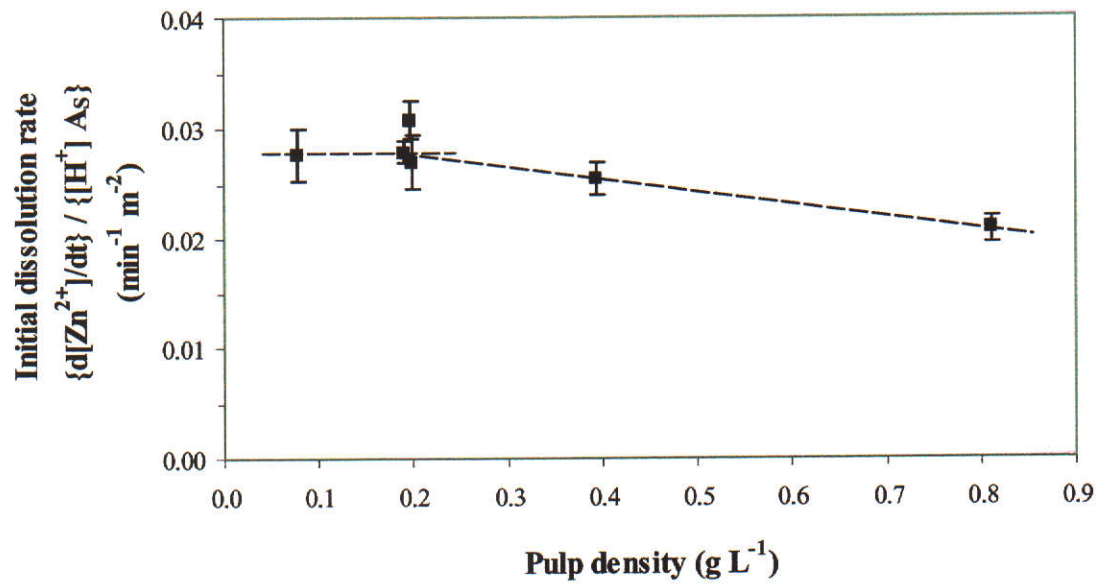

Figure 6.5 Effect of pulp density on initial dissolution rate at 150°C.
Initial rate corrected for variations in $[H^+]$ and surface area. $[H^+] = 0.024$ mol L^{-1}

6.1.3 *Effect of hydrogen ion concentration*

The effect of hydrogen ion concentration on the initial dissolution rate was measured at 150°C in H_2SO_4 concentrations from 0.1 to 0.5 mol L^{-1} using the 425.4 μm fraction. Figure 6.6 shows that the initial rate is directly proportional to $[H^+]$, i.e. the dissolution reaction is first order with respect to $[H^+]$. The hydrogen ion concentration was calculated using the method given in the Appendix.

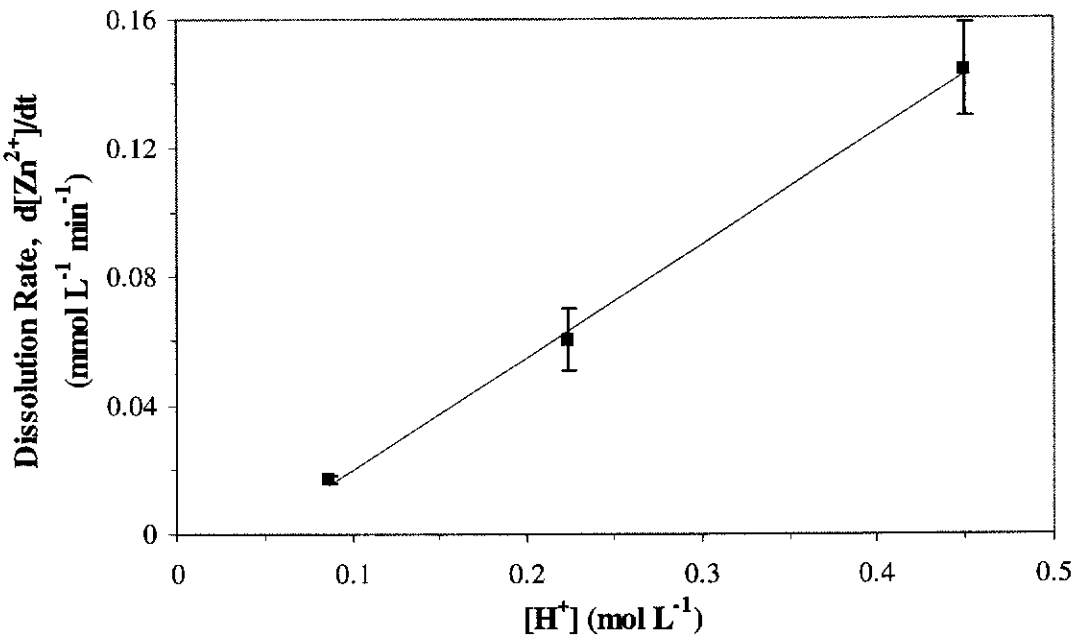

Figure 6.6 Effect of $[H^+]$ on dissolution rate of ZnS-F4 (425.4 μm) at 150°C. ZnS = 0.2 g L^{-1}

6.1.4 *Effect of surface area*

To determine the effect of surface area on the dissolution rate, two size fractions, 8.45 μm and 27.3 μm, were leached under conditions where the reverse reaction was negligible in the initial stages (Figure 6.7). Although only two data points were collected (as the coarse fractions attrition and are not useable), they lie on a straight line that passes through the origin, within experimental error, indicating a first order dependence of the forward reaction rate on the surface area.

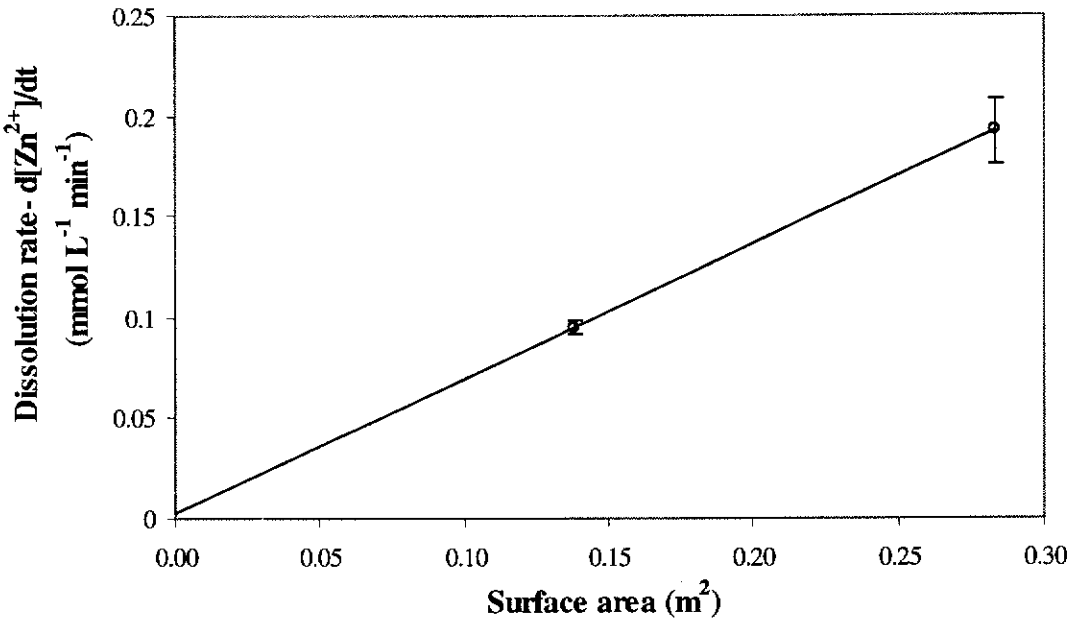

Figure 6.7 Effect of surface area on initial dissolution rate of ZnS in 0.024 mol L^{-1} H_2SO_4 at 150°C. ZnS = 0.2 g L^{-1}.

The observed first order relationships between the dissolution rate and surface area and $[H^+]$ confirm that at 150°C the forward reaction obeys the same relationship as is observed at temperatures below 70°C (Eqn. 6.2, p. 111).

This result also indicates that, although the material is porous, the entire surface (internal and external) in each of these size fractions is accessible to the leach solution.

6.1.5 Effect of zinc ion concentration

In the absence of added zinc sulfate, 48% zinc extraction was achieved. Increasing the concentration of Zn^{2+} in the leach solution to 2.0, 4.1 and 8.2 mmol L^{-1} decreased the extraction of zinc to 40%, 30% and 22% respectively, demonstrating the strong inhibiting effect of zinc ions on the dissolution rate (Figure 6.8).

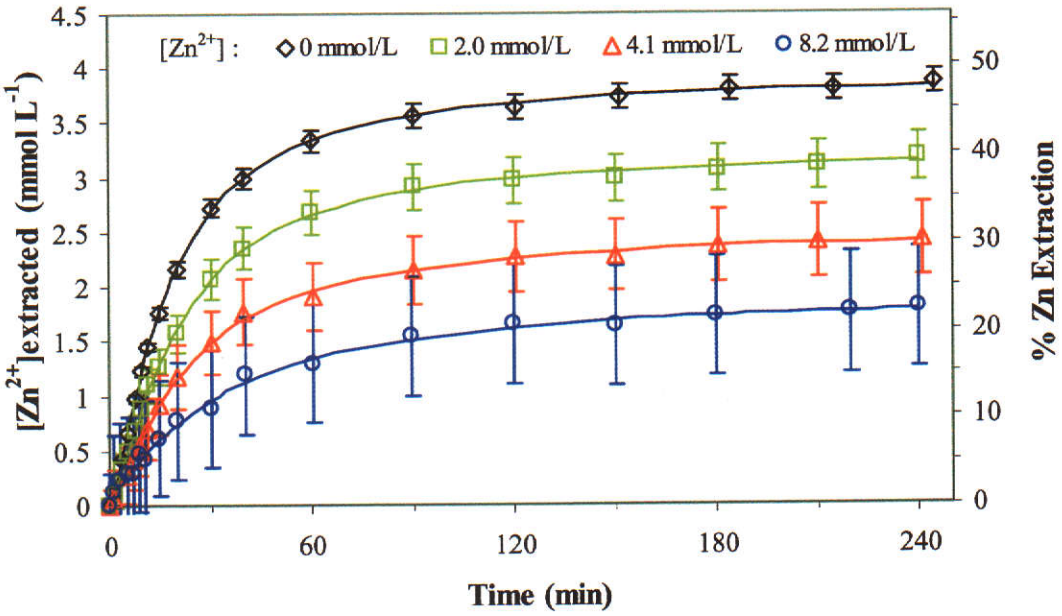

Figure 6.8 Effect of Added Zn^{2+} on the dissolution of ZnS (0.8 g L^{-1}) in 0.09 mol L^{-1} H_2SO_4. T = 150°C, stirring speed = 800 rpm, ZnS-F4 (425.4 µm)

The leach data in Figure 6.8 was used to determine the order of the reaction with respect to the concentration of zinc ions.

Re-arranging the dissolution equation (Eqn. 6.1) gives

$$\frac{k_f A_s[H^+] - d[Zn^{2+}]/dt}{A_s} = k_f[H_2S]^{0.5}[Zn^{2+}]^{0.5} \qquad (6.3)$$

If the order of reaction with respect to $[Zn^{2+}]$ is 0.5, then a plot of the left hand term in equation 6.3 versus $[Zn^{2+}]^{0.5}$ should yield a straight line. The value of $\frac{k_f A_s[H^+] - d[Zn^{2+}]/dt}{A_s}$ was determined for each leach at equivalent zinc extractions, rather than at equivalent leach times, in order to render constant the $[H_2S(aq)]$ term in the right hand side of equation 6.3, since at any given % zinc extraction the number of moles of ZnS leached in each leach are equivalent and hence the concentrations of $H_2S(aq)$ produced are also equivalent. By doing this, the only variable in the right hand side was the concentration of zinc, $[Zn^{2+}]$.

The term, $\frac{k_f A_s[H^+] - d[Zn^{2+}]/dt}{A_s}$, was evaluated as follows.

The surface area at a given % zinc extraction (A_s) was determined from the mass of ZnS present and the specific surface area at the given percentage, α, of ZnS reacted.

$$A_s = m(ZnS) \times A_{specific} \quad (6.4)$$

The mass of ZnS at a given percentage extraction, α, was calculated from the initial mass of ZnS ($m(ZnS)_o$) using equation 6.5.

$$m(ZnS) = (1 - \alpha/100) \times m(ZnS)_o \quad (6.5)$$

However, since the size fraction used in these leaches (425.4 μm) experiences attrition and as such its specific surface area increases with increasing time, a function expressing the specific surface area versus time relationship was required. This was determined using data from a leach where there was negligible reverse reaction in the initial stage (0.08 g L^{-1} leach in Figure 6.4). In this case, since the reverse reaction rate is negligible, the reverse reaction term in equation 6.1 can be neglected and the resulting equation rearranged to give the specific surface area, $A_{specific}$, as a function of time.

$$A_{specific} = \frac{d[Zn^{2+}]/dt}{k_f [H^+] m(ZnS)} \quad (6.6)$$

To minimise errors in calculating the specific surface area, dissolution rates were compared at low % zinc extractions, since at low % zinc extractions the leach times were similar and thus in each case the particles were agitated for similar periods of time. The greatest difference in leaching times was when comparing dissolution rates of leaches that had 3.5% Zn extraction, where the rate was measured after 2.6 minutes in one leach and after 5.9 minutes in another, i.e a difference of only 3.3 minutes.

The hydrogen ion concentration was taken as the initial hydrogen ion concentration,

since it was present in great excess and at the low zinc extractions, negligible reduction in its concentration would have occurred.

The overall dissolution rate ($d[Zn^{2+}]/dt$) was determined by taking the derivative of a polynomial fit to the leach data.

The forward reaction rate constant, k_f , used, was determined using a smaller size fraction (27.3 μm, Section 6.1.6.1, Table 6.2); the larger size fractions being unsuitable for this purpose since they experience attrition.

Plotting $\frac{k_f A_s[H^+] - d[Zn^{2+}]/dt}{A_s}$ versus $[Zn^{2+}]^{0.5}$ at three different zinc extractions, 0 %, 1.2 % and 3.5 %, yielded straight line relationships in each case, indicating that the order of reaction with respect to the concentration of zinc is 0.5 (Figures 6.9, 6.10 and 6.11).

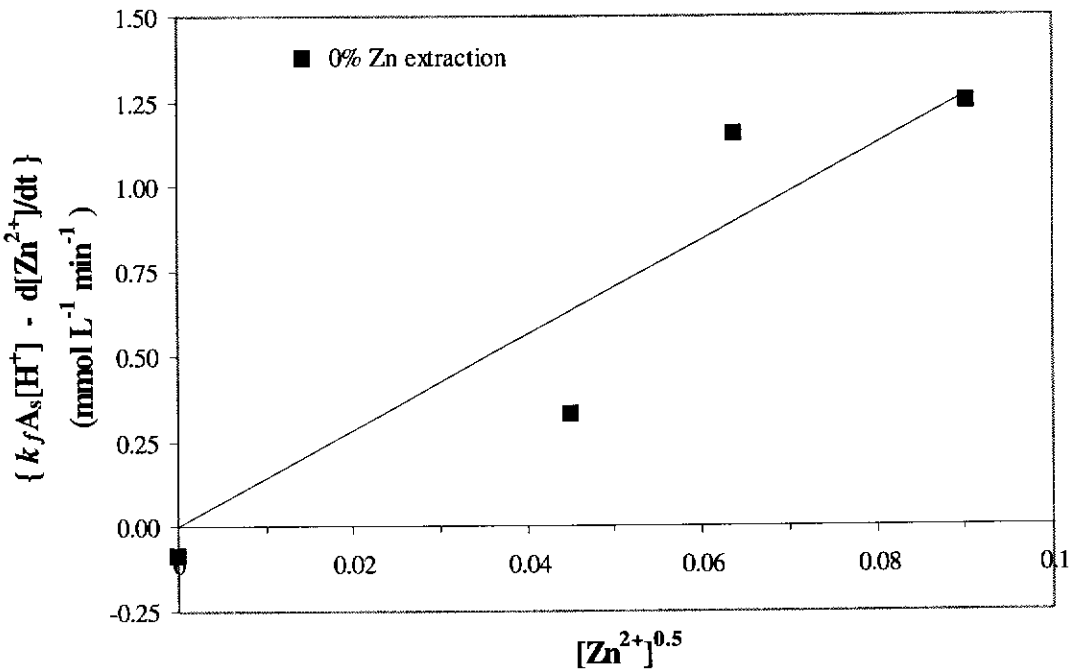

Figure 6.9 Plot of $[Zn^{2+}]^{0.5}$ versus the rate of the reverse reaction at 0% zinc extraction.

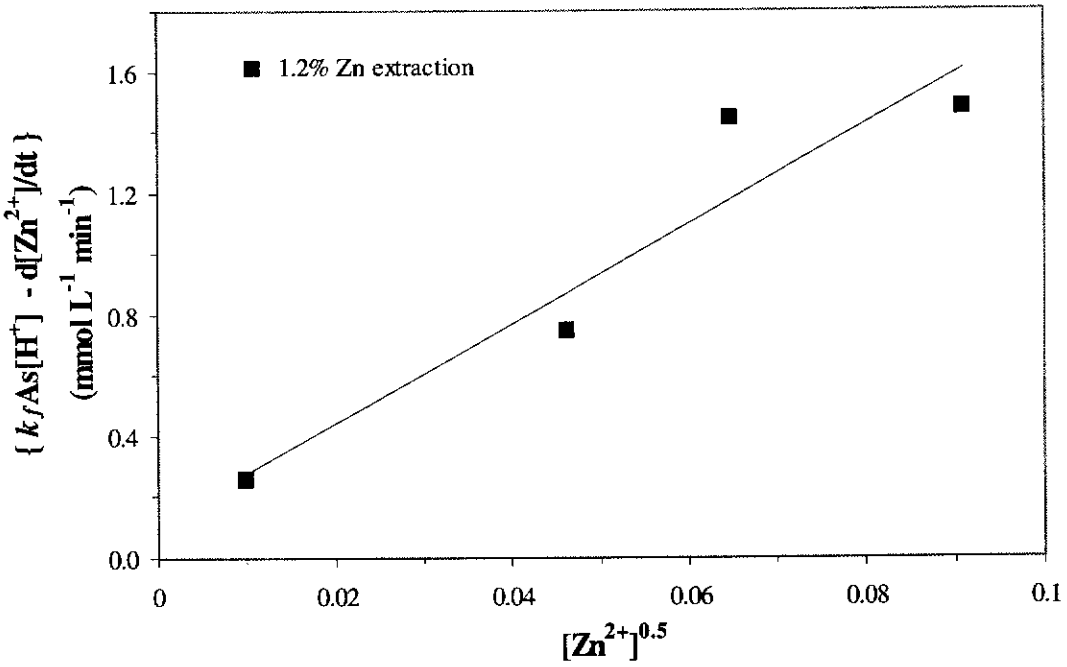

Figure 6.10 Plot of $[Zn^{2+}]^{0.5}$ versus the rate of the reverse reaction at 1.2% zinc extraction.

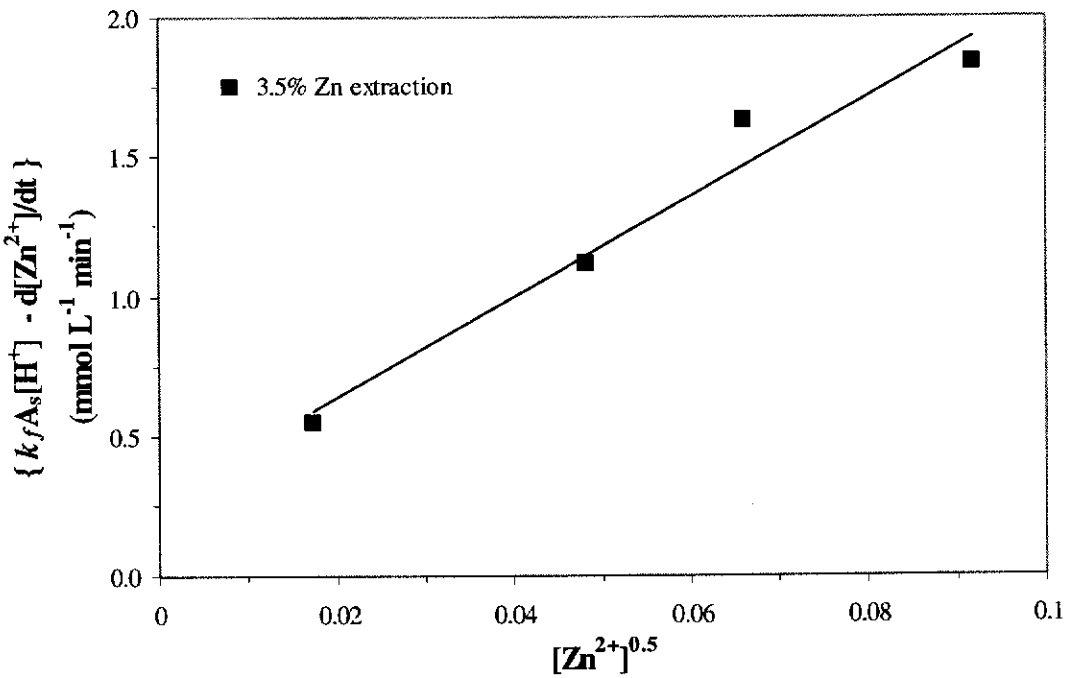

Figure 6.11 Plot of $[Zn^{2+}]^{0.5}$ versus the rate of the reverse reaction at 3.5% zinc extraction.

6.1.6 Confirmation of the rate equation by comparison of calculated and experimental leach curves

Experimental $[Zn^{2+}]$ versus time leach curves were compared with calculated curves at 100°C and 150°C to confirm that the rate of dissolution of ZnS in H_2SO_4 obeys equation 6.1. The 27.3 μm fraction was used for this purpose. The 425.4 μm fraction was unsuitable because its surface area is affected by agitation.

To enable the curves to be calculated it was necessary to:

a) determine k_f and k_r, from experimental data

b) obtain expressions for $[H^+]$, $[H_2S(aq)]$ and A_s in terms of $[Zn^{2+}]$

6.1.6.1 Determination of the rate constants, k_f and k_r

The forward reaction rate constant, k_f , was determined from measurements of the initial rate in experiments conducted under conditions (Table 6.1) such that the initial rate could be expressed by equation 6.2, i.e conditions whereby the initial rate of the reverse reaction was negligible.

Table 6.1 Conditions used to determine k_f at 100°C and 150°C, using ZnS-F2 (27.3 μm).

Temperature (°C)	$[H_2SO_4]$ (mol L^{-1})	ZnS pulp density (g L^{-1})
100	0.1	0.5
150	0.024	0.2

From a comparison of leaches at 150°C and 100°C, run under conditions given in Table 6.1, it is evident that the conditions chosen for the 100°C leach also render its reverse reaction rate negligible in the initial stage. In Figure 6.12 it is apparent that the 150°C leach attains equilibrium in a shorter period of time (~60 min) compared to the 100°C leach (≥ 160 min). Hence, the time at which the rate of the reverse reaction becomes significant would occur earlier in the 150°C leach. Since it was established that in the initial stages of the 150°C leach, under the conditions used, the contribution of the reverse reaction is negligible (see 6.1.2), it must also be negligible in the 100°C leach.

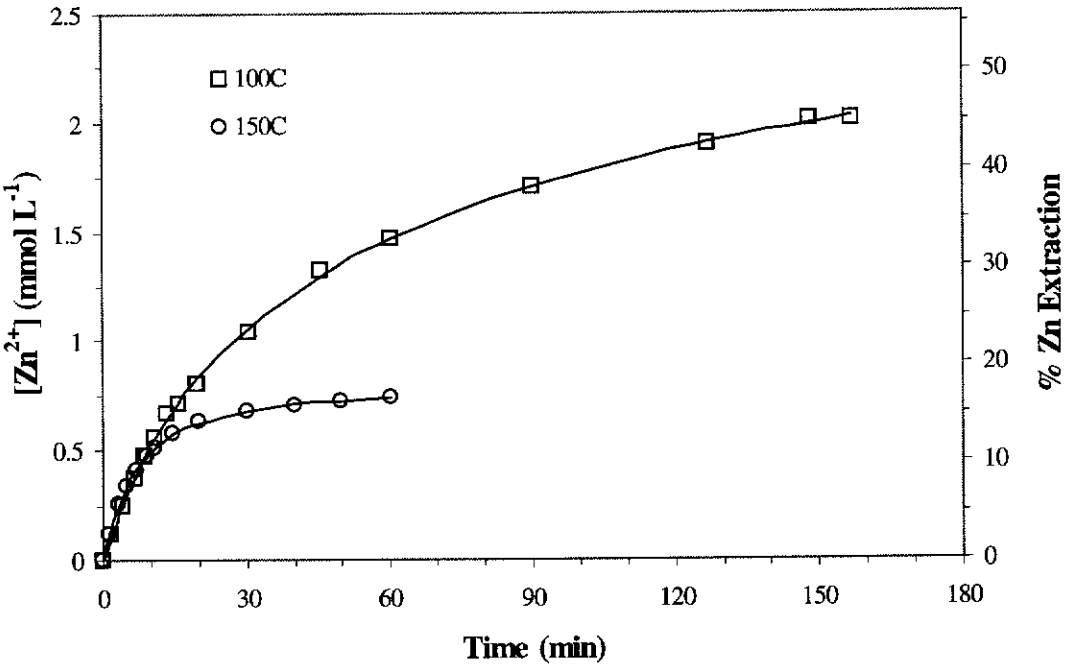

Figure 6.12 Comparison of leaches at 100°C and 150°C conducted under conditions given in Table 6.1.

The forward reaction rate constant, k_f, was evaluated using the initial dissolution rate ($\{d[Zn^{2+}]/dt]_o$), initial surface area (A_{so}) and initial molar hydrogen ion concentration ($[H^+]_o$). The initial surface area (A_{so}) and concentration of sulfuric acid ($[H_2SO_4]_o$) were always known and the initial hydrogen ion concentration was calculated from $[H_2SO_4]_o$ (using the method given in the Appendix).

The dilution of the sulfuric acid solution, by the addition of a known amount of water used for injecting ZnS into the pressure vessel, was taken into account. In addition, solution volume increases due to elevated temperatures were included in the calculations. At 100°C, literature values for the density of sulfuric acid are published (Perry and Green 1997), enabling the solution volume to be calculated from the mass of solution. However, at 150°C, no literature values were available and since the sulfuric acid concentrations were low (0.024 mol L^{-1}), volume increases due to temperature were calculated using the known mass of water and its density at 150°C (Ghiorso and Sack 1995).

Zinc ion concentrations were measured for samples taken throughout the experiment. The initial dissolution rate, $(d[Zn^{2+}]/dt)_o$, was obtained by fitting a polynomial to $[Zn^{2+}]$ versus time plots and differentiating the polynomial to obtain the slope (rate) at t = 0 min.

The equilibrium constants, K_c, were determined by substituting the measured equilibrium concentrations of Zn^{2+} and calculated equilibrium concentrations of $H_2S(aq)$ and H^+ into equation 6.7.

$$K_c = \frac{[Zn^{2+}]_{eq}[H_2S]_{eq}}{[H^+]^2_{eq}} \tag{6.7}$$

where $[Zn^{2+}]_{eq}$, $[H_2S]_{eq}$ and $[H^+]_{eq}$ are the equilibrium molal concentrations of the species in solution.

At equilibrium the forward and reverse reaction rates are equivalent.

$$k_f A_s [H^+]_{eq} = k_f A_s [H_2S(aq)]^{1/2}_{eq} [Zn^{2+}]^{1/2}_{eq} \tag{6.8}$$

Combining equations 6.7 and 6.8 gives an expression relating the equilibrium constant to the rate constants

$$K_c = \left(\frac{k_f}{k_r}\right)^2 \tag{6.9}$$

Using the equilibrium constants and forward reaction rate constants, the reverse reaction rate constants were calculated using equation 6.9. The results are summarised in Table 6.2

Table 6.2 Equilibrium and rate constants for the dissolution of ZnS-F2 (27.3 μm) in sulfuric acid at 100°C and 150°C.

Temperature (°C)	k_f ($\times 10^{-3}$) (min^{-1} m^{-2})	k_r ($\times 10^{-1}$) (min^{-1} m^{-2})	K_c ($\times 10^{-4}$)
100	2.50 ± 0.13	1.10 ± 0.19	5.16 ± 0.63
150	28.3 ± 1.5	9.0 ± 1.6	9.8 ± 1.3

From the equilibrium and rate constants, K_c, k_f and k_r, the terms, A_s, $[H^+]$ and $[H_2S(aq)]$ can then be determined throughout the progress of the reaction as functions of $[Zn^{2+}]$.

6.1.6.2 Expressions for surface area (A_s), $[H^+]$ and $[H_2S(aq)]$ in terms of $[Zn^{2+}]$

The variables, A_s, $[H^+]$ and $[H_2S(aq)]$ were derived as functions of $[Zn^{2+}]$ on the basis of the following assumptions:

The zinc sulfide material used behaves as a collection of uniformly sized solid spheres. This assumption is reasonable, since, even though the material is porous, the entire surface (internal and external) is accessible to the leach solution (see 6.1.4).

As the density of sulfuric acid solutions at temperatures above 100°C was not available, it was assumed that the density of the dilute solution was equivalent to the density of water. Errors introduced by this assumption are likely to be negligible as there is only 0.7% difference between the density of water (0.9578 g mL^{-1}) and 1% H_2SO_4 (0.9645 g mL^{-1}) at 100°C (Perry and Green 1997). To calculate the volume increase due to elevated temperatures, the mass of water in solution was calculated and its density at the given temperature obtained from data tables published by Ghiorso and Sack (1995).

It was assumed that the solubility of H_2S in the sulfuric acid solutions used (0.024 mol L^{-1} and 0.1 mol L^{-1}) was equivalent to its solubility in pure water at the temperatures of interest (100–200°C). Although Henry's constants for H_2S in 0.125

mol L^{-1} H_2SO_4 have been reported by Corriou, Gely and Viers (1988), they were not used in this work as they were considered to be in error. The authors report that they had difficulties with their experimental method. At high temperatures, H_2S was very corrosive toward unprotected parts of the tantalum-lined autoclave and above 150°C, it was oxidised by H_2SO_4 to elemental sulfur (Eqn. 6.10)

$$H_2S + H_2SO_4 \rightarrow S^o + \text{“}H_2SO_3\text{”} + H_2O \qquad (6.10)$$

where “H_2SO_3” denotes a complex mixture of ions and undissociated species.

These difficulties led them to conclude that above 100°C, their data has up to 20% error. Furthermore, comparison of Henry's constants for H_2S in pure water obtained by Corriou, Gely and Viers (1988) with other published values confirms that at 200°C the data of Corriou, Gely and Viers is in error (Figure 6.13).

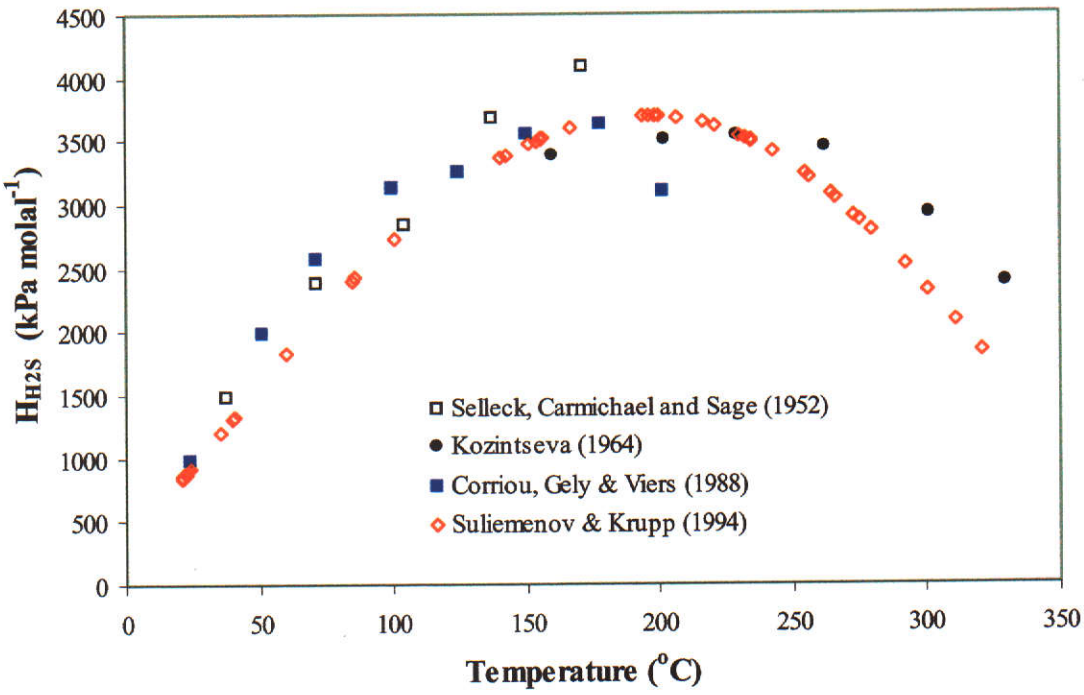

Figure 6.13 Comparison of literature values for Henry's constant (H_{H2S}) for H_2S in pure water.

Hence, the values reported by Corriou, Gely and Viers (1988) were not used. Instead, the most recent literature values of Henrys constants for H_2S in water,

determined by Suleimenov and Krupp (1994), were used.

It was assumed that Henry's constant for H_2S in water is equivalent to that for H_2S in the sulfuric acid solutions used (0.024 mol L^{-1} and 0.1 mol L^{-1}) at the temperatures of interest (100–200°C), since at 25°C, in sulfuric acid concentrations of 0.025 mol L^{-1} and 0.1 mol L^{-1}, Henry's constant increases by only 0.4 and 1.6% respectively relative to its value for pure water (Corriou, Gely and Viers 1988; Suleimenov and Krupp 1994).

Surface area as a function of $[Zn^{2+}]$

The surface area (A_s) for the assemblage of particles can be expressed by equation 6.10 by assuming that it consists of N spherical particles, each having the same radius, r.

$$\begin{aligned} A_s &= 4\pi r^2 \times N \\ &= 4\pi r^2 \times \{m / (4/3\ \pi r^3 \rho)\} \\ &= 3\,m / \rho r \end{aligned} \qquad (6.11)$$

where N = total number of particles
m = mass of ZnS
r = average particle radius
ρ = density of ZnS

Substituting $r = r_o(1-\alpha)^{1/3}$

where r_o = initial average particle radius
α = fraction of ZnS reacted

$$A_s = \frac{3m}{\rho\, r_o\, (1-\alpha)^{1/3}}$$

$$= \frac{3m}{\rho\, r_o\, (m/m_o)^{1/3}}$$

$$A_S = \frac{3m_o^{1/3}m^{2/3}}{\rho r_o}$$

$$= \frac{3m_o^{1/3}}{\rho r_o}(m_o - [Zn^{2+}]V_{soln}W_m)^{2/3}$$

$$= \frac{3m_o}{\rho r_o}\left(1 - \frac{[Zn^{2+}]V_{soln}W_m}{m_o}\right)^{2/3} \quad (6.12)$$

$$= C_1\left(1 - C_2[Zn^{2+}]\right)^{2/3} \quad (6.13)$$

where $C_1 = 3\ m_o / (\rho\ r_o)$

$C_2 = V_{soln}\ W_m / m_o$

V_{soln} = volume of solution in reactor

W_m = molecular weight of ZnS

m_o = initial mass of ZnS

Including a factor for surface area roughness and porosity gives the surface area to zinc concentration relationship

$$A_s = F_R\ C_1\left(1 - C_2[Zn^{2+}]\right)^{2/3} \quad (6.14)$$

where F_R = Roughness factor = $\frac{A_{s,meas(t=0)}}{A_{s,calc(t=0)}}$

The mass of ZnS removed from the reactor by sampling was negligible and ignored in the calculations.

$[H^+]$ as a function of $[Zn^{2+}]$

For every mole of Zn^{2+} formed, two moles of H^+ are consumed

$$ZnS + 2H^+ \leftrightarrow Zn^{2+} + H_2S$$

The concentration of hydrogen ions at any time during the reaction, $[H^+]$, is given by equation 6.15, where $[H^+]_o$ is the initial hydrogen ion concentration and $[Zn^{2+}]$ is the concentration of zinc ions at time, t.

$$[H^+] = [H^+]_o - 2[Zn^{2+}] \quad (6.15)$$

$[H_2S(aq)]$ as a function of $[Zn^{2+}]$

The concentration of aqueous H_2S was calculated knowing that the total number of moles of H_2S (gaseous and aqueous species) is equivalent to the total number of moles of Zn^{2+} produced.

$$n(H_2S)_{total} = n(H_2S(aq)) + n(H_2S(g)) \quad (6.16)$$

$$n(H_2S)_{total} = m(H_2S(aq)) \times m(H_2O) + n(H_2S(g)) \quad (6.17)$$

$n(H_2S(g))$ was calculated, assuming ideal gas behaviour, using H_{H_2S} (kPa, molal) and $V_{hdspc.}$

Where:

H_{H_2S}	= Henry's constant (kPa kg mol^{-1})
V_{hdspc}	= volume of headspace (L)
$m(H_2S(aq))$	= molality of $H_2S(aq)$ (mol kg^{-1})
R	= 8.314 $JK^{-1}mol^{-1}$
T	= Temperature (K)
$p(H_2S(g))$	= pressure of $H_2S(g)$ (kPa)
$m(H_2O)$	= mass of H_2O (kg)

Combining the ideal gas law

$$n(H_2S(g)) = p(H_2S(g))\, V_{hdspc} / RT \quad (6.18)$$

and Henry's law

$$p(H_2S(g)) = H_{H_2S}\, m(H_2S(aq)) \quad (6.19)$$

gives

$$n(H_2S(g)) = H_{H_2S}\, m(H_2S(aq))\, V_{hdspc} / RT \qquad (6.20)$$

Substituting equation 6.20 into 6.17 gives

$$n(H_2S)_{total} = m(H_2S(aq)) \times m(H_2O) + H_{H_2S}\, m(H_2S(aq))\, V_{hdspc} / RT$$

$$= m(H_2S(aq)) \left(m(H_2O) + \frac{H_{H_2S}\, V_{hdspc}}{RT} \right) \qquad (6.21)$$

which can be rearranged to give an expression for the molality of $H_2S(aq)$

$$m(H_2S(aq)) = \frac{n(H_2S)_{total}}{\left(m(H_2O) + \frac{H_{H_2S}\, V_{hdspc}}{RT} \right)} \qquad (6.22)$$

Converting the concentration of $H_2S(aq)$ from molality (mol kg^{-1}) to molarity (mol L^{-1}).

$$[H_2S(aq)] = \frac{m(H_2S(aq)) \times m(H_2O)}{V_{soln}}$$

$$= \frac{n(H_2S)_{total} \times m(H_2O)}{\left(m(H_2O) + \frac{H_{H_2S}\, V_{hdspc}}{RT} \right) \times V_{soln}} \qquad (6.23)$$

where $m(H_2O) = m(soln) - m(H_2SO_4)$

$= SG_{soln} \times V_{soln} - [H_2SO_4(g/L)]_{soln} \times V_{soln} \times 1000$

with m(soln) and SG_{soln} being, respectively, the mass and specific gravity of the solution.

Using

$$n(H_2S)_{total} = n(Zn^{2+})$$

$$= [Zn^{2+}]\, V_{soln}$$

and substituting into equation 6.23 gives

$$[H_2S(aq)] = \frac{[Zn^{2+}]\,m(H_2O)}{\left(m(H_2O) + \frac{H_{H_2S}\,V_{hdspc}}{RT}\right)} \tag{6.24}$$

$$[H_2S(aq)] = C_3 \times [Zn^{2+}] \tag{6.25}$$

$$\text{where} \quad C_3 = \frac{m(H_2O)}{\left(m(H_2O) + \frac{H_{H_2S}\,V_{hdspc}}{RT}\right)} \tag{6.26}$$

Substituting these variables into equation 6.1 and expressing k_r in terms of K_c and k_f using equation 6.9 gives $d[Zn^{2+}]/dt$ as a function of $[Zn^{2+}]$.

$$d[Zn^{2+}]/dt = F_R\,C_1\left(1 - C_2\,[Zn^{2+}]\right)^{2/3} \times \left(k_f\left([H^+]_o - 2[Zn^{2+}]\right) - \frac{k_f}{\sqrt{K_c}}[Zn^{2+}]^{1/2}\left(C_3[Zn^{2+}]\right)^{1/2}\right) \tag{6.27}$$

The integrated form of equation 6.27 was not obtainable by analytical means. It was solved for $[Zn^{2+}]$ numerically using the 4th order Runge – Kutta method (Billo 1997).

In addition, since in the gathering of data for the experimental leach curves, solution samples of known volume were taken from the reactor, affecting the solution and headspace volumes, the same stepwise reduction in solution volume at given sample times was replicated when solving equation 6.27 to obtain the calculated leach curves. Hence the constants C_2 and C_3 , being dependent on the solution and headspace volumes were allowed to vary accordingly, so that valid comparisons between the experimental and calculated leach curves could be made.

6.1.6.3 Errors in calculated leach curves

The errors in the calculated leach curves are represented by the upper and lower limit lines in Figures 6.14, 6.15 and 6.16. The upper limit lines were obtained by solving equation 6.27 using the maximum values for the equilibrium constants (K_c) and forward reaction rate constants (k_f) at 100°C and 150°C, whereas the lower limit lines were obtained using the minimum values.

The error in K_c was calculated from the errors in the equilibrium concentrations of $Zn^{2+}(aq)$, $H_2S(aq)$ and $H^+(aq)$. In determining these error values, the errors introduced by solution sampling during the reaction were taken into account. The resulting errors in the equilibrium constants were 13.5% at 100°C and 16.2% at 150°C.

Two other potential sources of error, namely, re-precipitation of ZnS after filtering, and reaction between $H_2S(aq)$ and H_2SO_4 were considered as they had the potential to affect the measured equilibrium constants. Since the equilibrium constant decreases with temperature and it could reasonably be expected that on sampling, zinc sulfide would re-precipitate. However, there was no evidence to suggest that re-precipitation of ZnS occurred when solutions at elevated temperatures were sampled and cooled to room temperature.

The sampling procedure involved:

a) collecting the solution in a sample cylinder

b) transferring hot sample solution via 15 cm of pvc tubing to a syringe

c) immediate filtration of the sampled solution using a syringe filter.

It was assumed that no precipitation occurred between steps a) and c), a period of about 30 seconds. No precipitates were observed in the filtered solutions, indicating that no ZnS precipitation occurred after filtration. Thus, this potential source of error can be ignored.

The possibility of the removal of both H_2S and H_2SO_4 via reaction 6.28 was also considered.

$$3H_2S + H_2SO_4 \rightarrow 4S^{\circ} + 4H_2O \qquad (6.28)$$

This reaction has been shown to occur in dilute sulfuric acid (0.02 to 0.18 mol L^{-1}) at elevated temperatures (254°C to 340°C) (Bichowsky 1921). Corriou (1988) also found evidence of this reaction occurring at temperatures as low as 140°C when leaching ZnS in 0.1225 mol L^{-1} H_2SO_4. They found that more H_2SO_4 was consumed than expected, based on the ZnS dissolution reaction stoichiometry (Eqn. 2.28, p. 23) and concluded that additional H_2SO_4 may have been removed by its reaction with H_2S (Eqn. 6.28).

However, in this work, in leaches conducted using 0.025 and 0.1 mol L^{-1} H_2SO_4 and at temperatures up to 200°C, no reaction between H_2SO_4 and H_2S was observed. If consumption of H_2S by H_2SO_4 had occurred then it is expected that the dissolution of ZnS would have increased. However, the leach curves do not show evidence of this (Figures 6.5, 6.7 and 6.10).

The error in k_f was determined from the errors in the initial rate of Zn^{2+} production, $(d[Zn^{2+}]/dt)_o$ and the initial hydrogen ion concentration. The error in $(d[Zn^{2+}]/dt)_o$ was determined by fitting 2nd and 3rd order polynomials to the leach data and obtaining the standard deviation in the slopes of these at t=0. The resulting errors in k_f at 100°C and 150°C were 5.2%.

6.1.6.4 Experimental and calculated leach curves

The close agreement between experimental leach curves and calculated $[Zn^{2+}]$ versus time curves obtained using equation 6.1, confirms that this equation describes the dissolution of ZnS in sulfuric acid at 100°C (Figure 6.14) and 150°C (Figure 6.15).

Experimental data from leaches of varying pulp density at 150°C also agreed with calculated data (Figure 6.16).

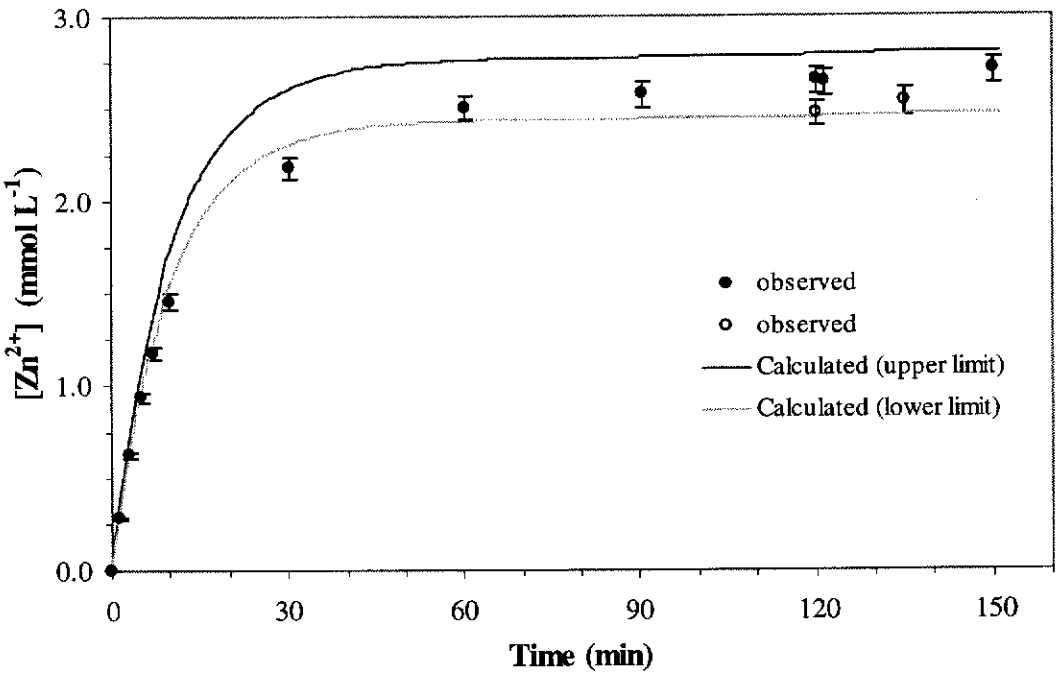

Figure 6.14 Comparison of calculated and observed values for the dissolution of ZnS (1.6 g L^{-1}) in H_2SO_4 (0.1 mol L^{-1}) at 100°C.

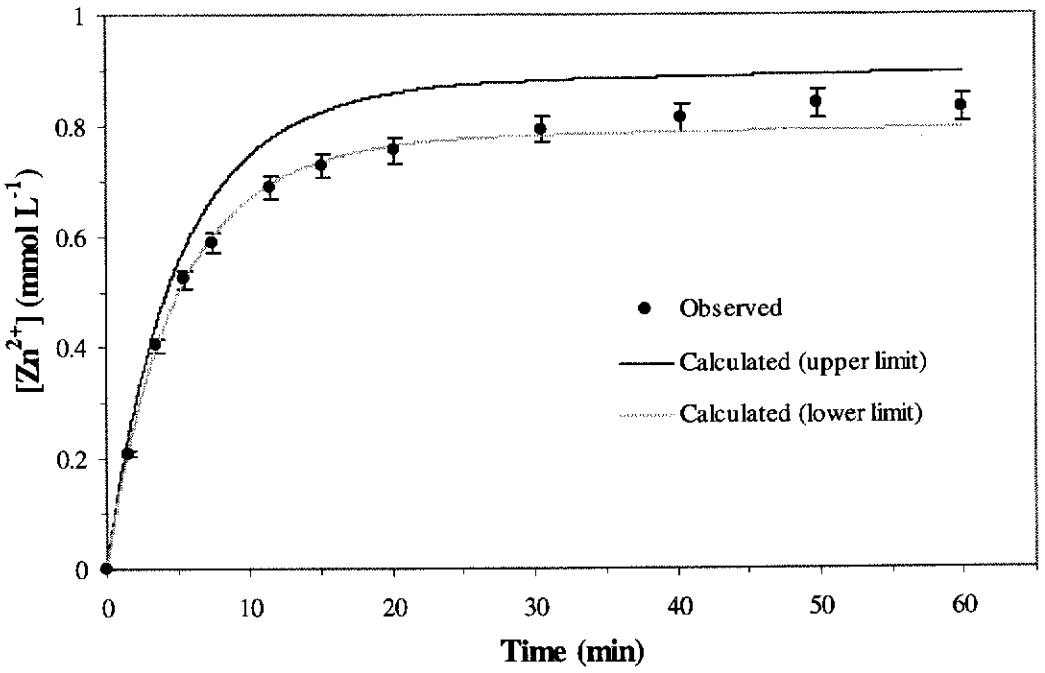

Figure 6.15 Comparison of calculated and observed values for the dissolution of ZnS (0.4 g L^{-1}) in H_2SO_4 (0.024 mol L^{-1}) at 150°C.

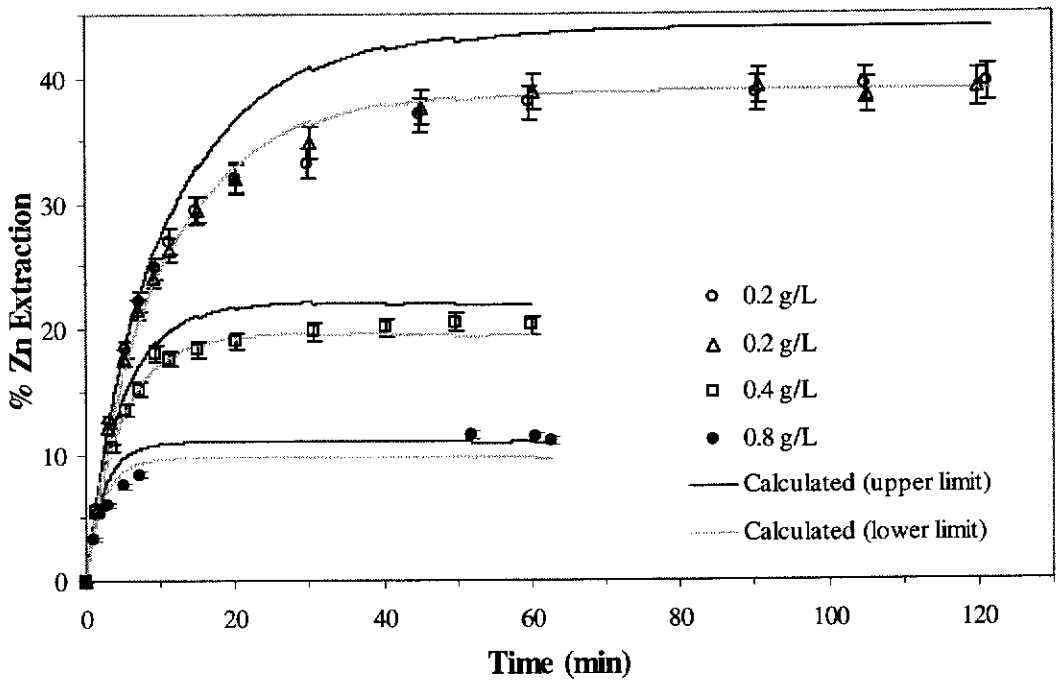

Figure 6.16 Comparison of calculated and observed % zinc extractions at varying pulp densities for the dissolution of ZnS in H_2SO_4 (0.024 mol L^{-1}) at 150°C.

In the period leading up to equilibrium, the observed leaching values were consistently closer to the lower calculated limit. This is probably the result of some of the particles being caught up in crevices among the internal fittings of the pressure vessel. At the completion of a leach, unreacted ZnS was always found in the screw thread of the bolt of the spacer between the thermocouple well and stirrer shaft. ZnS also gathered at places where the internal cooling coils pressed against the wall of the vessel. This would have caused the mass and hence surface area of ZnS in contact with the solution to be reduced, resulting in a reduction in the dissolution rate and thus decreased zinc extractions compared to those calculated using equation 6.27. The removal of ZnS from the leach solution would not have affected the final equilibrium zinc extraction, which is what is observed (Figures 6.14 - 6.16).

6.2 EFFECT OF TEMPERATURE

The effect of varying the temperature from 100°C to 200°C was examined in order to determine its effect on the initial rate and the equilibrium constant and enable the activation energy and reaction enthalpy to be determined.

6.2.1 Effect of temperature on initial rate

At 200°C the rate of dissolution of ZnS is rapid. Consequently, to reduce the rate to a measurable value, the coarser size fraction, ZnS-F4 (425.4 μm), was used. The leach curves are given in Figure 6.17, and show the dissolution rate increasing with increasing temperature.

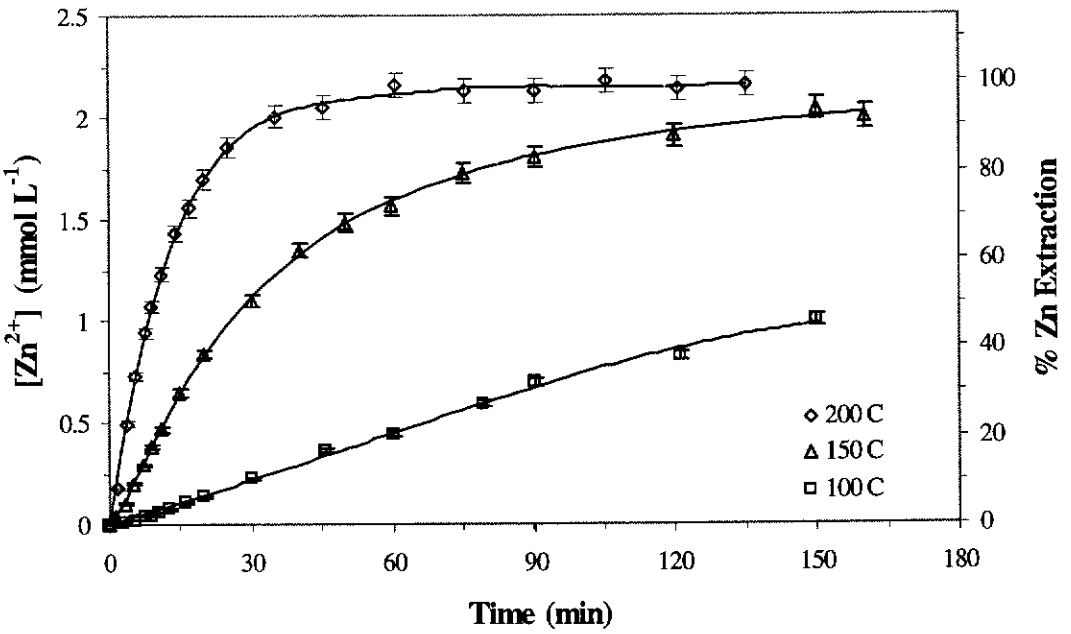

Figure 6.17 Effect of temperature (100 – 200°C) on dissolution of ZnS-F4 (425.4 μm) (0.2 g L^{-1}) in 0.1 mol L^{-1} H_2SO_4.

The true forward reaction rate constant, k_f, was not able to be determined since the initial specific surface area, Φ, in contact with the leach solution was unknown, because of the attritioning of the coarse particles used.

Hence, a pseudo-rate constant, k_f', was used. The derivation of the equation for k_f' is given below.

Rearranging equation 6.2 (p. 111) gives the expression for k_f.

$$k_f = \frac{\dfrac{d[Zn^{2+}]_o}{dt}}{A_{s_o}[H^+]_o} \tag{6.29}$$

$$k_f = \frac{\dfrac{d[Zn^{2+}]_o}{dt}}{m(ZnS)_o \, \Phi \, [H^+]_o} \tag{6.30}$$

where

$\dfrac{d[Zn^{2+}]_o}{dt}$ = initial dissolution rate

A_{s_o} = initial surface area

Φ = specific surface area

$m(ZnS)_o$ = initial mass of ZnS

$[H^+]_o$ = initial concentration of hydrogen ions

$$k_f' = \frac{\left(\dfrac{d[Zn^{2+}]}{dt}\right)_o}{m(ZnS)_o \, [H^+]_o} \tag{6.31}$$

$$k_f = \frac{k_f'}{\Phi} \tag{6.32}$$

As the logarithmic form of the Arrhenius equation is,

$$\ln k_f = \ln z - E_a/RT \tag{6.33}$$

substituting k_f' for k_f gives

$$\ln k_f' = \ln \Phi + \ln z - E_a/RT \tag{6.34}$$

The Arrhenius plot of k'_f yielded an apparent activation energy of 56 ± 11 kJ mol^{-1} for the forward reaction (Figure 6.18).

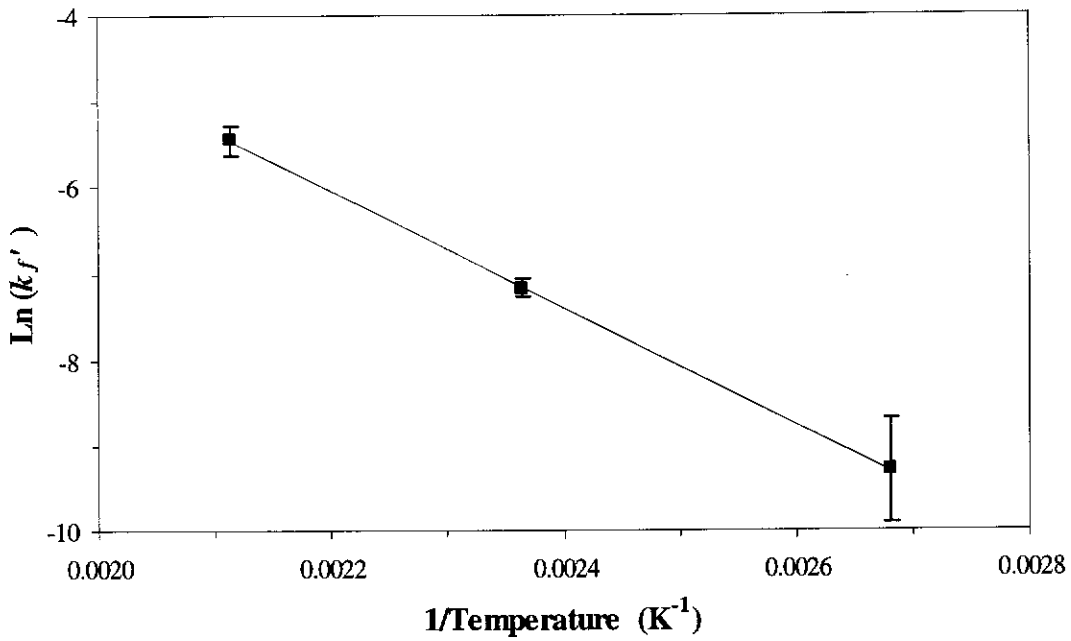

Figure 6.18 Arrhenius plot for forward reaction.
ZnS-F4 (425.4 μm) in 0.09 mol L^{-1} H_2SO_4.

6.2.2 Effect of temperature on the equilibrium

To determine the effect of temperature on the equilibrium constant, ZnS-F4 (425.4 μm) at 0.8 g L^{-1} was leached in 0.1 mol L^{-1} H_2SO_4 at 100°C, 150°C and 200°C. Increasing the temperature from 100°C to 200°C increased the extent of zinc extraction at equilibrium from 31% to 67% (Figure 6.19).

The equilibrium constants, K_c, based on molal concentrations of species in solution, were calculated at each temperature using equation 6.7 (p. 124), where $[Zn^{2+}]_{eq}$, $[H_2S]_{eq}$ and $[H^+]_{eq}$ are equilibrium concentrations.

$$K_c = \frac{[Zn^{2+}]_{eq}[H_2S]_{eq}}{[H^+]^2_{eq}} \qquad (6.7)$$

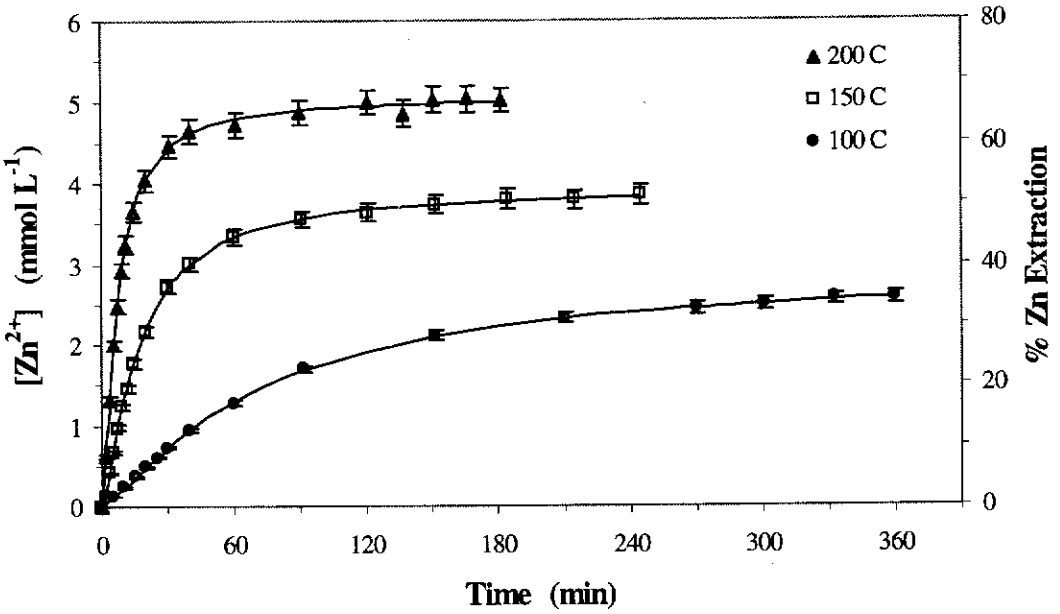

Figure 6.19 Effect of temperature (100°C - 200°C) on extent of dissolution of ZnS. ZnS-F4 (425.4 μm) = 0.8 g L^{-1}, $[H_2SO_4]$ = 0.09 mol L^{-1}

$[Zn^{2+}]_{eq}$ was measured from samples of the solution taken at equilibrium. $[H_2S]_{eq}$ and $[H^+]_{eq}$ were calculated from $[Zn^{2+}]_{eq}$ by the methods given in section 6.1.6.2.

These experimental equilibrium constants are presented, along with published values obtained using a wurtzite (58%)/ sphalerite (42%) mixture (Corriou, Gely and Viers 1988) in Table 6.3. To make valid comparisons between equilibrium constants obtained in this work and values reported by Corriou, Gely and Viers (1988), the data in this work was also evaluated using the same Henry's constants as used by Corriou, Gely and Viers. Although their equilibrium constants were measured in 0.125 mol l^{-1} H_2SO_4, whereas those in this work were measured in 0.1 mol L^{-1} H_2SO_4, the differences are likely to be negligible.

Table 6.3 Equilibrium constants (molality based) for dissolution of ZnS in sulfuric acid (0.09 mol L^{-1}) at 100 – 200°C.
(a) – Suleimenov and Krupp (1994), *(b)* – Corriou, Gely and Viers (1988)

Temp. (°C)	K_c ($\times 10^{-4}$)		
	This work		Corriou, Gely and Viers (1988)
	Using H_{H_2S} in H_2O [a]	Using H_{H_2S} in 0.125 mol L^{-1} H_2SO_4 [b]	
100	4.99 ± 0.81	4.78	2.08
150	12.6 ± 2.2	13.2	6.42
200	28.3 ± 5.5	33.9	47.8

Corriou, Gely and Viers' equilibrium constants at 100°C and 150°C are lower than the values in this work, possibly because their measurements of the solution concentrations of zinc and hydrogen ions were performed after cooling the autoclave. On cooling, since the equilibrium constant decreases with decreasing temperature, it is possible that re–precipitation of ZnS occurred. Consequently, their measured equilibrium constants are likely to be lower than the actual values. In contrast, at 200°C, their equilibrium constant (47.8×10^{-4}) is higher than that observed in this study (28.3×10^{-4}). Even when Corriou, Gely and Viers' value for Henry's constant was used to calculate the equilibrium constant at 200°C, there was still a significant difference between their result and that of this study. A possible reason for this is that hydrogen sulfide may have reacted with their pressure vessel, since they state that hydrogen sulfide was very corrosive toward the unprotected parts of the vessel. This would result in a decrease in the concentration of aqueous hydrogen sulfide, leading to an increase in the zinc ion concentration. This would not pose a problem if the equilibrium constant were determined from measured values of the aqueous zinc ion, hydrogen sulfide and hydrogen ion concentrations. However, they calculated the concentration of aqueous hydrogen sulfide from the measured concentration of zinc ions only, and since the concentration of aqueous hydrogen sulfide is directly proportional to the concentration of zinc ions, any increase in the zinc ion concentration results in an increase in the calculated concentration of hydrogen sulfide. Consequently these higher measured concentrations of zinc ions and calculated concentrations of aqueous hydrogen sulfide, would have caused the

calculated value of the equilibrium constant to be higher than the true value.

The enthalpy of reaction was determined using the van't Hoff isochore (Atkins 1982)

$$\frac{d\ln K}{dT} = \frac{\Delta H_m^o(T)}{RT^2} \tag{6.35}$$

This is rearranged using the relationship

$$\frac{d(1/T)}{dT} = -\frac{1}{T^2} \tag{6.36}$$

$$\text{i.e. } \frac{dT}{T^2} = -d(1/T) \tag{6.37}$$

to give

$$\frac{d\ln K}{d(1/T)} = -\frac{\Delta H_m^o(T)}{R} \tag{6.38}$$

From a plot of $\ln(K_c)$ vs 1/T over the range 100 – 200°C (Figure 6.20), the enthalpy was found to be 25.4 ± 0.7 kJ mol^{-1}, which compares favourably with the enthalpy calculated from thermodynamic data (30.5 kJ mol^{-1}) (Romankiw and de Bruyn 1965).

In this system the enthalpy of reaction (ΔH) is equal to the difference between the activation energies for the forward and reverse reactions (Castellan 1983),

$$\Delta H = E_{a,\,fwd} - E_{a,\,rev} \tag{6.39}$$

Using this equation (Eqn. 6.39), similar enthalpies of 25 and 24.6 kJ mol^{-1} have been calculated over the range 25 – 54°C from published activation energies for the dissolution of synthetic and pure natural sphalerite (Crundwell and Verbaan 1987). Additionally, an enthalpy of 27.6 kJ mol^{-1} was observed over the range 0.5 – 65°C for the dissolution of a 75% sphalerite – 25% wurtzite mixture in sulfuric acid (Romankiw and de Bruyn 1965). The similarity of these values determined at

ambient temperatures with that determined at 100-200°C in this work, suggests that the mechanism at 100°C to 200°C is the same as that at ambient temperatures.

In the only other reported study at elevated temperatures, Corriou, Gely and Viers (1988), using a synthetic ZnS (42% sphalerite, 58%wurtzite), observed that the enthalpy varied from 23.3 kJ mol^{-1} between 25 and 100°C, to 50.8 kJ mol^{-1} between 110 and 150°C and to 106.9 kJ mol^{-1} between 160 and 200°C. The enthalpy observed at the lower temperatures (25–100°C) is consistent with this and other work mentioned above. However, the increase in enthalpy they observed at higher temperatures was not observed in this study. As stated previously, Corriou, Gely and Viers mentioned that H_2S reacted with unprotected parts of their pressure vessel; this may have been a cause of their increasing enthalpy with increasing temperature. The increase in enthalpy from 150 – 160°C was explained by the onset of the reaction of H_2S with H_2SO_4, removing H_2S from the system (Eqn. 6.28). The results in this study did not suggest this effect, as the extraction of zinc did not continually increase with time (Figure 6.19). This would be expected if H_2S was reacting with H_2SO_4 and, as such, being removed from the system.

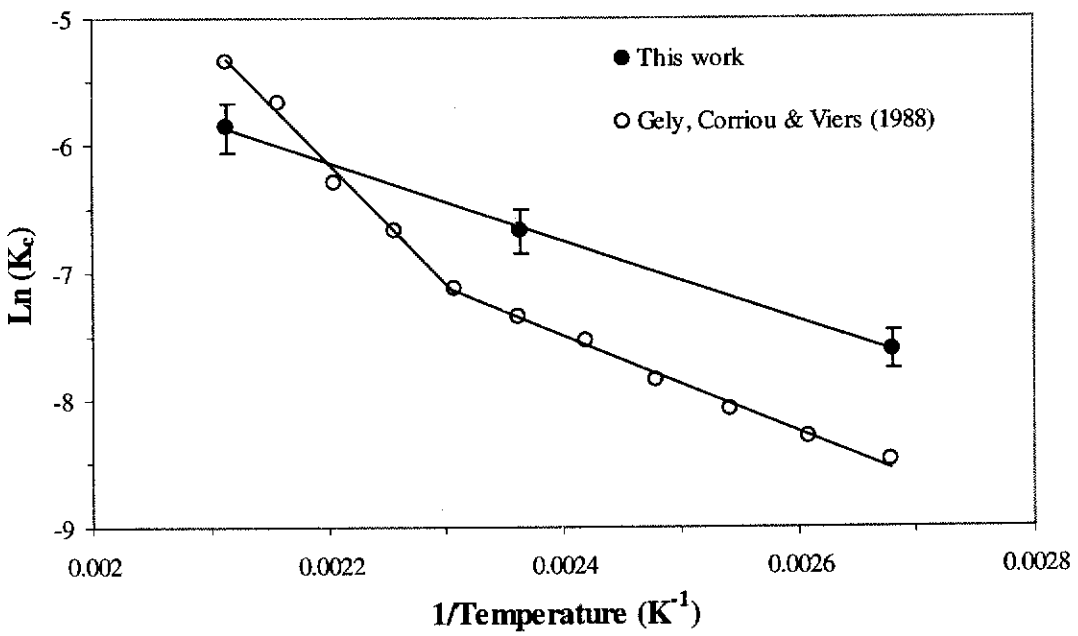

Figure 6.20 Ln (K_c) *vs* reciprocal temperature.

Using the equilibrium constants (Table 6.3) and pseudo forward reaction rate constants, k_f', pseudo rate constants for the reverse reaction, k_r', were calculated at 100, 150 and 200°C.

$$k_r' = \frac{k_f'}{\sqrt{K_c}} \tag{6.40}$$

From an Arrhenius plot of k_r' (Figure 6.21), the activation energy for the reverse reaction was calculated to be 45 ± 15 kJ mol^{-1}, which, within error, is similar to that obtained by Romankiw and De Bruyn (1965) (32.6 ± 4.2 kJ mol^{-1}) over the range 0.6°C – 65°C and slightly higher than values obtained by Crundwell and Verbaan (1987) (25.4 kJ mol^{-1}) over the range 25°C – 54°C.

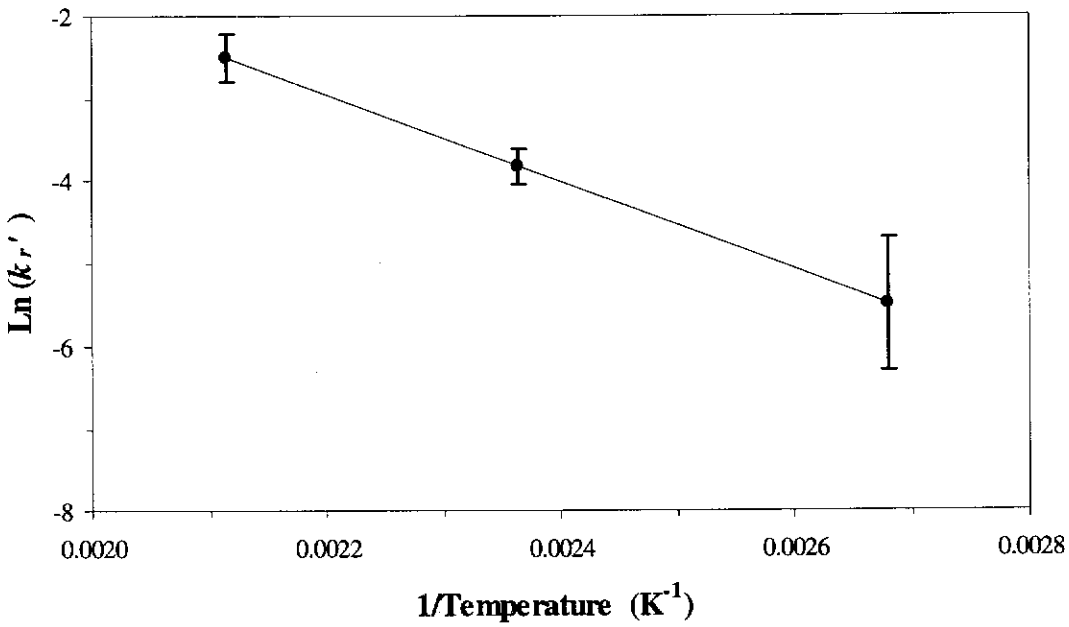

Figure 6.21 Arrhenius plot for reverse reaction.
ZnS-F4 (425.4 μm) in 0.09 mol L^{-1} H_2SO_4.

6.3 SUMMARY

The rate equation for the dissolution of ZnS at ambient temperatures (< 65°C) (Eqn. 6.1, p. 110) also describes the dissolution of ZnS in sulfuric acid at 100 and 150°C.

Equilibrium constants were determined at 100°C, 150°C and 200°C and rate constants for the forward and reverse reactions determined at 100°C and 150°C (Table 6.4).

Table 6.4 Equilibrium and rate constants for the dissolution of ZnS in H_2SO_4 at 100 - 200°C.

Temp (°C)	K_c	k_f	k_r	Source
100	**4.99×10^{-4}**	**2.50×10^{-3}**	**1.10×10^{-1}**	**This work**
	2.08×10^{-4}	–	–	(Corriou, Gely and Viers 1988)
150	**1.26×10^{-3}**	**2.83×10^{-2}**	**9.05×10^{-1}**	**This work**
	6.42×10^{-4}	–	–	(Corriou, Gely and Viers 1988)
200	**2.83×10^{-3}**	–	–	**This work**
	4.78×10^{-3}	–	–	(Corriou, Gely and Viers 1988)

This gives a picture of the ZnS - Zn^{2+} equilibrium in H_2SO_4 in the absence of oxidising or reducing agents. As can be seen ZnS is not very soluble in H_2SO_4, even at elevated temperatures, but if H_2S can be removed from the system then dissolution should proceed unhindered.

The activation energies for the forward and reverse reactions in the range 100°C to 200°C are also similar to those observed at ambient temperatures (see Table 6.5), suggesting that there is no change in the dissolution mechanism on increasing the temperature to 200°C.

Table 6.5 Apparent activation energies for the dissolution of ZnS in H_2SO_4.

Temp. (°C)	$E_{a, fwd}$ (kJ mol^{-1})	$E_{a, rev}$ (kJ mol^{-1})	Material	Source
0.6 – 65	46.4 ± 4.2	32.6 ± 4.2	75% sphalerite, 25% wurtzite, synthetic	Romankiw and De Bruyn (1965)
25 – 54	43.9	31.6	sphalerite, natuaral	Crundwell and Verbaan (1987)
25 – 54	37.9	25.4	sphalerite, synthetic	Crundwell and Verbaan (1987)
100 – 200	**56 ± 11**	**45 ± 15**	**sphalerite, synthetic**	**This work**

7 PRESSURE LEACHING OF ZINC SULFIDE IN H_2SO_4 AND SO_2

Sulfuric acid leaching of zinc sulfide is limited by the generation of H_2S, which inhibits dissolution. The removal of H_2S would allow dissolution to proceed. One possible method of removing H_2S is to react it with SO_2. This would be of commercial benefit as waste SO_2 from the roasting stage would be converted to elemental sulfur. This section addresses the effect of SO_2 on the ZnS / H_2SO_4 reaction.

7.1 EFFECT OF SO_2 ON THE DISSOLUTION KINETICS OF ZnS IN H_2SO_4

Since the dissolution of ZnS in H_2SO_4 (Eqn. 2.28, p. 23)

$$ZnS + H_2SO_4(aq) \leftrightarrow ZnSO_4(aq) + H_2S(aq)$$

involves competing forward and reverse reactions, the effect of SO_2 on each of these reactions was examined.

The effect of SO_2 on the forward reaction was examined at low ZnS pulp densities (0.2 g L^{-1}), where the contribution of the reverse reaction to the dissolution rate is known to be negligible. To examine the effect of SO_2 on the reverse reaction the pulp density was increased to 2 g L^{-1} to ensure that the reverse reaction was significant.

7.1.1 *Effect of SO_2 on the forward reaction*

At 150°C the addition of SO_2 had negligible effect on the initial rate of the forward reaction (Figure 7.1), confirming, as found with studies at ambient temperatures, that SO_2 does not interact directly with ZnS. Even an eight-fold increase in $[SO_2(aq)]$ produced, within error limits, no change in the initial dissolution rates (Figure 7.2). Increasing the SO_2 concentration caused the longer term dissolution rate and the extent of leaching to decrease slightly. This is likely to be due to ZnS particles adhering to molten sulfur globules, which would reduce the surface area available for leaching. In the leach with the highest concentration of SO_2 (0.4 mol L^{-1}) the residue contained a large lump (~ 1 cm diam.) of solidified sulfur. It is likely that in this leach some of the ZnS particles were bound up in this molten sulfur. Only one ZnS / H_2SO_4 / SO_2 leach residue contained such a large lump of sulfur. In all the other leaches reported in this chapter, the sulfur in the residues was finely divided.

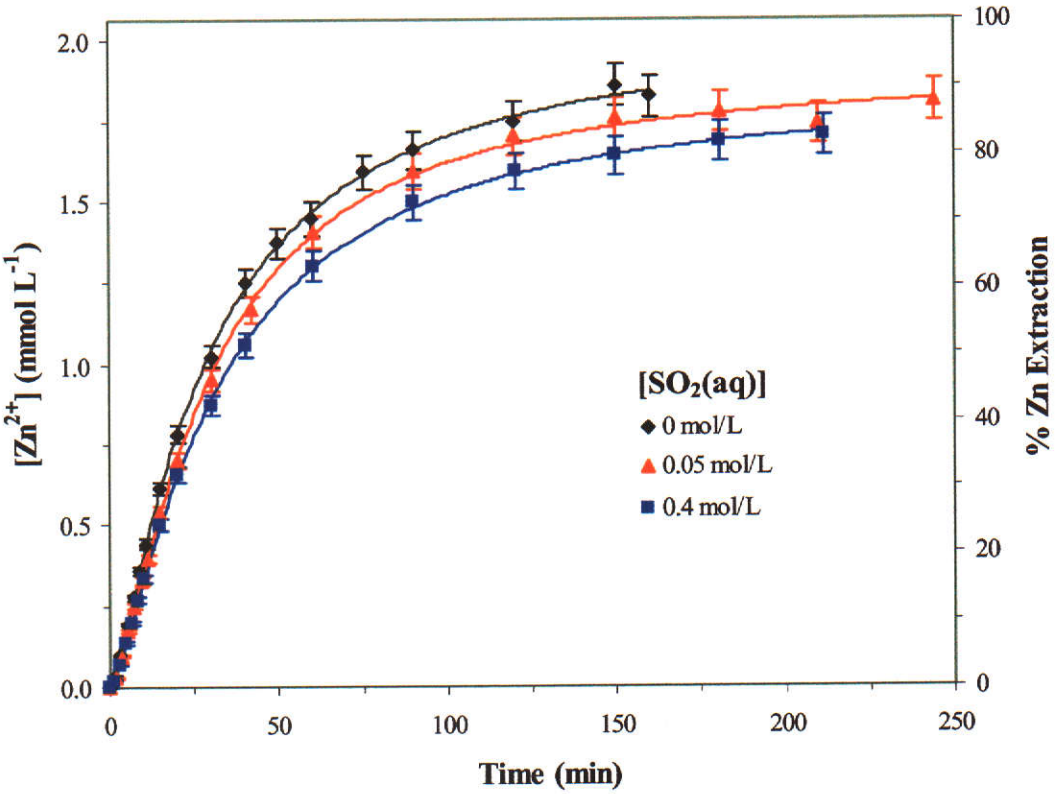

Figure 7.1 Effect of $[SO_2(aq)]$ on dissolution of ZnS in sulfuric acid under low pulp density conditions.
T = 150°C, $[H_2SO_4]$ = 0.1 mol L^{-1}, ZnS-F4 (425.4 µm) = 0.2 g L^{-1}

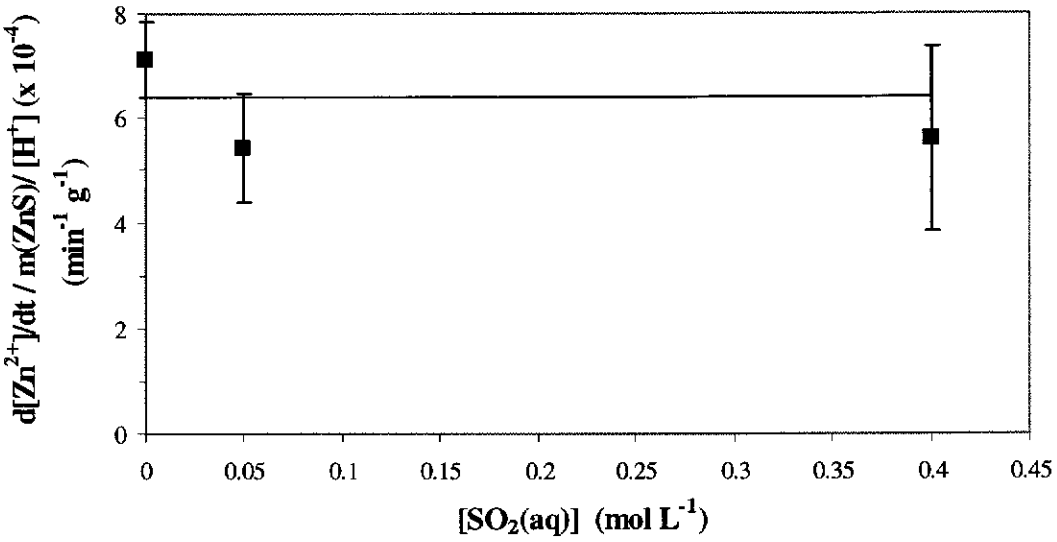

Figure 7.2 Effect of $[SO_2(aq)]$ on initial dissolution rate under low pulp density conditions.

7.1.2 Effect of SO_2 on the reverse reaction

To investigate the effect of SO_2 on the reverse reaction two size fractions were used, ZnS-F4 (425.4 μm) and ZnS-F2 (27.3 μm). The larger size fraction (425.4 μm) was employed in order to make qualitative observations, whereas the smaller fraction (27.3 μm) was used to examine quantitatively the effect of SO_2 on the kinetics of the reverse reaction. The larger size fraction was unsuitable for this purpose as it experiences attrition in the reactor and consequently its surface area at any given zinc extraction could not be estimated (see 6.1.1 and 6.1.2), but was used because of its slower dissolution rate at higher temperatures.

Variation of $[SO_2(aq)]$ using the ZnS–F4 (425.4 μm) fraction

The addition of SO_2 prevents the dissolution of ZnS in sulfuric acid from being constrained by the ZnS-H_2SO_4 equilibrium (Eqn. 2.23, p. 20), as with SO_2 present the extraction of ZnS increased (Figure 7.3). In the absence of SO_2 the dissolution of ZnS (2g L^{-1}) in sulfuric acid (0.1 mol L^{-1}) attains equilibrium after approximately 45 minutes with the zinc extraction limited to 20% (Figure 7.3). In the presence of SO_2, equilibrium was not attained and after four hours leaching the zinc extraction was 60% and still increasing (Figure 7.3). However SO_2 had no effect on the initial rate,

and it is only as the system approaches the ZnS-H_2SO_4 equilibrium position that the SO_2 leach rate begins to exceed the non-SO_2 leach rate (Figure 7.4). In addition, increasing the SO_2 concentration by a factor of five did not produce a corresponding increase in the rate of reaction (Figure 7.3).

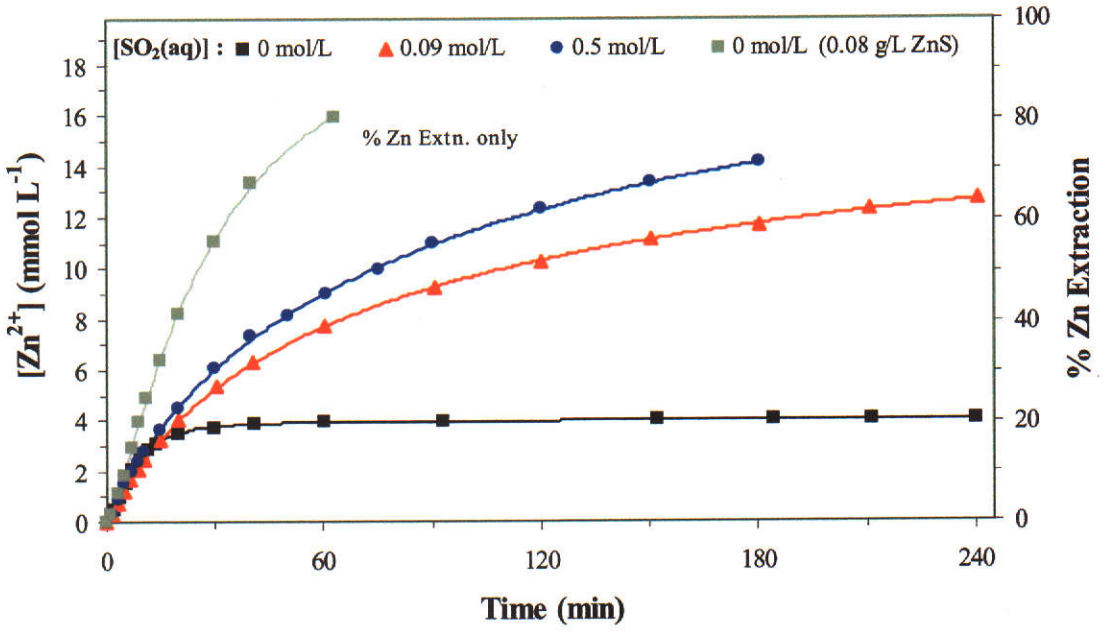

Figure 7.3 Effect of SO_2 on ZnS dissolution in 0.1 mol L^{-1} H_2SO_4 at 150°C. ZnS-F4 (425.4 µm) = 2 g L^{-1}

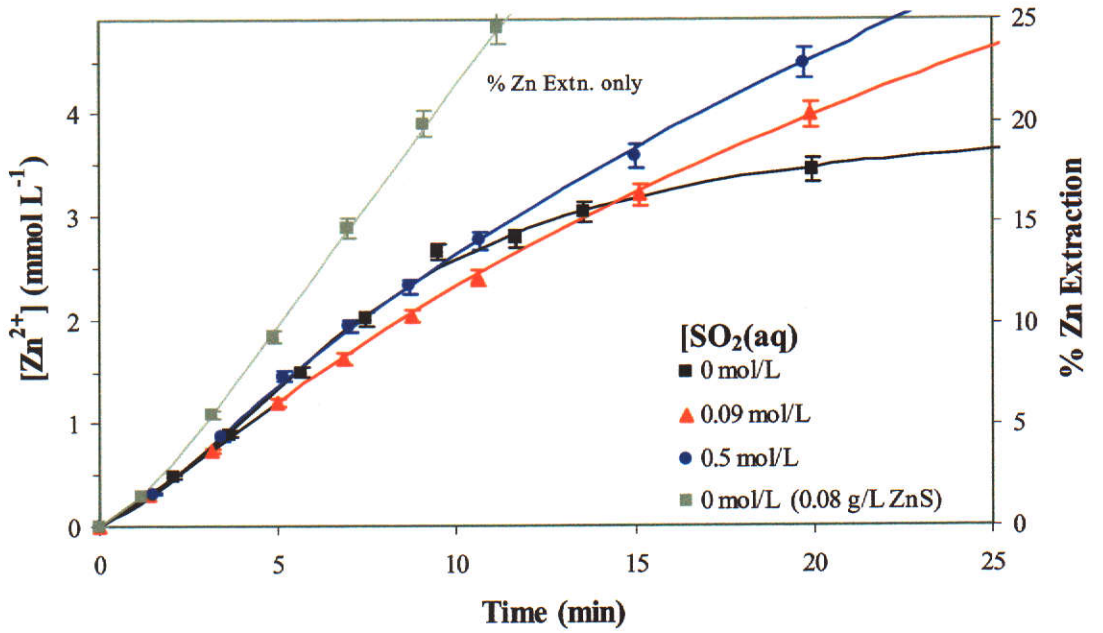

Figure 7.4 Effect of SO_2 on ZnS dissolution in 0.1 mol L^{-1} H_2SO_4 at 150°C – Initial stages. ZnS-F4 (425.4 µm) = 2 g L^{-1}

Variation of [SO_2(aq)] using the ZnS-F2 (27.3 μm) fraction

As would be expected, studies using the smaller size fraction (27.3 μm) in 0.024 mol L^{-1} H_2SO_4 at 150°C, yielded similar SO_2 leach results to the larger size fraction. SO_2 prevented the dissolution of ZnS from being constrained by the ZnS – H_2SO_4 equilibrium reaction (Figure 7.5). In the initial stages the dissolution rate in the presence of added SO_2 was the same as the rate without any added SO_2, and the dissolution rate was unaffected by variations in the concentration of SO_2 (Figures 7.5 and 7.6).

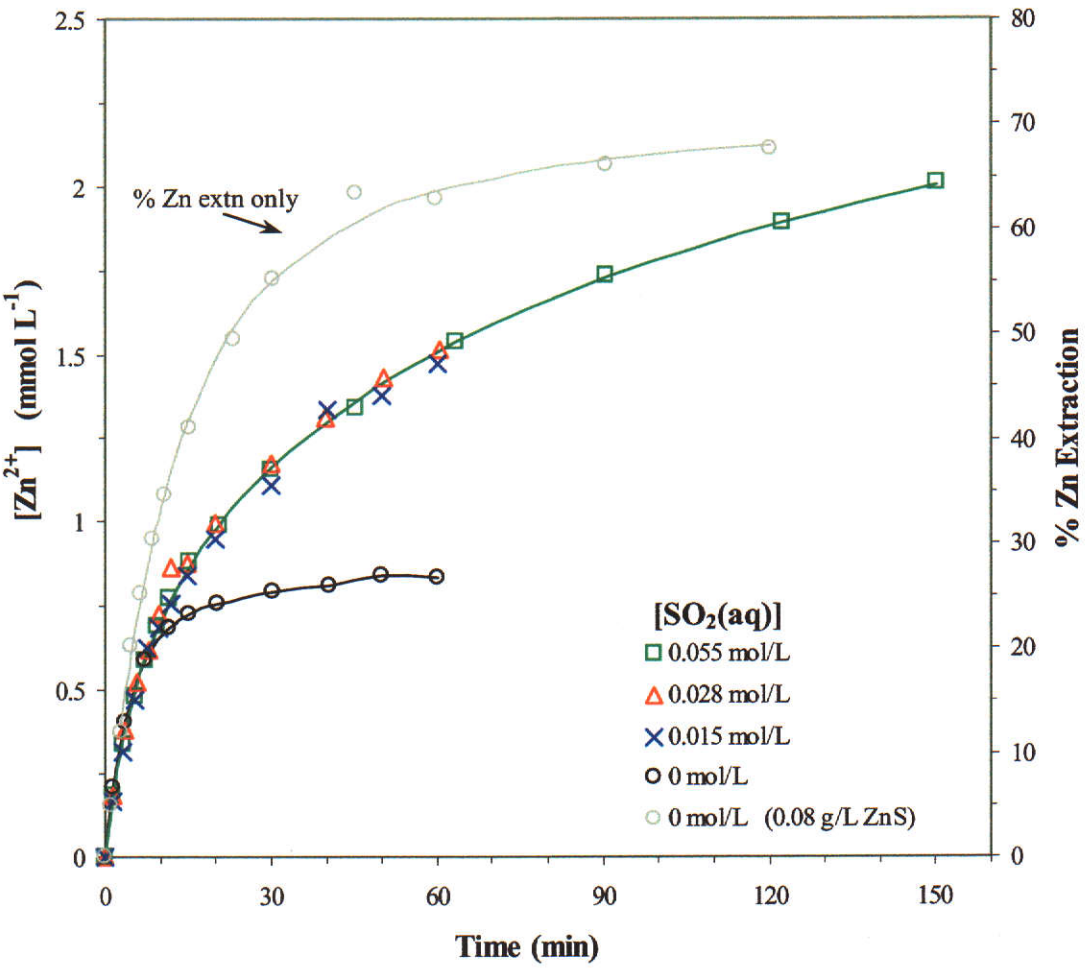

Figure 7.5 Effect of SO_2 on ZnS dissolution in 0.024 mol L^{-1} H_2SO_4 at 150°C. ZnS-F2 (27.3 μm) = 0.4 g L^{-1}

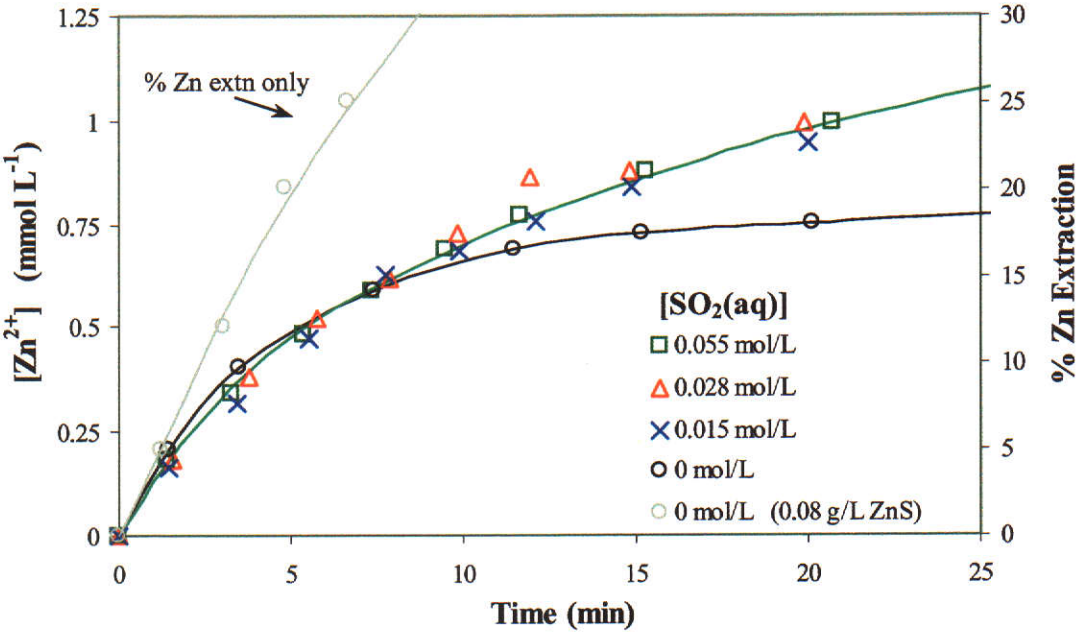

Figure 7.6 Effect of SO_2 on ZnS dissolution in 0.024 mol L^{-1} H_2SO_4 at 150°C- Initial stages. ZnS-F2 (27.3 μm) = 0.4 g L^{-1}

At 100°C leaches were conducted in 0.1 mol L^{-1} rather than 0.024 mol L^{-1} H_2SO_4 in order to obtain sufficiently fast leach rates. Although there were some fluctuations in the leach data, the results show that, for the leach times studied, SO_2 again has no effect on the dissolution of ZnS (Figures 7.7 and 7.8). The differences between leach curves are most likely due to experimental uncertainties.

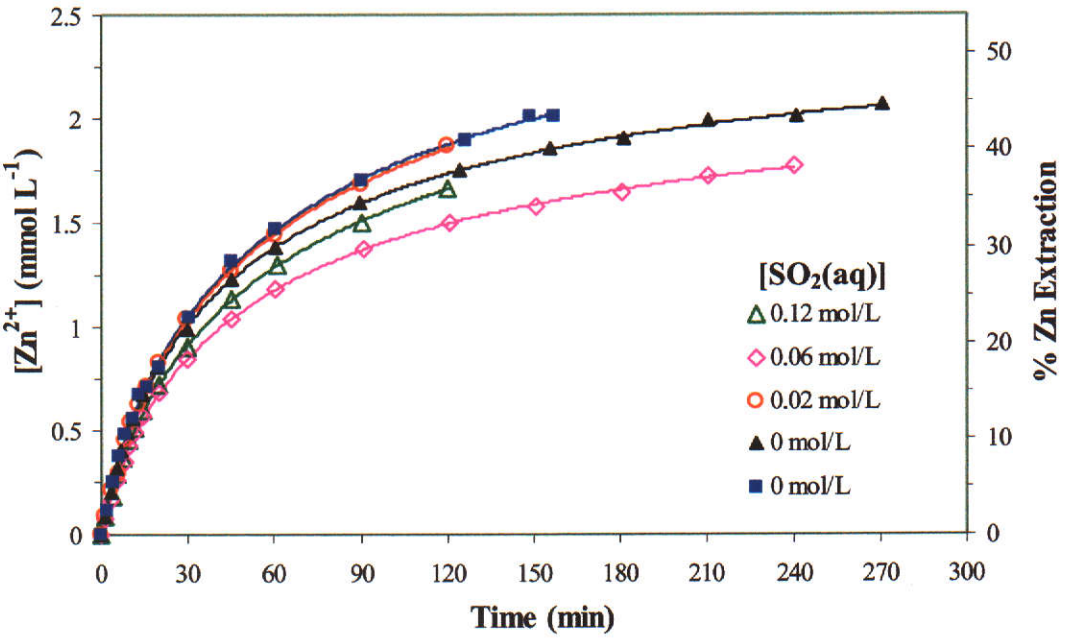

Figure 7.7 Effect of SO_2 on dissolution of ZnS F2 (27.3 μm) in 0.1 mol L^{-1} H_2SO_4 at 100°C. ZnS = 0.4 g L^{-1}

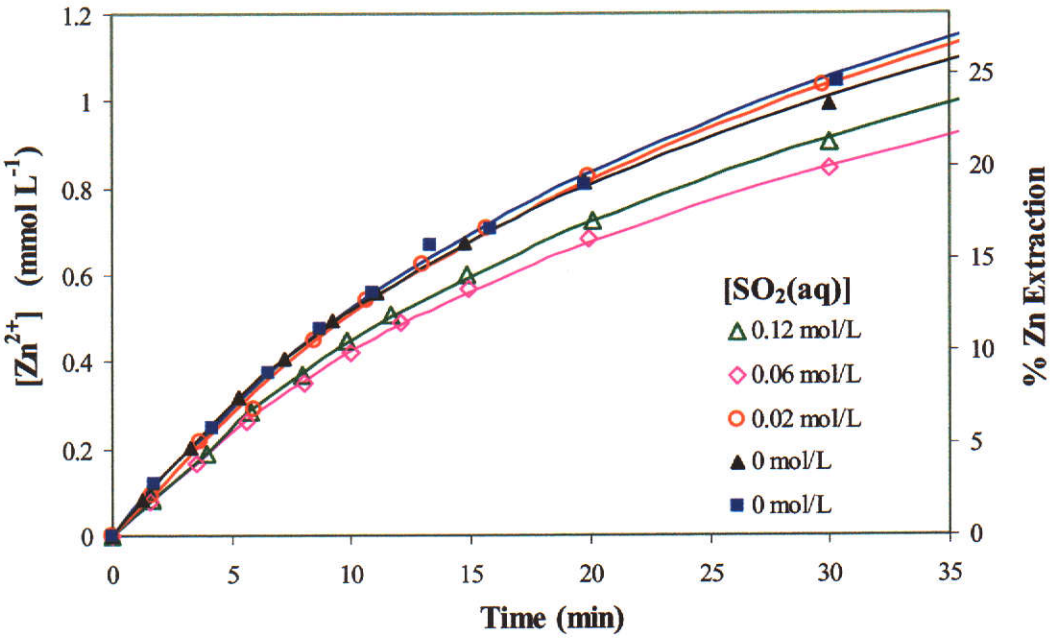

Figure 7.8 Effect of SO_2 on dissolution of 0.4 g L^{-1} ZnS-F2 (27.3 μm) in 0.1 mol L^{-1} H_2SO_4 at 100°C in the initial stages.

7.1.2.1 Evaluation of factors affecting dissolution kinetics

The observed increase in zinc extraction in the presence of SO_2 indicates that the dissolution is no longer constrained by the ZnS-H_2SO_4 equilibrium reaction (Eqn. 2.28, p. 23). This could be attributable to a number of causes:

- Increased acidity due to added SO_2
- Thermal decomposition of SO_2(aq)
- Removal of H_2S by SO_2

Increased acidity due to added SO_2

The increase in leaching cannot be attributed to increasing acidity due to the presence of "sulfurous acid" as the addition of SO_2 to the sulfuric acid solutions can be demonstrated to have had a negligible effect on the hydrogen ion concentration. The first dissociation constant for sulfurous acid decreases with increasing temperature, and at 150°C, $K_{a1}^{150^\circ C} = 3.16\times10^{-4}$ mol L^{-1} (Perrin 1982). At 25°C it is 1.39×10^{-2} mol L^{-1} (Huss and Eckert 1977). Based on this value at 150°C, the

addition of 0.5 mol L^{-1} SO_2 to 0.1 mol L^{-1} sulfuric acid would have increased the hydrogen ion concentration by only 0.0016 mol L^{-1}, which is only 1.6% and as such is negligible. Lower concentrations of SO_2 would have had even less of an effect on the hydrogen ion concentration. The highest concentration of SO_2 used in 0.024 mol L^{-1} H_2SO_4 was 0.055 mol L^{-1}. The presence of 0.055 mol L^{-1} SO_2 would have increased the concentration of hydrogen ions by only 3%. For the leaches at 100°C using 0.1 mol L^{-1} H_2SO_4, the highest SO_2 concentration was 0.12 mol L^{-1}, which also would have increased the hydrogen ion concentration by only 3% as well.

Thermal decomposition of $SO_2(aq)$

In Chapter 5 it was demonstrated that, in aqueous solutions of SO_2 at elevated temperatures (> 130°C), the dissolution of ZnS is promoted by sulfuric acid generated from the thermal decomposition of SO_2 (Eqn. 2.19, p. 17)

$$3SO_2 + 2H_2O \rightarrow S^o + 2H_2SO_4$$

Thus it is possible that this could also be occurring in the SO_2 / H_2SO_4 leach system, and be a cause for the increased zinc extractions.

The degree of SO_2 decomposition in this system was assessed by Raman analysis of the sulfate content in samples taken during the leach of ZnS (27.3 μm) in 0.024 mol L^{-1} H_2SO_4 containing the highest concentration of SO_2 (0.055 mol L^{-1}). The total sulfate concentration, as determined by summation of the Raman measured sulfate (980cm^{-1}) and hydrogen sulfate (1054 cm^{-1}) peak areas, remained constant throughout (Figure 7.9), indicating that thermal decomposition did not occur. If thermal decomposition of SO_2 had occurred, then according to equation 2.19 (p. 17) an increase in the sulfuric acid and hence sulfate concentration would have been expected. The second data point in Figure 7.9 was discounted, as it was clearly an outlier, on the basis of Q and Student's t-tests.

These observations agree with the work of Kuz'min and Postnikov (1935), who showed that the presence of hydrogen ions greatly reduces the rate of the thermal decomposition of SO_2, and explains why thermal decomposition was not observed.

Thermal decomposition would also not have occurred in the other leaches of ZnS (27.3 μm) in 0.024 mol L^{-1} H_2SO_4 at 150°C as they contained lower concentrations of SO_2, i.e., thermal decomposition of SO_2 can be ruled out as a cause for the increased dissolution of ZnS in these sulfuric acid solutions containing SO_2.

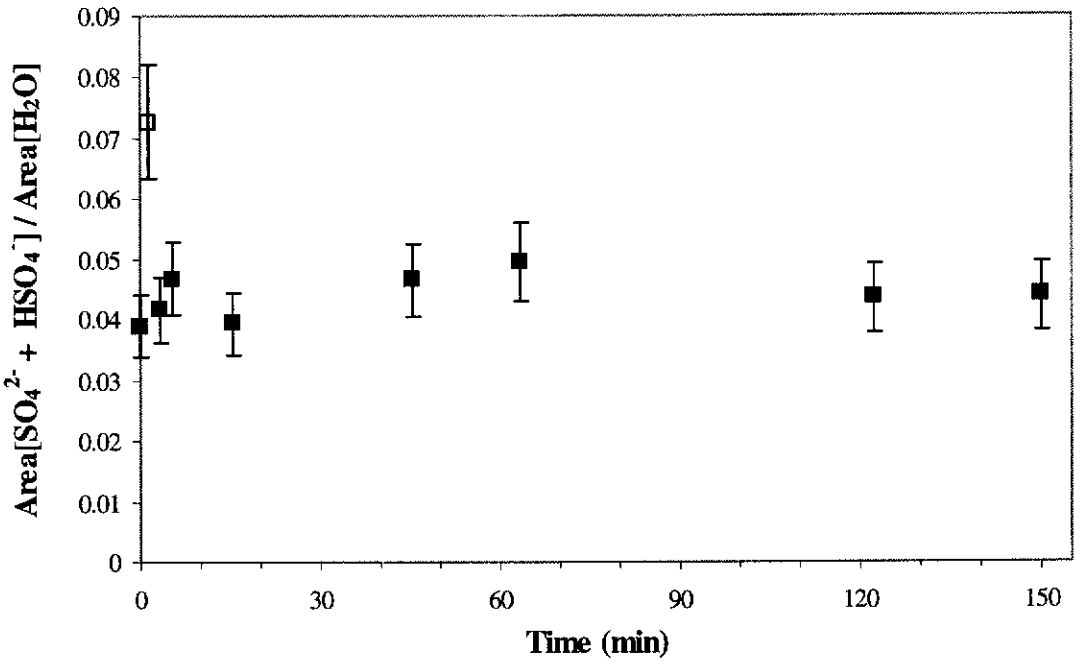

Figure 7.9 Areas of sulfate (980 cm^{-1}) and hydrogen sulfate (1054cm^{-1}) peaks relative to water (1650 cm^{-1}) in the Raman spectra of sampled solutions (514.532 nm Ar^+ line).

Removal of H_2S by SO_2

Since thermal decomposition of SO_2 and increased acidity can be ruled out as the means by which SO_2 increases the dissolution of ZnS, it is most likely to be due to its reaction with H_2S. The detection of elemental sulfur by Raman spectroscopy (Figure 7.10) indicates that reaction between SO_2 and H_2S takes place, since this is a known product of that reaction (Schroeter 1966d).

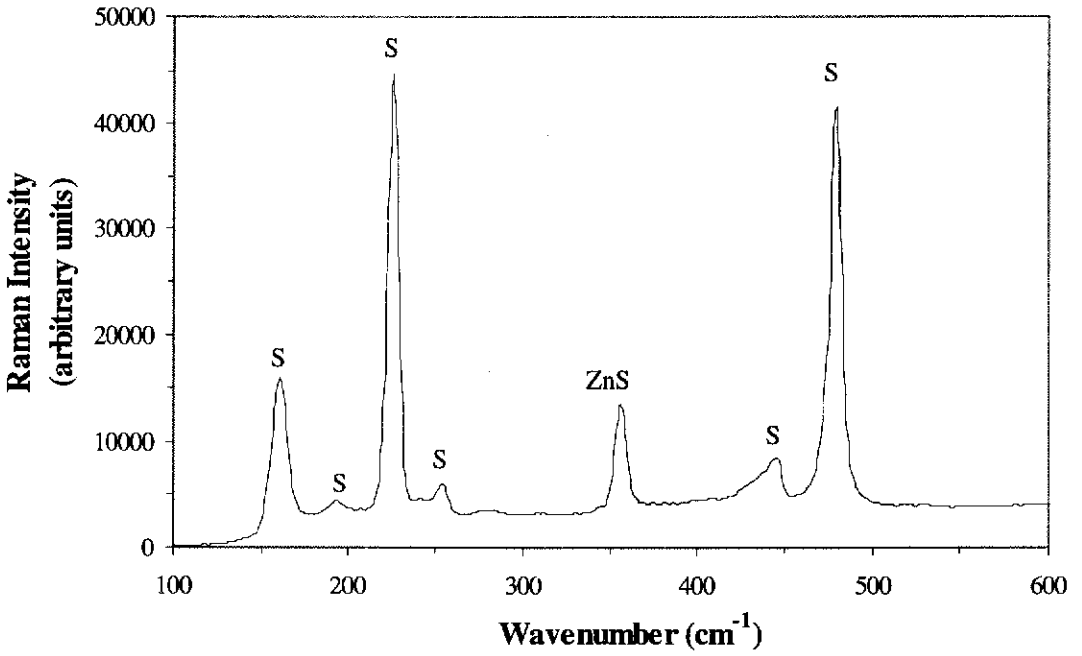

Figure 7.10 Dispersive Raman spectrum (He-Ne, 632.817 nm) of residue from ZnS / H_2SO_4 / SO_2 leach at 150°C showing the presence of elemental sulfur and ZnS.
Conditions: ZnS-F2 (27.3 μm) = 0.4 g L^{-1}, [H_2SO_4] = 0.024 mol L^{-1}, [SO_2(aq)] = 0.055 mol L^{-1}

However, SO_2 does not appear to be instantaneously or completely removing H_2S. If the removal of H_2S were instantaneous and complete, one would expect the H_2SO_4 / SO_2 leach curves to show no signs of inhibition. However, this was not the case. Included in Figures 7.3 and 7.4 and also in Figures 7.5 and 7.6 are leaches (denoted by the open squares) where inhibition due to the reverse reaction was minimal, as the pulp density was low (0.08 g L^{-1}). These are the leach curves that one would expect to observe if the reaction between SO_2 and H_2S was instantaneous and complete. That the SO_2 leaches did not achieve this rate may be due to a number of possible causes

- elemental sulfur produced in the reaction occluding the surface, inhibiting dissolution.
- the SO_2 + H_2S reaction not being instantaneous, leaving residual H_2S in solution.
- the SO_2 + H_2S reaction produces intermediates that inhibit ZnS dissolution in a similar manner to H_2S

Occlusion of the ZnS surface by molten sulfur

If we consider the possibility that H_2S is being removed by reaction with SO_2 to form elemental sulfur, but that the increase in dissolution rate is not observed due to molten sulfur occluding the solid, then it is possible to determine the extent of surface area occluded by the sulfur. Since there is no reverse reaction in this scenario, the dissolution rate is described by equation 6.2 (p. 111), i.e.

$$d[Zn^{2+}]/dt = k_f A_s [H^+]$$

Using the leach data from the ZnS / H_2SO_4 / SO_2 leach at 150°C with the highest initial concentration of SO_2 (i.e. 0.055 mol L^{-1}) (Figure 7.5), it was possible to calculate the surface area as a function of time throughout the leach. The rate, $d[Zn^{2+}]/dt$, was obtained from leach data, $[H^+]$ was calculated knowing the initial concentration of hydrogen ions and the number of moles of ZnS consumed and k_f was obtained from previous ZnS / H_2SO_4 leaches using the same size fraction ($k_f = 2.83\times10^{-2}$, Table 6.4). If elemental sulfur occlusion is occurring then the percentage of the total surface area covered by sulfur would have been 30% soon after the reaction commenced, increasing to 96% by the end of the leach (150 minutes) (Figure 7.11).

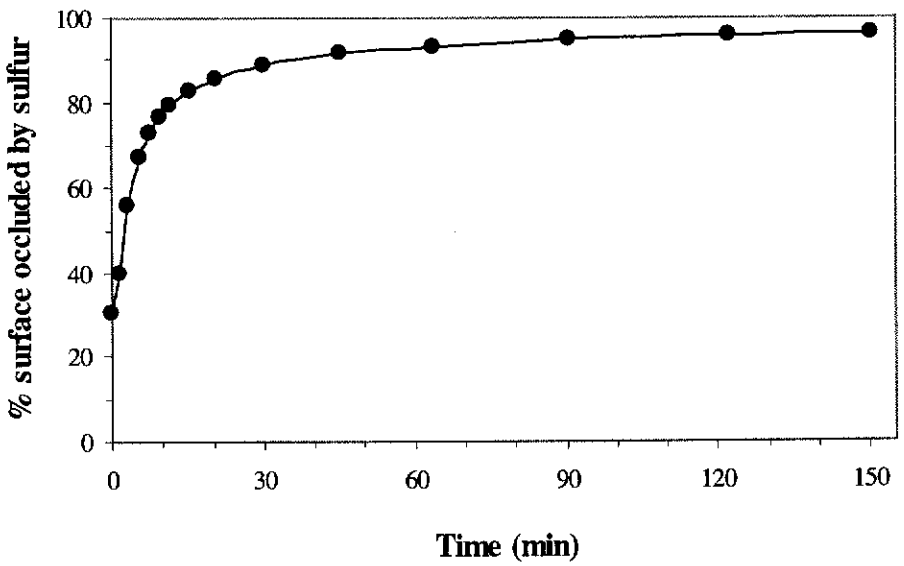

Figure 7.11 Calculated percentage of the ZnS surface that would be occluded by sulfur if sulfur is the only cause of inhibition.

However, scanning electron microscopy showed no evidence that sulfur occluded the unreacted ZnS particles. Images of the residue that had been mounted in resin and polished flat in order to show cross sectional views, indicated the presence of globules of sulfur, to which zinc sulfide particles adhered, however the majority of zinc sulfide particles existed as independent entities and were not attached to or occluded by elemental sulfur (Figures 7.12 and 7.13). No zinc sulfide was observed within the sulfur globules (Figure 7.13).

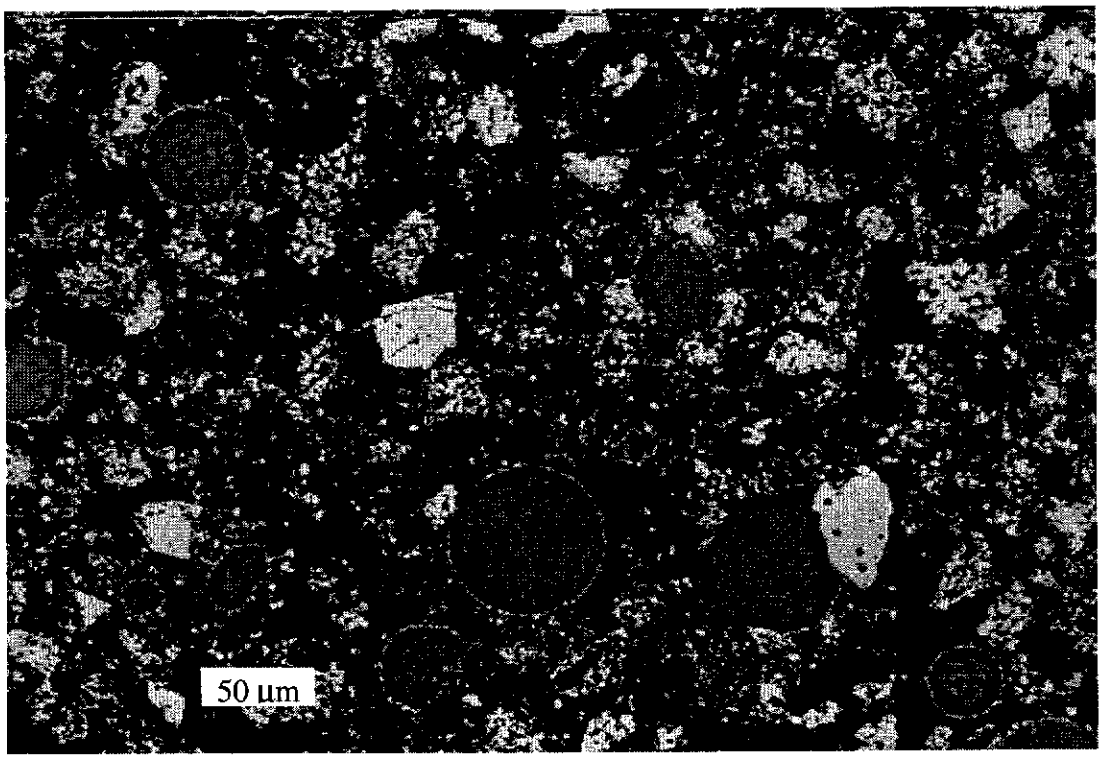

Figure 7.12 SEM image of residue from leach of ZnS in H_2SO_4 and SO_2 at 150°C, showing zinc sulfide (white) and sulfur (grey) in resin (black).

The calculated sulfur occlusion, according to this model, far exceeds the observed sulfur occlusion. Thus sulfur occlusion cannot account for the inhibition observed in ZnS / H_2SO_4 / SO_2 leaches.

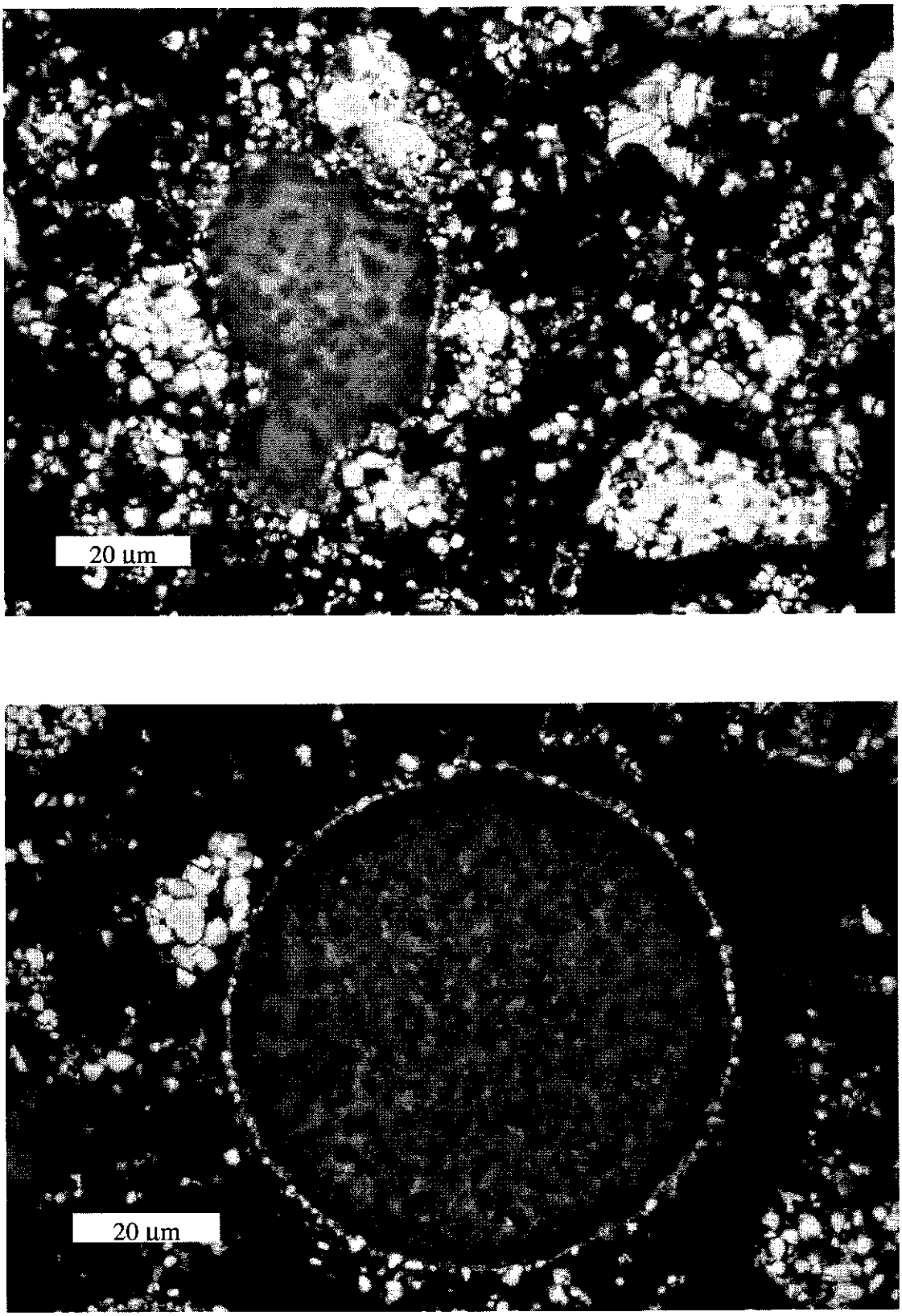

Figure 7.13 SEM images of sulfur globules from leach of ZnS in H_2SO_4 and SO_2 at 150°C, showing zinc sulfide (white) and sulfur (grey) in resin (black).

Evidence for the removal of $H_2S(aq)$

It was not possible to directly determine $H_2S(aq)$, however, its presence could be inferred by detection of $H_2S(g)$, since $H_2S(aq)$ is in equilibrium with $H_2S(g)$ (Eqn. 2.29, p. 23). Henry's constant for H_2S in water at 150°C is $K_H^{150^\circ C} = 3462$ kPa molal^{-1} (Suleimenov and Krupp 1994).

$$H_2S(aq) \leftrightarrow H_2S(g) \qquad K_H^{150^\circ C} = 3462 \text{ kPa molal}^{-1}$$

The relationship between $[H_2S(aq)]$ and $[H_2S(g)]$ at 150°C can be derived from equations (7.5 – 7.7) and is given in equation 7.8.

$$P_{H_2S} = K_H^{150^\circ C} \times [H_2S(aq)] \tag{7.5}$$

$$[H_2S(g)] = \frac{P_{H_2S}}{RT} \tag{7.6}$$

$$[H_2S(g)] = \frac{K_H^{150^\circ C}}{RT} \times [H_2S(aq)] \tag{7.7}$$

$$[H_2S(g)] = 0.984 \times [H_2S(aq)] \tag{7.8}$$

Only trace amounts of $H_2S(g)$ (< 0.6 μmol L^{-1}) were detected in the headspace. This is much lower than what would be expected if $H_2S(aq)$ was the cause of inhibition. If it is assumed that inhibition is due to residual $H_2S(aq)$ remaining after partial reaction with SO_2 then the concentration of residual $H_2S(aq)$ is given by equation 7.9. $[H_2S(g)]_{calc}$ can then be evaluated using the relationship in equation 7.8.

$$[H_2S(aq)] = \left[\frac{k_f A_{surf} [H^+(aq)] - d[Zn^{2+}(aq)]/dt}{k_r A_{surf} [Zn^{2+}(aq)]^{1/2}} \right]^2 \tag{7.9}$$

The observed concentrations of $H_2S(g)$ were well below values expected on the basis that H_2S was inhibiting dissolution (Figure 7.14).

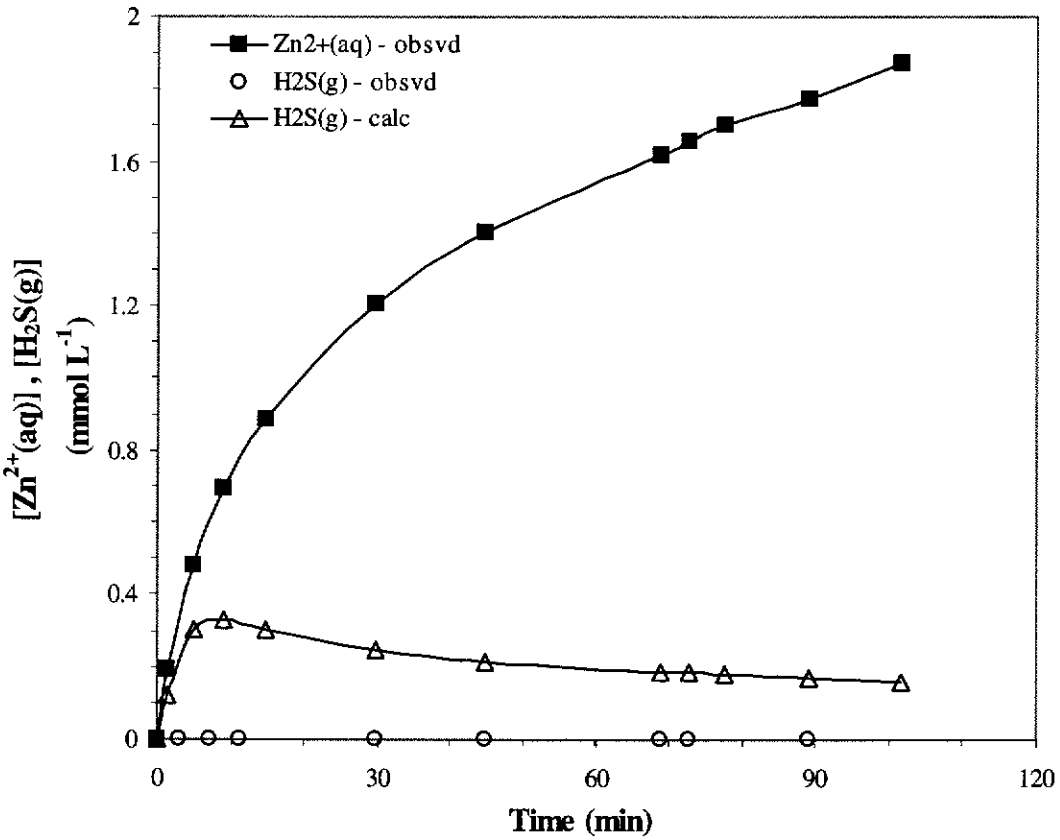

Figure 7.14 Observed concentrations of $H_2S(g)$ and calculated concentrations of $H_2S(g)$ based on ZnS dissolution inhibition by $H_2S(aq)$.
T = 150°C, ZnS-F2 (27.3 μm) = 0.4 g L^{-1}, $[H_2SO_4]$ = 0.024 mol l^{-1}, $[SO_2(aq)]$ = 0.0018 mol L^{-1}

Furthermore, reducing the pressure above the solution had no effect on the dissolution of ZnS (Figure 7.15). In one leach the headspace was not vented. In a similar leach, when the headspace was vented to atmosphere by opening a needle valve in the head of the reactor vessel it reduced the pressure by a factor of approximately two, from 1040 kPa to 550 kPa, over a period of 32 seconds. However, this produced no change in the dissolution of ZnS, which continued in the same manner as in the leach which was not vented.

The results indicate that $H_2S(g)$ was not present in the headspace. From this it can be inferred that H_2S is not present in the aqueous phase. Therefore, this also indicates that $H_2S(aq)$ is not the cause of inhibition.

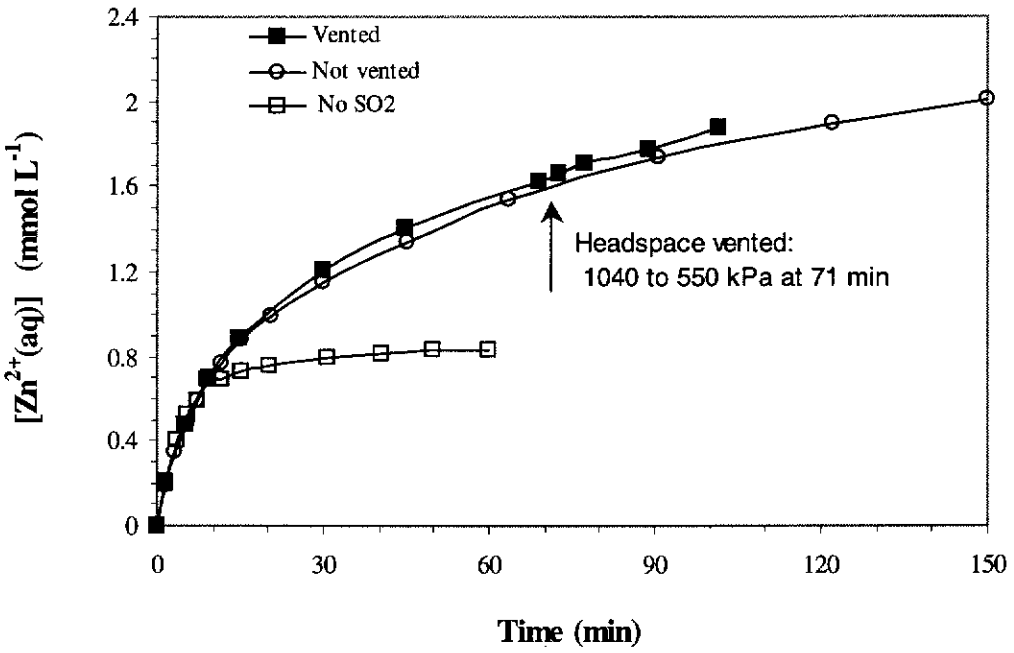

Figure 7.15 Effect of reducing headspace pressure on dissolution of ZnS in $SO_2 - H_2SO_4$. T = 150°C ZnS-F2 (27.3 μm) = 0.4 g L^{-1}, $[H_2SO_4]$ = 0.024 mol l^{-1}, $[SO_2(aq)]$ = 0.0018 (■) and 0.0055 (o) mol L^{-1}

Conversion of H_2S to reactive intermediates – the sulfane monosulfonate hypothesis

As the inhibition observed in H_2SO_4 / SO_2 leaches of ZnS is not due to occlusion by elemental sulfur or to the presence of $H_2S(aq)$, the only remaining option is that dissolution is inhibited by a "H_2S-like" species formed by reaction between H_2S and SO_2. Again, as in the ambient leaches, the most probable "H_2S-like" species that are produced in this reaction are sulfane monosulfonates ($^-S_xSO_3H$ and $^-S_xSO_3^-$). These have a terminal sulfur atom that is negatively charged (Meyer, Peter and Spitzer 1977) (Table 4.2, p. 91) and it is postulated that the zinc ion reacts with this species re-precipitating ZnS in the process.

Since $H_2S(g)$ is only observed in trace amounts, this suggests that the rate of the reaction between $SO_2(aq)$ and H_2S is fast.

The overall rate of dissolution of ZnS in H_2SO_4 / SO_2 is thus dependent upon the rate of removal or decomposition of the reactive sulfane monosulfonates into species that do not react with Zn^{2+} to precipiate ZnS, for example, polythionates, sulfate and

elemental sulfur (Eqns. 7.10 - 7.13)

$$ZnS + 2H^+ \rightarrow Zn^{2+} + H_2S \quad \text{fast} \quad (7.10)$$

$$SO_2 + H_2S \rightarrow M + P \quad \text{fast} \quad (7.11)$$

$$M + Zn^{2+} \rightarrow ZnS + P \quad \text{fast} \quad (7.12)$$

$$M \rightarrow P \quad \text{slow} \quad (7.13)$$

where M denotes sulfane monosulfonic acids and their anions

P denotes elemental sulfur and oxysulfur species that are unreactive toward Zn^{2+}.

As the concentration of SO_2 has no effect on the dissolution rate (Figure 7.5), it suggests that SO_2 is not involved in any decomposition reactions of the sulfane monosulfonates.

7.1.3 Evidence for sulfane monosulfonate hypothesis

Sulfane monosulfonates have not been observed in aqueous solutions and no attempt was made to observe them directly in this system. However, evidence supporting their proposed existence was obtained from observations of the effects of pulp density and added soluble zinc on the dissolution kinetics.

7.1.3.1 Effect of pulp density

Increasing the pulp density caused the dissolution rate of ZnS in a H_2SO_4 / SO_2 leach solution at 150°C to decrease (Figure 7.16). Although different SO_2 concentrations were used in each leach (0.05 and 0.09 mol L^{-1}), the leaches can be compared to each other as earlier experiments have shown that varying the SO_2 concentration has no effect on the dissolution rate (see Section 7.1.2).

The inhibition observed on increasing the pulp density is not due to the presence of H_2S(aq) or to occlusion by molten elemental sulfur, since these possible causes have

already been excluded (see 7.1.2.1). Consequently, the observed inhibition is due to some other factor, the most likely being the presence of aqueous "H_2S-like" species, of which the sulfane monosulfonates are the most probable.

The increase in inhibition with increasing pulp density is consonant with this view, since at higher pulp densities, with the larger surface area of ZnS, the rate of the forward reaction of equation 2.28 (p. 23)

$$ZnS + H_2SO_4(aq) \leftrightarrow ZnSO_4(aq) + H_2S(aq)$$

would be faster and consequently the rate of formation of sulfane monosulfonates would also be faster, resulting in higher concentrations of sulfane monosulfonates in solution and thus increased inhibition.

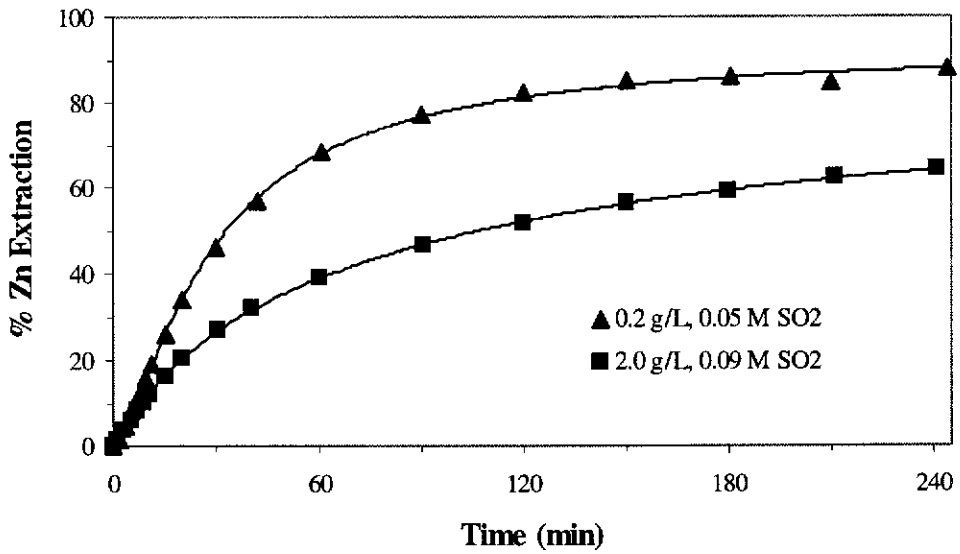

Figure 7.16 Effect of pulp density on dissolution of ZnS-F4 (425.4 μm) in SO_2– H_2SO_4. T = 150°C, $[H_2SO_4]$ = 0.1 mol L^{-1}

7.1.3.2 Effect of SO_2 in the presence of added zinc sulfate

When SO_2 is added to a leach with added soluble zinc (present as $ZnSO_4$), it has no effect on the dissolution rate in the initial stages and only affects it as the reaction approaches the non-SO_2 equilibrium position (Figure 7.17). Again, the inability of

SO_2 to remove the inhibition totally can be rationalised in terms of the sulfane monosulfonate hypothesis. SO_2 reacts with H_2S to form "H_2S-like" species, *viz.*, sulfane monosulfonates, which react with zinc ions in the same manner as $H_2S(aq)$, re-precipitating ZnS.

For comparison, a leach obtained using a low pulp density and without added zinc ions, in which the contribution of the reverse reaction to the initial rate is negligible, is included in Figure 7.17 (denoted by ×). This is the leach curve expected if SO_2 had removed all of the H_2S and converted it to an unreactive product. It is of interest to note that the initial dissolution rates with or without added SO_2 are always equivalent. This suggests that the rates of the reverse reactions, that of Zn^{2+} with $H_2S(aq)$ in the non-SO_2 leaches, and that of Zn^{2+} with the postulated sulfane monosulfonates in the SO_2 leaches, are equivalent.

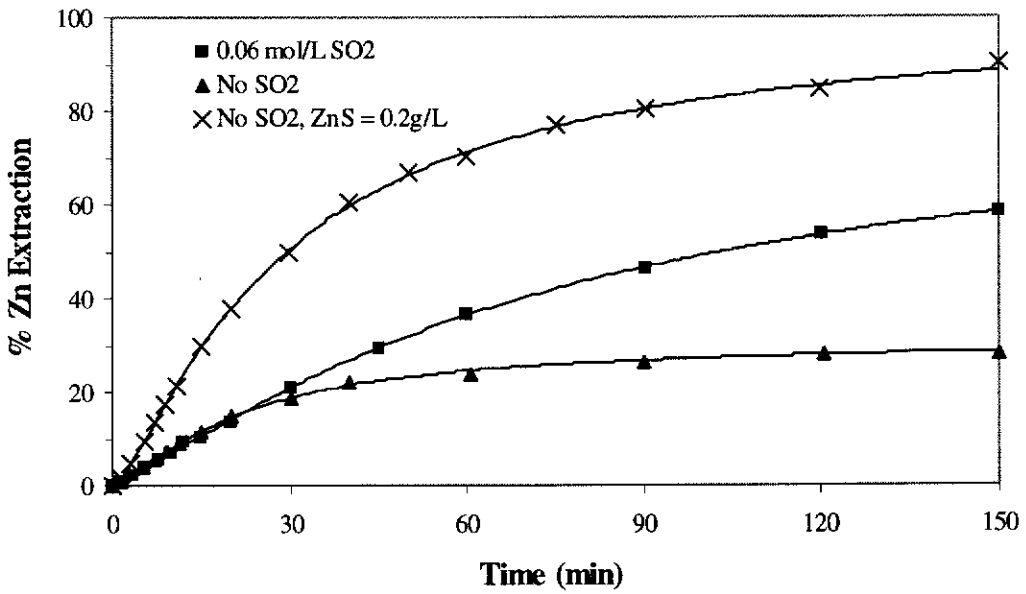

Figure 7.17 Effect of SO_2 on ZnS extraction in the presence of added $ZnSO_4$ (4 mmol L^{-1}). T = 150°C, ZnS-F4 (425.4 μm) = 0.8 g L^{-1}, [$ZnSO_4$] = 4 mmol L^{-1}, [H_2SO_4] = 0.1 mol L^{-1}.

7.1.4 Addition of SO_2 to ZnS – H_2SO_4 system at equilibrium

Previously described experiments were all performed with SO_2 present from the commencement of the leach. Figure 7.18 and Figure 7.19 show the leach curves for

the situations, at 100°C and 150°C, where SO_2 is added to the ZnS-H_2SO_4 system at equilibrium. Included in the figures are calculated curves for the cases where it is assumed that

- the removal of H_2S at equilibrium by reaction with SO_2 was instantaneous and any H_2S formed thereafter was also removed such that there was no inhibition due to H_2S(aq) or other "H_2S-like" species (i.e. no reverse reaction).

- the removal of H_2S present at equilibrium was instantaneous, but there was no further reaction between SO_2 and the H_2S generated as the ZnS continues to leach. i.e. after initial removal of H_2S present at equilibrium by reaction with SO_2, subsequent removal did not occur and the concentration of aqueous H_2S increased, causing inhibition.

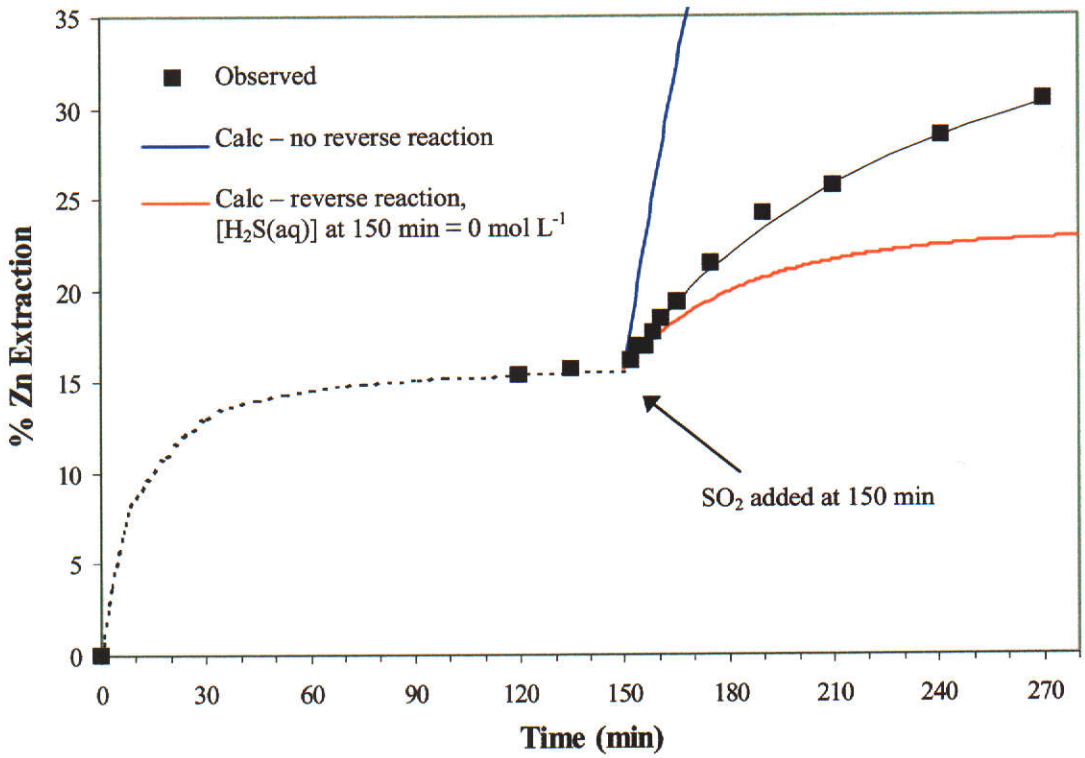

Figure 7.18 Effect of SO_2 on the ZnS / H_2SO_4 system at equilibrium at 100°C. [H_2SO_4] = 0.097 mol L^{-1}, pulp density = 1.6 g L^{-1}, [SO_2(aq)] = 0.12 mol L^{-1}, stirring speed = 800.

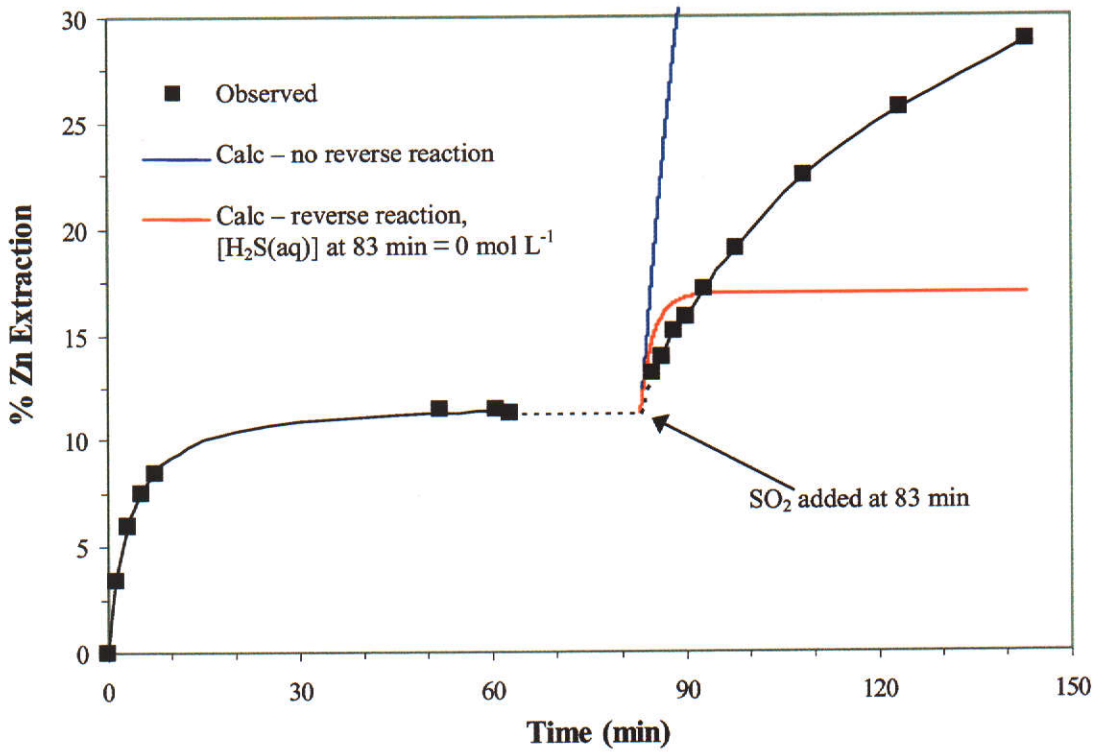

Figure 7.19 Effect of SO_2 on the ZnS / H_2SO_4 system at equilibrium at 150°C. $[H_2SO_4] = 0.024$ mol L^{-1}, pulp density = 0.8 g L^{-1}, $[SO_2(aq)] = 0.08$ mol L^{-1}, stirring speed = 800 rpm.

The observed leach curves suggest the H_2S present at equilibrium is consumed rapidly by SO_2 to produce species that do not react with Zn^{2+} to precipitate ZnS. Hence, it is likely that sulfane monosulfonates are not produced in this reaction, but that the products are elemental sulfur and sulfane disulfonates. If sulfane monosulfonates were produced then one would expect the leach rate to be initially zero, at the time of SO_2 addition, and then to gradually increase as the sulfane monosulfonates convert to elemental sulfur and sulfane disulfonates.

In contrast to the initial instant where SO_2 and H_2S react rapidly to produce species that do not precipitate ZnS, in the period immediately after this, the leaches exhibit inhibition typical of previous SO_2 leaches, suggesting the formation of sulfane monosulfonates.

Thus we have one situation where sulfane monosulfonates do not appear to be

produced by the SO_2 + H_2S reaction, and another situation where they do appear to be produced. Two possible reasons for this have been identified, as there are two differences between these situations.

Firstly, the sulfide species that reacts with sulfurous acid is likely to differ in each case. At the time of SO_2 addition to the ZnS / H_2SO_4 system at equilibrium, "sulfurous acid" species react with H_2S(aq) in solution, whereas after this time "sulfurous acid" species probably react with protonated sulfide species on or near the ZnS surface. This suggests that sulfane monosulfonates are produced by the surface reaction between sulfurous acid and protonated surface sulfide species, but not by the aqueous phase reaction between sulfurous acid and H_2S(aq).

Secondly, the concentration of H_2S(aq) that reacts with sulfurous acid is higher at the time of SO_2 addition than at times subsequent to this. It may be that the reaction of SO_2 with the comparatively higher concentrations of H_2S present at equilibrium ($\sim 10^{-4}$ mol L^{-1}) yields sulfane disulfonates whereas the reaction of SO_2 with the trace amounts of H_2S ($< 6 \times 10^{-7}$ mol L^{-1}) (see 7.1.2.1) present at subsequent times yields the "H_2S-like" sulfane monosulfonates.

7.1.5 Modelling the dissolution kinetics of ZnS in H_2SO_4 – SO_2 leach solutions

It is of interest to note that, in the initial stages, the dissolution rate of ZnS in H_2SO_4 is the same with or without SO_2 present (Figure 7.17). In this initial stage, the only difference in the two leaches is that the inhibiting species in the H_2SO_4 leach is H_2S(aq), whereas the inhibiting species in the H_2SO_4 / SO_2 leach is thought to be a sulfane monosulfonate. This suggests that the rates of the reverse reactions, that of Zn^{2+} with H_2S(aq) in the non-SO_2 leaches, and that of Zn^{2+} with sulfane monosulfonates in the SO_2 leaches, are equivalent. Assuming that the rate of reaction between Zn^{2+} and the sulfane monosulfonate species is equivalent to the rate of reaction between Zn^{2+} and H_2S(aq), it follows that the concentration of the sulfane monosulfonate species in the H_2SO_4 / SO_2 leach must be approximately equal to the concentration of H_2S(aq) in the H_2SO_4 leach. In the H_2SO_4 leaches at 150°C, the number of moles of H_2S(g) was approximately equal to the number of moles of

H_2S(aq) (Eqn. 7.10). Thus for every mole of Zn^{2+} produced approximately 0.5 mole of H_2S(aq) and 0.5 mole of H_2S(g) were produced. Similarly, in the H_2SO_4 / SO_2 leaches at 150°C, the number of moles of HSO_3S_xSH produced for every mole of Zn^{2+} must also have been 0.5. The sulfane monosulfonate that conforms to this restriction is disulfane monsulfonate (HS_2SO_3H), since it is reasonable to consider that one molecule of HS_2SO_3H is formed from one molecule of SO_2 or HSO_3^- and two molecules of H_2S, with the sulfonate group originating from SO_2(aq) or HSO_3^-(aq) and the sulfur atoms in the sulfane chain originating from H_2S.

In addition, if the rate of build-up of HS_2SO_3H is the same as the rate of build-up of H_2S(aq) then the reactions between SO_2(aq) or HSO_3^-(aq) and H_2S adsorbed on the ZnS surface must be fast with respect to the re-precipitation reaction.

Since the H_2SO_4 / SO_2 leach rate eventually exceeds the H_2SO_4 leach rate the sulfane monosulfonate species must decompose into species that do not react with Zn^{2+} to precipitate ZnS. Likely decompostion products are thus, the sulfane disulfonates and elemental sulfur. Figure 7.5 indicates that the concentation of SO_2 has no effect on the rate of the decompostion of the sulfane monsulfonate species. Based on these observations and assumptions this model can be represented by the following equations

$$d[Zn^{2+}]/dt = k_f A_s [H^+] - k_r A_s [HS_2SO_3H]^{1/2} [Zn^{2+}]^{1/2} \quad (7.14)$$

$$d[HS_2SO_3H]/dt = d[Zn^{2+}]/dt - k_w [HS_2SO_3H]^{\beta} \quad (7.15)$$

Since the reaction between SO_2 and H_2S yielding HS_2SO_3H appears to be instantaneous, the rate of formation of HS_2SO_3H is equivalent to the rate of formation of Zn^{2+}. Its rate of decomposition into elemental sulfur and/or other unreactive species is given by $k_w[HS_2SO_3H]^{\beta}$. This is a simplified model and does not take into account the many other side reactions that are possible in systems containing polythionates.

The model was applied to the H_2SO_4 / SO_2 (0.055 mol L^{-1}) leach of ZnS at 150°C, where SO_2 was present from the commencement of the leach (Figure 7.5). Using the the rate constants, k_f and k_r, previously obtained from leaches of ZnS in H_2SO_4 at

150°C (Table 6.5), the constants k_w and β were evaluated by fitting the model $[Zn^{2+}]$ versus time curve to the observed data. Using least squares fitting and allowing β and k_w to vary returned β = 2.66 and $k_w = 6.25\times10^4$. Using other fixed values for β also gave satisfactory fits to the data (Table 7.1 and Figure 7.20), however the rate constants for values of β ≥ 3 would appear to be unrealistically high (> 1.08×10^6).

Table 7.1 Values of β and k_w for the solution to equations 7.14 and 7.15.

β	k_w
1.5	3.96
2	2.55×10^2
2.5	1.65×10^4
2.66	6.25×10^4
3	1.08×10^6
3.5	7.08×10^7

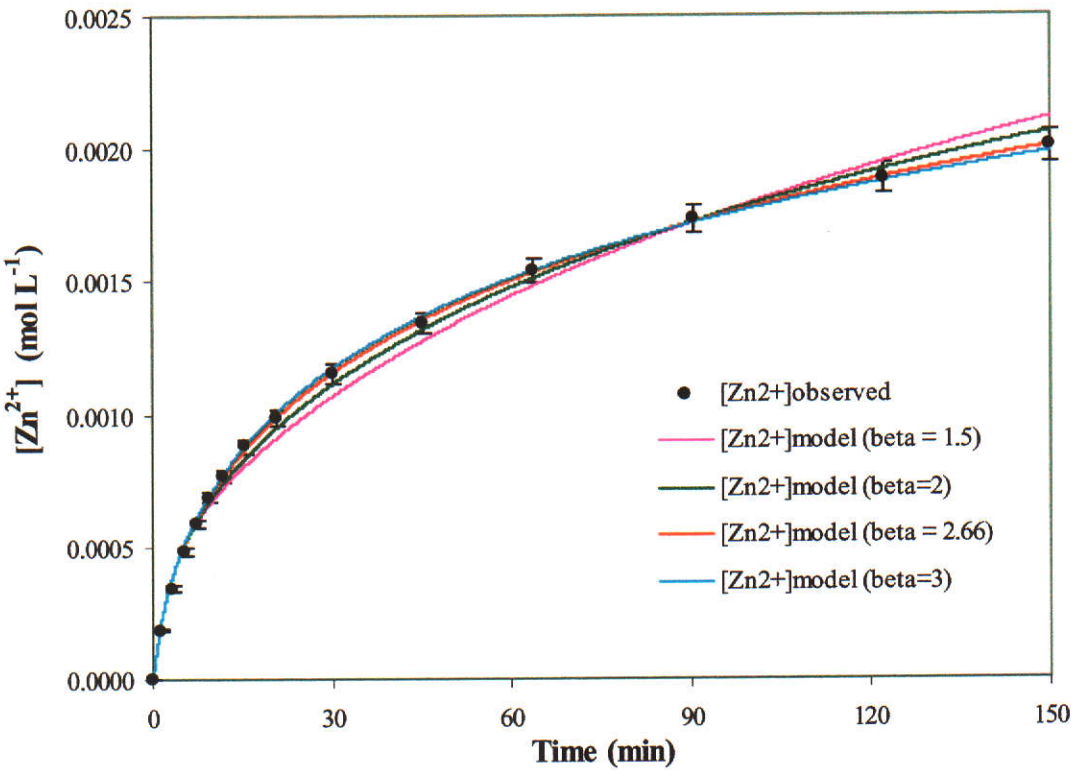

Figure 7.20 Effect of β on the fit of the model to a ZnS / H_2SO_4 / SO_2 leach at 150°C. Conditions: ZnS-F2 (27.3 μm) = 0.4 g L^{-1}, $[H_2SO_4]$ = 0.024 mol L^{-1}, $[SO_2]$ = 0.055 mol L^{-1}, 800 rpm.

The order of reaction with respect to HS_2SO_3H being greater than one, suggests that the kinetics of this reaction is not as simple as described by the above model. The higher order suggests that the decompostion reaction involves a number of steps, which is plausible, since in this system there are many possible side and sequential reactions that could be occurring where sulfane monosulfonates are being formed and decomposed (see Section 2.2.2.5). The existence of these equilibria would increase the order above one.

In addition, instead of ZnS only being re-precipitated by HS_2SO_3H, the re-precipitation of ZnS most probably occurs by reaction of $Zn^{2+}(aq)$ with sulfane monosulfonates of any chain length. It is probable that the higher sulfane monosulfonates are more reactive toward Zn^{2+}, since the longer the chain length the higher the negative charge on the sulfur atom at the end of the sulfane chain (Table 4.2, p. 91).

Evaluation of the leach data according to the diffusion controlled and interface reaction controlled shrinking particle models showed that neither model fitted the data. These negative observations supported the aforementioned dissolution mechanism. The lack of correlation with the diffusion controlled model supports the view that dissolution is not inhibited by a sulfur layer, since it suggests that dissolution is not diffusion controlled and hence that a layer does not cover the unreacted zinc sulfide. The lack of correlation with the interface reaction controlled model supports the view that the reaction is reversible, since it suggests the reaction is not an irreversible interface reaction controlled reaction.

7.1.6 Leaching at industrial pulp densities

To assess the commercial potential of SO_2 addition, the pulp density was increased to 150 g L^{-1}, as these conditions are close to those envisaged for an industrial situation. Figure 7.21 demonstrates the effectiveness of SO_2 in increasing the extent of ZnS dissolution in sulfuric acid at 100°C. The leach results suggest that upon addition of SO_2 a rapid reaction occurs between SO_2 and the H_2S present in the system from the

dissolution of ZnS by H_2SO_4. This rapid removal of H_2S allows the ZnS dissolution to rapidly increase. H_2S was evident prior to the addition of SO_2, as shown by the formation of a black precipitate on contacting a lead acetate solution, but after SO_2 addition it was only present at trace levels (Figure 7.22). The reaction between SO_2 and H_2S generated predominantly elemental sulfur with lesser amounts of tetrathionate, as shown by Raman spectroscopy (Figure 7.23).

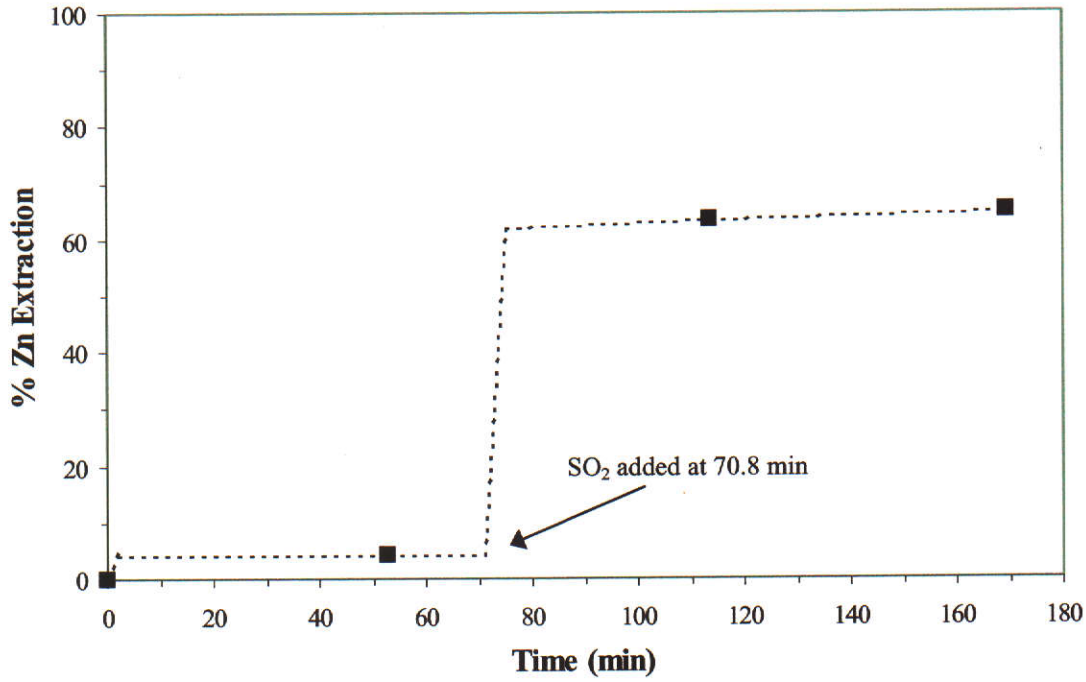

Figure 7.21 Effect of SO_2 addition to ZnS – H_2SO_4 system at equilibrium at 100°C.
$[H_2SO_4] = 1.6$ mol L^{-1}, $m(ZnS) = 200$ g, $m(SO_2)_{added} = 92$ g, solution volume = 1.36 L

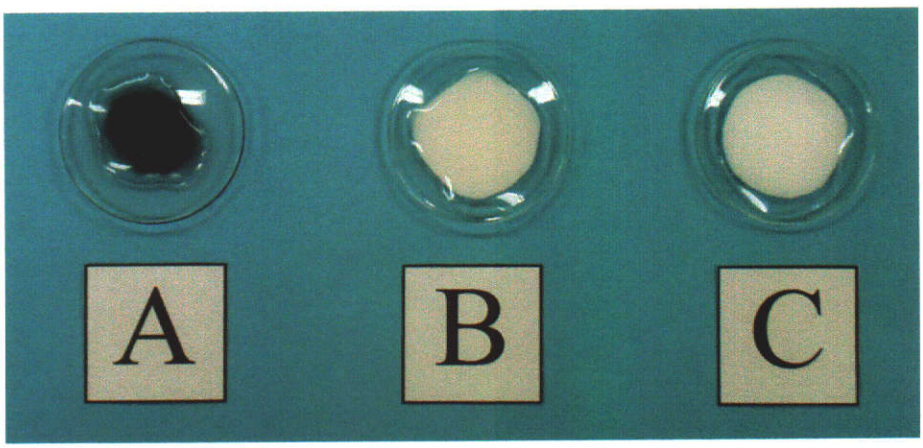

Figure 7.22 Lead acetate test results for headspace gases sampled from a 100°C leach.
(A) before addition of SO_2, (B) 10 minutes after addition of SO_2 and (C) 55 minutes after addition of SO_2.

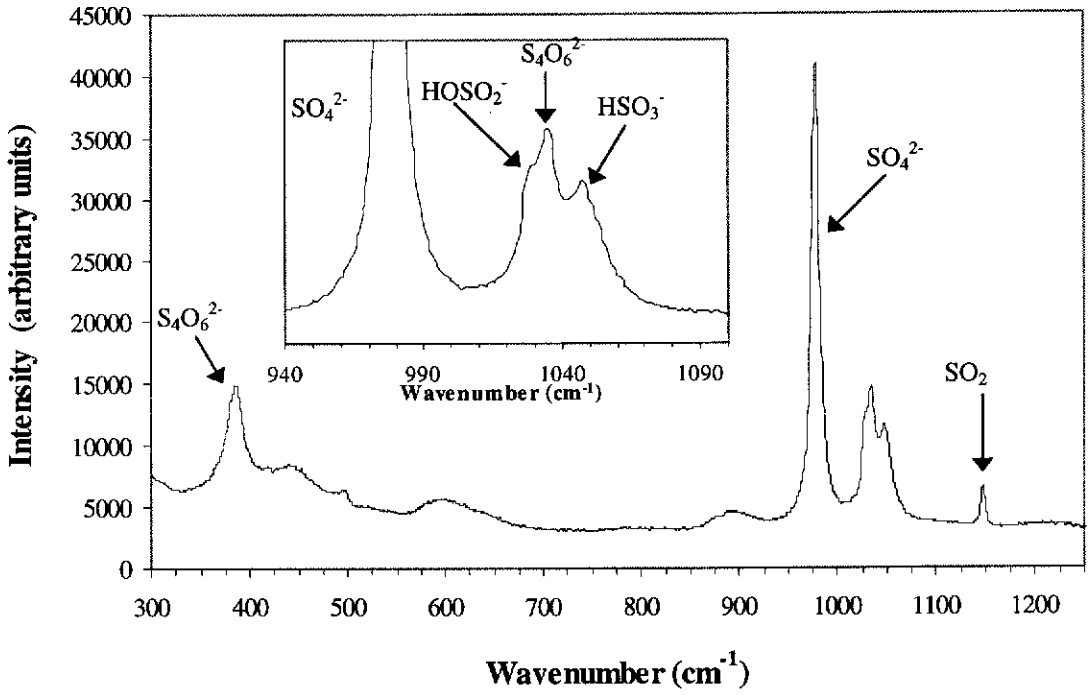

Figure 7.23 Dispersive Raman spectrum (He-Ne, 632.817 nm) of leach solution 100 min after addition of SO_2.
Conditions: T = 100°C, $[H_2SO_4]$ = 1.6 mol L^{-1}, m(ZnS) = 200 g, m(SO_2) added = 92 g, solution volume = 1.36 L

After the initial increase in zinc extraction, the dissolution rate experienced considerable inhibition. SEM images of mounted and polished cross sections of the leach residue suggest that the inhibition was due to the agglomeration of elemental sulfur with unreacted ZnS. Figure 7.24 shows the cross sectional view of a number of larger agglomerates consisting of ZnS and elemental sulfur. A close up view (Figure 7.25) of one of the agglomerates shows spheres of elemental sulfur (lighter grey circles) intimately mixed with unreacted ZnS (white). The black circles are holes and the dark grey irregular regions are the resin in which the sample was mounted. Within the large agglomerates, smaller agglomerates consisting of smaller spheres of elemental sulfur and surrounded by ZnS are also evident.

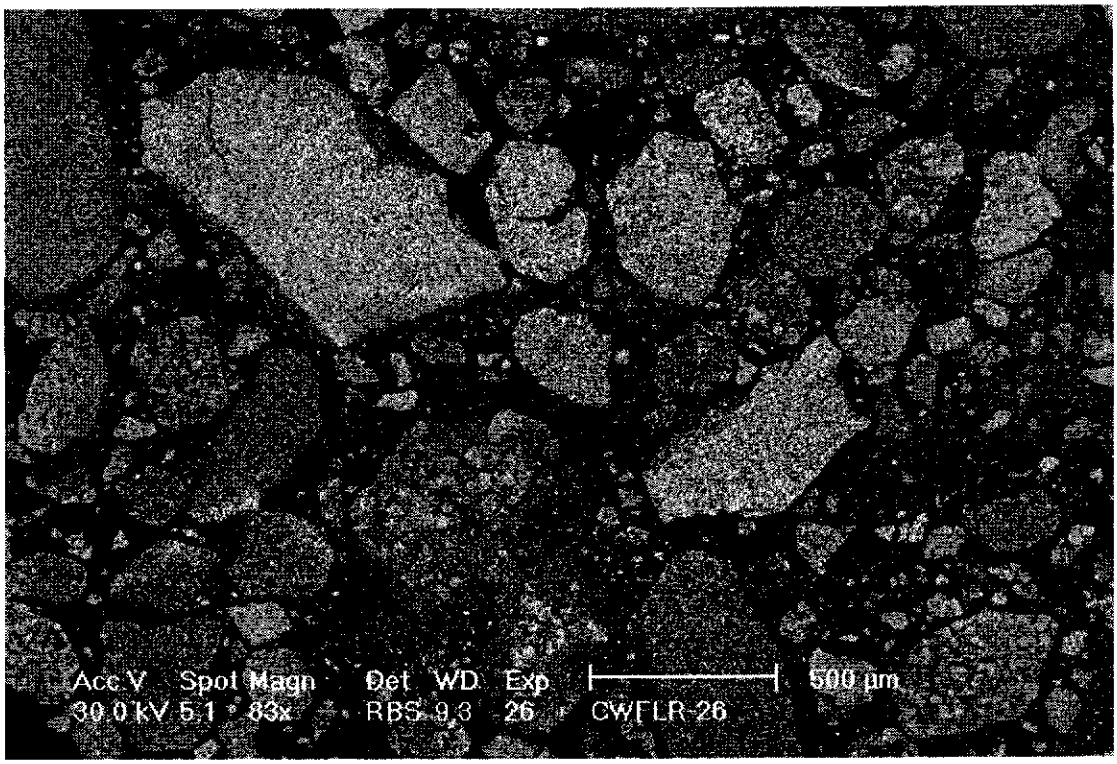

Figure 7.24 SEM image (back scatter) of the 100°C leach residue that had been mounted in resin and polished, showing agglomerates of zinc sulfide and elemental sulfur (grey) embedded in resin (black).

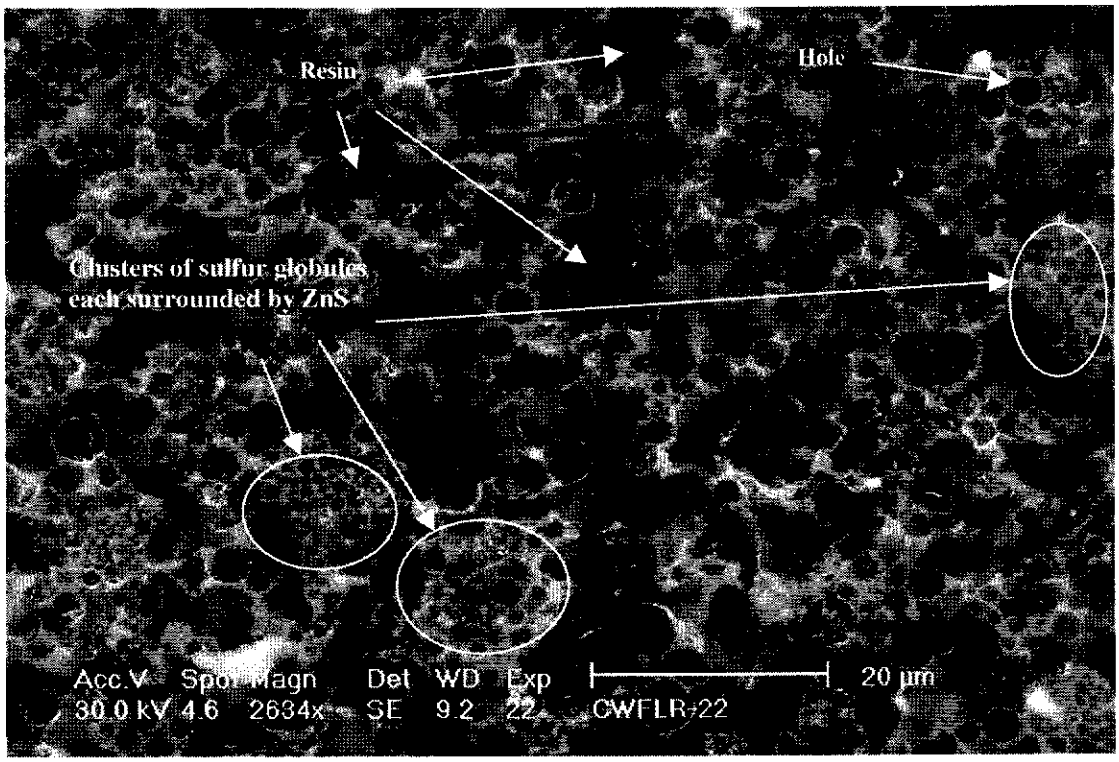

Figure 7.25 Close-up SEM image of the 100°C leach residue that had been mounted in resin and polished, showing spheres of sulfur (light grey circles) surrounded by very fine ZnS particles (white).

At 150°C, SO_2 was also able to increase the extent of ZnS dissolution in sulfuric acid. In this leach, the rapid initial rate is evident, with the zinc extraction increasing from 8% to 55% within 4 minutes.

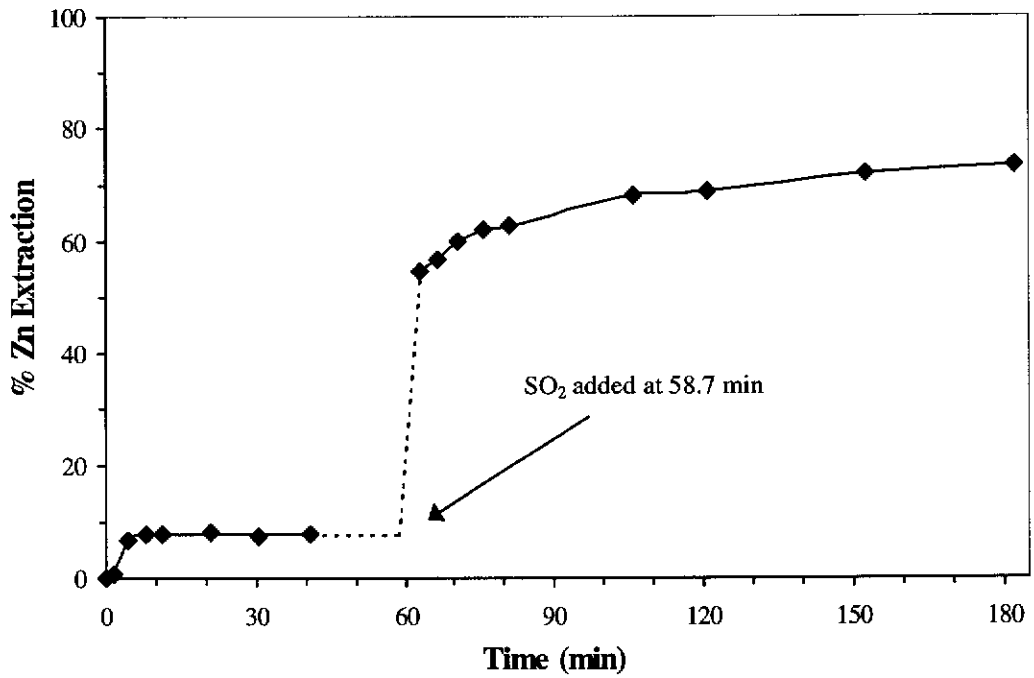

Figure 7.26 Effect of SO_2 addition to ZnS – H_2SO_4 system at equilibrium at 150°C. $[H_2SO_4]$ = 1.6 mol L^{-1}, m(ZnS-C) = 200 g, m(SO_2) = 92 g, solution volume = 1.36 L

However, as with the 100°C leach, this leach also experienced inhibition with the zinc extraction reaching only 72%, two hours after the addition of sulfur dioxide. Scanning electron microscopy images of the final leach residue that had been mounted in resin and polished to obtain cross sectional views (Figure 7.27), again showed agglomerates containing spheres of elemental sulfur (dark grey circles) and finely divided zinc sulfide particles (light grey regions) that were less than 0.5 μm (Figure 7.28b). The very bright particles contain barium, which is an impurity in the zinc sulfide. The spheres of elemental sulfur also contained zinc sulfide (Figure 7.28), indicating that some of the unreacted zinc sulfide was completely occluded by molten sulfur. Thus, the reduction in leach rate was due to the complete occlusion of some of the zinc sulfide in globules of elemental sulfur, and to the formation of agglomerates of zinc sulfide with elemental sulfur which reduced the surface area of zinc sulfide available for reaction.

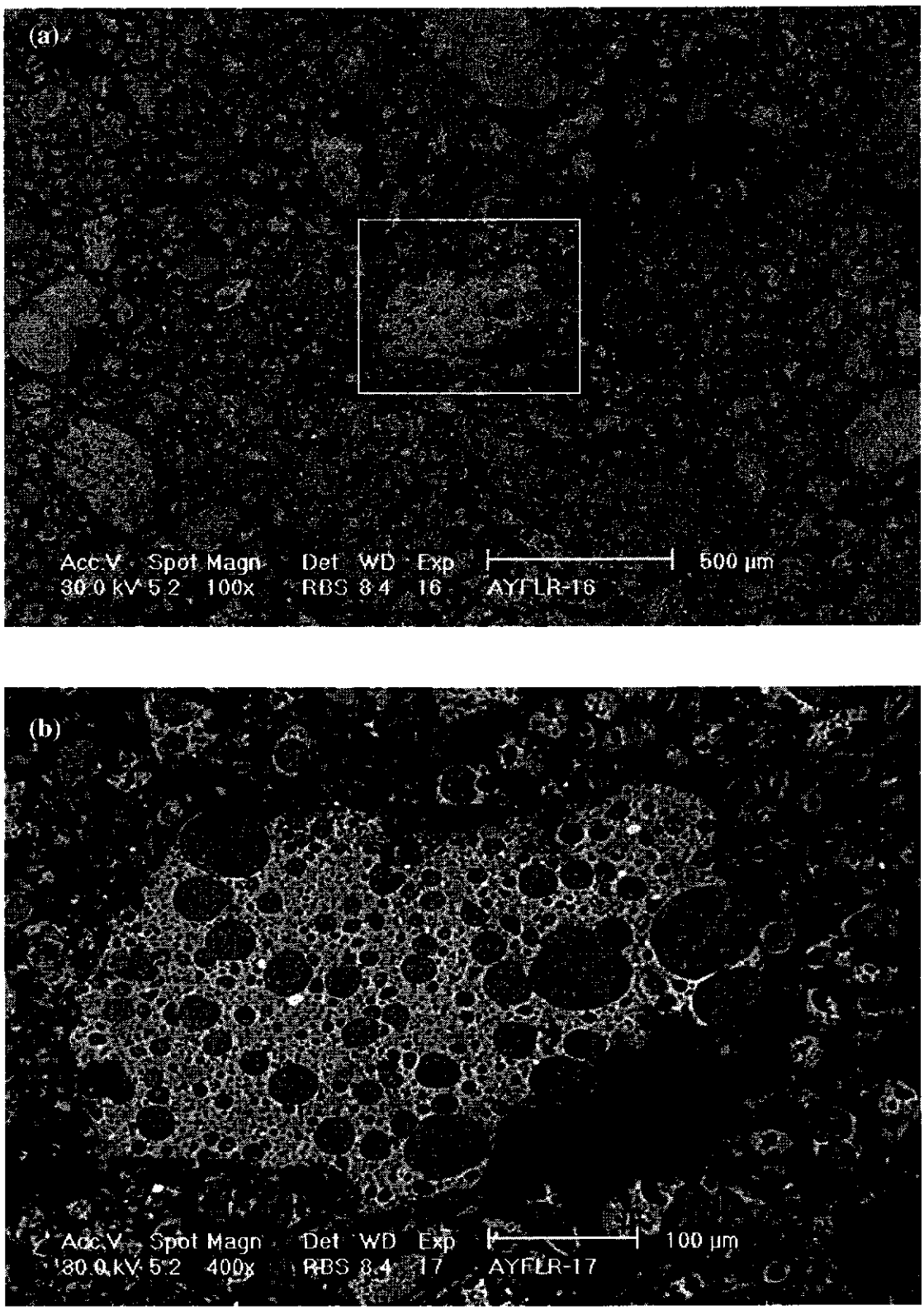

Figure 7.27 SEM images of the 150°C leach residue that had been mounted in resin and polished. The outlined section in (a) is magnified further in (b).

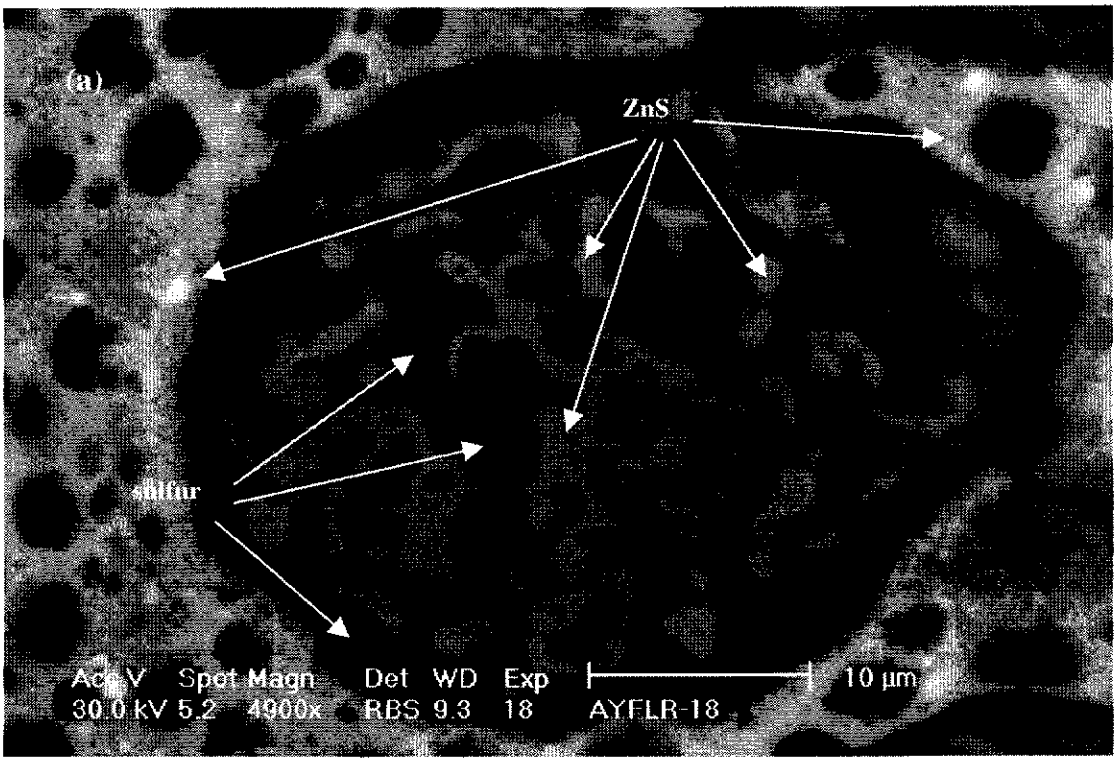

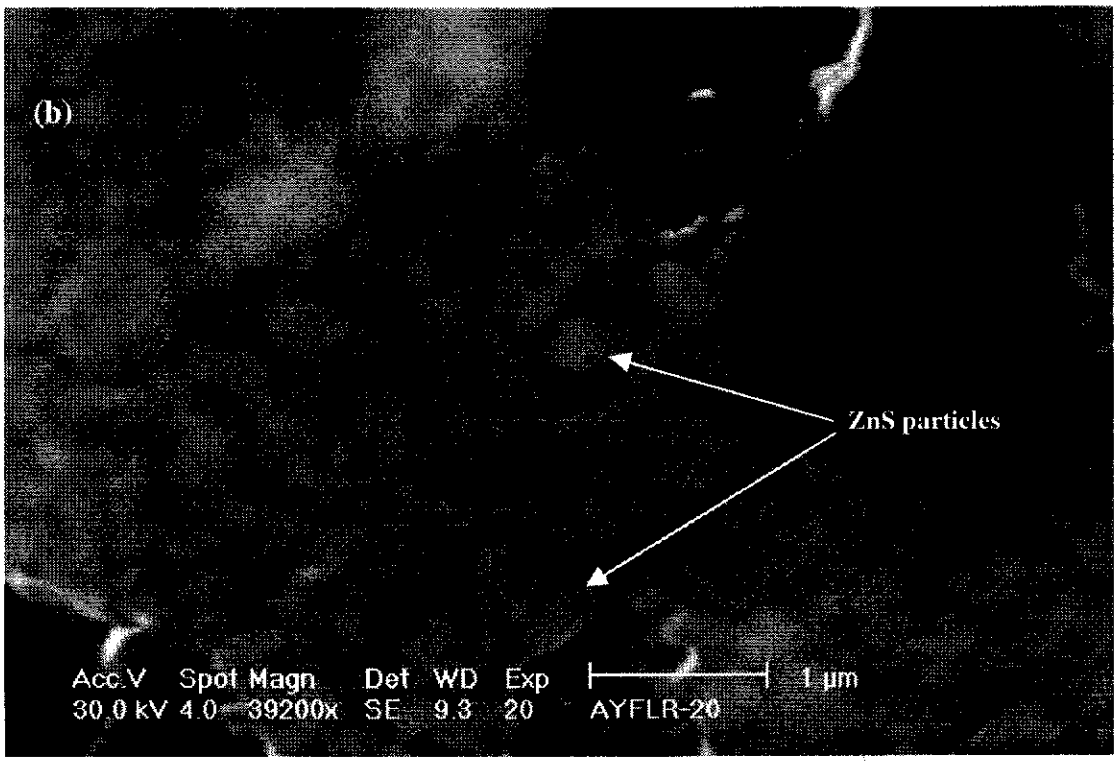

Figure 7.28 Close-up SEM images of the 150°C leach residue that had been mounted in resin and polished.
(a) – cross sectional view of globule of sulfur (dark grey) containing ZnS (light grey).
(b) – image of some of the unreacted zinc sulfide particles

That elemental sulfur was observed to inhibit the dissolution of zinc sulfide at high pulp densities but not at low pulp densities is probably due to the larger amounts of elemental sulfur generated at the higher pulp densities. With more elemental sulfur present in the system, agglomeration and occlusion of unreacted zinc sulfide occurs to a greater extent.

7.1.7 Comparison to other studies

The behaviour of the ZnS / H_2SO_4 / SO_2 system in this work is similar to that observed for the dissolution of PbS in HCl / SO_2 solutions, since this occurs by a similar two step process; non-oxidative dissolution of PbS followed by oxidation of H_2S to elemental sulfur by SO_2, and is also independent of SO_2 concentration (Han 1985).

In contrast, Tiwari (1977) observed that, when leaching ZnS in solutions containing sulfur dioxide and sulfuric acid (0.3 - 2 mol L^{-1}) at ambient temperature (26°C), the rate varied with the square root of sulfur dioxide concentration. The difference between the observations in this work and those of Tiwari may be due the difference in ZnS pulp densities, as the pulp density in Tiwari's study was 20 g L^{-1} whereas those in this study were fifty times lower, being only 0.4 g L^{-1}.

Also, in contrast to the observations in this work, Tiwari concluded that the dissolution rate is retarded by the formation of a tenacious film of elemental sulfur on the zinc sulfide surface. He observed that the initial reaction rate is high but that it rapidly decreases as the reaction progresses and proposed that in the initial stage, the dissolution rate is governed by the reaction of hydrogen ions with zinc sulfide, whereas in the latter stages, the rate is governed by the removal of H_2S by reaction with SO_2. Having determined that the rate of reaction between $H_2S(g)$ and SO_2 (aq) was so high that it could not be the rate determining step, he concluded that 'the rate of the H_2S / SO_2 reaction is very fast and hydrogen sulfide produced by the ZnS / H^+(aq) reaction is oxidised right on the surface of zinc sulfide and does not get a chance to diffuse away from the reaction interface to the bulk of the solution.'

He interpreted his observed kinetic data in the light of a sulfur growth model, which assumes that there is a sulfur layer covering the particle, whose thickness increases with time, and concluded that the rate of dissolution of zinc sulfide depends on the rate of diffusion of reactants (H^+, SO_2) and products (H_2S) through this sulfur layer.

However, Tiwari did not clearly establish that elemental sulfur occluded the ZnS particles. He only mentions that 'sulfur was seen on the surface of zinc sulfide particles', and there was no mention of how this observation was made.

In addition, his sulfur growth model does not satifactorily explain all of his observations. Instead of being diffusion controlled, his calculated activation energies (50.88 kJ mol^{-1} in 0.18 $molL^{-1}$ H_2SO_4 and 87.03 kJ mol^{-1} in 3.0 mol L^{-1} H_2SO_4) suggest that the reaction is interface reaction controlled. The activation energy for a diffusion controlled reaction is usually of the order of 21 kJ mol^{-1} or less, whereas that for an interface reaction controlled reaction is typically 40 - 105 kJ mol^{-1} (Sohn and Wadsworth 1979a).

According to the observations in this work which showed no occlusion by elemental sulfur at temperatures below the melting point of sulfur, but which did indicate that agglomeration of elemental sulfur and zinc sulfide occurs at high pulp densities, it is likely that in Tiwari's study the dissolution was inhibited by agglomeration rather than occlusion by a sulfur film, and his findings are not necessarily contradictory to this work.

7.2 SUMMARY

The dissolution of ZnS in H_2SO_4 / SO_2 solutions was found to proceed via non-oxidative acidic dissolution of ZnS followed by reaction between H_2S thus generated and $SO_2(aq)$ or $HSO_3^-(aq)$ to produce elemental sulfur and polythionates, predominantly tetrathionate.

At low pulp densities (0.4 g L^{-1}) the reaction between the generated H_2S and $SO_2(aq)$

or HSO_3^-(aq) species is postulated to occur at the sulfide surface, generating reactive intermediates, thought to be sulfane monosulfonates. The presence of SO_2 increases the extent of zinc extraction beyond that obtainable in sulfuric acid alone, however, the dissolution rate is independent of the SO_2 concentration. The rate of dissolution, however is slow, possibly due to the presence of sulfane monosulfonates, which may react with zinc ions to re-precipitate ZnS, the rate determining step then being the rate of removal of the inhibiting sulfane monosulfonates from the system. Direct inhibition by H_2S and occlusion by sulfur were shown not to be contributing factors to the inhibition.

At high pulp densities (200 g L^{-1}), the addition of SO_2 to ZnS / H_2SO_4 systems at equilibrium causes a marked increase in the dissolution rate, which rapidly slows. The reduction in rate is due to the agglomeration of particles of unreacted zinc sulfide and elemental sulfur, and at temperatures above the melting point of sulfur, occlusion of zinc sulfide within globules of molten sulfur also occurs.

8 SO_2 PRESSURE LEACHING OF A ZINC SULFIDE CONCENTRATE

To evaluate the potential of commercially using a ZnS / H_2SO_4 / SO_2 leaching process, experiments using a zinc concentrate from Elura, Australia, were conducted using 1.7 mol L^{-1} H_2SO_4 (170 g L^{-1}), as this is approximately the maximum strength that would likely be used in an industrial process. In an industrial situation, it is probable that liquor exiting from the electrolytic circuit would be used to leach the concentrate. Typically, the concentration of sulfuric acid in these liquors is around 180 g L^{-1}.

8.1 EFFECT OF SO_2 ON DISSOLUTION OF ELURA CONCENTRATE IN 1.7 MOL L^{-1} H_2SO_4

In the absence of SO_2, the dissolution of Elura concentrate (2 g L^{-1}) in 1.7 mol L^{-1} H_2SO_4 at 130°C was rapid with 94% extraction after 30 minutes (Figure 8.1). The pulp density and acidity were chosen such that in H_2SO_4 alone, equilibrium would not be attained. Consequently, the reverse reaction was negligible. However, when it was leached under the same conditions but with added SO_2, the dissolution rate and extent of dissolution decreased. In contrast to synthetic zinc sulfide, the dissolution of zinc concentrates was inhibited by molten elemental sulfur (m.p. = 119°C) produced in the leach which occluded the mineral surface. The presence of elemental sulfur, S_8, was confirmed by Raman spectroscopy (Figure 8.2).

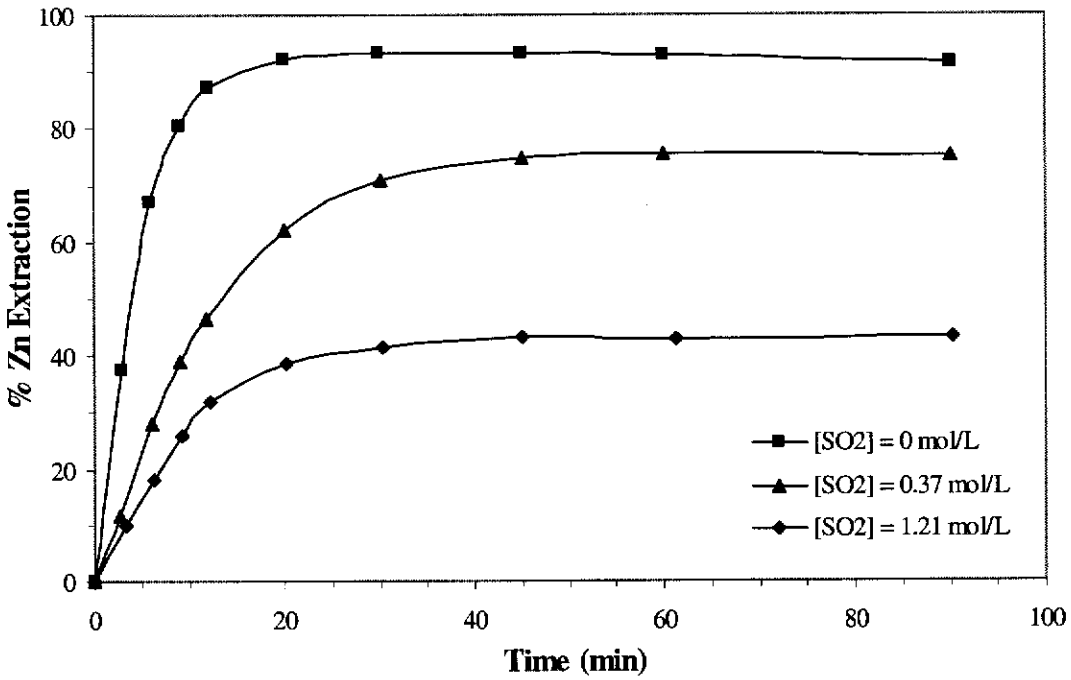

Figure 8.1 Effect of $[SO_2]$ on dissolution of Elura concentrate in 1.7 mol L^{-1} H_2SO_4 at 130°C. Pulp density = 2 g L^{-1}

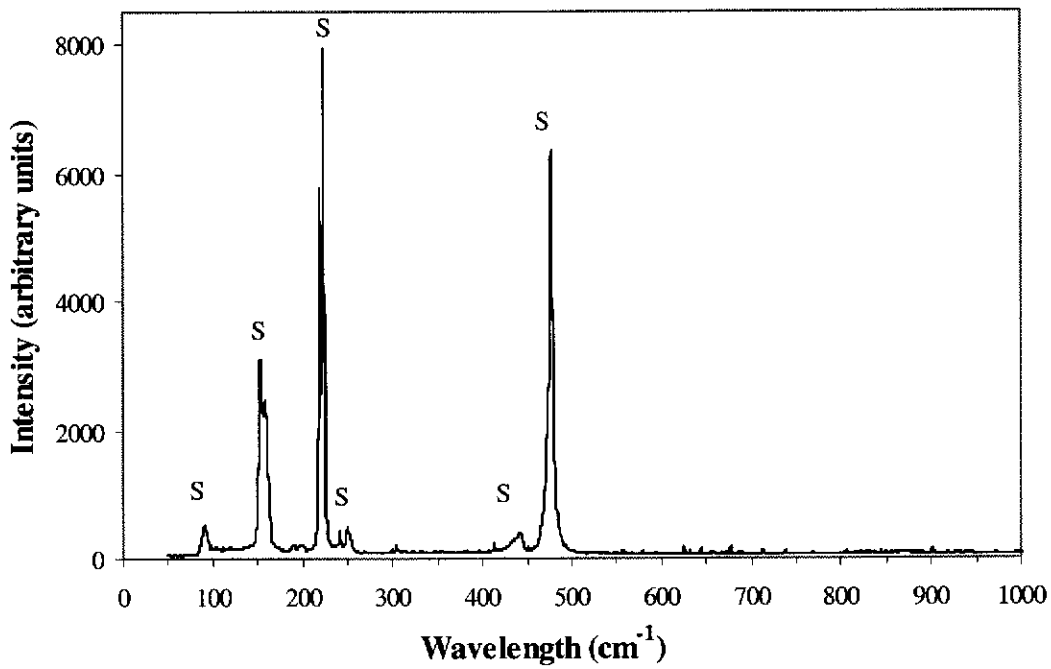

Figure 8.2 Dispersive Raman spectrum (He-Ne, 632.817 nm) of residue from SO_2 / H_2SO_4 leach of Elura C3 at 130°C.
$[H_2SO_4]$ = 1.7 mol L^{-1}, $[SO_2]$ = 1.21 mol L^{-1}, Pulp density = 2 g L^{-1}

Residues from samples taken throughout the leach were examined using scanning electron microscopy and X-ray analysis. This revealed the presence of agglomerates of mineral particles cemented together with molten sulfur. As the reaction progressed, the Elura concentrate-sulfur agglomerates continued to agglomerate further, forming larger agglomerates, reducing the surface area available for reaction, i.e. the sulfur globules acted as collectors for Elura concentrate particles, removing them from solution. Samples taken throughout the leach contained fewer free Elura concentrate particles and fewer agglomerates with time, indicating continual collection of Elura concentrate particles on molten sulfur and agglomeration of agglomerates as the reaction progressed (Figure 8.3a to Figure 8.3e). The leach curve that corresponds to these SEM images is shown in Figure 8.1 and is denoted by the diamond (♦) symbols. At the end of these leaches, there was often one large globule of sulfur impregnated with unreacted mineral plus smaller agglomerates.

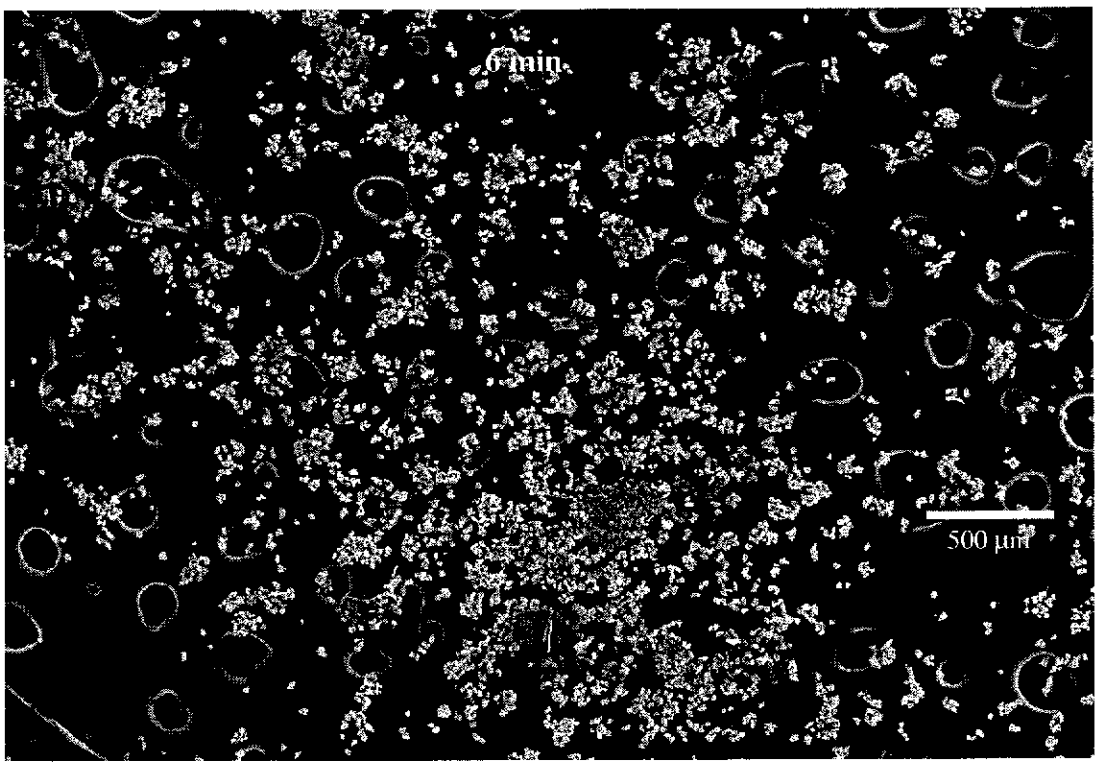

Figure 8.3 a) SEM image of Elura C3 residue after 6 minutes of leaching.

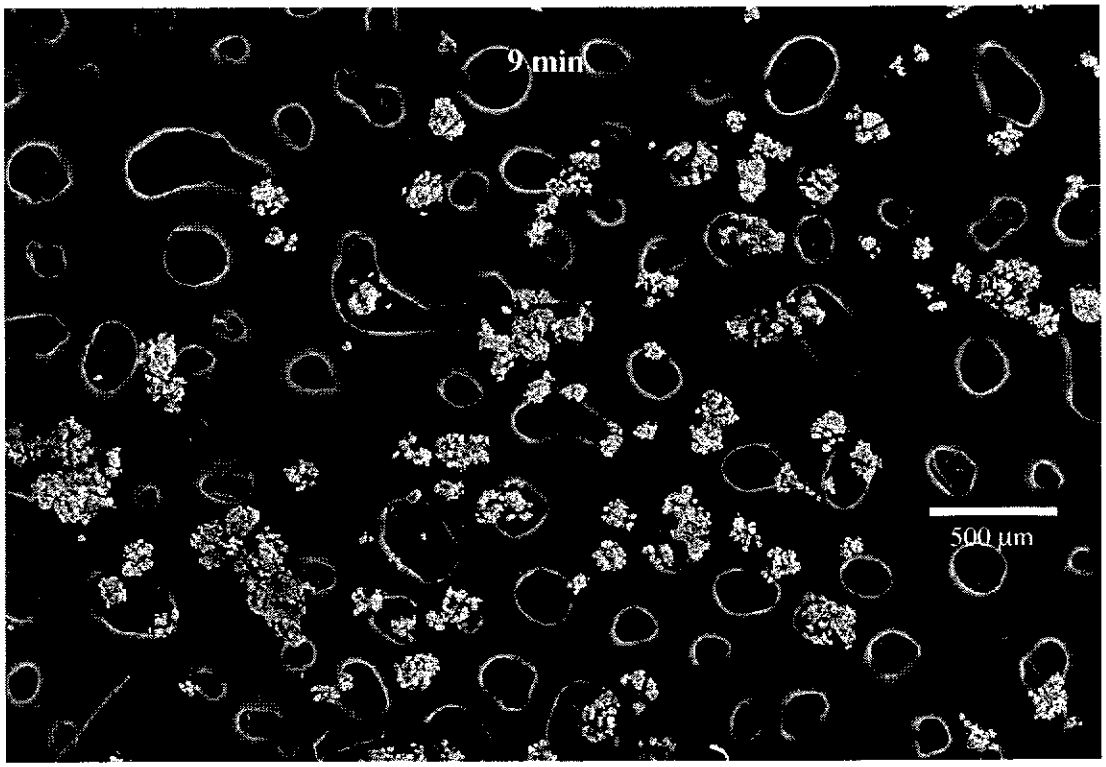

Figure 8.3 b) SEM image of Elura C3 residue after 9 minutes of leaching.

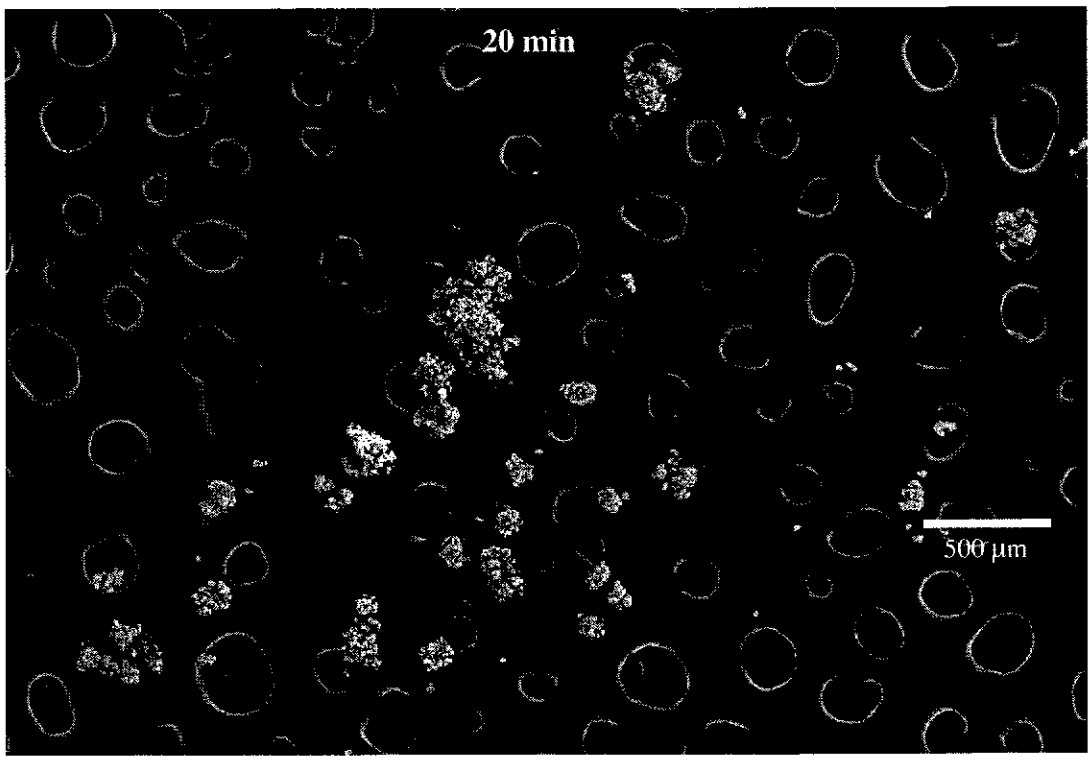

Figure 8.3 c) SEM image of Elura C3 residue after 20 minutes of leaching.

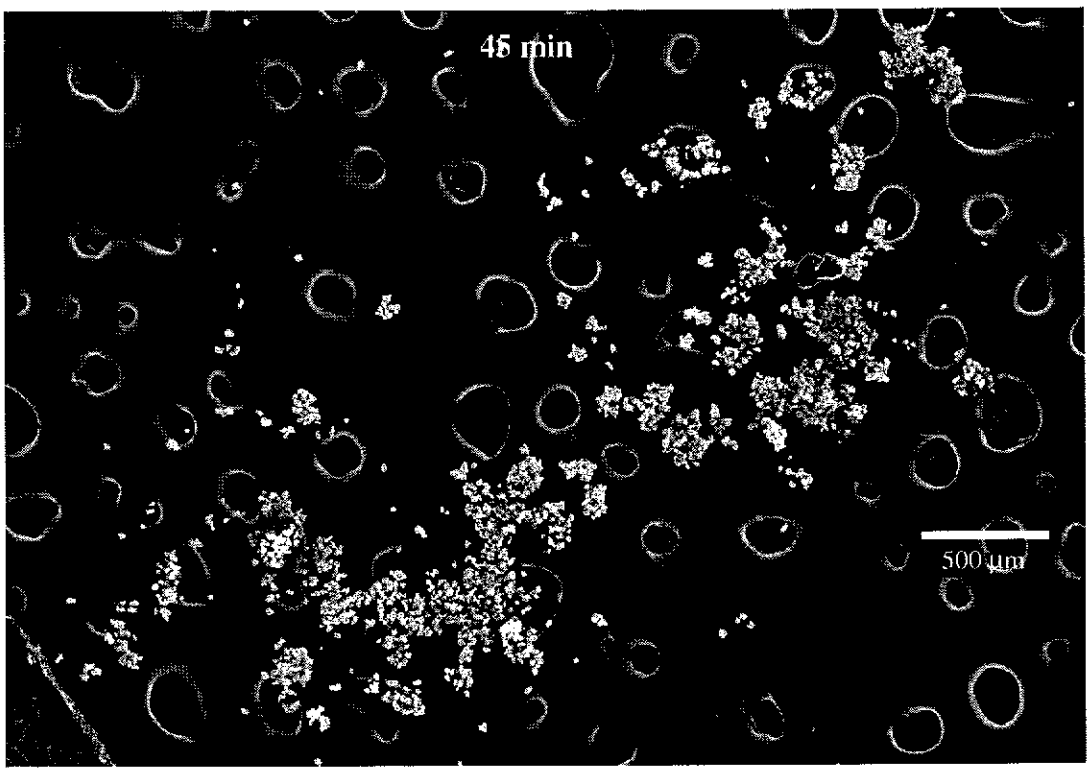

Figure 8.3 d) SEM image of Elura C3 residue after 45 minutes of leaching.

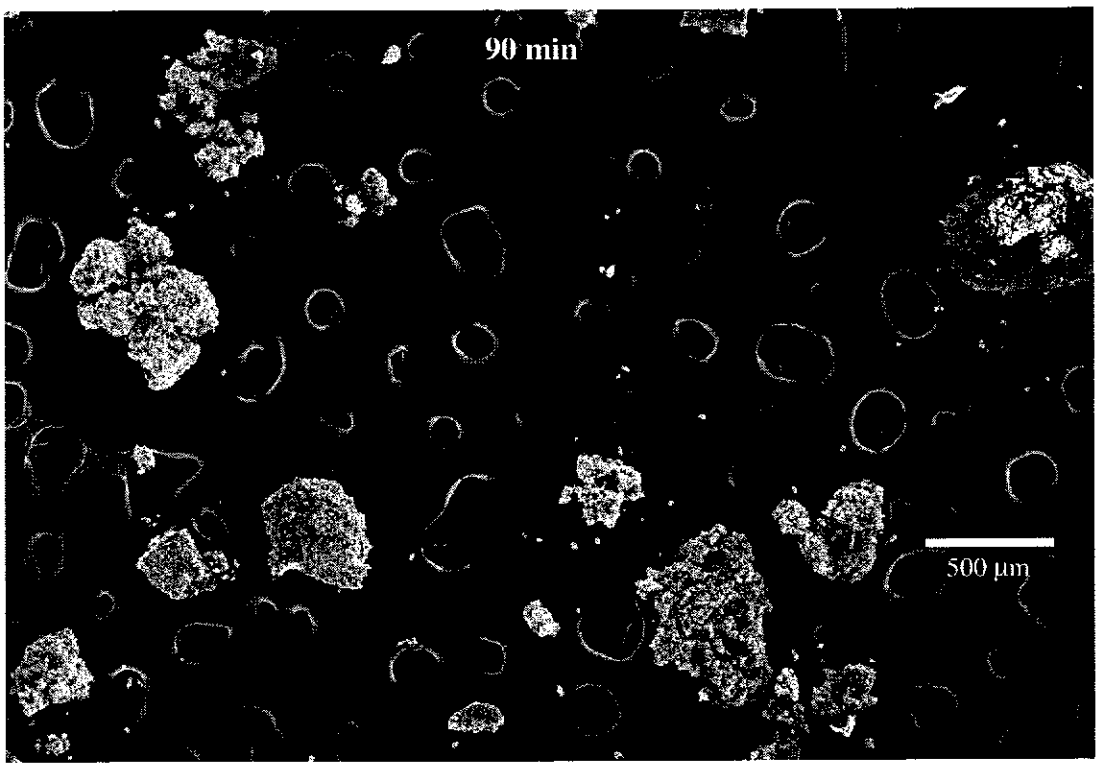

Figure 8.3 e) SEM image of Elura C3 residue after 90 minutes of leaching.

Figure 8.3 SEM images of residues taken throughout an SO_2 / H_2SO_4 leach of Elura C3 at 130°C, showing the increase in agglomerate size with increasing reaction time. $[SO_2(aq)]$ = 1.2 mol L^{-1} , $[H_2SO_4]$ = 1.7 mol L^{-1}, Pulp density = 2 g L^{-1}. The corresponding leach curve is shown in Figure 8.1 (♦).

As in the case of synthetic sphalerite, the sulfur was produced via the reaction between $SO_2(aq)$ and $H_2S(aq)$, generated by non-oxidative dissolution of sulfides in the concentrate (Eqn. 2.24, p. 20) Thermal decomposition of SO_2 (Eqn. 2.19 p. 17) is unlikely to have occurred since the high concentration of sulfuric acid would have inhibited that reaction (Kuz'min and Postnikov 1935).

The leach data presented above also give qualitative information regarding the kinetics of the sulfur forming $SO_2 + H_2S$ reaction (Eqn. 2.24, p. 20); the rate of sulfur production being reflected by the increased degree of inhibition in the leach rate. The results suggest that the rate of reaction is rapid as SO_2 affects the Elura concentrate dissolution rate from the commencement of the reaction (Figure 8.1). Also, agglomeration is observed after only 6 minutes (Figure 8.3a), at which time only about 10% Zn extraction had occurred (Figure 8.1).

The rate of sulfur production shows a strong dependency on concentration of $SO_2(aq)$. Increasing the concentration of $SO_2(aq)$ increased the rate of formation of sulfur and decreased the Elura concentrate dissolution rate (Figure 8.1), which is attributable to sulfur occluding the surface. This is in contrast to what was observed when leaching synthetic ZnS, where SO_2 had no effect on the dissolution rate. It would appear that the difference between the two systems is that Elura concentrate is wet by molten sulfur, whereas synthetic zinc sulfide is not.

8.2 EFFECT OF SURFACTANTS

Since occlusion by molten sulfur severely affects the rate of ZnS dissolution, it was necessary to find a surfactant that would prevent occlusion.

Elemental sulfur formation also occurs in the oxidative pressure leaching of zinc sulphide concentrates. Forward and Veltman (1959) found that at temperatures above the melting point of sulfur "the molten sulfur formed globules which wetted and occluded unoxidised sulfides", and to counter this, they optimised the conditions for the reaction to be carried out at 110°C, below the melting point of sulfur.

Subsequently it was found that by increasing the pulp density, the problem of sulfur wetting could be minimised and reaction temperatures of 150°C were feasible (Veltman and O'Kane 1968).

A significant breakthrough was made in the mid 1970's when it was found that the addition of certain surfactants (lignins, ligninsulfonates, tannin compounds, quebracho, tree bark extracts and alkylaryl sulfonates) prevented molten sulfur from occluding the unleached mineral (Kawulka, Haffenden and Mackiw 1975). This enabled the reaction temperature to be increased above the melting point of elemental sulfur and with the optimum reaction temperature being around 150°C the leaching rates were significantly increased.

Owusu and co-workers elucidated the probable mechanism by which surfactants increase zinc extractions. Owusu, Dreisinger and Peters (1995b) reported that calcium-based ligninsulfonic acid reduces the interfacial tension between liquid sulfur and aqueous zinc sulphate (0.8 - 2.0 mol L^{-1}) from 54 ± 1 mN m^{-1} to 29 ± 1 mN m^{-1} and increases the liquid sulfur-zinc sulphide (marmatite) - aqueous solution contact angle (from 80° ± 5° to 143° ± 5°). They concluded that surfactant is adsorbed at the liquid sulfur-aqueous phase interface and zinc sulfide (marmatite) - aqueous phase interface. As such the mineral surface is rendered both hydrophilic and "sulfophobic". The sulfur dispersion process is enhanced if the liquid sulfur-aqueous interfacial tension decreases as well, promoting the formation of smaller, spherical sulfur drops (Owusu and Dreisinger 1996). Table 8.1 lists interfacial tensions and liquid sulfur mineral contact angles for various surfactants (Owusu and Dreisinger 1996).

To gauge the effectiveness of surfactants in the SO_2 pressure leaching of zinc sulfide concentrate, sodium ligninsulfonate, quebracho and orthophenylenediamine were used as a representative set.

Adding the surfactants, sodium ligninsulfonate, orthophenylenediamine (OPD) and quebracho, to Elura concentrate / H_2SO_4 / SO_2 leaches increased the extent of zinc extraction (Figure 8.4). However complete dissolution of the concentrate was not possible, suggesting that partial occlusion of the mineral by sulfur still occurred.

Table 8.1 Interfacial tensions and liquid sulfur mineral contact angles for various surfactants.
Conditions: [Surfactant] = 0.3 g L^{-1}, $[ZnSO_4] = 1.5$ mol L^{-1}, T = 130-135°C, $p(N_2(g)) = 620$ kPa (from Owusu and Dreisinger (1996)).

Surfactant Type	Interfacial Tension (mN m^{-1})	Contact Angle (°)
None	54.4	80
Ligninsulfonate	27.0	143
Quebracho	44.8	128
Orthophenylenediamine	52.4	127
Tergitol	42.5	103
Napthalene sulfonic acid	22.0	155

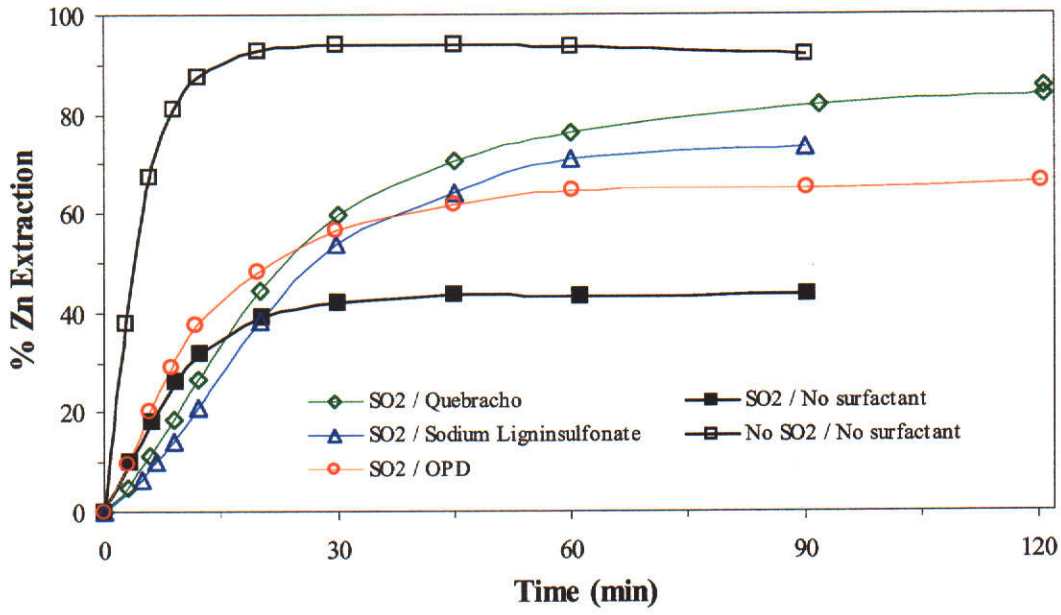

Figure 8.4 Effect of different surfactants on dissolution of Elura C3 in SO_2 / H_2SO_4.
T = 130°C, Surfactant = 0.3 g L^{-1}, $[H_2SO_4]$ = 1.7 mol L^{-1}, $[SO_2(aq)] = 1.2$ mol L^{-1}, Pulp density = 2 g L^{-1}, Stirring speed = 800 rpm.

In the presence of sodium ligninsulfonate and quebracho, the initial leach rates were slower than the rate in the absence of any surfactant, suggesting that these surfactants adsorb on the mineral surface and reduce the rate of dissolution initially. This effect was not observed with orthophenylenediamine, probably because, having a much lower molecular weight, the surfactant-sulfide surface interactions would have been weak and consequently any adsorption onto the mineral surface would have been weak. The inhibition in the leaches with quebracho and sodium ligninsulfonate did not appear to be due to the agglomeration of mineral particles with elemental sulfur

as very few agglomerates were found in the leach residues of samples taken in this period. A purple – brown residue, which may have resulted from the decomposition of quebracho in sulfuric acid, was observed amongst the residual zinc concentrate and may have also caused some inhibition. No further work was undertaken with orthophenylenediamine, for health and safety reasons, since it is a carcinogen.

Increasing the surfactant concentration from 0.3 g L^{-1} to about 0.8 g L^{-1}, in the case of sodium ligninsulfonate and quebracho, resulted in only small increases in zinc extraction (Figure 8.5).

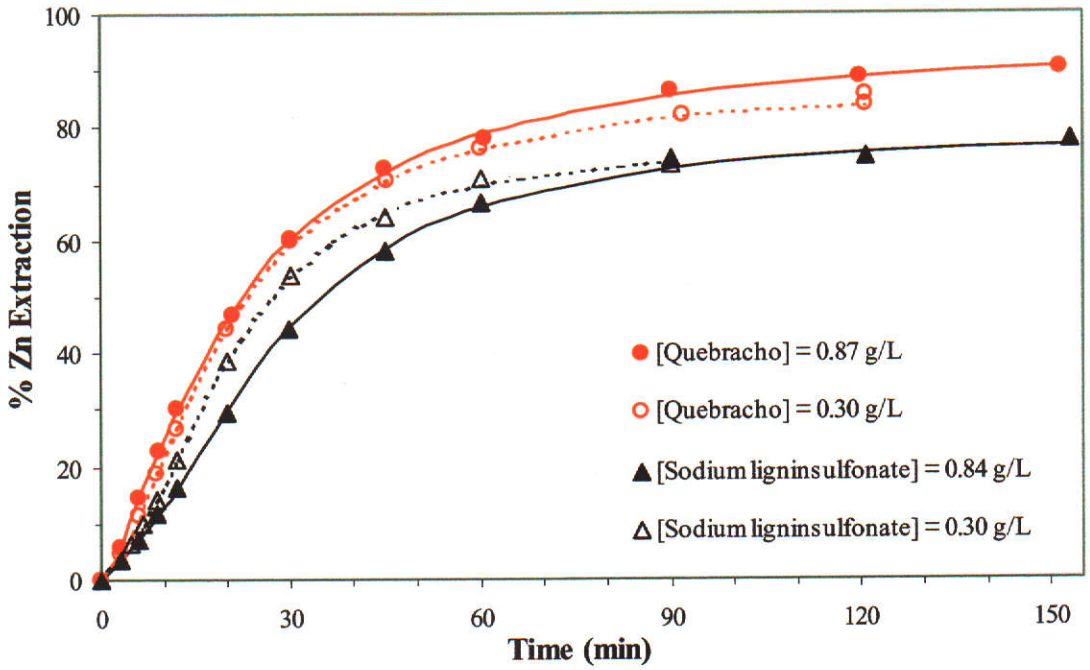

Figure 8.5 Effect of surfactant concentration on zinc extraction from Elura C3 in SO_2 / H_2SO_4 leach at 130°C.
$[H_2SO_4]$ = 1.7 mol L^{-1}, $[SO_2(aq)]$ = 1.2 mol L^{-1}, Elura concentrate = 2 g L^{-1}

Although quebracho or its decomposition products do slow and inhibit the non-oxidative dissolution of Elura concentrate in sulfuric acid, the degree of inhibition is much less than that observed when SO_2 is present (Figure 8.6). In the presence of 0.89 g L^{-1} quebracho, Elura zinc concentrate is almost completely leached in sulfuric acid, though the dissolution rate is less than when quebracho is absent. When sulfur dioxide is also present, the dissolution rate is further impeded, however with longer leaching times a similar degree of extraction may be achieved. This suggests that as the sulfur forms, the surfactant leaves the mineral surface and adsorbs onto the

sulfur, keeping it dispersed to a large extent, and the dissolution rate increases as evidenced by increased zinc extraction.

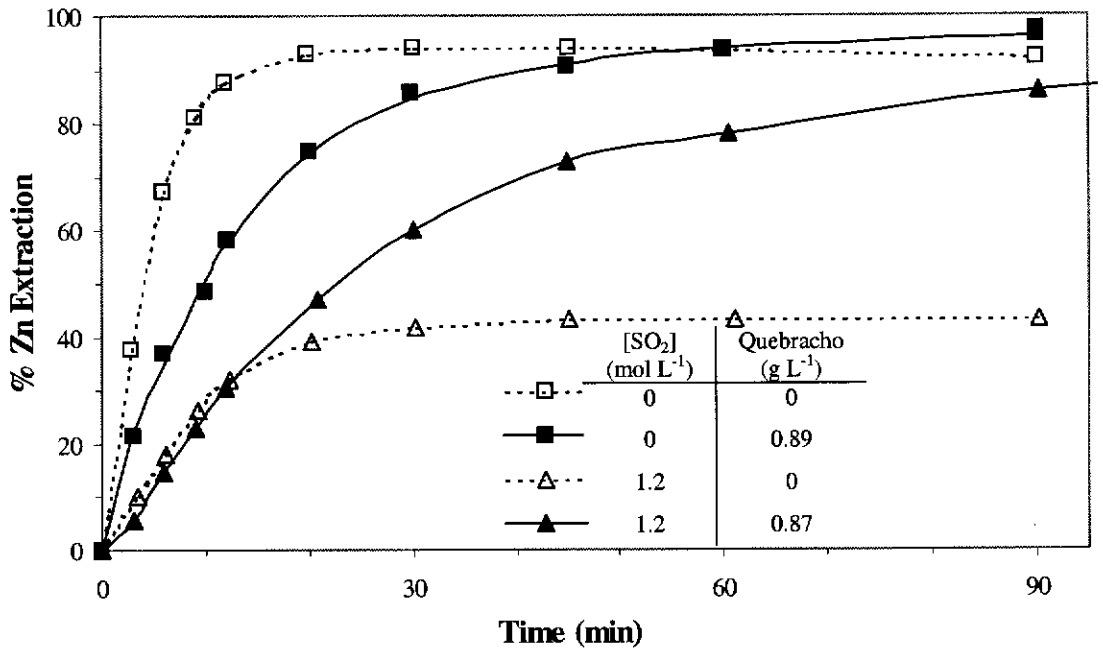

Figure 8.6 Effect of quebracho on the dissolution of Elura concentrate in H_2SO_4 (1.7 mol L^{-1}) with and without SO_2 at 130°C.

The surfactants, quebracho, orthophenylenediamine and sodium ligninsulfonate, are effective in keeping the mineral surface relatively free from sulfur occlusion in the H_2SO_4 / SO_2 leaching system. However, it appears that, in such solutions at elevated temperatures, they decompose by reaction with sulfuric acid and/or sulfur dioxide, reducing their effectiveness with time.

8.3 ADDITION OF SO_2 TO THE ELURA CONCENTRATE / H_2SO_4 SYSTEM AT EQUILIBRIUM

Sections 8.1 and 8.2 addressed the effect of sulfur dioxide on the dissolution of zinc concentrate in sulfuric acid under conditions such that the zinc concentrate / sulfuric acid system was far from equilibrium. This section addresses the effect of sulfur dioxide on the system when it is at equilibrium.

The addition of SO_2 to the zinc concentrate / H_2SO_4 system at equilibrium resulted in

increased zinc extraction (Figure 8.7), however, the increase was modest, from 53% to 63%.

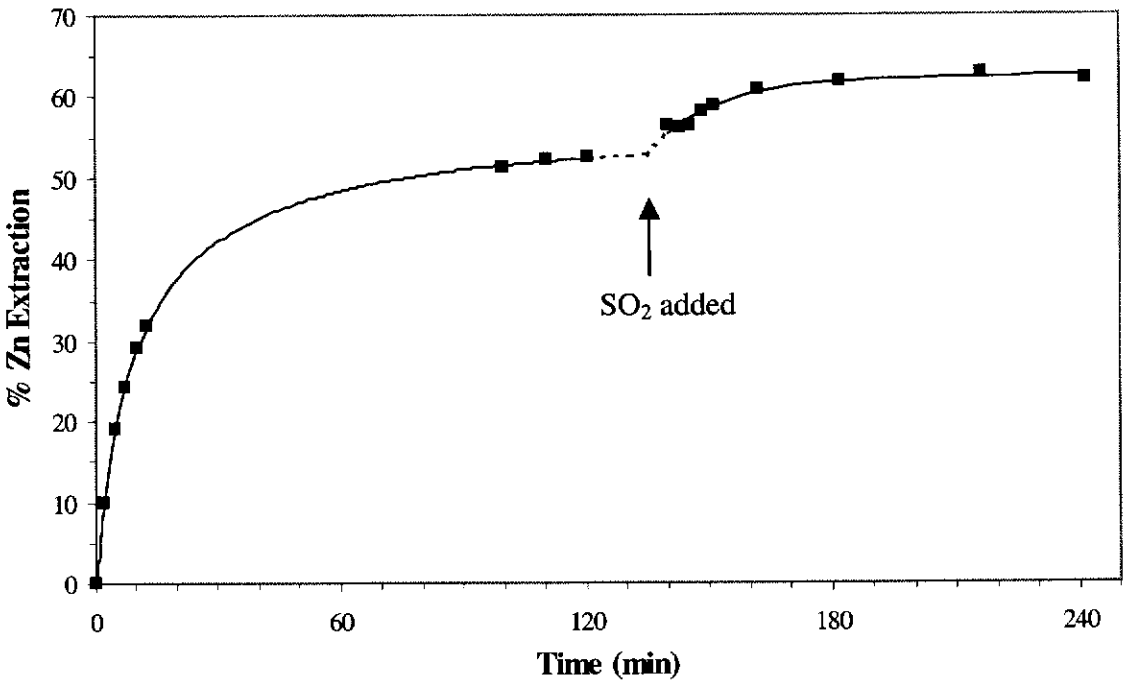

Figure 8.7 Effect of SO_2 addition to Elura C3 – H_2SO_4 system at equilibrium.
T = 150°C, $[H_2SO_4]$ = 0.50 mol L^{-1} , pulp density = 4.1 g L^{-1} [Quebracho] = 0.1 g L^{-1}.
SO_2 (65.5 g) added at 134.6 min, $[SO_2(aq)]$ = 0.7 mol L^{-1}

Solid samples taken prior to addition of SO_2 were free flowing fine grains, whereas in samples taken after the addition of SO_2 the grains were not free flowing but adhered together (Figure 8.8), indicating that molten sulfur, observed in the partially leached solids, was inhibiting dissolution. Figure 8.8 shows agglomerates of zinc concentrate particles (light grey) with elemental sulfur (dark grey) and also zinc concentrate particles attached to spheres of elemental sulfur. A close-up view of the agglomerate in the top right corner of Figure 8.8 is shown in Figure 8.9, showing mineral particles fixed in a sulfur globule.

Even though quebracho (0.1 g L^{-1}) was present in the leach solution, it appears to have been ineffective. It may be that by the time SO_2 was added (135 minutes into the leach), the quebracho had decomposed to some extent. It is also likely that the added SO_2 reacted with the quebracho, as the solution prior to addition of quebracho was light brown, whereas after the addition of SO_2 it was colourless.

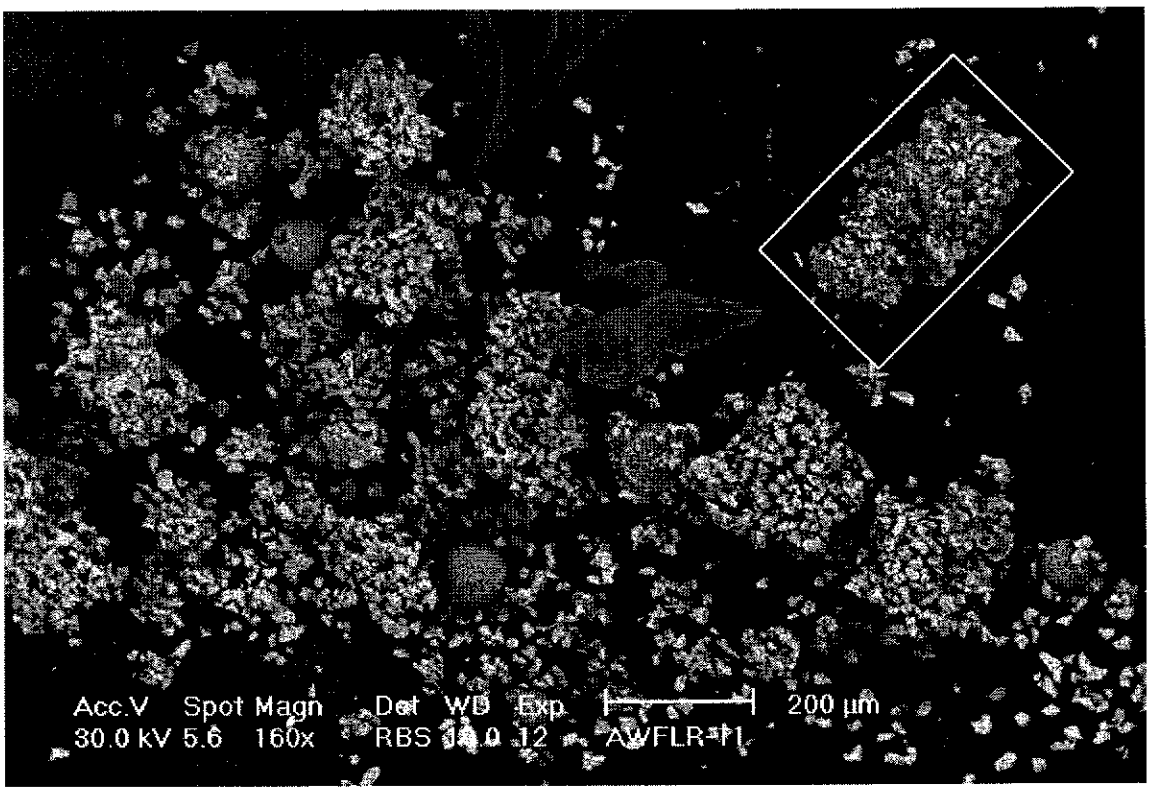

Figure 8.8 SEM image of residue taken after SO_2 addition to a leach of Elura C3 in H_2SO_4. The leach conditions are given in Figure 8.7.

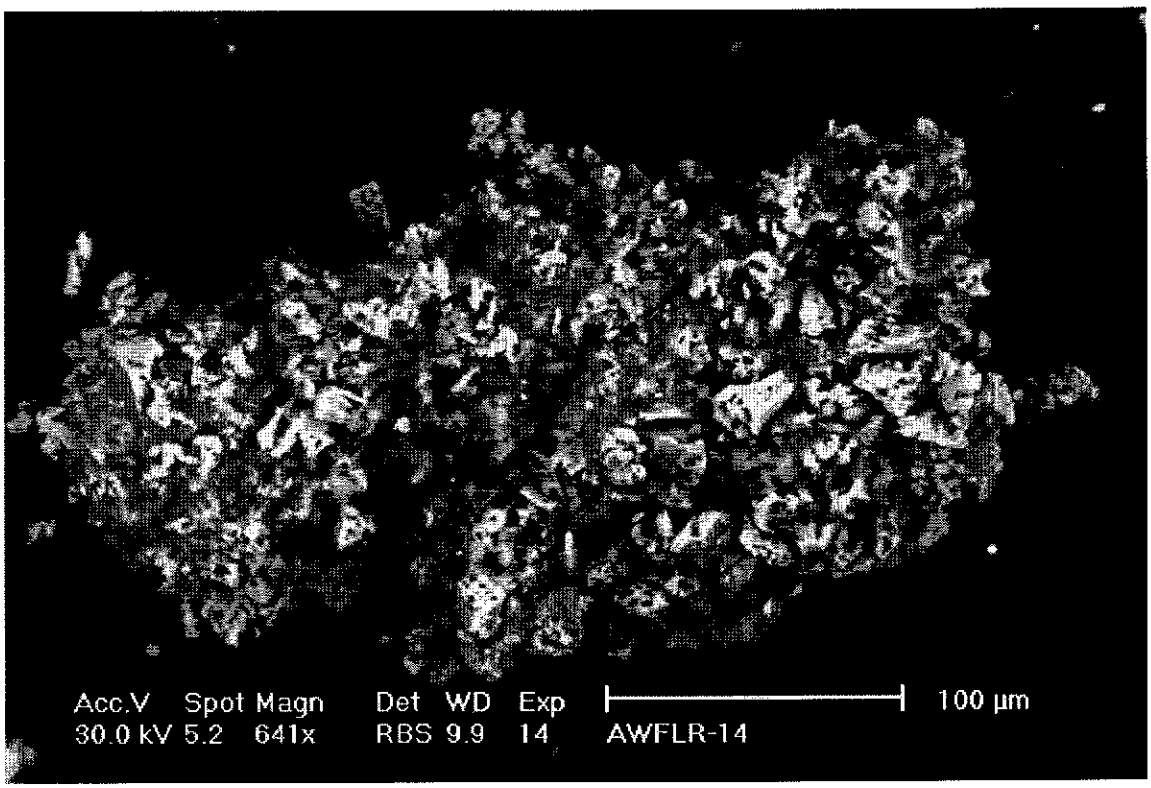

Figure 8.9 Close-up view of an agglomerate of Elura zinc concentrate and elemental sulfur. A magnified view of the outlined agglomerate in Figure 8.8. The leach conditions are given in Figure 8.7.

8.4 LEACHING ELURA CONCENTRATE AT HIGH PULP DENSITIES IN H_2SO_4 / SO_2

Leaches, using high pulp densities (160 – 220 g L^{-1}), were conducted at 100, 150 and 180°C and in all cases poor zinc extractions were obtained. At 100°C, 5% zinc was extracted and at 150°C and 180°C approximately 10% zinc was extracted. In the 100°C leach, Elura concentrate was slurried with water and heated to 100°C. At this point, the zinc extraction was 7.3%, indicating that in the concentrate some of the ZnS had been oxidised to $ZnSO_4$. After addition of sulfuric acid the zinc extraction decreased slightly to 3.8% (Figure 8.10). The reduction in % zinc extraction was most probably due to precipitation of ZnS by reaction between Zn^{2+} and H_2S generated via the acidic dissolution of pyrite, FeS_2, which is also present in Elura concentrate. The presence of H_2S(aq) was indicated by the detection of H_2S (g) in the headspace after the addition of sulfuric acid. SO_2 was then added and, although it removed H_2S from the system, it had negligible effect on the % Zn extraction which only increased slightly to 4.7%. In a comparable leach using synthetic ZnS instead of zinc concentrate, the % Zn extraction increased from 4% to 63% (Figure 7.21).

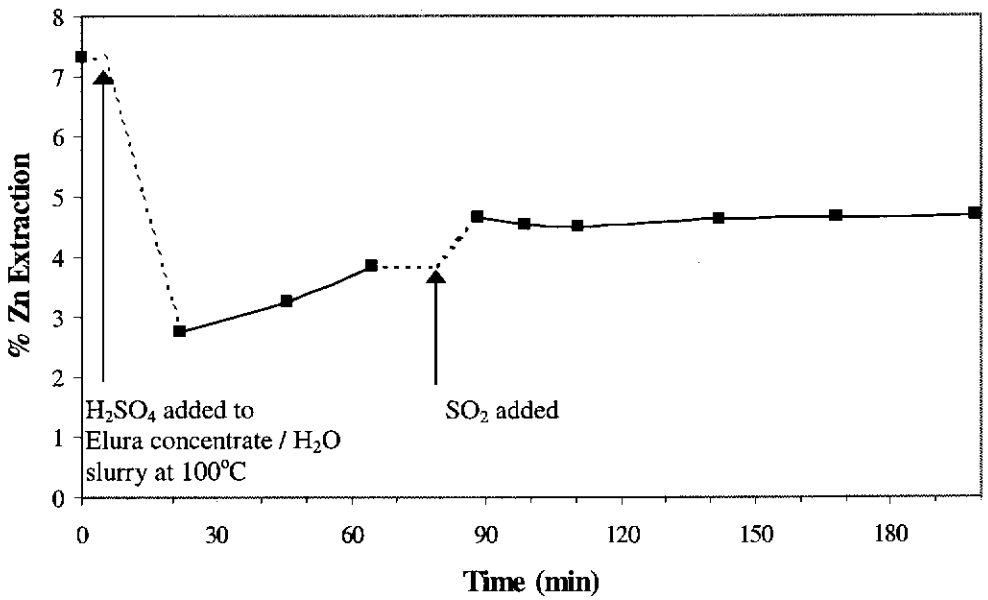

Figure 8.10 Leach of Elura concentrate (Elura Bulk #2) in H_2SO_4 / SO_2 at 100°C.
Conditions: Pulp density = 160 g L^{-1}, $[H_2SO_4]$ = 1.8 mol L^{-1}, n(SO_2)added = 1.7 moles, $[SO_2(aq)]_{calc}$ = 1.2 mol L^{-1}

The inability of H_2SO_4 / SO_2 solutions to successfully leach zinc from Elura zinc concentrate may, again, be due to the formation of sulfane monosulfonates which, being "H_2S – like", inhibit dissolution of ZnS.

Inhibition was not due to a build-up of H_2S. In the 100°C leach, 6.5 and 24 minutes after the addition of SO_2(g), the headspace gas was tested for H_2S and in each case the lead acetate test for H_2S was negative. Elemental sulfur could not have occluded the mineral as it was only present in trace amounts. In addition, the residues contained none of the agglomerates that are typically observed when molten sulfur is present.

It was considered possible that an insoluble solid may have precipitated onto the mineral surface, however Raman spectroscopy did not reveal any unusual features, the spectra of the 150°C and 180°C leach residues being similar to that of the unleached mineral (Figure 8.11).

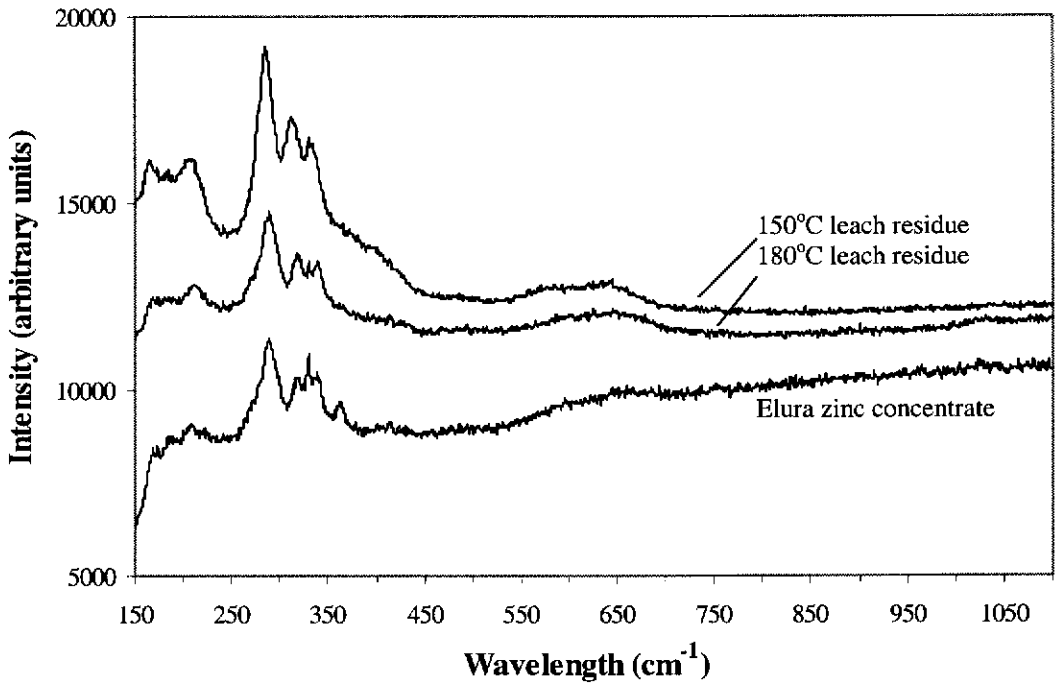

Figure 8.11 Raman spectra of Elura concentrate (Elura Bulk #1) and residues from leaches in H_2SO_4 / SO_2 at 150°C and 180°C.
Conditions: At 150°C, pulp density = 221 g L^{-1}, [H_2SO_4] = 1.8 mol L^{-1}, n(SO_2)added = 1.8 moles, [$SO_2(aq)]_{calc}$ = 1.3 mol L^{-1}, [Quebracho] = 0.2 g L^{-1}, [Sodium ligninsulfonate] = 0.1 g L^{-1}.
At 180°C, pulp density = 205 g L^{-1}, [H_2SO_4] = 1.7 mol L^{-1}, n(SO_2)added = 1.6 moles, [$SO_2(aq)]_{calc}$ = 1.1 mol L^{-1}, [Quebracho] = 0.2 g L^{-1}, [Sodium ligninsulfonate] = 0.1 g L^{-1}.

It is unlikely that the surfactants used in these leaches, quebracho (0.2 g L^{-1}) and sodium ligninsulfonate (0.2 g L^{-1}), or their decomposition products would have inhibited the leach by occluding the mineral surface since they were present in minor quantities; the amount of zinc concentrate in each leach being 221 g L^{-1} and 205 g L^{-1} at 150 and 180°C, respectively.

8.5 SUMMARY

At low pulp densities (~2 g L^{-1}) the dissolution of Elura zinc concentrate in SO_2 / H_2SO_4 solutions at 130°C experienced strong inhibition due to occlusion of the unreacted mineral by molten elemental sulfur, which is a product of the reaction. Mineral particles clustered around sulfur globules forming agglomerates which increased in size as the reaction progressed. This was in contrast to similar leaches using synthetic zinc sulfide, where neither occlusion nor agglomeration were observed and it appears that Elura zinc concentrate is more readily wet by molten elemental sulfur than is synthetic zinc sulfide.

Occlusion by molten sulfur was minimised by using the surfactants, quebracho, sodium ligninsulfonate and orthophenylenediammine, which all acted to increase the extent of zinc extraction, however some inhibition still remained. Quebracho was found to be the most effective of the surfactants tested.

Surprisingly, at high pulp densities (~200 g L^{-1}), the presence of SO_2 in a sulfuric acid leach solution had no effect on the zinc extraction. This particular resistance of Elura zinc concentrate at high pulp densities to leaching by SO_2 / H_2SO_4 solutions compared to synthetic zinc sulfide pulps at corresponding pulp densities, was not attributable to the formation of a reaction inhibiting surface layer or to the presence of $H_2S(aq)$, and seems to suggest that the dissolution of ZnS in zinc concentrates is inhibited by the reverse reaction between Zn^{2+} and aqueous "H_2S-like" species, namely the sulfane monosulfonates.

9 CONCLUSIONS

The feasibility of using aqueous solutions of sulfur dioxide to leach zinc concentrates was investigated in four stages.

Firstly, studies of the dissolution of synthetic ZnS in aqueous solutions of SO_2 were undertaken at ambient temperature to elucidate the role of SO_2 in the dissolution of ZnS. These established that SO_2 does not directly attack the sulfide, but that the active leaching agent is the hydrogen ion generated by the dissolution of SO_2 into water forming sulfurous acid. The dissolution is first order with respect to the concentration of hydrogen ions. The observed half order dependence of the rate on $[SO_2(aq)]$ also supports this position, since in sulfurous acid the concentration of H^+ due to the hydrolysis of $SO_2(aq)$

$$SO_2(aq) + H_2O \leftrightarrow H^+(aq) + HSO_3^-(aq)$$

$$K_{a1}^{25^\circ C} = 0.0139 \text{ mol } L^{-1} \text{ (Huss and Eckert 1977)}$$

has a half order dependence on $[SO_2(aq)]$.

$$[H^+(aq)] = 0.1179[SO_2(aq)]^{0.5}$$

The view that ZnS dissolves oxidatively via reaction with aqueous SO_2 is thus untenable and it is apparent that non-oxidative dissolution takes place via hydrogen ions.

$$ZnS + H^+ \rightarrow Zn^{2+} + HS^-$$

Tetrathionate, observed in solution, is thus not an initial product of the dissolution reaction, as considered by Larsen (1984), but results from the reaction of $H_2S(aq)$ or $HS^-(aq)$ with the sulfurous acid species, $SO_2(aq)$ and $HSO_3^-(aq)$. Elemental sulfur is also a product of this reaction.

Additionally, it appears that prior to the formation of these stable sulfur containing products (tetrathionate and elemental sulfur) that sulfane monosulfonates ($^-SS_nSO_3^{2-}$, n = 1 - 5) are formed. These are postulated on the basis that the dissolution of ZnS is inhibited by either increasing the pulp density of ZnS or by the addition of zinc ions. This inhibition was not attributable to either $H_2S(aq)$ or occlusion by elemental sulfur, and is thus considered to be due to an aqueous species that is "H_2S-like", in that it reacts with zinc ions to reprecipitate ZnS. The sulfane monosulfonates are postulated since these have a negatively charged sulfur atom at the sulfane end of the sulfur chain and may thus behave like H_2S toward zinc ions (Meyer, Peter and Spitzer 1977). These are thought to be produced as one of the initial products of the reaction of $SO_2(aq)$ with $H_2S(aq)$ or $HS^-(aq)$. This reaction is thought to occur at the ZnS / solution interface since gaseous H_2S was not detected, implying the absence of significant concentrations of $H_2S(aq)$ or $HS^-(aq)$ in the bulk solution. If these species were present , then at the pHs under which these experiments were conducted (pH < 2) $H_2S(g)$ would have been expected to have been observed.

The rate of ZnS dissolution in aqueous solutions of SO_2 was found to be rather slow at ambient temperature. Increasing the temperature increased the dissolution rate, but at temperatures of 150°C and above (to 200°C), the dissolution rate was also accelerated by the *insitu* generation of hydrogen ions from the thermal decomposition of $SO_2(aq)$.

$$3SO_2(aq) + 2H_2O \rightarrow S^o + 2H_2SO_4$$

In the second part of the work, the kinetics and equilibria of dissolution of ZnS in H_2SO_4

$$ZnS + 2H^+ \leftrightarrow Zn^{2+} + H_2S$$

were investigated at elevated temperatures, since it had been demonstrated that the active leaching agent is the hydrogen ion.

The rate equation for the dissolution of ZnS in H_2SO_4 which has been determined at ambient temperatures (Crundwell and Verbaan 1987; Romankiw and de Bruyn 1965) to be

$$d[Zn^{2+}]/dt = k_f A_s [H^+] - k_r A_s [H_2S(aq)]^{1/2} [Zn^{2+}]^{1/2}$$

was found to be applicable at elevated temperatures (100 – 150°C). Rate constants for the forward and reverse reactions, together with activation energies and equilibrium constants are as follows.

Temp (°C)	K_c	k_f	k_r	$E_{a,\,fwd}$ (kJ mol^{-1})	$E_{a,\,rev}$ (kJ mol^{-1})
100	4.99×10^{-4}	2.50×10^{-3}	1.10×10^{-1}	56 ± 11	45 ± 15
150	1.26×10^{-3}	2.83×10^{-2}	9.05×10^{-1}		
200	2.83×10^{-3}	–	–		

The dissolution of ZnS in H_2SO_4

$$ZnS(s) + 2H^+(aq) \leftrightarrow Zn^{2+}(aq) + H_2S(aq)$$

is limited as the equilibrium favours the reactants even at 200°C.

In the third part of the work, the combination of H_2SO_4 and SO_2 as a lixiviant for ZnS was examined with the expectation that SO_2 would remove H_2S and thus enhance leaching.

The addition of SO_2 to the ZnS / H_2SO_4 system did remove $H_2S(aq)$, allowing increased zinc extraction, but the effect was much less than expected and differed depending on the pulp density.

At low pulp density (0.5 g L^{-1}) the rate of synthetic ZnS dissolution in a H_2SO_4 / SO_2 solution is the same as that in a H_2SO_4 solution in the initial stages, but eventually exceeds it. The dissolution rate is slower than that expected if H_2S(aq) were being removed from the system, and this, together with the absence of other possible inhibiting factors, *viz.* the presence of H_2S(aq) and occlusion by molten elemental sulfur, suggests that "H_2S – like" aqueous species that are able to react with Zn^{2+} ions to reprecipitate ZnS are present. The sulfane monosulfonates are again postulated as possible species.

At high pulp densities (200 g L^{-1}), similar to those expected in an industrial situation, the addition of sulfur dioxide to a slurry of the powder in sulfuric acid at equilibrium, rapidly increases the dissolution of ZnS. However, after the initial rapid dissolution (7% to 54% Zn extraction), which generates elemental sulfur and polythionates, the reaction is inhibited by elemental sulfur, which forms agglomerates with unreacted ZnS, even at temperatures below sulfur's melting point, and the rate slows considerably. At high pulp densities elemental sulfur affects the dissolution kinetics whereas it has no effect at the lower pulp densities. This is possibly due to the large amounts of elemental sulfur produced in the high pulp density leaches. The use of a suitable surfactant would probably enable the dissolution to proceed to completion.

Finally, to examine the possibility of using sulfur dioxide leaching in an industrial situation, leaches were also performed using a zinc concentrate. At low pulp densities (2 g L^{-1}) and in H_2SO_4 / SO_2 leach solutions at 130°C, the dissolution is impeded by molten sulfur, which causes the mineral particles to agglomerate as they adhere to the globules of sulfur. However, this was overcome to some extent by the addition of surfactants, which prevented molten sulfur from occluding the mineral surface. Of the surfactants tested, orthophenylenediamine, quebracho and sodium ligninsulfonate, the most effective was quebracho, even though it showed signs of decomposition in H_2SO_4 and H_2SO_4 / SO_2 at 130°C. Alternative, more stable surfactants are required for possible commercialisation of the process.

The relatively promising extractions obtained at low pulp densities were not achievable at high pulp densities (160-200 g L^{-1}), with the zinc extraction being only approximately 10%. This observation is similar to that previously observed by Sobol

and Frash (1974) who reported a zinc extraction of only 0.5%. No causes for the observed inhibition were found, but it may be that inhibition is due to aqueous species, as yet unobserved, such as the sulfane monosulfonates.

The identification of the aqueous species present in solution is worthy of future research in order to ascertain the cause of inhibition. Once identified, it may be possible to develop strategies to prevent them forming, or for their further reaction, and consequently the use of H_2SO_4 / SO_2 leach solutions may still yet prove to be viable to be included as part of the zinc roast - leach - electrowin process.

In the event that direct SO_2 addition to a H_2SO_4 leach is not feasible, the side stream reaction of SO_2 gas with H_2S from a zinc concentrate acid leach may be achievable. A simplified schematic diagram of a possible process is given below, showing the sulfur producing route (in dashed boxes) alongside the existing RLE route (Figure 9.1).

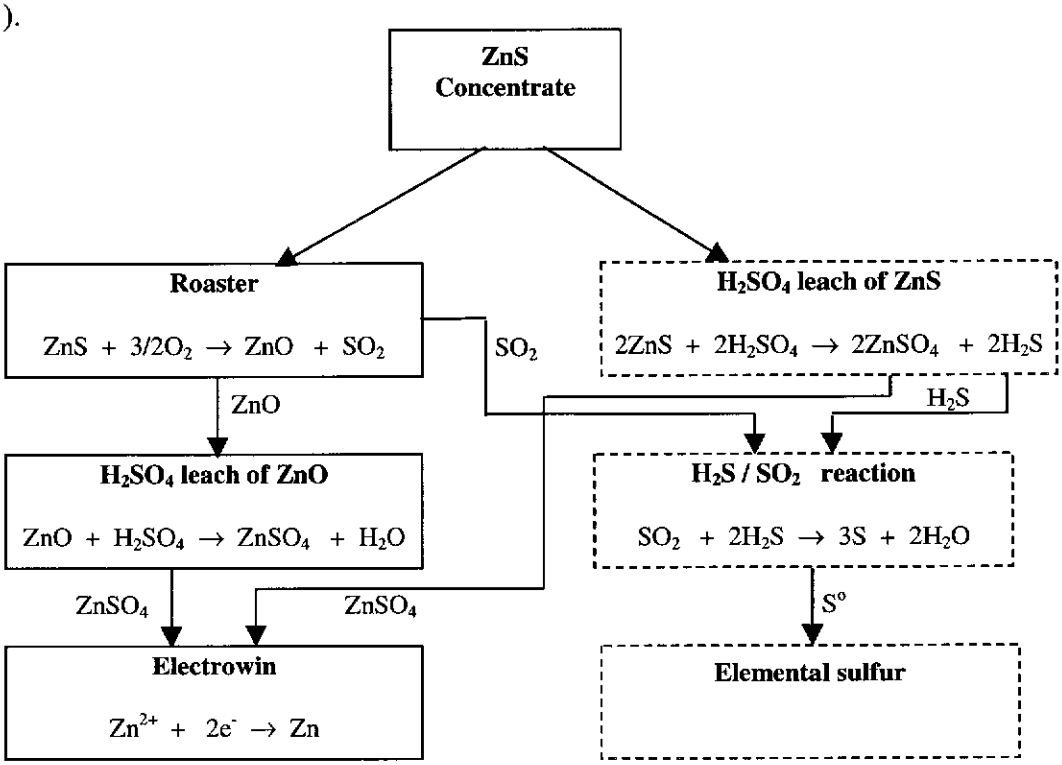

Figure 9.1 Possible leaching process incorporating an elemental sulfur producing route alongside existing RLE route.

An advantage of such a process is that elemental sulfur is a more saleable product than sulfuric acid. Also, the roasting costs would be reduced as only one third of the ore would require roasting, in order to achieve the required SO_2 : H_2S ratio.

REFERENCES

Adams, R. W. and Matthew, I. G. 1981, 'Leaching of metal sulphide concentrates at atmospheric pressure using SO_2/O_2 mixtures', *Proceedings of the Australasian Institute of Mining and Metallurgy,* vol. 280, pp. 41-53.

Archer, D. G. and Wang, P. 1990, 'The dielectric constant of water and Debye-Huckel limiting law slopes', *Journal of Physical and Chemical Reference Data,* vol. 19, no. 2, p. 371.

Atkins, P. W. 1982, *Physical Chemistry,* 2nd edn, Oxford University Press, Oxford, p. 931.

Balaz, P. and Ebert, I. 1991, 'Oxidative leaching of mechanically activated sphalerite', *Hydrometallurgy,* vol. 27, pp. 141-150.

Barbieri, R. and Sosi, S. 1961, 'The reaction between H_2S and SO_2. Studies with ^{35}S on the polythionates and thiosulphate.', *La Ricerca Scientifica,* vol. 1, no. 1, pp. 5-11.

Berezowsky, R. M. G. S., Collins, M. J., Kerfoot, D. G. E. and Torres, N. 1991, 'The commercial status of pressure leaching', *Journal of Metals,* vol. 43, no. 2, pp. 9-15.

Bichowsky, F. R. 1921, 'Equilibrium in the reaction between sulfur dioxide and water', *Journal of the American Chemical Society,* vol. 44, pp. 116-132.

Billo, E. J. 1997, *Excel for Chemists,* Wiley-VCH, Inc., New York, .

Bjorling, G. 1954, 'Uber die laugung von sulfidmineralien unter sauerstoffdruck (Leaching of sulfide minerals under pressure)', *Metallwissenschaft und Technik,* vol. 8, pp. 781-784.

Bobeck, G. E. and Su, H. 1985, 'The Kinetics of Dissolution of Sphalerite in Ferric Chloride Solution', *Metallurgical Transitions B,* vol. 16B, pp. 413-423.

Brierley, J. A. and Brierley, C. L. 2001, 'Present and future commercial applications of biohydrometallurgy', *Hydrometallurgy,* vol. 59, pp. 233-239.

Brual, G. B., Byerley, J. J. and Rempel, G. L. 1983, 'Kinetic and mechanistic study of FeS dissolution in aqueous sulfur dioxide solution', *Hydrometallurgy,* vol. 9, pp. 307-331.

Buban, K. R., Collins, M. J., Masters, I. M. and Trytten, L. C. 2000, 'Comparison of direct pressure leaching with atmospheric leaching of zinc concentrates', in *Lead-Zinc 2000,* eds. J. E. Dutrizac, J. A. Gonzalez, D. M. Henke, S. E. James and A. H.-J. Siegmund, The Minerals, Metals and Materials Society, Pittsburgh, PA, USA, pp. 727-738.

Castellan, G. W. 1983, *Physical Chemistry,* 3rd edn, Addison-Wesley Publishing Company, Reading, .

Chalkley, M. E., Collins, M. J. and Ozberk, E. 1993, 'The behaviour of sulphur in the Sherritt zinc pressure leach process', in *World Zinc '93,* ed. I. G. Matthew, The Australian Institute of Mining and Metallurgy, Hobart, Tasmania, pp. 325-331.

Collins, M. J., McConaghy, E. J., Stauffer, R. F., Desroaches, G. J. and Krysa, B. D. 1994, 'Starting up the Sherrit Zinc Pressure Leach Process at Hudson Bay', *Journal of Metals,* no. April, pp. 51-58.

Connick, R. E., Tam, T. M. and von Deuster, E. 1982, 'Equilibrium constant for the dimerization of bisulfite ion to form $S_2O_5^{2-}$', *Inorganic Chemistry,* vol. 21, p. 103.

Corriou, J.-P., Gely, R. and Viers, P. 1988, 'Thermodynamic and kinetic study of the pressure leaching of zinc sulfide in aqueous sulfuric acid', *Hydrometallurgy,* vol. 21, pp. 85-102.

Crundwell, F. K. 1987, 'Kinetics and mechanism of the oxidative dissolution of a zinc sulphide concentrate in ferric sulphate solutions', *Hydrometallurgy,* vol. 19, pp. 227-242.

Crundwell, F. K. 1988, 'The influence of the electronic structure of solids on the anodic dissolution and leaching of semiconducting sulphide minerals', *Hydrometallurgy,* vol. 21, pp. 155-190.

Crundwell, F. K. and Verbaan, B. 1987, 'Kinetics and mechanisms of the non-oxidative dissolution of sphalerite (zinc sulphide)', *Hydrometallurgy,* vol. 17, pp. 369-384.

Davis, R. E. 1958, 'Displacement reactions at the sulfur atom. I. An interpretation of the decomposition of acidified thiosulfate', *Journal of the American Chemical Society,* vol. 80, pp. 3565-3569.

De Maeyer, L. and Kustin, K. 1963, 'Fast reactions in solution', *Annual Review of Physical Chemistry,* vol. 14, pp. 5-34.

Driessens, Y. P. M., Fowler, T. A. and Crundwell, F. K. 1999, 'A comparison of the bacterial and chemical leaching of sphalerite at the same solution conditions', in *International Biohydrometallurgy Symposium '99*, Spain, pp. 201-208.

Dutrizac, J. E. 1992, 'The leaching of sulphide minerals in chloride media', *Hydrometallurgy,* vol. 29, pp. 1-45.

Dutrizac, J. E. and MacDonald, R. J. C. 1974, 'Ferric ion as a leaching medium', *Minerals Science and Engineering,* vol. 6, no. 2, pp. 59-100.

Dutrizac, J. E. and MacDonald, R. J. C. 1978, 'The dissolution of sphalerite in ferric chloride solutions', *Metallurgical Transactions B,* vol. 9B, pp. 543-551.

Foerster, F. and Janitzki, J. 1931, 'Beiträge zur kenntnis der schwefligen säure und ihrer salze IX. Über die einwirkung von schwefliger säure auf die sulfide von eisen, zink und mangan', *Zeitschrift fur anorganische und allgemeine chemie,* vol. 200, pp. 23-45.

Foerster, F., Lange, F., Drossbach, O. and Seidel, W. 1923, 'Beiträge zur Kenntnis der schwefligen Säure und ihrer Salze. 1. Über die Zersetzung der schwefligen Säure und ihrer Salze in wäßriger Lösung.', *Zeitschrift fur anorganische und allgemeine chemie,* vol. 128, p. 245.

Forward, F. A. and Veltman, H. 1959, 'Direct leaching zinc-sulfide concentrates by Sherritt Gordon', *Journal of Metals,* vol. 11, no. December, pp. 836-840.

Foss, O. 1961, 'Thiosulphate catalysis on rearrangements of higher polythionates', *Acta Chemica Scandinavica,* vol. 15, no. 7, p. 1610.

Foss, O. and Kringlebotn, I. 1961, 'Displacement of sulphite groups of polythionates by thiosulphate', *Acta Chemica Scandinavica,* vol. 15, no. 7, pp. 1608-1609.

Fugleberg, S. and Järvinen, A. 1998, *Method for leaching zinc concentrate in atmospheric conditions,* WO 98/06879, Outokumpu Base Metals Oy, (patent).

Ghiorso, M. S. and Sack, R. O. 1995, 'Chemical Mass Transfer in Magmatic Processes IV. A Revised and Internally Consistent Thermodynamic Model for the Interpolation and Extrapolation of Liquid-Solid Equilibria in Magmatic Systems at Elevated Temperatures and Pressures', *Contributions to Mineralogy and Petrology,* vol. 119, pp. 197-212.

Habashi, F. (ed.) 1997, *Handbook of Extractive Metallurgy,* Wiley-VCH, Weinheim; Chichester, (a) p. 645, (b) p. 652, (c) p. 653, (d) p. 1100.

Han, M. K. 1985, *Kinetics of Dissolution of Lead-Sulfide in Hydrochloric Acid Solutions Saturated with Sulfur Dioxide (Electrochemical, Reaction Mechanism, Selective Leaching)*, Doctor of Philosophy in Metallurgy, University of Utah.

Hansford, G. S. and Vargas, T. 1999, 'Chemical and electrochemical basis of bioleaching processes', in *International Biohydrometallurgy Symposium '99*, Spain, pp. 13-25.

Henderson, W. E. and Weiser, H. B. 1913, 'The action of sulfurous acid upon the sulfides of iron, zinc and manganese', *Journal of the American Chemical Society,* vol. 35, pp. 239-244.

Heunisch, G. W. 1977, , *Inorganic Chemistry,* vol. 16, no. 6, p. 1411.

Horner, D. A. and Connick, R. E. 1986, 'Equilibrium quotient for the isomerization of bisulfite ion from HSO_3^- to SO_3H^-', *Inorganic Chemistry,* vol. 25, pp. 2414-2417.

Huss, A., Jr. and Eckert, C. A. 1977, 'Equilibria and ion activities in aqueous sulfur dioxide solutions', *The Journal of Physical Chemistry,* vol. 81, no. 24, pp. 2268-2270.

Jin, Z. M., Warren, G. W. and Henein, H. 1993, 'An investigation of the electrochemical nature of the ferric chloride leaching of sphalerite', *International Journal of Mineral Processing,* vol. 37, pp. 223-238.

Jin, Z.-M., Warren, G. W. and Henein, H. 1984, 'Reaction kinetics of the ferric chloride leaching of sphalerite - an experimental study', *Metallurgical Transactions B,* vol. 15B, pp. 5-12.

Kask, T. and Teder, A. 1998, 'Elimination of methyl mercaptan from the kraft pulping process with polythionate and polysulphide solutions', *Paper and Timber,* vol. 80, no. 1, pp. 49-58.

Kawulka, P., Haffenden, W. J. and Mackiw, V. N. 1975, *Recovery of zinc from zinc sulphides by direct pressure leaching,* US Patent No. 3,867,268, Sherritt Gordon Mines Limited, Toronto, Ontario, Canada, (patent).

Keller, J. L. 1956, *Removal of sulfur dioxide from gases containing the same,* US Patent No. 2,729,543, (patent).

Kozak, Z. 1987, 'Hydrogen sulfide oxidation by sulfur dioxide in solutions', *Wiadomosci Chemiczne,* vol. 41, pp. 99-120.

Kunda, W. and Rudyk, B. 1970, 'Aqueous reduction of sulphur dioxide by pyrrhotite to elemental sulphur', *Canadian Metallurgical Quarterly,* vol. 9, no. 4, pp. 551-561.

Kuz'min, L. L. and Postnikov, V. F. 1935, 'The reaction of sulfur dioxide with water under pressure', *Journal of Chemical Industry (Moscow),* vol. 12, pp. 571-580.

Kwong, V. and Meissner, R. E. 1995, 'Rounding up sulfur', *Chemical Engineering,* vol. 102, no. 2, p. 74.

Larsen, D. M. 1984, *Hydrometallurgy of metal sulphites: A study of leaching and recovery in the zinc sulphide-sulphur dioxide system*, Ph.D. Thesis, University of Sydney.

Larsen, D. M. and Linkson, P. B. 1993, 'Thermodynamics of the zinc-sulfur dioxide - water system', *Metallurgical Transactions B,* vol. 23B, pp. 409-417.

Linkson, P. B. 1985, 'Sulfite hydrometallurgy - innovative technology?', in *Chemeca 85*, pp. 157-161.

Linkson, P. B. and Larsen, D. M. 1984, 'Hydrometallurgical extraction of zinc using sulphur dioxide', in *Institute of Chemical Engineering Symposium Series No. 87 (Chemical Reaction Engineering)*, pp. 627-634.

Littlejohn, D., Walton, S. A. and Chang, S. 1992, 'A Raman study of the isomers and dimer of hydrogen sulfite ion', *Applied Spectroscopy,* vol. 46, no. 5, pp. 848-851.

Lochmann, J. and Pedlik, M. 1995, 'Kinetic anomalies of dissolution of sphalerite in ferric sulfate solution', *Hydrometallurgy,* vol. 37, pp. 89-96.

Locker, L. D. and deBruyn, P. L. 1969, 'The kinetics of dissolution of II-IV semiconductor compounds in nonoxidising acids', *Journal of the Electrochemical Society,* vol. 116, no. 12, pp. 1659-1664.

Lotens, J. P. and Wesker, E. 1987, 'The behaviour of sulphur in the oxidative leaching of sulphidic minerals', *Hydrometallurgy,* vol. 18, pp. 39-54.

Magers, W. W. 1940, *"Diss. Halle Ads" cited in* Kask, T. and Teder, A. 1998, 'Elimination of methyl mercaptan from the kraft pulping process with polythionate and polysulphide solutions', *Paper and Timber,* vol. 80, no. 1, pp. 49-58.

Majima, H. and Awakura, Y. 1985, 'Leaching of oxides and sulphides in acidic chloride media', in *Extraction Metallurgy '85*, pp. 607-627.

Majima, H., Awakura, Y. and Misaki, N. 1981, 'A kinetic study on nonoxidative dissolution of sphalerite in aqueous hydrochloric acid solutions', *Metallurgical Transactions B,* vol. 12B, pp. 645-649.

Makovetskii, A. E. 1934, , USSR Patent No. 37699, (patent).

Masters, M., Doyle, B. N. and Weir, D. R. 1989, 'Direct pressure leaching of Australian zinc concentrates', in *Non-ferrous Smelting Symposium*, Port Pirie, South Australia, pp. 99-110.

Meyer, B. and Ospina, M. 1982, 'Raman spectrometric study of the thermal decomposition of aqueous tri- and tetrathionate', *Phosphorous and sulfur,* vol. 14, pp. 23-36.

Meyer, B., Peter, L. and Spitzer, K. 1977, 'Trends in the charge distribution in sulfanes, sulfanesulfonic acids, sulfanedisulfonic acids, and sulfurous acid', *Inorganic Chemistry,* vol. 16, no. 1, pp. 27-33.

Meyers, R. A., Hamersma, J. W. and Kraft, M. L. 1975, 'Sulfur dioxide pressure leaching. New pollution-free method to process copper ore.', *Environmental Science and Technology,* vol. 9, no. 1, pp. 70-71.

Miaskiewicz, K. and Steudel, R. 1994, 'Structures, Energies and Vibrational spectra of four isomers of hydrogendioxothiosulfate(IV) anion ($H_2S_2O_2^-$) and of the related anion $ClSO_2^-$: an *ab-initio* molecular-orbital study', *Journal of the Chemical Society, Dalton Transactions,* pp. 2919-2923.

Micromeritics 1991, *SediGraph 5100 Particle Size Analysis System Operator's Manual*, Report V3.00.

Nicol, M. J. 1983, 'The non-oxidative leaching of oxides and sulphides: An electrochemical approach', in *3rd International Symposium on Hydrometallurgy*, eds. K. Osseo-Asare and J. D. Miller, AIME, Warrendale, PA, pp. 177-195.

Nikolaev, N. S., Ivanov, N. A. and Akulova, K. S. 1939, 'The reaction of hydrogen sulfide with sulfur dioxide in aqueous solution', *Journal of Applied Chemistry (USSR),* vol. 12, p. 1013.

Ospina, M. 1982, *Formation and decomposition of sulfur oxyacids*, PhD Thesis, University of Washington.

Owusu, G. and Dreisinger, D. B. 1996, 'Interfacial properties determinations in liquid sulfur, aqueous zinc sulfate and zinc sulfide systyems', *Hydrometallurgy,* vol. 43, pp. 207-218.

Owusu, G., Dreisinger, D. B. and Peters, E. 1995a, 'Effect of surfactants on zinc and iron dissolution rates during oxidative leaching of sphalerite', *Hydrometallurgy,* vol. 38, pp. 315-324.

Owusu, G., Dreisinger, D. B. and Peters, E. 1995b, 'Interfacial effects of surface-active agents under zinc pressure leach conditions', *Metallurgical and Materials Transactions B,* vol. 26B, pp. 5-12.

Palencia Perez, I. and Dutrizac, J. E. 1991, 'The effect of the iron content of sphalerite on its rate of dissolution in ferric sulphate and ferric chloride media', *Hydrometallurgy,* vol. 26, pp. 211-232.

Pay, Z. P., Yermakova, A., Kundo, N. N. and Kirillov, V. A. 1994, 'Sulphur production in the processes of purification and conversion of hydrocarbon raw materials', *Chemistry for Sustainable Development,* vol. 2, pp. 423-425.

Perrin, D. D. 1982, *Ionisation Constants of Inorganic Acids and Bases in Aqueous Solution,* 2nd edn, Pergamon Press .

Perry, R. H. and Green, D. W. (eds.) 1997, *Perry's Chemical Engineers' Handbook, 7th Edn,* New York, McGraw-Hill, .

Peters, E. 1993, "Macro-model for zinc pressure leach' in Hydrometallurgy. Fundamentals, Technology and Innovations', in *Milton E. Wadsworth (IV) International Symposium on Hydrometallurgy*, eds. J. B. Hiskey and G. W. Warren, Society for Mining, Metallurgy and Exploration, Inc., Salt Lake City, Utah, pp. 3-20.

Roche, E. G. 1993, *Confidential Internal Pasminco Research Centre Report H336A*, Pasminco Research Centre, Report H336A.

Romankiw, L. T. and de Bruyn, P. L. 1965, 'Kinetics of dissolution of zinc sulfide in aqueous sulfuric acid', in *Unit Processes in Hydrometallurgy*, eds. M. E. Wadsworth and F. T. Davis, Gordon and Breach, London, pp. 45-66.

Rumpf, B. and Maurer, G. 1992, 'Solubilities of hydrogen cyanide and sulfur dioxide in water at temperatures from 293.15 to 413.15 K and pressures up to 2.5 MPa', *Fluid Phase Equilibria,* vol. 81, pp. 241-260.

Ryabinina, A. F. and Oshman, V. A. 1972, 'Thermal decomposition of aqueous sulfur dioxide solutions', *Transactions of Ural Institute of Forestry and Forest Industries,* vol. 28, pp. 182-189.

Sand, W., Gehrke, T., Jozsa, P.-G. and Schippers, A. 1999, 'Direct versus indirect bioleaching', in *International Biohydrometallurgy Symposium '99*, Spain, pp. 27-49.

Schenk, P. W. and Steudel, R. 1965, , *Angewandte Chemie, International Edition English,* vol. 4, p. 402.

Schmidt, H., Steudel, R., Sülzle, D. and Schwarz, H. 1992, 'Generation and Characterization of Dihydroxy Disulfide, HOSSOH: The Chainlike Isomer of Thiosulfurous Acid', *Inorganic Chemistry,* vol. 31, no. 6, pp. 941-944.

Schmidt, M. 1965a, 'Preparation of unusual sulfur rings', in *Elemental Sulfur*, ed. B. Meyer, Interscience, New York, NY, pp. 327-335.

Schmidt, M. 1965b, 'Reactions of the sulfur-sulfur bond, p.308-314', in *Elemental Sulfur*, ed. B. Meyer, Interscience, New York, NY, pp. 301-326.

Schmidt, M. and Heinrich, H. 1958, 'Reaktion von schwefliger Säure mit elementarem Schwefel', *Angewandte Chemie,* vol. 70, p. 572.

Schmidt, M. and Siebert, W. 1973, 'Chapter 23. Sulphur', in *Comprehensive Inorganic Chemistry*, eds. J. C. Bailar, Jr., H. J. Emeréus, S. R. Nyholm and A. F. Trotman-Dickenson, Pergamon Press, New York, pp. 886-887.

Schroeter, L. C. 1966, *Sulphur Dioxide,* Pergamon Press Inc. (a) p. 13, (b) p. 17, (c) pp. 93-94, (d) pp. 91-92, (e) p. 89, (f) p. 90.

Scott, P. D. and Nicol, M. H. 1977, 'The kinetics and mechanisms of the non-oxidative dissolution of metal sulphides.', in *Trends in Electrochemistry*, eds. J. O. M. Bockris, D. A. J. Rand and B. J. Welch, Plenum Press, New York, pp. 303-316.

Scott, P. D. and Nicol, M. J. 1978, *The kinetics of the leaching of zinc sulphide concentrates in acidic solutions containing ferric sulphate*, National Institute for Metallurgy, Randburg, Report 1949.

Silberman, Y. I. and Fridman, V. M. 1946, 'On the reaction between hydrogen sulphide and sulphites. On the mechanism of the reactions taking place in the preparation of sodium thiosulphate.', *Zhurnal obshschei khimii,* vol. 16, pp. 309-324.

Siu, T. and Jia, C. Q. 1999, 'Kinetic and mechanistic study of reaction between sulfide and sulfite in aqueous solution', *Industrial and Engineering Chemistry Research,* vol. 38, no. 10, pp. 3812-3816.

Slavik, I. 1961, 'Über die Zersetzung des Schwefeldioxyds unter Bedingungen der Sulfitkochung', *Svensk Papperstidning,* vol. 64, no. 11, p. 427.

Sobol, S. I. and Frash, T. M. 1974, 'Sulfur dioxide in the autoclave technology of processing sulfide raw material.', *Tsvetnye Metally,* vol. 2, pp. 14-21.

Sobol, S. I. and Timoshenko, E. M. 1992, 'Pyrrhotite leaching by sulfur dioxide to solve the Norilsk Complex problems.', *Tsvetnye Metally,* vol. 5, pp. 8-10.

Sohn, H. Y. and Wadsworth, M. E. (eds.) 1979, *Rate Processes of Extractive Metallurgy,* Plenum Press, New York, (a) p. 135, (b) pp. 141-143, (c) pp. 146-148

Stanczyk, M. H. and Rampacek, C. 1960, *Dissolution of zinc from sphalerite at elevated temperatures and pressures*, U.S. Department of the Interior
Bureau of Mines, Tuscaloosa, Report 5848.

Staples, B. R., Holcomb, G. R. and Cramer, S. D. 1992, 'Calculation of pH for high - temperature sulfate solutions at high ionic strengths', *Corrosion,* vol. 48, no. 1, pp. 35-41.

Steudel, R., Gobel, T. and Holdt, G. 1988, 'The molecular composition of hydrophilic sulfur sols prepared by acid decomposition of thiosulfate', *Zeitschrift fur Naturforschung,* vol. 43b, pp. 203-218.

Steudel, R., Gobel, T. and Holdt, G. 1989, 'The molecular nature of the hydrophylic sulfur prepared from aqueous sulfide and sulfite (Selmi sulfur sol)', *Zeitschrift fur Naturforschung.,* vol. 44b, pp. 526-530.

Steudel, R., Holdt, G., Gobel, T. and Hazeu, W. 1987, 'Chromatographic separation of higher polythionates $S_nO_6^{2-}$ (n = 3...22) and their detection in cultures of *thiobacillus ferroooxidans*; molecular composition of bacterial sulfur secretions', *Angewandte Chemie, International Edition English,* vol. 26, no. 2, pp. 151-153.

Suleimenov, O. M. and Krupp, R. E. 1994, 'Solubility of hydrogen sulfide in pure water and in NaCl solutions, from 20 to 320°C and at saturation pressures.', *Geochimica et Cosmochimica Acta,* vol. 58, no. 11, pp. 2433-2444.

Suleimenov, O. M. and Seward, T. M. 1997, 'A spectrophotometric study of hydrogen sulphide ionisation in aqueous solutions to 350°C', *Geochimica et Cosmochimica Acta,* vol. 61, no. 24, pp. 5187-5198.

Sulzle, D., Verhoven, M., Terlouw, J. K. and Schwarz, H. 1988, 'Generation and characterization of sulfurous acid (H_2SO_3) and of its radical cation as stable species in the gas phase', *Angewandte Chemie, International Edition English,* vol. 27, no. 11, pp. 1533-1534.

Takala, H. 1999, 'Leaching of zinc concentrates at Outokumpu Kokkola plant', *Erzmetall,* vol. 52, no. 1, pp. 37-42.

Teder, A. and Wilhelmsson, A. 1975, 'The kinetics of the reaction between sulfide and sulfite in aqueous solution', *Svensk Papperstidning,* vol. 78, no. 13, pp. 480-487.

Thom, G. C. 1977, *The characterization of the metal-sulfide sulfur dioxide reaction in aqueous media*, Ph.D. Thesis, The American University.

Thom, G. C., Waters, P. F. and Hadermann, A. F. 1978a, 'Formation and decomposition of thiosulfate in the ferrous sulfide-sulfur dioxide reaction', *Inorganic Chemistry,* vol. 17, no. 6, pp. 1693-1696.

Thom, G. C., Waters, P. F. and Hadermann, A. F. 1978b, 'A study of the metal sulfide-sulfur dioxide reaction in aqueous media by reaction pressure characterization and ultraviolet spectrophotometry', *Hydrometallurgy,* vol. 3, pp. 373-396.

Thorne, P. C. L. and Roberts, E. R. 1948, *Fritz Ephraim Inorganic Chemistry p.573,* 5th edn, Interscience, New York, .

Timoshenko, E. M., Sobol, S. I., Nagornaya, T. V. and Morozov, V. A. 1991, 'Solid products from autoclave leaching of pyrrhotite by sulfur dioxide.', *Tsvetnye Metally (Moscow),* vol. 11, pp. 17-20.

Tiwari, B. L. 1977, *The kinetics of oxidation of zinc sulfide and hydrogen sulfide by sulfur dioxide in aqueous sulfuric acid*, Eng. Sc. D. Thesis, Columbia University.

Tributsch, H. 1999, 'Direct versus indirect bioleaching', in *International Biohydrometallurgy Symposium '99*, Spain, pp. 51-60.

Tronev, V. G. and Bondin, S. M. 1939, 'Oxidation of ZnS and transference of Zn into aqueous or alkali solution at air pressure', *Comptes Rendus de l'Academie des Sciences de l'URSS,* vol. 23, no. 6, p. 541.

Urban, P. 1975, *Removal of H_2S from a gas stream containing H_2S and CO_2,* 3,859,414, Universal Oil Products Company, Des Plaines, Ill., (patent).

van der Heijde, H. B. and Aten, A. H. W., Jr. 1953, 'Tracer studies on the formation of sulfur from hydrogen sulfide and sulfur dioxide in aqueous solutions', *Journal of the American Chemical Society,* vol. 75, pp. 754-755.

Vazarlis, H. G. 1987, 'Hydrochloric acid - hydrogen peroxide leaching and metal recovery from a Greek zinc-lead bulk sulphide concentrate', *Hydrometallurgy,* vol. 19, pp. 243-251.

Veltman, H. and Bolton, G. L. 1980, 'Direct pressure leaching of zinc blend with simultaneous production of elemental sulphur. A state of the art review.', *Erzmetall,* vol. 33, pp. 76-83.

Veltman, H. and O'Kane, P. T. 1968, 'Accelerated pressure leaching of zinc sulphide concentrates', in *97th Annual Meeting of the AIME*, New York.

Vogel 1979, *Textbook of Quantitative Inorganic Analysis,* 4 edn, Longman, London.

Volynskii, N. P. 1971, 'Mechanism of Wackenroder's reaction', *Russian Journal of Inorganic Chemistry,* vol. 16, no. 2, pp. 158-161.

Wagner, H. and Schreier, H. 1978, , *Phosphorous and Sulfur,* vol. 4, p. 281.

Warren, G. W., Henein, H. and Jin, Z.-M. 1985, 'Reaction mechanism for the ferric chloride leaching of sphalerite', *Metallurgical Transactions B,* vol. 16B, pp. 715-724.

Williamson, M. A. and Rimstidt, J. D. 1992, 'Correlation between structure and thermodynamic properties of aqueous sulfur species', *Geochimica et Cosmochimica Acta,* vol. 56, pp. 3867-3880.

Wohler, L., Martin, F. and Schmidt, E. 1923, 'Formation of sulphur by the action of sulphur dioxide on calcium sulphide, zinc sulphide and iron sulphide', *Zeitschrift fur Anorganische und Allgemeine Chemie,* vol. 127, pp. 273-294.

APPENDIX

ESTIMATION OF HYDROGEN ION CONCENTRATIONS AT ELEVATED TEMPERATURES

Using the concentration of sulfuric acid and the temperature, the hydrogen ion concentration was estimated using the method given by Staples, Holcomb and Cramer (1992).

The first dissociation of sulfuric acid is complete

$$H_2SO_4(aq) \rightarrow H^+(aq) + HSO_4^-(aq) \qquad (A.1)$$

but the second dissociation is incomplete and its equilibrium constant is given by equation A.3

$$HSO_4^- \xleftrightarrow{K_2^o} H^+ + SO_4^{2-} \qquad (A.2)$$

$$K_2^o = \frac{a_{H^+}\, a_{SO_4^{2-}}}{a_{HSO_4^-}} \qquad (A.3)$$

where a_i is the activity of the respective ionic species.

The concentration equilibrium constant is

$$Q_2 = \frac{m_{H^+}\, m_{SO_4^{2-}}}{m_{HSO_4^-}} \qquad (A.4)$$

The equilibrium constants, K_2^o and Q_2, are related via the activity coefficients, γ_i.

$$K_2^o = \frac{a_{H^+}\, a_{SO_4^{2-}}}{a_{HSO_4^-}}$$

$$= \frac{\gamma_{H^+}\, \gamma_{SO_4^{2-}}}{\gamma_{HSO_4^-}} \times \frac{m_{H^+}\, m_{SO_4^{2-}}}{m_{HSO_4^-}}$$

$$= \frac{\gamma_{H^+}\, \gamma_{SO_4^{2-}}}{\gamma_{HSO_4^-}} \times \; Q_2 \qquad \text{(A.5)}$$

The activity coefficients, γ_i, for the respective ionic species were expressed using the extended Debye-Huckel limiting law expression

$$\ln \gamma_i = -\frac{z_i^2\, S_T\, I^{1/2}}{1 + A_2\, I^{1/2}} \qquad \text{(A.6)}$$

where

S_T is the Debye-Huckel limiting law slope for the activity coefficient at temperature T for a univalent electrolyte.

I is the ionic strength,

$$I = \tfrac{1}{2} \sum z_i^2 m_i \qquad \text{(A.7)}$$

with z_i and m_I being respectively the charge and molality of the species.

A_2 is an adjustable parameter.

Substituting equation A.6 into equation A.5 gives an expression for the concentration equilibrium constant

$$\ln Q_2 \;=\; \ln \frac{m_{H^+} m_{SO4^{2-}}}{m_{HSO_4^-}} \;=\; \ln K_2^o + \frac{4\, S_T I^{1/2}}{1 + A_2 I^{1/2}} \qquad \text{(A.8)}$$

The terms K_2^o, S_T, and A_2 are temperature dependent. The equation for K_2^o, from 298 K to 623 K, is

$$\ln K_2^o = 199.0185 - 6658.95/T - 31.81 \ln T \quad \text{(A.9)}$$

and the equation for the parameter S_T is

$$S_T = 3 A_f \quad \text{(A.10)}$$

where A_f is the limiting law slope for the osmotic coefficient. Values for A_f at the temperatures used in this work are given in Table A.1

Table A.1 Selected values of the Debye-Huckel Limiting Law Constant for the Osmotic Coefficient (from (Archer and Wang 1990))

Temperature (°C)	A_f (kg mol^{-1})
100	0.45989
150	0.52682
200	0.61715

The equation for A_2 is given by

$$A_2 = 0.78688 + 5.792 \times 10^{-3} t - 3.3027 \times 10^{-8} t^3 \quad \text{(A.11)}$$

where t is in °C.

The concentration equilibrium constant for the desired temperature is calculated by substituting equations A.9, A.10 and A.11 into equation A.8.

The equilibrium hydrogen ion and sulfate concentrations, m_{H^+} and $m_{SO_4^{2-}}$, are related to the initial concentration of sulfuric acid ($m_{H_2SO_4\ (t=0)}$) and the equilibrium concentration of bisulfate via the equations

$$m_{SO_4^{2-}} = m_{H_2SO_4\ (t=0)} - m_{HSO_4^-} \quad \text{(A.12)}$$

$$m_{H^+} = 2m_{H_2SO_4\ (t=0)} - m_{HSO_4^-} \quad \text{(A.13)}$$

The equilibrium concentrations of $H^+(aq)$, $SO_4^{2-}(aq)$ and $HSO_4^-(aq)$ were calculated by inserting the initial concentrations of these species into a equation A.12, which is a rearranged form of equation A.8, and allowing the concentration of bisulfate ($m_{HSO_4^-}$) to vary until a solution was obtained.

$$\ln\frac{m_{H^+}m_{SO_4^{2-}}}{m_{HSO_4^-}} - \ln K_2^o - \frac{4S_T I^{1/2}}{1+A_2 I^{1/2}} = 0 \qquad (A.14)$$

The equilibrium hydrogen ion concentration was obtained by substituting the equilibrium bisulfate concentration into equation A.13.

For the estimation of the hydrogen ion concentration in ZnS / H_2SO_4 leaches that had attained equilibrium, the removal of hydrogen ions by reaction with ZnS was taken into account.